MECHANICAL AND CHEMICAL PROPERTIES OF ROTATOR CUFF TENDONS

Dr Umme Salma Chaudhury

MB BChir, MA, MRCS

Submitted in partial fulfilment of the requirements for the degree of

DOCTOR OF PHILOSOPHY

St Hugh's College
Nuffield Department of Orthopaedics, Rheumatology and Musculoskeletal Science
Department of Zoology
University of Oxford

Supervisors: Professor Andrew Carr and Professor Fritz Vollrath

Trinity Term 2011

CONTENTS PAGE

Acknowledgements

Firstly I must thank Andrew Carr for his mentorship, support, encouragement and above all his friendship. He has been an absolute pleasure to work with, and to learn from, and has made work a wonderful and fun place.

Thank you to my parents for encouraging and believing in me, and my fantastic sisters Siddiquah and Sawda for their unfaltering love, adoration and care. Thank you to Sahir for supporting my quest to obtain a PhD and for tolerating a transatlantic relationship. Thanks to everyone who has encouraged me and guided me: Fritz, Chris, Cedric, Philippa, Dao, Mark, Emanuelle and Professor Ferguson. Osnat has always been there to help me and is a wonderful confidante. Thanks to everyone at the Botnar, NDORMs and zoology for making this a memorable experience, and for helping to me form lifelong friendships: Steve, Raj, Tom, Hannah, George, Paul, Richie, Beardo, Raewyn, Sarah S, Fujia, Tom, Imke, Bjoern, David P, Cushla, Tracey, Loretta, Bridget, Kim, Cynthia, Matthew, Karolina, Asma, Uday, and Clarence. A special thanks to Andy Price, Johnny Rees, Chris Little and all the UKUFF surgeons who helped me to collect specimens.

Funding

Thank you to the various funding bodies that have contributed in some form to my research, or my research unit:

Jean Shanks Foundation, Lord Nuffield Orthopaedic Trust and the National Institute for Health Research, Musculoskeletal Biomedical Research Unit.

Abstract

Shoulder disease is the third most common musculoskeletal problem, and rotator cuff tendon tears account for the greatest proportion of shoulder complaints. Rotator cuff tears are estimated to affect between 5-30% of adults, with higher incidences of tearing and failure to heal in elderly patients, placing a huge socioeconomic burden on an ageing British population. Serious concern arises as a large proportion of technically correct surgical repairs re-rupture. The intra-articular environment of the tendon often precludes normal healing and surgical repair is often necessary to improve pain and restore some function. It is feasible that there may be an inherent physiological or biomechanical defect in the tissue that prevents complete healing without some further augmentation to the surgical repair. Improved understanding of the biochemical and biomechanical changes in torn rotator cuff tendons may help to reduce the high rerupture rates. This study aimed to characterise normal, and different sized rotator cuff tendon tears from small samples obtained intraoperatively to try to use tests that may potentially be clinically useful in the future.

Tendon samples were mechanically tested using dynamic shear analysis, a form of rheology, to overcome gripping and slippage problems of very small specimens. It was found that torn tendons had a significantly reduced storage modulus compared to normal tendons, particularly for massive tears. Chemical analysis of tendons using Fourier transform infrared spectroscopy revealed that partial and different sized rotator cuff tendon tears are chemically distinguishable. The onset of rotator cuff tear pathology is mainly due to an alteration of the collagen structural arrangements, with associated changes in lipids and carbohydrates. Collagen structural changes in small and massive tendons were quantified using differential scanning calorimetry, which allows measurement of collagen thermal properties as a reflection of their structural integrity. Small and massive tendon tears had reduced thermal properties and hence reduced collagen integrity when compared to normal tendons, although there was no difference between the two tear groups. Gene expression differences between the small, massive tears and normal tendons were studied using microarray analysis, and revealed that the different groups were biologically distinguishable. Microarray gene profiles of human rotator cuff tendon tears suggested a key pathogenesis role for

various extracellular matrix (ECM) genes, such as aggrecan, matrix metalloproteinases (MMPs) and a disintegrin and metallopeptidases (ADAMs).

Rotator cuff tendon tears involve complex gene and biochemical changes, which particularly affect collagen and ECM components. These may interact and result in reduced mechanical properties of torn tendons. A growing interest has been shown in augmenting rotator cuff tendon repairs, for example with repair patches. Mechanical assessment of four commercially available repair patches has demonstrated wide variations between all patches and at least some reduced mechanical properties when compared to human rotator cuff tendons. Surgeons should be aware of the need to address and improve the biology and the mechanical properties of torn rotator cuff tendons when treating and possibly repairing these defects. The differences in different sized rotator cuff tendon tears should also be appreciated, as all tears are not a uniform homogenous group. It is possible that the future may increasingly involve tailoring treatments to specific tear characteristics, although much greater work is required in this area.

Manuscripts arising from this work

- **S. Chaudhury**, S E Gwilym, J Moser, A J Carr. 'Surgical options for patients with shoulder pain'. 2010: 6 (4), 217-226. Nature Reviews Rheumatology.

- **S. Chaudhury**, C Holland, F Vollrath, A J Carr. 'Dynamic Shear Analysis; A Novel Technique For Comparing Normal And Torn Rotator Cuff Tendons'. 2011: 93-B(7):942-8. Journal of Bone and Joint Surgery (British).

- **S. Chaudhury**, C Dicko, M Burgess, F Vollrath, A J Carr. 'Biochemical characterisation of normal and torn rotator cuff tendons using fourier transform infrared spectroscopy'. 2011 93-B(3):370-7. Journal of Bone and Joint Surgery (British).

- **S. Chaudhury**, C Holland, D Porter, U Tirlapur, F Vollrath, A J Carr. 'Differential Scanning Calorimetry of Normal and Different Sized Rotator Cuff Tendon Tears'. 2011 May 11 doi: 10.1002/jor.21450 (Epub). Journal of Orthopaedic Research.

- **S. Chaudhury**, C Holland, M S Thompson, F Vollrath, A J Carr. 'Mechanical Properties of Repair Patches and Comparability to Human Rotator Cuff Tendons'. 14 Nov 2011, DOI: 10.1016/j.jse.2011.08.045. [Epub, ahead of print]. Journal of Shoulder and Elbow Surgery.

- **S Chaudhury,** R Murphy, A J Carr. Tendon Tissue Engineering: The Potential Application of Stem Cells, Biological Factors and Repair Scaffolds To Improve Rotator Cuff Tendon Tears. Comprehensive Biotechnology (Second Edition), 2011. 5:291-310

- **S. Chaudhury**, X Zhidao, P Hulley, E Marchi, A J Carr. 'Gene Profile Changes Between Small and Massive Human Rotator Cuff Tendon Tears Compared to Normal Tendons'. Manuscript in preparation.

Prizes and Awards Related to Thesis

1. **Shortlisted for Best Paper Prize.** 'Genetic Profiling of Normal and Different Sized Rotator Cuff Tears Using Microarrays'. SECEC, Nice, France, 2011.

2. **Henry Kessler Prize: Awarded 1st Prize for best presentation.** 'Determining Mechanical Differences Between Normal and Torn Rotator Cuff Tendons Using Dynamic Shear Analysis'. British Elbow & Shoulder Society Scientific Meeting; London, UK, 2009.

3. **Runner up for best presentation.** 'Using Fourier Transform Infrared Spectroscopy to Differentiate Between Normal and Torn Rotator Cuff Tendons'. British Elbow & Shoulder Society Scientific Meeting; London, UK, 2009.

Declaration

I hereby declare that the work presented herein is original and the sole making of the author,

Ms Salma Chaudhury

Glossary of Terms and Abbreviations

Acromioplasty: surgical removal of the front edge of the acromion process of the scapula as a treatment for rotator cuff pathology.

Alcian Blue: A copper phthalocyanin dye that stains connective tissue mucopolysaccharides and a number of epithelial mucins blue.

Arthroscopic / Arthroscopy: keyhole surgery to a joint.

Bursa: a small synovial fluid filled sac found in the body that sits between moving tissue planes to facilitate movement and reduce friction between he layers.

Complementary DNA (cDNA): single-stranded DNA that is complementary to a certain sequence of messenger RNA and synthesized by the action of RNA-dependent DNA polymerase.

Differential Scanning Calorimetry (DSC): measures the temperatures and heat flows associated with transitions in materials as a function of time and temperature, within a controlled atmosphere.

Denaturation Enthalpy: is a measure of the energy required to fully denature all the collagen present and is thought to correspond to the relative amount and distribution of triple helical structure within the sample

Deoxyribonucleic Acid (DNA): a nucleic acid that carries the genetic information in the cell and is capable of self-replication and synthesis of RNA.

5-([4,6-dichlorotriazin-2-yl]amino)fluorescein (DTAF): A fluorescein derivative fluorescent stain which reacts with amino groups and N-terminal amino acids of proteins at neutral pH.

Dynamic Shear Analysis (DSA): is based upon rheometry, the study of flow and deformation of matter whereby samples are measured for their response to a shearing (side-to-side) mechanical stress.

Extracellular Matrix (ECM): substance produced by cells and excreted to the extracellular space within the tissues, serving as a scaffolding to hold tissues together and helping to determine their characteristics.

Food and Drug Authority (FDA): an agency in America responsible for regulating and supervising safety of foods, pharmaceuticals and related products.

Fourier Transform Infrared Spectroscopy (FTIR): all molecules can be excited to higher vibrational states, using light at specific wavelengths which correspond with the frequency of excited vibration modes of the bending or stretching motion of the molecule. This allows the absorption positions to be mapped and the chemical composition to be identified.

Full Thickness Rotator Cuff Tear: refers to structural failure and tissue disruption that spans the full width of at least one of the four muscles and tendons that form the rotator cuff.

Glyceraldehyde-3-phosphate Dehydrogenase (GAPDH): is an enzyme of glycolysis and gluconeogenesis, that catalyzes the production of 1,3-bisphosphoglycerate from glyceraldehyde 3-phosphate.

Glenohumeral joint: the 'ball and socket' joint of the shoulder. Articulation between the glenoid fossa of the scapula (the 'socket'), and the head of the humerus (the 'ball').

Glycosaminoglycans: a group of high molecular weight linear polysaccharides with various disaccharide repeating units and usually occurring in proteoglycans.

Graft: transplanted living tissue.

Haematoxylin and Eosin (H&E): a mixture of hematoxylin in distilled water and aqueous eosin solution, employed universally for routine tissue examination.

Immunohistochemistry: involves localising protein antigens in tissue cells, through specific antibody-antigen binding which is bound to a dye and allows visual identification.

Immunoglobulin (Ig): a class of proteins present in the serum and cells of the immune system, that function as antibodies.

Microarray: involves the use of glass plates or 'chips' with DNA probes bonded to it, which hybridize with labelled cDNA samples and are scanned to measure fluorescence levels that are relative to cDNA abundance.

Magnetic Resonance Imaging (MRI): a type of non-ionising medical imaging that uses a strong magnetic field to evaluate body tissues. MRI is generally used to assess the soft tissues of the body.

Messenger Ribonucleic Acid (mRNA): a form of RNA, transcribed from a single strand of DNA, that carries genetic information required for protein synthesis from DNA to the ribosomes.

Partial Thickness Tears: any tear that involves rotator cuff disruption that does not extend all the way through the tendon.

Polymerase Chain Reaction (PCR): amplifies a specific DNA sequence through the binding of primers containing complementary DNA sequences.

Proteoglycans: are heavily glycosylated glycoproteins consisting of a "core protein" with one or more covalently attached glycosaminoglycan (GAG) chain(s) occurring in the extracellular matrix of connective tissue.

Revolutions per minute (RPM): a measure of the frequency of a rotation, measuring the number of full rotations per minute around a fixed axis.

Ribonucleic Acid (RNA): single-stranded molecules transcribed from DNA, containing a linear sequence of nucleotide bases that is complementary to the DNA strand from which it is transcribed.

RNA Integrity Number (RIN): is an algorithm to allow assessment of the integrity of total RNA within samples.

Rotator Cuff: a group of four muscles and tendons (supraspinatus, infraspinatus, teres minor and subscapularis) attached between the shoulder blade and the humerus that act to stabilize and rotate the glenohumeral joint.

Rotator Cuff Repair: surgical procedure of reconstructing a torn rotator cuff tendon, normally by reattaching the tendon to bone using sutures and a bone anchoring technique.

Scaffold: a temporary structure, which in the case of tendon repair offers physical support to the healing tissue.

Shear Modulus: the ratio of shear stress to the shear strain.

Stress: is a measure of the average force per unit area of a surface within the body on which internal forces act.

Strain: the ratio of elongation with respect to the original length.

Synovium: the non-cartilaginous, soft tissue lining of synovial joints and bursae in the body (e.g. glenohumeral, hip and knee joints).

Tensile (Young's) Modulus: this modulus is measured as the tangent of the initial, linear portion of a stress-strain curve.

Toughness: the amount of energy per volume that a material can absorb and undergo plastic deformation before rupturing.

$\mathbf{T_{onset}}$: is defined as the onset of the endotherm on the thermogram. This is proposed to represent breaking of the water-amide hydrogen bonds, resulting in increased mobility of the protein chain backbone and resulting in a ordered to disordered transition.

T_{peak}: is the peak of the endotherm, and reportedly corresponds to the temperature at which the majority of proteins fall out of solution.

List of Figures

List of Tables

1 CHAPTER 1: BACKGROUND

1.1 Socioeconomic Burden of Rotator Cuff Disease

The ball and socket shoulder joint affords a huge degree of mobility, by partially sacrificing stability. Stability is partly offered by the four muscles that make up the rotator cuff. The first surgical repair of a rotator cuff tear is often accredited to Codman who is thought to have performed the procedure in 1909, and his classic observations were extensively described in 1934 [1]. Rotator cuff degeneration and tears pose a significant management challenge by imposing a huge functional, economic and social burden. Prevalence of shoulder problems in the UK has been estimated at 14% in the general population [2], with higher estimations in several other countries such as Japan where the prevalence is estimated at 20.7% [3, 4]. 1-2% of British adults consult their general practitioner (GP) annually with a new onset of shoulder pain [2], and it has been suggested that 40-50% of all patients in the UK consult their general practitioners for shoulder pain at some stage [5]. Shoulder problems are the third most common cause of musculoskeletal problems following spine and knee problems [6], and accounted for 2.4% of all GP consultations in the UK [7] and 4.5 million visits to physicians in the USA in 2002 [8]. Rotator cuff tears are one of the most common causes of shoulder pain and dysfunction [9]. Although some cases of shoulder pain do improve with treatment and rest, 40% of patients still have persistent or recurrent symptoms a year after presenting to their GP [10]. While there are many causes of shoulder pain such as impingement, frozen shoulder, calcific tendonitis and osteoarthritis, this thesis will only focus on rotator cuff tears.

Census information from the United States predicts that 17 million people potentially face the risk of disability from rotator cuff failure [11]. Rotator cuff pathology accounts for 30-70% of shoulder problems [12, 13], a significant proportion is attributable to rotator cuff tears. Cadaveric studies have estimated that the prevalence of rotator cuff tears in adults is 5-30% [14, 15]. MRI and USS studies have estimated similar prevalence rates of 15-23% for asymptomatic rotator cuff tears [16, 17]. However it is important to note that not all tears are symptomatic [18]. A study which followed patients with asymptomatic tears found that over 5 years, 51% of patients became symptomatic, although some patients were lost during follow up [19]. Presence of a rotator cuff tear has been found to correlate with inferior shoulder scores [20].

As rotator cuff tears increase with age [12, 21, 22], particularly over the age of fifty years [23], an aging population means the socioeconomic burden of this problem will only increase. The incidence of rotator cuff tears is increased by the presence of co-morbidities such as rheumatoid arthritis. 24-52% of patients with rheumatoid arthritis over the age of 50 years were found to have at least one rotator cuff tear [24, 25]. Tears can impair the ability to work or perform household tasks [26, 27] and result in increased time off from work [28-30]. The intra-articular synovial environment of the damaged tendon often precludes normal healing. Surgical repair may be required and more than 300,000 surgical repairs are performed annually in the USA for rotator cuff pathologies, at an average cost of $14,000 [31]. It is difficult to accurately quantify the economic cost of rotator cuff disease to the NHS in the UK. The annual financial burden of rotator cuff surgeries in the USA has been estimated to be $3 billion, including treatment, evaluation and management [31].

Current surgical treatment strategies of suture repair, tendon grafts or synthetic grafts are often unsuccessful with high reported failure rates of between 13-94% [32-36]. Re-rupture has serious clinical consequences and has been shown to correlate with poorer outcomes [33]. Managing larger tears is particularly challenging as they are associated with a higher incidence of re-rupture [37, 38]. Importantly, pre-operative tear size seems ineffective as a sole indicator to predict clinical and functional repair following surgery.

1.2 The Healthy Shoulder

1.2.1 Anatomy of the Shoulder

Tendons are composed of fibrous connective tissue that connects muscle to bone, and generate movement of a joint. The shoulder joint is a complex joint which offers a wide range of motions that are actively and passively contributed to by numerous soft tissue structures. While the shoulder joint consists of a ball and socket joint, it offers a low level of bony constraint, as the glenoid fossa is relatively shallow compared to the humeral head. Thus soft tissue support plays a vital role in shoulder mechanics, and arises from muscles, ligaments and other passive stabilisers. Stability of the shoulder joint is partly offered by the four deep muscles that span the glenohumeral joint, and are attached to the proximal humerus and the scapula (See Figure 1-1). The four muscles form the rotator cuff and include the supraspinatus, infraspinatus, teres minor and subscapularis muscles. The rotator cuff muscles function to actively elevate the arm and rotate the humerus with respect to the scapula. Dynamic stabilisation of the glenohumeral joint is also offered by compressing the humeral head into the glenoid. Additionally the rotator cuff muscles can cancel

out opposing or unwanted forces acting on the glenohumeral joint, such as lattisimus dorsi or trapezius.

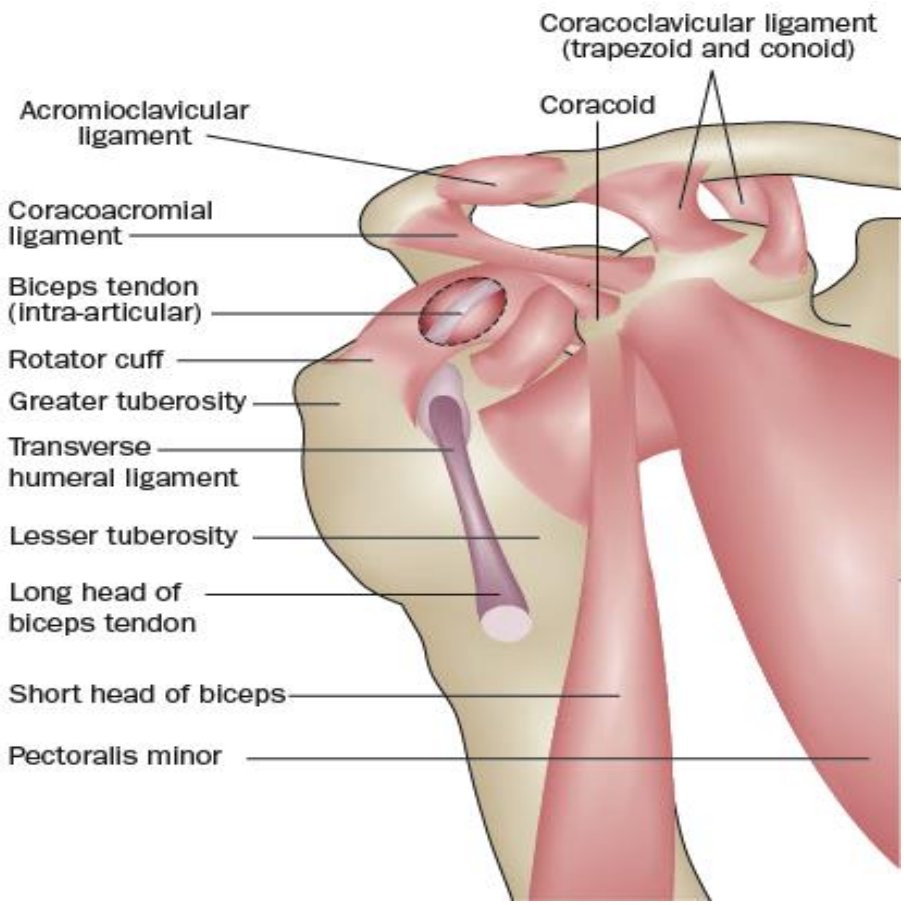

Figure 1-1: Diagram showing the anatomy a normal shoulder. Image obtained from Elsevier Ltd © Carr, A. J. & Hamilton, W. Orthopaedics in Primary Care 2nd edition (2005).

1.2.1.1 Supraspinatus

Supraspinatus originates from the supraspinatus fossa found on the superior aspect of the scapula spine, and inserts into the highest point on the humeral greater tuberosity (see Figure 1-2). This insertion point is shared by the insertion of the coracohumeral ligament anteriorly and infraspinatus posteriorly. Supraspinatus initiates abduction and stabilises the humeral head in the glenoid fossa at the start of elevation [39]. Fibrous tissue derived from the coraco-humeral ligament encases the anterior margin and bursal surface of supraspinatus [40]. The nerve supply is from the suprascapular nerve and fibres from the C5 nerve root.

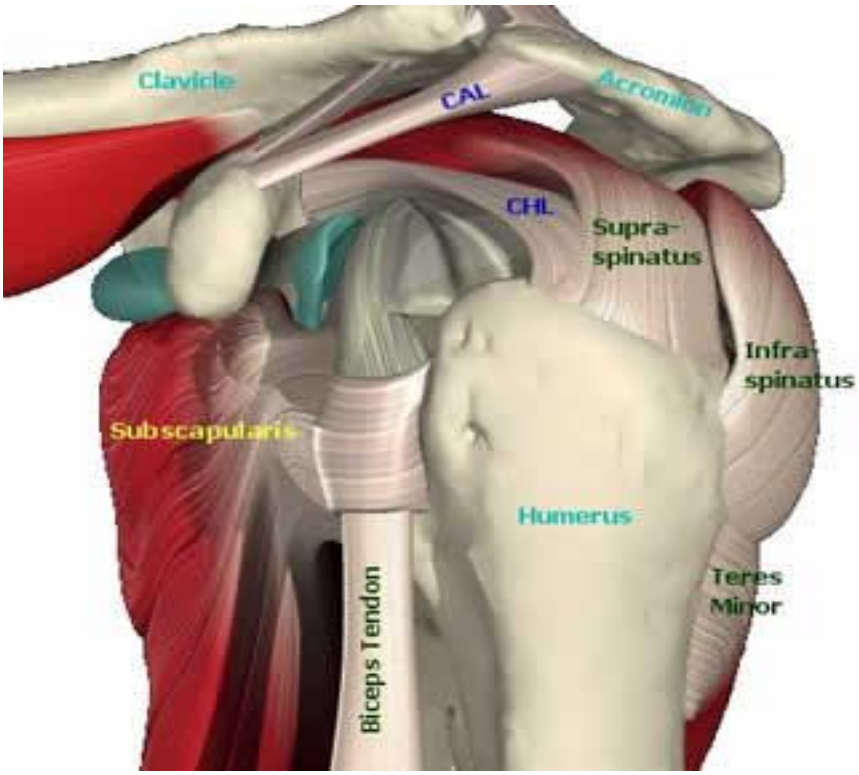

Figure 1-2: Diagram showing the anatomy of the rotator cuff tendons. Image obtained from Yeovil Shoulder and Elbow Service webpage; www.yess.uk.com/patient_information.anatomy.

1.2.1.2 Infraspinatus

Infraspinatus is a pennate muscle, originating from the infraspinatus fossa found inferior to the spine of the scapula and inserts into the middle of the greater tuberosity. One of the primary functions of infraspinatus is to externally rotate the shoulder [41]. It also depresses the humeral head and prevents superior translation. Infraspinatus has the same nerve supply as supraspinatus.

1.2.1.3 Teres Minor

Teres minor originates from the upper lateral border of the scapula, and inserts into the greater tuberosity, inferior to the insertion of infraspinatus. In addition to infraspinatus, teres minor also helps to externally rotate the shoulder after thirty degrees from neutral, as well as to adduct it [41]. Teres minor is supplied by the posterior branch of the axillary nerve, with fibres from the C5-6 nerve root.

1.2.1.4 Subscapularis

Subscapularis is a multipennate muscle originating from the anterior aspect of the scapula. The upper portion of the tendon inserts into the lesser tuberosity, while the lower portion inserts just below the lesser tuberosity into the humerus. Subscapularis internally rotates, has a role in adduction and depresses the humeral head to restrict anterior displacement [42]. A gap exists between the supraspinatus anteriorly and subscapularis superiorly termed the rotator interval, into which projects the coracoid medially and the long head of biceps laterally. There is dual innervation from the upper subscapular nerve, with fibres from the C5 nerve root, and the lower subscapular nerve with fibres from C5-6 nerve roots.

1.2.1.5 Additional Soft Tissue Support

A thick bundle of fibres from the coracohumeral ligament are termed the rotator cable and defined as a structure that runs perpendicular to the axis of the supraspinatus tendon to transversely span the distal attachments of the supraspinatus and infraspinatus tendons. Biomechanical studies have indicated that the cuff attachments distal to the rotator cable (termed the rotator crescent) are relatively stress shielded [43]. It has been proposed that if tears occur within the rotator crescent, the rotator cable is able to dissipate load from the rotator cuff muscles to the attachments of the cable, which is why repairing the ends of the rotator cuff cable is strongly recommended.

The relatively shallow glenoid is a cuff of fibrocartilagenous tissue around the margins, termed the glenoid labrum. Further reinforcement of the joint is achieved through a fibrous capsule lined by a synovial membrane, which is relatively taut at rest anteriorly, superiorly and posteriorly to prevent subluxation. The capsule becomes taut inferiorly on abduction.

The joint and capsule are further reinforced by ligaments: 3 glenohumeral ligaments which are incorporated within the capsule, and the coracohumeral ligament superiorly. The tendon of the long head of the biceps brachii originates from the supraglenoid tubercle and passes through the joint space, travelling along the intertubercular groove. The long head of biceps brachii makes an important contribution to rotator cuff tendon function. Running over part of the long head of biceps is the broad transverse humeral ligament.

To facilitate movement within the shoulder joint and reduce friction, several bursae exist which are fibrous synovial lined sacs containing synovial fluid.

1.2.2 Shoulder Forces

The shoulder is subjected to both tensile loads as well as compressive and shear forces. The rotator cuff muscles rotate the humerus about its head, and also provide a joint centring force and concavity compression. The combined rotator cuff muscle tension directly restrains the centre of the humeral head onto the centre of the glenoid. When a compressive force is applied to the shoulder, there is a tendency for the musculature to press the spherical humeral head into the centre of the concave articular surface of the glenoid. Values suggested for this joint compressive load are between 22-62 N [44]. Rotator cuff muscle data and morphology have been studied using finite element modelling based upon cadaveric data [45-47]. This data has been applied to detailed models of shoulder kinematics [48]. Some attempts have been made to quantify the relative strength of each of the rotator cuff muscles. In a small study focusing on the potential moment arm (Ncm^{-1}) exerted about the humeral head by each rotator cuff muscle, 5 cadavers were examined and it was determined that the relative contributions of each of the cuff muscles were as follows: subscapularis 53%, infraspinatus 22%, supraspinatus 14% and teres minor 10% [49]. The mechanical properties vary within individual rotator cuff tendons. As an example, supraspinatus tendons display the greatest ultimate load anteriorly (411 N) compared to the middle (152 N) and posterior (88 N) aspects of the tendon [50]. Mechanical differences also exist between the joint and bursal sides [51], with the bursal side displaying almost twice the failure strain and failure stress and that of the joint side [52].

Each muscle has a maximum threshold for its mechanical properties in terms of strength or maximum elongation. Tendon damage and subsequent tears can occur when these parameters are exceeded. Tendons are viscoelastic materials and their mechanical response will vary with the rate or duration of loading [53]. As tendons are viscoelastic but have fairly low energy dissipation (5-10%), they act as good elastic energy storing modalities in limbs. Tendon stress-strain curves display properties of stress, relaxation and creep [54]. The region of the initial slope at low stress is called the 'toe region' of the graph and represents the elastic behaviour of the tendon (see Figure 1-3). Below 2% strain the lack of significant change in stress is thought to represent flattening of the crimp pattern of tendon fibrils and fibre realignment. After removal of all crimp, fibres are assumed to be taut and the highly aligned fibre arrangement allows forces to be transmitted along the long axis of the tendon and results in increasing stiffness. Up to 4% strain, changes are reversible, and correlate with the physiological strain range. Once strain exceeds 4%, the tendon enters a linear phase of deformation where microscopic failure is thought to occur as the energy provided overcomes and breaks forces between collagen fibres, allowing the fibres to slide past each other. Although tear propagation has been reported to occur as low as 1.7% in supraspinatus tendons [55]. Macroscopic failure is proposed to occur above 8%, and complete failure can occur rapidly beyond this point [56].

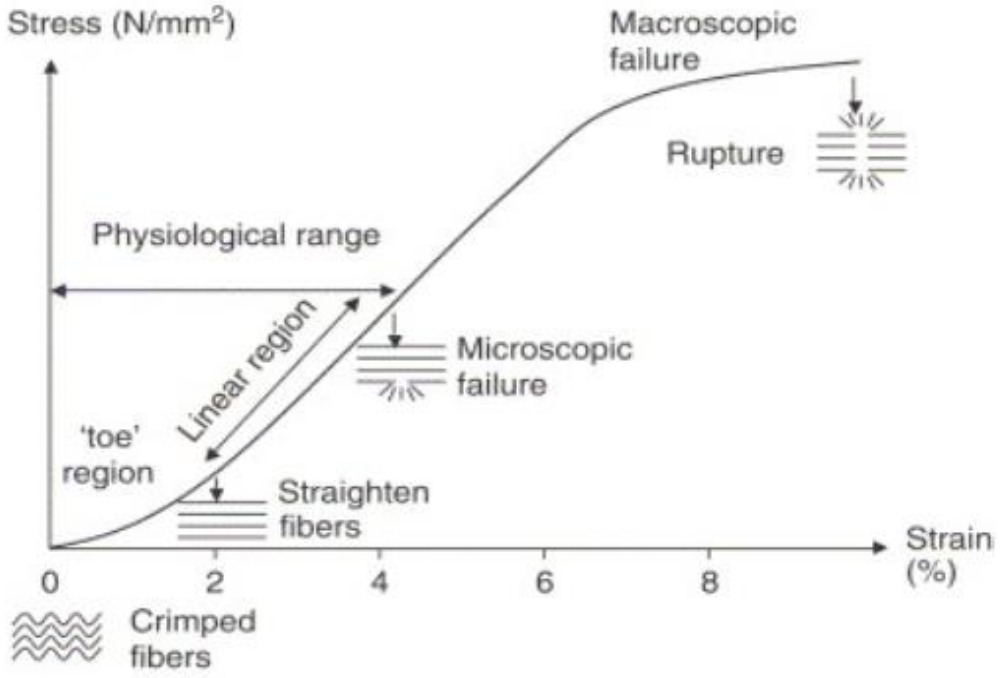

Figure 1-3: Image of representative tendon stress-strain curve. Microscopic failure is thought to occur above 4-6% strain, and macroscopic failure occurs by the time 8% strain has been reached. Image taken from Wang *et al.*, [57]

1.2.3 Rotator Cuff Vascularity

The blood supply of the rotator cuff is derived from multiple sources. Supraspinatus and the anterosuperior portion of the cuff are supplied by branches of the thoracoacromial artery. Infraspinatus and teres minor are primarily supplied by the suprascapular and posterior circumflex humeral arteries. Subscapularis is primarily supplied by the anterior circumflex humeral artery, with some contributions from the posterior humeral circumflex artery. Small contributions to the rotator cuff arise from the subscapular artery. The rotator cuff microvasculature is slight atypical

as it does not have a synovial sheath or a true paratenon, and so vessels connect to the rotator cuff through the periosteum, musculotendinous junction and bursal surface.

1.2.4 Tendon Microstructure

Tendon has a complex multi-hierarchical structure (see Figure 1-4). Collagen molecules assemble into triple helices, which then form collagen fibrils which can lengthen in time, and aggregate to form subfascicles, which group together to form fascicles, that ultimately form collagen fibres. Fibre bundles are sheathed in connective tissue termed endotenon. The entire tendon is enclosed by epitenon. Most tendon elements are primarily arranged in parallel to each other along the long axis of the tendon, and thus load is applied along them. Tendon has been described as 'in effect a unidirectional fibre reinforced composite with a matrix of low stiffness' [53]. Morphological studies of human supraspinatus have revealed independent fascicles that can slide past one another during movement of the arm [58].

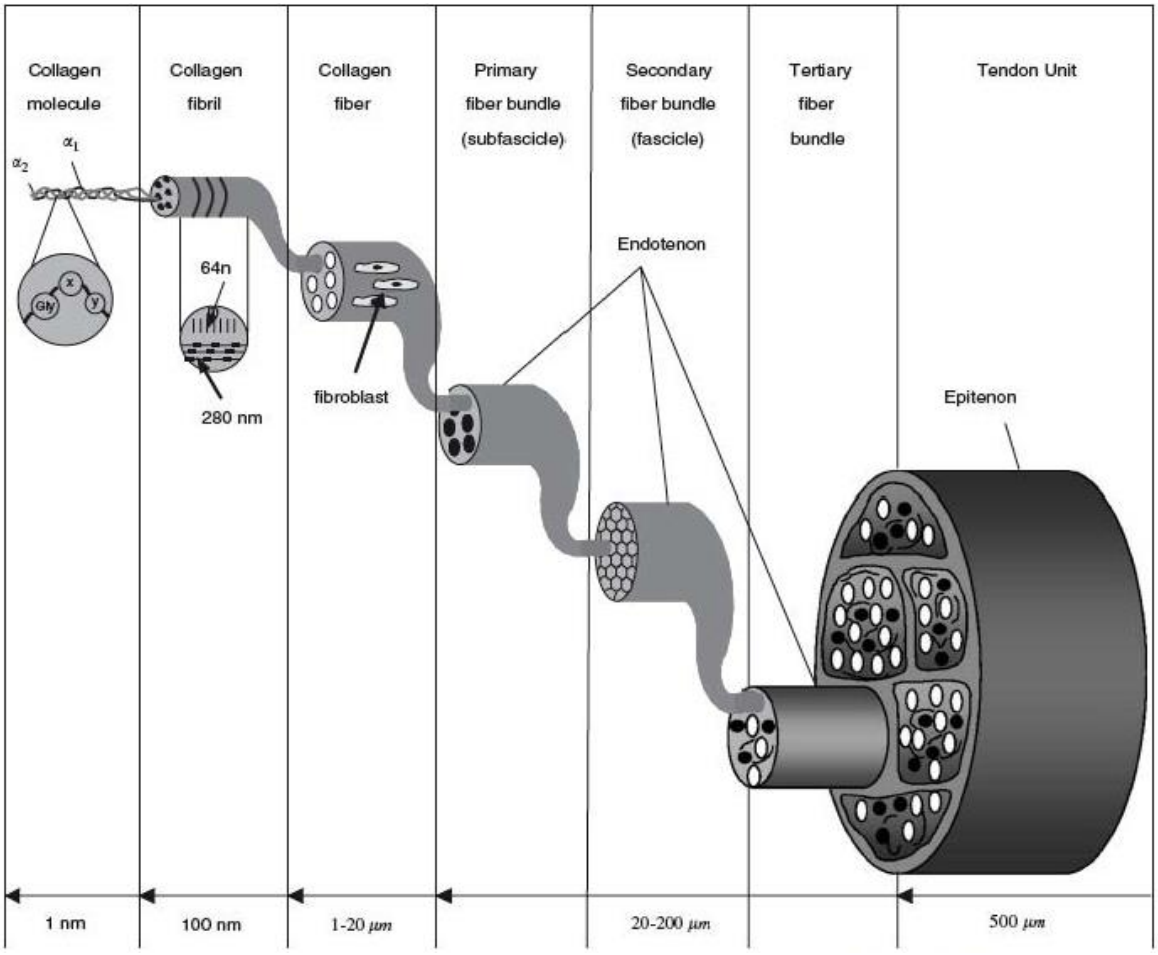

Figure 1-4: Diagram representing tendon microstructure, demonstrating the hierarchical organisation. Image taken from Silver *et al.*, [59].

Rotator cuff tendons have a complex microstructure, and five histologically distinct layers of the supraspinatus and infraspinatus have been described by Clark and Harryman, following their study of intact cadavers [40]:

- 1st layer – superficial layer of coracohumeral ligament with obliquely orientated fibres
- 2nd – large bundles consisting of closely packed, parallel tendon fibres
- 3rd – smaller bundles, of more randomly orientated tendon fibres. Tendons fuse in the third layer with interdigitating tendon fibres.

- 4th – loose connective tissue with some thick bands of collagen fibres
- 5th – joint capsule.

Based upon another cadaveric study of the shoulder, Nakajima *et al.*, have also described histological differences between the joint and bursal sides, between 2 to 17 mm from the tendon insertion [52]. The joint side tendons were described as being thinner and more transversely orientated near the insertion side. On the bursal side, the musculotendinous junction was found to be closer to the insertion site.

As the rotator cuff tendons approach their insertion, they fuse to allow them to work in unison. Four tendon zones have been described at the healing enthesis: tendon, unmineralized fibrocartilage, mineralized fibrocartilage and bone. These zones are thought to permit effective dispersion of loads and stresses, rather than concentrating forces in any one area and thus making the tendon less prone to rupture, as well as facilitating changes in abduction/adduction angles [60, 61].

A myotendinous junction has been described, wherein the collagen fibrils of the tendon strongly anchored to muscle by being inserted at an angle into deep recesses formed by myocyte processes. This structure is thought to increase the surface area of the tendon anchoring and thus can dissipate tensile stresses generated by contraction of the muscle [60].

1.2.5 Tendon Extracellular Matrix

Tendons are composed of 55% water (wet weight) [62], cells and the extracellular matrix (ECM). Collagen subfascicles are embedded in an ECM, which allows neighbouring subfascicles to interact with one another. ECM interactions with collagen increase tendon stiffness and resistance to bending, but it is still much less stiff than bone [53]. The ECM is formed primarily from collagen, but also proteoglycans, glycosaminoglycans, and elastin. Cells are usually found in between or attached to collagen fibres. While tendons are relatively acellular, they consist of tenocytes and tenoblasts, which both have long spindle shapes, with the latter being more immature and active, fibroblasts and chondrocyte like cells in fibrocartilagenous areas [63]. Tenocytes and fibroblasts secrete ECM components such as tropocollagen, proteoglycans and glycosaminoglycans. The ECM components are in a constant state of flux, and are constantly being synthesised, remodelled and degraded [64].

1.2.5.1 Collagen

The most common constituent of tendon is collagen, accounting for 65-80% of its dry mass [65]. Collagen fibres are embedded in an ECM consisting of proteoglycans and water. Collagen fibres are cross-linked and arranged parallel to the loading axis of the tendon. At rest, a crimp pattern exists within tendon at a periodicity of 20 nm on average [59]. During initial loading of tendons, energy is thought to be absorbed during the lengthening out of the crimp pattern, resulting in the toe region seen in tendon stress-strain curves (see Figure 1-3). The most common form of tendon collagen is type I collagen, which has been estimated to form 95% of the collagen total [66]. Type

III collagen is located within the endotenon rather than within fascicles, and accounts for approximately 3% of all collagens. Increased levels have been identified at the edges of tears, in degeneration and in older patients [67].

1.2.5.2 Proteoglycans

Proteoglycans such as decorin, lumican and fibromodulin have been demonstrated to play an important role in guiding and stabilising collagen fibril formation and maturation, as well as providing compressive strength [68, 69]. 1 % of tendon weight is due to proteoglycans which are strongly hydrophilic macromolecules and thus thought to contribute to swelling, but smaller quantities exist in tendons than are found in knee cartilage and meniscus [70]. The most frequently found proteoglycans in the tendon include biglycan, decorin and aggrecan [71]. Decorin is largely bound to the collagen fibril surface and its glycosaminoglycan chain extends laterally from the fibril, formed primarily by dermatan sulphate [72]. The force within tendons is directly transmitted through collagen fibrils rather than through interfibrillar coupling such as a proteoglycan bridge [73].

1.2.5.3 Glycosaminoglycans

Glycosaminoglycans are polysaccharides containing amino sugars, with the most common examples in the tendon being chondroitin sulphate, followed by dermatan sulphate and hyaluronic sulphate [71]. Supraspinatus tendons were found to have higher levels of glycosaminoglycans such as chondroitin sulphate than other tendons such as the biceps [74, 75]. A few possible

explanations about the role of proteoglycans/glycosaminoglycans have been proposed. They may facilitate the movement between collagen bundles, which helps to relieve shear stress at tissue bends. As proteoglycans and glycosaminoglycans are observed between collagen fibres, a common belief is that they form strong electrostatic interactions with collagen and act as lubricants to facilitate sliding between collagen fibres when loads are placed through muscles [58, 75]. Glycosaminoglycans are proposed to act as 'cross-links' that transfer axial forces between contiguous collagen fibrils [76]. It has also been suggested that they may help to protect the tendon's vasculature supply during compression, as proteoglycans have been observed around tendon vessels [63].

1.2.5.4 Elastin

Elastin forms 1-2% of the tendon mass. This protein is also secreted by fibroblasts, and plays a role in cross-linking collagen to allow stretch and recoil, and recovery of shape flowing muscle contraction [77].

1.3 Rotator Cuff Tendon Tears

In order to address the high surgical rerupture rates and improve patient outcomes, there is a need for improved understanding of why rotator cuff tendons initially fail, and subsequently fail to heal. Failure of rotator cuff surgery primarily occurs at the suture-tendon interface [78]. It is feasible that there may be an inherent physiological or biomechanical defect in the tissue that prevents complete healing without further augmentation to the surgical repair. Furthermore to address

tendon healing, regional variations in tendon also need to be addressed, which may explain why regenerating the transition zones described previously and achieving successful structural healing following surgical repair is difficult.

To date tendons, particularly rotator cuff tendons, have often been studied using animal models or intact specimens from cadavers. While animal models provide useful information, they are unable to accurately replicate the chronic degenerative pathology of human rotator cuff tendons. Cadaveric studies are usually limited to intact human tissue, which does not always replicate the mechanical and chemical properties of damaged rotator cuff tendons that are difficult to successfully repair.

A continuing spectrum of disease has been proposed for rotator cuff tendons, ranging from tendinopathy to full thickness massive tears. This thesis will focus upon full thickness tears only.

1.3.1 Types of Rotator Cuff Tendon Tears

1.3.1.1 Full Thickness Rotator Cuff Tears

Rotator cuff tears refer to full thickness disruption of one of the four muscles that form the rotator cuff and help to stabilise the shoulder. A classification system of full thickness tears based upon tear size has been proposed by Post *et al*., who has classified tears as small (< 1 cm), medium (< 3 cm), large (< 5 cm) and massive (> 5 cm) according to the greatest diameter of he tear [79]. Rotator cuff tears have been proposed to be part of a spectrum or cascade of disease ranging from reversible tendonitis, irreversible tendonitis, partial tears, small through to massive full thickness tears and

finally cuff tear arthropathy [6]. Each of these stages can involve calcific tendonitis, but this is often transient and is outside of the scope of this study.

1.3.1.2 Partial Thickness Rotator Cuff Tears

Any tears that involve rotator cuff fibre disruption but do not extend all the way through the cuff are termed partial thickness tears. Ellman has proposed a classification system for this group of tears based upon radiographic imaging which describes 3 features: location (articular, bursal, or interstitial), tear area (measured in mm^2) and grade (grade 1 < 3 mm, grade 2 is 3-6 mm, and grade 3 is > 6 mm deep)[80].

1.3.1.3 Cuff Tear Arthropathy

Neer coined this term in 1983 to describe severe rotator cuff tendon insufficiency associated with arthritic changes of the glenohumeral joint [81].

1.3.2 Aetiology of Rotator Cuff Failure

Tendinopathy describes tendon injury that results in pain or tearing of any tendon, whereas tendonitis describes tendon inflammation. Microtearing of the tendon is termed tendinosis and is a histological diagnosis [82].

Rotator cuff tears can be classified according to their presumed aetiology, as being either acutely traumatic or chronic degenerative; extrinsic or intrinsic; mechanical or biochemical; or based upon anatomy as articular, bursal or interstitial. Acutely traumatic tears are presumed to occur in

tendons without evidence of pathological abnormalities, wherein excessive force exceeds the tendons withstanding capabilities and it tears. There is widespread literature about rotator cuff tendon failure associated with sports which is assumed to be due to overuse involving activities such as swimming, throwing and overhead activities etc. Chronic degenerative tendons are more common and assumed to occur in tissues that involve a combination of changes of normal ageing in conjunction with some abnormal active pathological processes.

A more common classification for the pathogenesis of rotator cuff disease involves extrinsic (extratendinous) factors such as impingement beneath the coracoacromial arch, and intrinsic (intratendinous) degeneration which may or may not be related to ischaemia and usually worsens with age [83].

1.3.2.1 Extrinsic Causes of Rotator Cuff Tears

Mechanical factors have been shown to contribute to tendon tears, such as excessive loading which can damage the tendon body and result in inflammation of the tendon sheath [84]. A large Japanese cross-sectional study identified a history of trauma as a risk factor for rotator cuff tears [4]. The tensile strength of tendons is a function of its thickness and collagen content. Once the tendon is stretched beyond its elastic threshold, then failure may ensue with inflammation of the tendon sheath and/or tendon degeneration [85]. Tendon damage can also occur when microtrauma forces are applied within the tendon's physiological threshold but the normal reparative mechanisms are overwhelmed [85]. Overuse has been suggested as a contributing factor to the development of rotator cuff tendon tears as tears are often more symptomatic in the dominant rather than the non-

dominant arm [4, 21]. However overuse cannot be used as a sole explanatory factor, as the majority of tears (more than 70% estimated by one study) occur in sedentary individuals who only do light work [86].

Supraspinatus is the most frequently torn rotator cuff muscle [87]. Extrinsic causes of rotator cuff tendon failure were proposed by Neer in 1972, who suggested that more than 95% of rotator cuff tears occur when mechanical contact occurs between the rotator cuff tendons and the overlying coracoacromial arch [88, 89]. Neer described three progressive stages of impingement: (1) oedema and haemorrhage, (2) fibrosis and tendonitis and (3) rotator cuff and biceps tendon tears with acromial bony spurs [90]. A 2-dimension finite element model has suggested that subacromial impingement generates high stress concentrations in and around the critical zone [91]. A correlation between rotator cuff tears and associated impingement due to the acromial shape has been proposed by Bigliani *et al.*, [92]. He suggested that tears are contributed to by "spurs" at the antero-inferior margin of the acromion, particularly a hook shaped acromion rather than a flat shape, as well as changes in the coracoid and coracoacromial ligament [88, 89]. The supraspinatus outlet can be reduced by thickening of the coracoacromial ligament. It has been proposed that different glenoid and humeral versions can act via by both an extrinsic mechanism by narrowing the subacromial space, and contribute to intrinsic degeneration by increasing the shear stress on the rotator cuff [93]. Extrinsic causes cannot explain all rotator cuff tendinopathies and tears. It has been proposed that rather than being a primary cause for rotator cuff tendon failure, impingement occurs secondary to intrinsic rotator cuff tendon failure which impairs tendon function and results in superior migration of the humeral head, narrowing of the subacromial space

and impingment against the acromion and coracoacromial ligament [94]. The relationship between rotator cuff tears and impingment was also studied by Ozaki *et al.*, who examined 200 cadaveric shoulders and found pathological changes in the acromial undersurface with bursal tears rather than articular tears [95]. They therefore hypothesised that articular tears occurred due to a degenerative process.

1.3.2.2 Mechanical Changes In Rotator Cuff Tears

The effects of rotator cuff tears on muscle moment arms were simulated using finite element modelling [96]. The study concluded that the torn tendons were associated with associated with reduced moment arms when compared to intact tendons, which would reduce the effectiveness of muscles. An MRI study found that the glenoid version of rotator cuff tears was significantly different compared to controls, with retroversion being predictive of anterior cuff tears and anteversion being predictive of posterior cuff tears [97]. Full thickness rotator cuff tears have been shown to have an association with increased glenoid inclination angle [98].

Rotator cuff tears are prone to heal with the formation of scar tissue at the tendon-bone interface, thus this regenerated tissue is usually weaker and more prone to fail [99, 100]. Tissue near the tendon-bone attachment, or enthesis, has been shown to have a low degree of fibre alignment [54]. Using finite element modelling, higher stress concentrations have been suggested at the edges of tears [51]. Itoi *et al.,* suggested that supraspinatus tears are associated with decreased strength [101]. Following artificially created tears in human cadaveric supraspinatus tendons, Reilly *et al,*. demonstrated alterations in strain [102]. A small study looking at 20 patients with partial and full

thickness supraspinatus tears compared to their normal contralateral shoulder, found that after intrarticular or intrabursal local anaesthetic blocks, there was a significant increase in strength in abduction and external rotation. However it may be argued that the decreased strength in torn tendons is due to pain rather than an inability to transmit mechanical load. Following rotator cuff tears, it was found that the remaining intact tendons had decreased mechanical properties with a decreased modulus but increased cross-sectional areas [103]. A study looking at the morphology of rotator cuff tendon tears found that full thickness tendon tears had a significantly decreased muscles fibre length and increased functional tendon length (extramuscular tendon length plus tear length) when compared to partial thickness tears and normal tendons [104].

1.3.2.3 Intrinsic Changes of Rotator Cuff Failure

Codman proposed in 1934 that intrinsic mechanisms related to inherent tissue changes within the tendon played a significant role in the aetiology of rotator cuff tendon tears [1]. The biology of tendons is important, and this theory is supported by the fact that the incidence of tears increases with age, and poorer outcomes are seen following smoking [105, 106]. Nobuhara *et al.,* found that 97% of 189 repairs performed for massive tears were in patients aged 45 years and above, and 81% of patient tendon biopsies showed degeneration [107]. Degenerative changes are likely to play a key role in the pathogenesis of tears, as they are more likely to rupture than normal tendons during physiological loading [61, 108]. A large cadaveric study found these changes in 97% of spontaneously ruptured tendon tears ranging from the Achilles to biceps brachii, but also in 33%

of normal tendons [109]. Degeneration was defined as tendon thinning, presences of granulation tissue and partial thickness tears. As degeneration was found to increase with age, distinguishing pathological degeneration from normal physiological age related degeneration is complex, but the levels of degeneration between normal and ruptured tendons have been shown to be different even in advanced age groups [110, 111]. Degenerative changes of the rotator cuff tendon are likely to affect mechanical properties, as the increasing degeneration has been found to result in decreasing ultimate tensile stress [112]. Sperling *et al*., found that patients under the age of 50 years are more likely to suffer from traumatic tears [113]. Variable results for the effect of age on healing have been reported. Boileau *et al*., and Tibone *et al*., reported better healing outcomes in younger patients, whereas Watson *et al*., and Grauer *et al*., reported poorer outcomes in younger patients under the age of 55, although results may have been confounded by other factors such as differences in repair techniques [114-117].

The role of biological factors in the aetiology of rotator cuff tendon tears is further supported by evidence that some patients have a greater genetic predisposition to the development of rotator cuff tendon pathologies and symptoms thereof, [118, 119] and to earlier disease progression [120].

Alterations in the biochemical environment of torn tendons have been demonstrated. Factors implicated in the pathophysiology of rotator cuff tears include apoptosis genes [121], cytokines [122], oxygen free radicals [123] and growth factors such as TGF-β [124] and matrix metalloproteinases [122]. It has been suggested that tendon tears occur when the healing mechanism within tendons are overwhelmed [85].

1.3.2.4 Changes in Cellularity and Metabolism

Tear propagation may be encouraged by the presence of fewer cells at the edges of tears [125], which have an altered metabolism [126] and are less able to synthesize and degrade the ECM to repair the structural damage. Supraspinatus tendons usually have higher rates of collagen turnover than other tendons such as biceps tendons [64], so any disruption in the turnover is also likely to affect the collagen and proteoglycan content [127].

An increase in inflammatory cells has been noted in small and medium sized tears, compared to larger tears and controls [125]. Rats subjected to overuse activities were found to have hyperplasia and hypertrophy of fibroblasts [128]. Cells within the compressive regions of rotator cuff tendons have been identified which synthesise aggrecan and type II collagen, and as such are interpreted as signs of chondrogenesis [70]. Tenocytes have been shown to be responsive to loads [129]. Chondroplasia has been proposed as an adaptation to hypoxia secondary to compressive loading or overuse [130, 131]. The exact mechanism is unknown, but a higher incidence of chondroplasia has been detected in the articular side of rotator cuff tendon tears, and areas of few fibroblasts [110, 125].

Metabolic changes are thought to occur in conjunction with increasing age. Evidence of decreased protein synthesis was found in older tenocytes, and a greater shift towards anaerobic metabolism with age [132, 133].

1.3.2.5 Extracellular Matrix Changes

Changes within the ECM of rotator cuff tendons have been demonstrated, and may underlie reduced ability to withstand mechanical loads, ultimately increasing the predisposition to tendons rupturing. Torn tendons often heal by forming scar tissue, which initially contains a higher proportion of type III collagen [134, 135]. Type III collagen fibre bundles are smaller and less organized and form fewer cross-links than type I collagen, and this may contribute to the reported reduction in tissue strength seen in torn tendons [136-139]. ECM changes in torn rotator cuff tendons have been demonstrated previously, including increased collagen III, reduced collagen I, altered metalloproteinases and an accumulation of glycosaminoglycans and lipids [140, 141]. Interestingly the total collagen content has not been found to change with age, but did decrease with degeneration [74]. Torn tendons have been shown to have altered chemical compositions with varying levels of proteoglycans [74], glycoproteins [142], atrophy [143] and chondrocyte markers [144].

Remodelling of the tendon ECM has been demonstrated in response to load, ageing and injury [71, 145]. An imbalance in ECM remodelling has been suggested in torn rotator cuff tendons, primarily mediated through changes in expression of matrix metalloproteinases (MMPs) and tissue inhibitors of matrix metalloproteinases (TIMPs) [141]. MMPs are a family of proteoloytic enzymes that can cleave and degrade components of the ECM, particularly collagen. MMPs can be classified into subgroups based upon substrate specificity and cellular localisation: collagenases (e.g. MMP-1, -8, -13), stromelysins (e.g. MMP -3, -10, -11), gelatinases (e.g. MMP-2,- 9) and membrane type MMPs (e.g. MMP 14 to 17, -24, -25). ADAMTs (A Disintegrin And Metalloproteinase with

Thrombospondin Motifs) are proteases that specifically have a metalloproteinase domain and contribute to ECM collagen regulation. ADAMTs have some interactions with various inflammatory processes, for example ADAMTs1 interacts with vascular endothelial growth factor (VEGF), the latter having been implicated in playing a role in angiogenesis and cell migration in rotator cuff tears [146].

Supraspinatus tendinpathy has been shown to result in decreased MMP-3 (stromelysin-1) mRNA expression, and both a decrease and increase in MMP-2 (gelatinase A) [147, 148]. Additionally increases in MMP-1, 9 (gelatinase B) and 13 and TIMP 2, 3 and 4 have been detected in the rotator cuff tendon in naturally occurring tears and following changes in loading [64, 149, 150]. Increased MMP-1 and MMP-13 levels have been measured in synovial fluid taken from shoulders with torn rotator cuff tendons [151]. A study looking at the effect of overstressing and stress deprivation on MMP modulation, found increased MMP-1, -9 and -14 as well as increased ADAMTs-1 in stress deprived tendon areas as well as increased aggrecan [152]. Conversely, overstressing of tendons caused increased MMP-13 and also aggrecan, in ovine supraspinatus models, highlights a correlation between MMPs and mechanical loading. Specifically, MMPs appear to be sensitive to the level of strain, and upregulation of MMP-13 was noted following fatigue loading of rat patellar tendons and cultured tenocytes at 1.7% strain, which resulted in overt microstructural damage [153]. Yet a lower strain rate of 0.6%, which only produced microstructural damage, caused downregulation of MMP-13 and interleukin-1β (IL-1β). Some MMPs appear to be sensitive to both increased and decreased stress levels in rat supraspinatus tendons, with increased expression of MMP -3, -13 and TIMP-2 following stress deprivation caused by detaching tendons from their

insertions. This relationship was much greater in supraspinatus tendons when compared to Achilles tendons. Conversely, intermittent cyclical compression of attached supraspinatus tendons resulted in increased MMP-13 expression in supraspinatus tendons only, and not in the comparator Achilles tendon group. Hence stress deprivation may contribute to the progression of supraspinatus tendinopathy

These ECM related pathways are likely to have important mechanical and healing implications, and as an example inhibition of MMP-13 has been shown to improve histological healing, with improved mechanical healing following doxycycline mediated inhibition [154, 155]. Conversely, quinolone drugs have been proposed to play a role in tendinopathy, via an IL-1β mediated release of MMP-3 [156, 157]. However, another study examining inhibition of matrix metalloproteinases in rat models demonstrated improved histological healing, but interestingly there no difference was found in mechanical properties [158].

Increased amyloid deposition has been reported in chronic rotator cuff tendon tears compared to acute tears, although this may be confounded by the reported correlation with increasing age [159]. Mucoid and lipoid degeneration have been reported in tendons, with accumulation of mucoid patches and vacuoles, and lipid accumulation respectively [60]. Muscle atrophy and fatty infiltration into the muscle have also been demonstrated, and are associated with poorer outcomes following repairs [160, 161]. Increased amyloid deposition has been noted in rotator cuff tendon tears. Cole *et al.*, reported a greater incidence of amyloid deposition in chronic tears (70%) compared to acute tears (25%), although a non-significant correlation with age was noted [162]. Glycosaminoglycans are proposed to play a role in amyloid protein folding, by rendering amyloid

less susceptible to proteolytic degradation. Alterations of this mechanism may contribute to structural disruption and ultimately tendon failure [162].

1.3.2.6 Stress Related Changes

Stress to the tendon can be mechanical but also biological, and oxidative or hypoxic stress can occur following both mechanical and biological insults. Different stress related pathways have been shown to be altered in tendinopathies. One such pathway related to stress involves heat shock proteins, which are thought to protect cells against oxidative induced necrosis or apoptosis and increase tendon healing, as they play a role in assembly, folding and transport of proteins. Heat shock proteins (HSP) also have been shown to activate the innate immune system to induce pro-inflammatory cytokines. HSP-27 in particular inhibits cytochrome C and is throught to prevent cells from undergoing apoptosis. A small microarray study by Murell *et al*., found upregulation of heat shock proteins 27 and 70 following oxidative stress in torn rotator cuff tendons [163]. However these changes are not specific to torn tendons, as increased expression of HSPs was also noted in matched intact supraspinatus samples obtained from the same patients with tears.

A role for abnormal apoptosis has been implicated in rotator cuff tendinopathy. While apoptosis is part of the regulation processes involving normal cell turnover, aberrations can occur. It has been shown that tenocytes from diseased or overused rotator cuff tendons demonstrate features of programmed cell death or apoptosis [126, 164, 165]. Following tendon strain, changes in stress

activated protein kinases can induce apoptosis [165, 166]. Apoptosis has been shown to be increased by cytokines, glucocorticoids, and reactive oxygen species (ROS) [121].

Atrophy related genes have been proposed to play an important role in pathogenesis of chronic rotator cuff tears. Another pathway which has been shown to be altered in rotator cuff tears is related to cell death and cell cycle inhibition, are the transcription factor forkhead (FOX) genes. FOXO changes have been shown to induce muscle atrophy by inducing atrogin-1 and MURF1 genes [143]. Furthermore an effect of tear size has been demonstrated on forkhead related genes. PCR analysis from human rotator cuff tears revealed that FOXO1A was upregulated in massive tears compared to small tears and controls, whereas FOXO3A was downregulated in massive tears [143]. Massive tears were also found to display upregulation of UBE2B and UBE3A, genes related to the ubiquitin-proteosome pathway, which also plays a role in regulating atrophy. Ubiquitination renders myofibrils susceptible to proteosomal degradation.

Hypoxia may also play a role in tendinopathy, either as a causative factor or as an adaptation to injury. A decrease in hypoxia-inducible factor 1 (HIF-1) was measured in rats subjected to overuse. Other apoptotic inhibitors have also been implicated in tendinopathies and include cFLIP receptor and caspase 3 and 8 [121, 167]. Torn rotator cuffs express increased levels of the DNA (deoxyribonucleic acid) repair enzyme Apr/Ref-1, which is thought to signify attempted repair of hypoxia induced DNA or mitochondrial damage [168]. Alterations in nitric oxide synthases and oxygen free radicals following mechanical loading and reperfusion induced ischaemia have also been implicated in the pathogenesis of stress-induced rotator cuff tendinopathies [169] . Increased

expression of the antioxidant peroxiredoxin 5 has been measured in tendinopathy [170], and may play a normal role in protecting against cellular damage.

Increased pro-inflammatory cytokines have also been measured following rotator cuff injury, such as interleukin (IL)-1β, -1α, -1 and -6 and cyclo-oxygenase (COX) -2 and -3 [171, 172].

However neither the extrinsic nor intrinsic theories of aetiology can fully explain rotator cuff tendon tears. Belief in the extrinsic theory alone has been largely superseded, as tears can occur without acromial or other mechanical stresses. It is therefore likely that rotator cuff tendon tears are contributed to by a complex interaction of intrinsic changes resulting in extrinsic contributions. MacGillivray *et al*., have proposed a degeneration-microtrauma model for cuff tearing, that suggests that while tissue injury may initiate tears, susceptible individuals produce a maladaptive response to this injury which results in progression to full-thickness rotator cuff tendon tears (see Figure 1-5) [173].

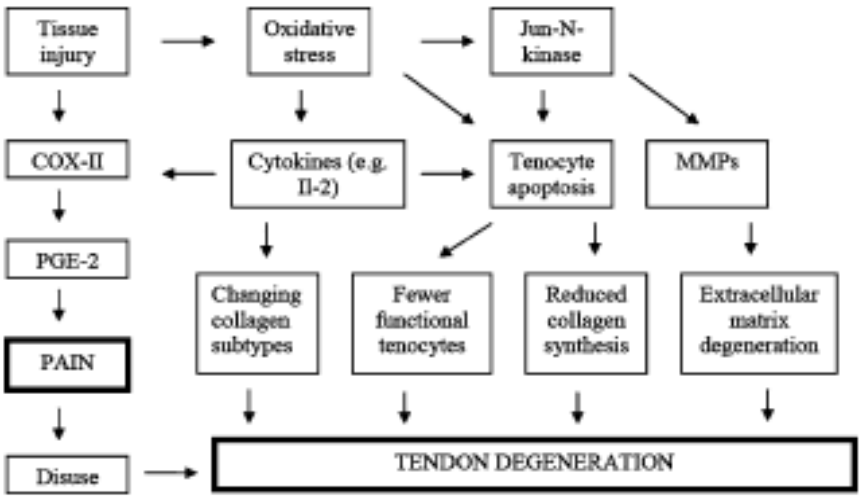

Figure 1-5: A degeneration-microtrauma model for cuff tearing has been proposed by MacGillivray *et al.*, indicating the complex multi-factorial pathways contributing to potential tendon failure. Image taken from MacGillivray *et al.* [173].

At present the aetiology and progression of rotator cuff tendon tears are not fully understood, which may explain why there is currently no definitive or curative treatment.

1.3.2.7 Vascular Changes

Codman proposed that the perfusion of rotator cuff tendons played a significant role in the development of tendon pathology [174]. A few studies have suggested that the supraspinatus tendon has reduced vascularity close to its bony insertion [175]. An avascular zone has been reported approximately 1 cm from the supraspinatus insertion [176], and this area has been termed the 'critical zone' and represents an area of vessel anastomoses [177]. It has been observed that tendon degeneration and rupture often occur at watershed areas, and thus reduced vascularity has been proposed as an important predisposing factor. The supraspinatus tendon most commonly ruptures at or near its insertion into the greater tuberosity, at the so-called critical zone [177]. This under-perfused area was found to be more evident on the articular side of the tendon [178]. The area of avascularity has been proposed to increase with age [179]. A review of randomised clinical trials comparing the use of topical nitroglycerin (GTN) patches to rehabilitation for the treatment of chronic supraspinatus tendinopathy found improved outcomes in terms of patient related pain, increased tendon force measures, functional measures and patient outcome [180].

However theories of hypovascularity causing or contributing to tears has been questioned by studies reporting a hyperaemic response in the tear edges, in both the bursal and articular sides as well as at the distal stump at the insertion site [130, 181]. While the exact mechanism is unclear, the mechanism underpinning the improvement may be vasodilatation.

1.3.3 Imaging of Tears

Plain radiographs of the shoulder are a useful first line investigation as they can help to identify bony abnormalities, arthritic and calcific changes as well as tumours. X-rays have limited diagnostic accuracy for soft tissue conditions such as rotator cuff tears. Ultrasound (USS) is a cheap and rapid modality, which is increasingly performed in outpatient clinics by either radiologists or trained surgeons as part of a 'one stop' clinic. Due to its high accuracy USS is useful in the detection of many soft tissue pathologies of the shoulder [182]. CT scans have some limitations in the detection of soft tissue lesions, particularly partial thickness tears, resulting in less frequent employment of this technique. High accuracy in the detection of rotator cuff tears has been demonstrated with CT arthrography (CTA) [183]. MRI is considered by many as the investigation of choice for rotator cuff lesions [184, 185], and some studies have suggested that MRI is a more accurate diagnostic tool than USS [182, 184]. However a meta-analysis of studies revealed that MRI and USS have comparable sensitivity and specificity for diagnosing both full and partial thickness rotator cuff tears [186]. The same analysis found that MRI arthrography (MRA) MRA had greater sensitivity and specificity for the detection of rotator cuff tears when

compared to USS and MRI. MRA is particularly accurate for diagnosing certain conditions such as partial thickness tears [187]. The disadvantages of MRA are the additional time, expertise required, cost and the need for an intra-articular injection with its associated risk of joint infection. The effectiveness of any imaging modality, particularly MRI, is reduced when the clinical picture and indications are unclear [188, 189]. Due to the high incidence of asymptomatic pathology and risk of both false positive and false negative results with any imaging modality, it is imperative to order investigations appropriately, with clear indications and when the results will alter management.

1.3.4 Management of Tears

1.3.4.1 Conservative Treatment

Regardless of the size of the tear, some cases can be effectively treated with a trial of a combination of advice, exercises, simple analgesics and anti-inflammatory medication [190] as some patients are able to 'compensate' with good active shoulder function, despite a rotator cuff tear [191].

More severe or persistent cases may require physiotherapy or gluococorticoid injections (with or without local anaesthetic). These interventions have variable outcomes in the literature ranging from excellent to no better than placebo. Unfortunately evidence for long lasting benefit from these treatments is weak and repeated use of injections may be harmful.

The evidence for the effectiveness of common conservative treatment strategies, such as oral NSAIDs and glucocorticoid injections, is weak [192, 193] and addresses the pain and inflammation

rather than reversing the underlying pathophysiology. A Cochrane review of steroid injections found that subacromial glucocorticoid injections showed short term benefits over a placebo in some trials, particularly for improving abduction [192]. Glucocorticoid injections were not found to have any advantages over oral NSAIDs [193]. Repetitive injections may be inappropriate as there is an association with cell death [194], inhibition of tenocyte migration and proliferation of synovial fibroblast proliferation [142] as well as slowing of healing [195], which may impair repair. It has been suggested that corticosteroid injections may be detrimental to tendon strength as they damage collagen ultra-structure [74], causing increased collagen disorientation [196] and weaken collagen fibres [197-199], thus increasing the likelihood of rupturing [200]. There have been some reported cases of tendon rupture [194], subacromial joint infections [201] and deleterious effects on glenohumeral cartilage [202] following glucocorticoid injections.

1.3.4.2 Surgical Management of Full Thickness Tears

The intra-articular environment of the damaged tendon often precludes normal healing. If conservative strategies fail after a 3 to 6 month period, then surgery may be considered to restore stability and improve pain and function. The first surgical repair of a rotator cuff tear is reported to have occurred in 1909 [203]. Indications for surgery usually involve sudden onset of severe symptoms and pathology or a combination of failed conservative care, persistent or worsening pain and functional disruption. Despite developments in techniques and repair materials, current surgical treatment strategies are often unsuccessful in the long term. Currently a variety of surgical techniques are undertaken to manage rotator cuff tears such as arthroscopic repair, mini-open repair, open repair (all of which can be done with or without a subacromial decompression) or less

commonly with a biceps tenodesis, debridement, tendon transfer or synthetic grafts. Different repair techniques include a single row medially, a single row laterally, a double row of suture anchors and a double-row transosseous equivalent technique. For both partial thickness and massive tears debridement is sometimes performed. The type of surgery employed will depend not only upon the diagnosis but also upon the patient profile.

While repair of rotator cuff tears is usually advocated for painful tears with functional impairment, some uncertainty exists as to exactly when to operate and what features should guide this decision. Of grave concern is that a large proportion of technically correct surgical repairs re-rupture, with reported failure rates between 13-94% [33-36]. Larger tears seem to be associated with higher incidences of rerupturing [204] irrespective of the surgical technique employed [205]. Higher incidences of rerupturing are associated with larger tears [32, 35, 204, 206] and increasing age [33, 207]. Other factors which have been suggested to influence surgical outcomes include fatty infiltration of the cuff [208-210], and co-morbidities such as smoking [211] and time elapsed before surgery [212].

Rotator cuff tears associated with systemic diseases such as rheumatoid arthritis are an additional surgical challenge [213]. What is surprising is that despite failure of the surgical repair a majority of patients report improved pain levels [32, 205] and satisfaction [205] post-operatively. However, patients whose repairs remain intact do relatively better in terms of function [205] and strength [38] but are no different in terms of pain scores than the re-ruptured group.

Many symptomatic tears respond to non-surgical management [214] and some patients with tears demonstrate marked improvement following arthroscopic subacromial decompression and rotator cuff debridement without cuff repair [215]. An argument in support of repairing tears is that without surgical intervention there is a significant likelihood of tear progression [19] and subacromial decompression alone does not reduce this risk [216]. In cases of massive tear where a complete repair is not possible various strategies including tendon transfers and incorporation of the biceps tendon have been employed but in the absence of any controlled data it is unclear how effective these approaches are [217].

There is currently no evidence proving the superiority of one surgical approach over another [218]. This lack of evidence is reflected in the significant variation in surgical opinion, decision making and treatment strategies used to manage rotator cuff tears [219].

The absence of definitive and reparative treatment requires further investigation into the biology of rotator cuff tears, so that appropriate treatment strategies can be employed. At present the same treatment modalities are often undertaken across the spectrum of rotator cuff tears (i.e. from partial through to massive tears), and it may be that a more in depth understanding of the disease process will reveal that a more tailored treatment approach is required for tears of different sizes.

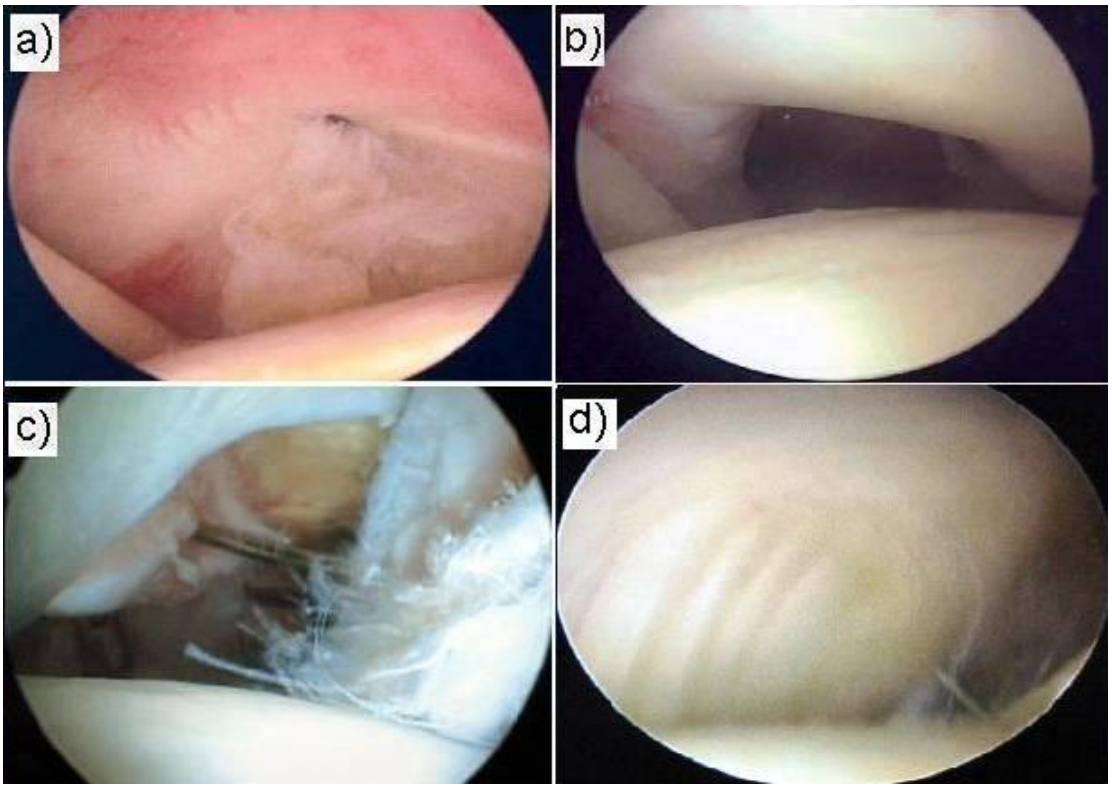

Figure 1-6: Photographs showing rotator cuff tears. a) Small partial thickness rotator cuff tear of the joint surface. b) A medium sized full thickness tear. c) A large full thickness tear with supraspinatus detachment anteriorly, and fraying of the long head of biceps. d) A partial thickness tear of the rotator cuff. Photographs taken during operative procedures at the Nuffield Orthopaedic Centre, Oxford, with permission from patients.

1.3.4.3 Management of Partial Thickness Rotator Cuff Tears

Management of partial thickness rotator cuff tears is a controversial subject without widespread consensus, even though they are more prevalent than full thickness rotator cuff tears [220]. Classically patients were treated conservatively, and if this failed there was a progression to arthroscopic debridement with or without subacromial decompression. There is some uncertainty regarding the risk of progression to full thickness tears. Cordasco *et al.*, [221] demonstrated that

lesions involving less than 50% of the thickness of the cuff did progress in the long term. If symptoms fail to settle with conservative measurements then subacromial decompression may be beneficial. Some favourable results have been reported following debridement of partial thickness tears with subacromial decompression [222] as well as following open repair of partial thickness tears involving >50% of the tendon but no controls were available [223]. Repair of partial thickness tears are also associated with high failure rates, with one series reporting 100% failure [224].

1.3.4.4 Management of Irreparable Rotator Cuff Tears

Tears are deemed irreparable when it is impossible to connect the tendon back to its insertion footprint without unacceptable degrees of tension, or poor tendon quality that prevents purchase of a suture. Goutallier *et al*., have demonstrated that fatty degeneration of infraspinatus or subscapularis muscles is associated with less favourable outcomes after repair [225]. Debridement and subacromial decompression have been reported to improve pain, function [56] and patient satisfaction [226].

1.4 Understanding Tear Size Related Changes in Rotator Cuff Tendons

There is increasing evidence to support the idea of a progressive multistage disease process where small tears have different characteristics to larger tears. There is some evidence to suggest that different sized rotator cuff tears may have different mechanical properties. Rokito *et al*., found a trend between tear size and the recovery of shoulder strength after repair, with large and massive

tears being weaker [227] and taking longer to regain strength compared to small and medium tears [228].

Recent evidence suggests that both the cellular and ECM composition of the torn tendon edge change significantly as the tear size increases [118, 125]. Matthews *et al.*, reported that compared to normal tendons, small rotator cuff tears had an increase in the numbers of inflammatory cells and fibroblasts, which then decreased as tear size increased [125]. Increased chondroplasia was also detected in larger (medium to massive) tears compared to normal controls and small tears [125].

In addition, the metabolism and therefore possibly the viability of tendons, also diminishes as tear size increases [229]. Using a multistage disease model Benson *et al.,* have shown that this apoptotic process progresses as tear size increases, and may be induced by hypoxia [230].

1.5 Scope of this thesis

This thesis aims to address whether there are mechanical and chemical changes in torn human rotator cuff tendon specimens compared to normal intact tendons. Current diagnosis of rotator cuff tears relies solely upon radiographic imaging of tear size, and there are no clinical means for identifying rotator cuff pathologies at an earlier stage or for assessing repair potential. The aims of this thesis are driven by the clinical need to identify rotator cuff tendon abnormalities that may preclude successful healing, with the hope that this information can be used to stratify appropriate

clinical treatment. Understanding the mechanics and biology of human tendon specimens is likely to be key, as animal models cannot accurately and comprehensively replicate the complex anatomy, chronic degeneration and biology that contributes to rotator cuff tendon tears.

As the size of rotator cuff tears correlates with different failure rates, it is possible that there are biomechanical differences between different tear sizes. Hence this thesis sets out to use a multistage disease model to investigate the mechanical, biochemical, structural and genetic properties of rotator cuff tears. It is hoped that by gaining a better understanding of the intrinsic changes seen in rotator cuff tears, it may be possible to identify earlier biomarkers of rotator cuff tear pathologies. This may potentially guide earlier diagnosis of disease, better monitoring of disease progression and response to treatment, and potentially may be used to predict possible treatment or surgical outcomes. Understanding any differences between different tear sizes may offer valuable insight into the pathophysiology of rotator cuff tears, and help to guide clinicians and researchers as to which tendon healing or reparative mechanisms need to be addressed to improve treatment outcomes. It is also hoped that by understanding the mechanisms that underlie failure, treatment of this pathology can be better directed to try to reduce the high failure rates of current surgical repairs. Potentially this study may identify targets for treatments, and parameters of normal rotator cuff tendons that need to be replicated by repair grafts. Thus the study will also encompass an assessment of the mechanical suitability of commercially available repair grafts. This study will focus only on rotator cuff tears, with impingement and other shoulder related problems remaining outside of the scope of this thesis.

1.6 Aims of this thesis

This thesis aims to characterise whether there are differences between normal and torn rotator cuff tendons, and different sized rotator cuff tendon tears. There is a strong clinical need to try to identify patients early who have rotator cuff tendinopathy and a reduced repair potential, so that treatment can be instituted earlier with the aim of obtaining improved clinical outcomes. The motivation for this study is to determine whether different stages of disease can be better distinguished, identified earlier and whether treatment modalities need to be streamlined to particular tear types in a manner that is not routinely practised currently. I shall aim to achieve this by answering a number of questions:

1. Do normal and torn rotator cuff tendons have different mechanical properties, and do different stages of rotator cuff tendon tears have different mechanical properties? Chapter 2 will explore the deformation of normal and different sized human rotator cuff tendon specimens in response to shear forces.

2. Are normal and torn rotator cuff tendons chemically distinguishable, and are different stages of rotator cuff tears chemically distinguishable? Chemical compositional fingerprints will be obtained from normal and different sized rotator cuff tendon tear specimens using Fourier Transform Infrared Spectroscopy (FTIR) in Chapter 3.

3. Do normal and torn rotator cuff tendons have changes in their collagen composition that may affect their thermal properties? Further analysis of the collagen composition and potential

differences in structure will be undertaken in Chapter 4 with differential scanning calorimetry which allows quantification of subtle structural changes in small tendon specimens.

4. Is there a difference in the gene expression profile of normal and torn rotator cuff tendon tears, and different stages of rotator cuff tendon tears? Genetic differences which may underlie different sized rotator cuff tendon tears will be explored using microarray technology in Chapter 5, with RT-PCR and immunohostochemistry to understand changes in gene and protein expression.

5. Do different commercially available rotator cuff repair patches have differences in their mechanical properties and in their suitability to support human rotator cuff tendon repair? Chapter 6 will explore how well the mechanical properties of repair patches are suited to human rotator cuff tendon specimens, by subjecting them to both tensile failure testing, and shear loading using dynamic shear analysis. These parameters will be compared to published values for human rotator cuff tendons and experimentally derived rotator cuff tendon shear values.

Chapter 7 will try to explore the potential implications of the findings of this thesis, and place it into a wider context of understanding the biology behind rotator cuff tendon failure and its relevance for surgical repairs. Many questions have arisen from the work in this manuscript, and future experimental works shall be addressed in Chapter 8.

2 COMPARING THE MECHANICAL PROPERTIES OF NORMAL AND TORN ROTATOR CUFF TENDONS USING TENSILE TESTING

2.1 Abstract

2.1.1 Background

This study aimed to develop a novel method for quantitatively determining any differences in the mechanical properties of healthy intact rotator cuff tendons in comparison to torn tendons. It was hypothesised that intact and torn rotator cuff tendons would have altered structural and mechanical characteristics.

Improved understanding of the biomechanics of rotator cuff tendons may help to reduce the high rerupture rates observed after rotator cuff repairs. This study aims to develop a novel method for quantitatively determining differences in the mechanical properties of healthy and torn rotator cuff tendons. To overcome problems of stress risers at the grip-tendon interface that can obscure mechanical measurements of small tendons, a novel solution of Dynamic Shear Analysis (DSA) is presented. DSA is a form of rheology, and allows the study of material deformation and minimises clamping effects by subjecting samples to oscillatory deformation under compression. The storage modulus of tendons was calculated and used as an indicator of mechanical integrity.

2.1.2 Methods

Rotator cuff tendon specimens were obtained during shoulder surgery from 100 patients. These included 82 tears, which were classified according to the size of the tear and compared to 18 controls matched for age and sex. All 3 mm-sized biopsy samples were subjected to DSA using oscillatory deformation under compression. The storage modulus (G') was calculated and used as an indicator of mechanical integrity.

2.1.3 Results

A number of significant differences between the moduli of normal and diseased rotator cuff tendons were observed. Healthy tendons had a significantly higher modulus than torn tendons, indicating that torn tendons are mechanically weaker than normal tendons ($p = 0.0032$, unpaired t-test). Further analysis of the modulus of different tear sizes showed that normal tendons had a significantly higher mean shear modulus than tendons with massive tears ($p < 0.01$, Bonferroni's multiple comparison test).

2.1.4 Conclusion

This case control study utilised DSA to demonstrate that samples from healthy rotator cuff tendons have a significantly higher modulus than samples taken from torn tendons. DSA allows the determination of shear mechanical properties of small rotator cuff tendon specimens obtained intra-operatively, which may in turn assist treatment decisions and guide surgeons to repairs which

may require further augmentation. This study provides some preliminary insight into the mechanisms that may contribute to high rates of failure of rotator cuff repairs.

2.2 Introduction

Tenocytes from diseased rotator cuff tendons can demonstrate features of programmed cell death or apoptosis [126, 164]. Recent evidence suggests that both the cellular and ECM composition of the torn tendon edge change significantly as the tear size increases [118, 125]. In addition, it has been shown using a multistage disease model that the metabolism, and therefore presumably the viability of tendons, also diminishes as tear size increases [229]. It is yet to be determined whether these affect the mechanical properties. This study aimed to investigate whether the alterations in cellular and ECM changes seen in rotator cuff tendon tears potentially manifested as changes in the mechanical properties of tendons. Improved understanding of the biomechanics of rotator cuff tendons may help reduce high rerupture rates observed after rotator cuff repairs. Hence the purpose of this study was to establish whether the mechanical properties of torn human rotator cuff tendons are distinguishable from normal rotator cuff tendon using small samples that are obtained at surgery.

2.2.1 Hypothesis

It was hypothesised that torn rotator cuff tendons would have reduced mechanical properties compared to normal tendons.

2.2.2 Methods and Materials

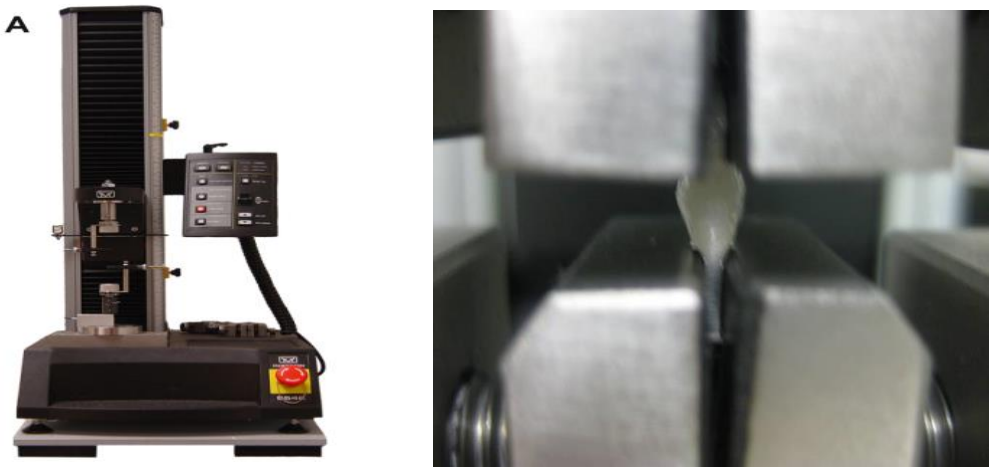

Figure 2-1: A) Photographs of an instron machine used to test tensile properties of rotator cuff tendons. B) Example of a small tendon piece held between 2 large clamps, with only a small testing gauge length.

Human rotator cuff tendon biopsies were obtained prospectively from patients who were undergoing surgical repair of rotator cuff tears. Biopsies were taken from the edge of the rotator cuff tear. Rotator cuff tears were diagnosed pre-operatively with either an ultrasound or a MRI. Matched case-controls were obtained from patients during shoulder hemiarthroplasties or anterior shoulder stabilisations in whom there was no evidence of rotator cuff disease or tears and no evidence of macroscopic damage during surgery. Most specimens were tiny, measuring only a few milimeters in width and diameter, although a small number of larger specimens were obtained, as shown in Figure 2-2. Rotator cuff tendon specimens were collected intraoperatively either from the Nuffield Orthopaedic Centre, ethics number 09/H0606/11 or as part of the national multi-centric UKUFF trial (see appendix 1), ethics number 07/Q1606/49.

Figure 2-2: Figure demonstrating the range of small pieces of rotator cuff biopsies samples taken intraoperatively, which range from 4 mm to 30 mm in width, and 2 to 5 mm in height.

Using both human rotator cuff and bovine tendons, I tried numerous attempts to successfully clamp the small tendon ends so that I could apply a uniaxial tensile load to test the mechanical properties of the tendon, including testing the specimen to failure. A common problem faced when testing the mechanical properties of small tendon samples is that of stress risers at the clamp-tendon interface which can obscure or invalidate measurements [231]. Gripping tendons adequately is an extremely difficult technique, and can alter the tensile properties of tendons [232]. Unfortunately despite several attempts with different methods, I have been unsuccessful in preventing my small tendon specimens from failing at the clamp-tendon interface rather than at the mid-substance of the tendon. I have outlined below a few of the methods attempted:

- Different designed grips, including serrated, straight and curved grips
- Gluing the tendon ends using cyanoacrylate (super-glue)
- Super-gluing the tendon ends and then applying sandpaper to improve grip

- Using cryoclamps, where the clamp and the end of the tendon were immersed in liquid nitrogen

- Embedding the ends in epoxy (araldite) and embedding within plastic holders (See Figure 2-3)

- Embedding the tendon in a collagen matrix (See Figure 2-3).

Successful tensile testing has previously been achieved using cryoclamps [233, 234], although the freezing clamp environment does not replicate the physiological state. Another reported technique involved air-drying the tendon ends to be clamped, while wrapping the rest of the tendon in a saline soaked tissue [235]. It is important to realise that no current clamping method is ideal or without problems. Any form of clamping will crush tendon ends and concentrate stress at the clamp-tendon interface. Many mechanical studies of tendon have involved freezing and then thawing tendons, but questions about the effects of this have been raised by some studies which found that freezing/thawing alters the mechanical properties and reduces Young's modulus [236-240]. However other studies have not shown any effect of freezing on mechanical properties [241, 242].

Figure 2-3: Some of the different modalities tried to clamp tendons. A) using sandpaper with differing coarseness B) encased within plastic holders and araldite C) embedded within a collagen matrix

2.2.3 Results

Various experimental settings were tried, such as changing the load cell to generate more force (see Figure 2-4), and altering gripping conditions. Unfortunately all attempts to grip the tendons were unsuccessful. Below is included an example of results from a tensile testing experiment, using sandpaper and superglue to grip the tendon edges (see Figure 2-5). Slippage of the tendon from the grip was noted in repeat experiments, rendering this technique unsuitable for obtaining consistent tensile failure results.

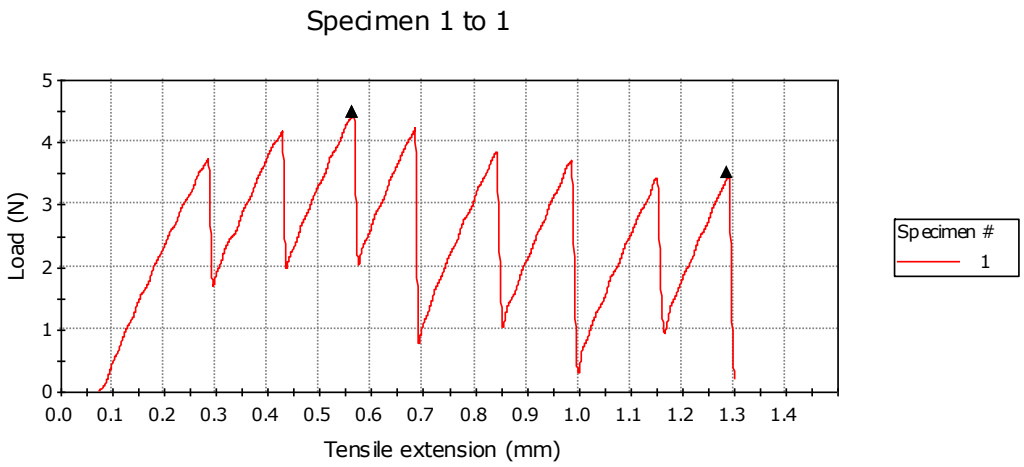

Figure 2-4: Using a 5N load cell, the irregular result demonstrate that the samples were slipping and this load cell was too small, as the 5N maximum kept being approached during tensile extension of the tendon. Thus a load cell with a larger capacity was required, and a 500N load cell was used.

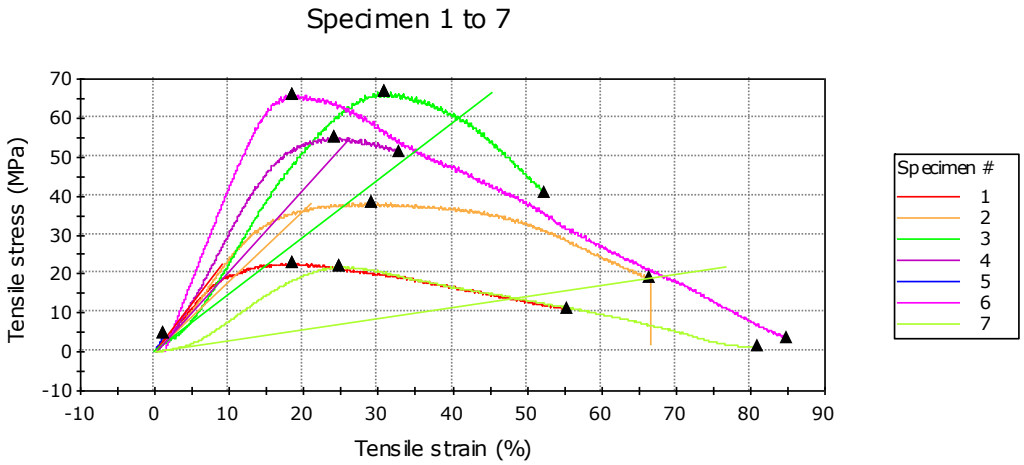

Figure 2-5: A stress strain graph showing tensile testing of supraspinatus tendon using a 500N load cell. The different specimen numbers represent different failed gripping techniques, such as gripping with sandpaper and superglue. Slippage of the tendon from the clamp occurred prior to any tendon midsubstance failure.

2.3 Comparing the mechanical properties of normal and torn rotator cuff tendons using dynamic shear analysis

2.3.1 Introduction

A major problem which prevents the tensile mechanical testing of small tendon samples is that of stress risers at the clamp-tendon interface which can obscure or invalidate measurements [231, 243]. Despite a wide body of literature and experience of tensile testing, to my knowledge there have been no studies comparing the tensile properties of normal and torn human rotator cuff tendons obtained intra-operatively due to the technical difficulties encountered with tensile testing of such surgical specimens. To obtain a comprehensive understanding of rotator cuff mechanics, it is important to appreciate that addition to tensile forces, shear forces are also important in the load bearing environment of the normal and diseased rotator cuff tendon.

The shoulder is subject to multi-directional forces involving shear and compression during the wide range of complex shoulder joint movements [244-248]. In addition to uniaxial tensile testing, shear analysis is highly relevant as rotator cuff tendons are structurally inhomogenous [40] anisotropic [171] materials which are affected by the direction of mechanical loading. During different shoulder movements it is likely that the rotator cuff tendons undergo a combination of tensile and shear loading. The region-specific changes in mechanical properties have been demonstrated in many studies that show a non-linear response to loading. A higher modulus of elasticity, strain to yield point and higher ultimate strain were detected on the joint side compared

to the bursal side, and as such it has been proposed that the joint (or articular) side is more prone to rupturing [52, 234, 249]. Mechanical differences have also been detected in the anterior-posterior direction, with higher mechanical values measured in anterior portions of the tendon (modulus, failure load, and failure stress), and mechanical properties are also affected by changes in arm position [50, 234]. Evidence of differences in the compressive stiffness of supraspinatus have also been presented between the bursal and articular sides [250]. Greater strains have been demonstrated near the tendon insertion compared to the mid-tendon and tendon-muscle junctions [234]. The magnitude of the strain has been shown to differ across the thickness of the tendon [251].

Reilly *et al.*, have proposed that shearing forces cause an intratendinous delamination, which results in increasing tendon strain and ultimate propagation into a full thickness tear [102]. Studies have shown that humeral elevation and joint angle alter not only the location of tear initiation and intratendinous strain [176] but also result in differences in strain between the articular and bursal surfaces [234]. The angle of abduction has been shown to alter the tension in repairs of small tears [252]. Interestingly, significant differences in strains placed on small rotator cuff tendon repairs only became apparent at certain glenohumeral abduction angles [253], however there was no significant difference in strains for repairs of large tears.

Newer methods to characterise the mechanical properties of tissue samples have included atomic force microscopy [254], nanoindentation [255] and elastography [256]. Both atomic force microscopy and nanoindentation provide high resolution information about the material properties of individual collagen fibres. However a technique which provided gross material properties of

the entire tendon specimens was required to meet my aims. Elastography provides useful information about stiffness in particular, but a more global assessment of mechanical parameters was desirable for this study. Therefore a different approach for characterising tendon specimens was undertaken.

2.3.1.1 Dynamic Shear Analysis

To overcome the problem of gripping, dynamic shear analysis (DSA) was developed, which is a relevant technique for studying heterogenous materials and avoids clamping artefacts. DSA is based on rheometry, the study of flow and deformation of matter whereby samples are measured for their response to a shearing (side-to-side) mechanical stress. Rheology is derived from the Greek work *Rhea*, meaning to flow. The concept of rheology was first introduced by the philosopher Simplicius, who stated '*panta rei*', which means 'everything flows' [257]. All solids have been shown to flow given enough time and/or force, even mountains. Different materials flow and deform differently in response to such stresses; a spoonful of mayonnaise spreads easily but leaves an indentation within the jar, whereas a spoonful of honey does not spread as easily but there is no residual indentation thus giving significant insights into their mechanical properties. Samples classically respond to deformation in two ways; either as an elastic, where stress is independent of strain or in a viscous manner, where strain is proportional to the rate of strain but independent of the stress [258]. However most biological materials respond to deformation in a non-linear or viscoleastic manner. Performing DSA on tendons allows us to calculate the bulk storage modulus (G′) [259] of tendons which in turn provides an overall indicator of mechanical integrity. Rheology has been used to characterise the shear properties of many biological tissues

such as cartilage [260], vocal chords [52] and fibrotic livers [261]. Fibrotic liver was shown to be 3 times stiffer than healthy liver, and it was proposed that this assessment could help to guide the extent of surgical resection intraoperatively.

The novel technique of DSA enables the study of small human tendon specimens, and thus provides the potential for further investigation of the role of mechanical properties in understanding the disease mechanisms underlying rotator cuff tendon tears and failure to heal post-operatively, as well as predicting the success of surgery. Understanding the mechanical properties of the tissue adjacent to a tear edge may provide insight which could help to identify tears which are likely to propagate or re-rupture, thus affecting clinical treatment.

2.3.2 Hypothesis

Working from a null-hypothesis of no discernible differences, it was nevertheless expected that torn rotator cuff tendons would have altered structural and mechanical characteristics compared to normal tendons.

2.3.3 Methods and Materials

2.3.3.1 Patients and Specimen Collection

Rotator cuff tendon biopsies were obtained during open surgical repair of rotator cuff tears in a prospective case-controlled, cross-sectional and non-randomized study. Rotator cuff tears were

diagnosed pre-operatively with ultrasound. Exclusion criteria included patients who had previously had surgery of their shoulder, or connective tissue disorders, or osteoarthritis, or rheumatoid arthritis of the shoulder. 82 chronic full-thickness biopsies were taken from the anterior edge of articular sided rotator cuff tears (aged 47-83 years, mean age of 65.2 years). The size of the tear was measured intra-operatively and classified according to size as small, medium, large and massive as per Post *et al's.*, classification [79]. Matched case-controls were obtained from patients aged 20 to 89 (n = 18, mean age 58.8 years, 9 males and 9 females) during shoulder hemiarthroplasties or anterior shoulder stabilisations in whom there was no history of rotator cuff problems, and intra-operatively no visual evidence of rotator cuff disease or tears as their tendons appeared grossly normal. Specimens were obtained both from the local hospital, Nuffield Orthopaedic Centre, Oxford, and from a national multi-centre trial, UKUFF, which aims to measure the clinical and cost effectiveness of different types of rotator cuff repairs (see Appendices for details). Ethical approval was obtained for this study, and fully informed consent was obtained from all patients enrolled in this study

Tendon specimens were immediately preserved in 10% formalin and stored at room temperature. Initially there was a concern that formalin fixation of specimens may alter the mechanical properties. However as all tendon specimens underwent the same fixation protocol, any effects should be uniformly present amongst all specimens. Also the aim of this study was to look for relative differences between normal and torn tendons, and different diseased states. Two separate 3 mm circular biopsies were taken from each specimen.

2.3.3.2 Rheological Assessment

A Bohlin Gemini 200 HR Nano rheometer (Malvern Instruments, Worcestershire, UK) was used (see Figure 2-6).

Figure 2-6: Photographs of a rheometer used to test shear properties of rotator cuff tendons. Small 3mm biopsies are tested between two parallel plates.

Two readings using separate 3 mm biopsy samples were taken from each tendon specimen and valid results averaged. The samples were loaded between two parallel plates, in the centre of the plate, within an environmental chamber kept at 37ºC and 100% humidity to avoid drying out (see Figure 2-6). The environmental chamber was filled with wet tissue around the measuring geometry to ensure that the samples did not dry out. Three modes of deformation can be applied using dynamic shear analysis: oscillation, shear and extensional flow. This study focused on oscillatory tests as they are non-destructive, as a sinusoidal strain is applied to samples at a fixed frequency within the linear viscoelastic region of the specimen. Previous studies have also shown the importance of testing tendons in subfailure ranges which are consistent with *in-vivo* loading, rather than just focusing on the linear region of loading and at failure [262]. The upper plate moves

sinusoidally between a fixed strain and a force is transmitted through the samples, and the stress response from the tendon samples is recorded over a range of frequencies (ω).

Placing a sinusoidal strain on a linear viscoelastic material results in a sinusoidal stress at the same frequency, but will be phase shifted ahead by an angle δ (see Figure 2-7). The resulting strain peak (γ0), stress peak (σ0) and difference in phase (δ) were measured for each frequency. The stress-strain relationship can be represented as having a component in phase with the strain (representing the elasticity) and a component 90^{o} out of phase with the strain (representing the viscosity) [263]. These values were used to calculate the complex modulus (G*), which can be divided into the elastic (storage) modulus and loss modulus. The elastic (storage) modulus (G′) represents the amount of energy stored within the sample during the strain cycle (see Figure 2-7). The loss modulus (G") can also be calculated, and represents the amount of energy dissipated through friction during the strain cycle, but the loss modulus is assumed to be negligible for tendon as it an elastic solid with no significant viscosity.

2.3.3.2.1 Establishing Test Parameters

It was important to establish the linear viscoelastic region (LVR) as this is the region of strain where samples respond elastically and thus return to their original material properties at the start of the experiment without sustaining destructive damage. During a pilot study, 3 mm circular tendon biopsies were subjected to increasing oscillatory strains at a fixed frequency, and the modulus response was measured to ensure that it remained linear, and there was no change in the G' values. As the LVR is frequency dependent, a frequency sweep was performed, and strain was

applied to tendon specimens over a range of frequencies 100, 50, 10, 1 and 0.1 Hz. To try to avoid the possibility of specimen damage, the lowest strain from which consistent modulus readings were obtained within the LVR was used (0.001). Additionally in order to minimise any damage induced through loading/unloading specimens were only tested once. Prior to the study, the criteria for valid modulus readings were set as a) a thrust of approximately 20 g and b) approximately a 1mm gap between the two parallel plates within which the tendon was compressed. A target strain of 20g ensured that tendon specimens did not slip between the plates. Samples were subjected to a standard oscillatory test (0.623 - 39.6 rad/s, 0.001 strain) (see Figure 2-7). Zhu *et al.,* have suggested that the physiological range of frequencies is 0.01-20 Hz [260]. Hence the average storage modulus across all frequencies was used to indicate the mechanical integrity of tendons. The observer was blinded to the size of the tear in this comparative case control study.

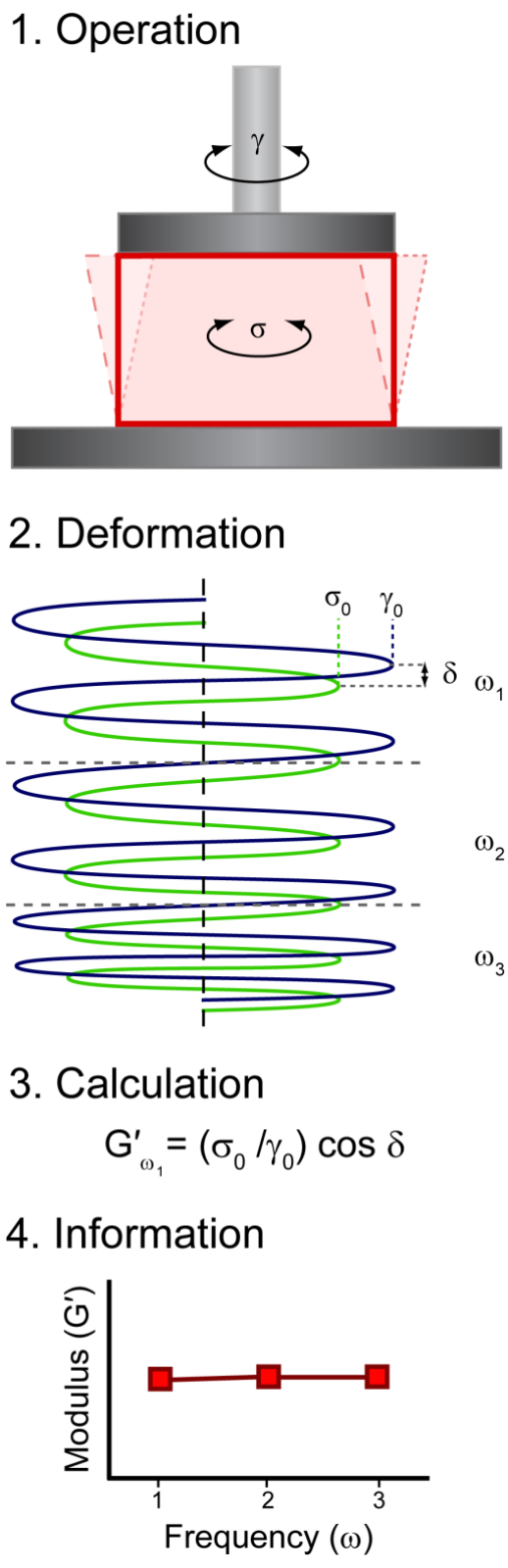

Figure 2-7: Introducing Dynamic Shear Analysis as a means for testing small tendon samples. Step 1, Operation; samples are compressed to a known force between two parallel plates in which the upper plate moves at a fixed strain and records the stress response. Step 2, Deformation; samples are subjected to a sinusoidal strain wave over a range of frequencies (ω). The resulting strain peak (γ0), stress peak (σ0) and difference in phase (δ) are measured for each frequency. Step 3, Calculation; these values are used to calculate the elastic (storage) modulus G′. Step 4, Information; the average values of the modulus readings are then used as an indicator of the mechanical integrity of the tendon. Figure produced with permission from Chris Holland.

2.3.3.2.2 Establishing Test to Test Variability

In order to assess the reproducibility of the measurements, a study was performed to assess the test-retest variability. Three millimetre circular biopsies from 7 human rotator cuff tendon specimens were preserved in formalin, and tested to measure the shear storage modulus, G'. The same specimens were then retested a week later. As shear testing occurs at sub-failure strains, it was assumed that no damage had occurred to the tendon during the initial testing. It is possible that some damage may have occurred during loading of specimens, although due care was taken to avoid this. The test-retest variability found that the correlation coefficient was 0.78 and the error standard deviation was 3202.8 Pa. The variability between the two measurements was small, but useful to know prior to interpretation of any actual test data.

2.3.3.3 Influence of Preoperative Factors

In order to verify that the changes were related to the presence of a tear and the extent of a tear, it was necessary to determine whether there were additional associations with tendon modulus, which may have been confounding variables. Possible effects of age, sex, hand dominance and length of formalin preservation were also studied (see Table 2-1 which provides details about preoperative factors).

Table 2-1: Table showing the categories of specimens tested (n=100), with illustration of some preoperative variables such as age, gender, hand dominance and length of preservation in formalin.

	Normal	All Tears Combined	Small	Medium	Large	Massive
Size of Tear	-	-	< 1cm	1-3cm	>3-5cm	>5cm
Number of Patients (n)	18	82	18	24	21	19
Average Age (years)	58.8	65.2	65.7	64.5	64.3	66.4
Female:Male (n)	9:9	31:51	6:12	11:13	9:12	5:14
Dominant:Non-dominant (n)	12:6	59:23	11:7	21:3	14:7	13:6
Average Time in Formalin (weeks)	7	7	6	7	8	7

2.3.3.4 Effect of Formalin Preservation

As the specimens were preserved in formalin for different lengths of time it was necessary to determine whether such storage may have confounded any of the results by causing a time related alteration of the material stiffness.

The actual effect of preservation in formalin also needed to be addressed. Tendons were collected from seven different ovine and bovine sources. From the same piece of animal tendon, two 3 mm circular biopsies were taken. One fresh specimen was tested fresh. It was then placed in formalin

for a week and the storage modulus was reassessed. The two values were then compared to look for any significant differences between the two groups.

2.3.3.5 Comparison of DSA to Tensile Mechanical Properties

As the traditional method of determining tendon mechanical properties is to assess tensile properties, I performed a preliminary study to compare shear and tensile test parameters from the same specimens. To assess whether DSA was sensitive enough to determine differences between tendons with different mechanical properties, tendons from different sources and locations were obtained: from human (Achilles), bovine (Achilles, superficial and deep flexor) and porcine tendons (Achilles). Six separate specimens from each different source were taken. The specimens were tested to determine the storage modulus, as described above, and the initial modulus (Young's modulus) was measured as an indicator of tensile parameters. The initial modulus was chosen as a relevant comparator as the DSA was also performed in the subfailure region of tendon mechanical properties. Strips of tendons measuring 2 mm in width and 2 mm in thickness were taken, with a length of 30 mm and a gauge length of 15 mm. Tests were performed at room temperature, using an Instron 5542 machine (Instron, Massachusetts, USA) fitted with a 500 N load cell (Honeywell Sensotec, Ohio, USA). To overcome stress-risers or failure at the clamp-tendon interface, a notch was created at the centre of the tendon resulting in a 1mm central width to encourage mid-tendon failure. Samples were tested at a rate of 10 mm/min until failure. Tendons are frequently preconditioned using cyclical loading patterns prior to testing to regulate any viscoelastic effects during specimen loading. However I was unable to precondition my specimens as the Instron 5542 used did not have the appropriate programme to allow this.

2.3.3.6 Statistical Methods

A pre-study power calculation indicated that 17 specimens per tear type were needed in order to detect an effect size of 1 standard deviation with a certainty of 90% (power, 0.9), and a 5% level of error (alpha < 0.05). An unpaired t-test was used to search for differences between normal and torn tendons. Further examination to determine the effect of tear size on modulus was performed using a one-way ANOVA. A Bonferroni multiple comparison test was used to compare individual tear classes and to account for a possible type-I error associated with multiple statistical tests. Bartlett's test for equal variances was also performed. The effect of gender and hand dominance was studied with unpaired t-tests. Correlation studies looking for an association between the modulus and a particular variable, such as age and length of preservation in formalin, were analysed with a Pearson rank correlation. All tests were two tailed and a $p < 0.05$ and alpha < 0.05 were considered significant. GraphPad Prism 5 software was used (GraphPad Software Inc, La Holla, CA).

2.3.4 Results

2.3.4.1 Effect of Tears

A significant difference was detected between normal and torn rotator cuff tendons (see Figure 2-8), demonstrating that healthy tendons had a higher modulus and thus greater mechanical

integrity than torn tendons (unpaired t-test, p = 0.032).

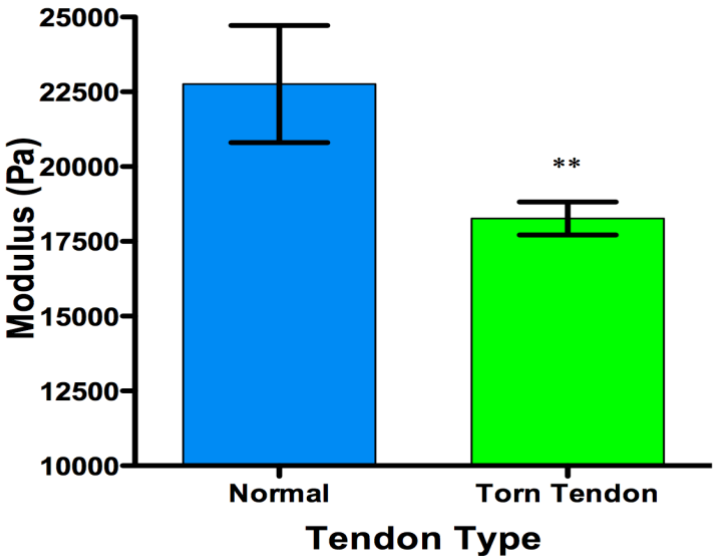

Figure 2-8: Comparison of the storage modulus of normal and torn tendons. Torn tendons have a significantly lower modulus, unpaired t-test p=0.0322, indicating that torn tendons are less stiff. ** p< 0.05. Bars represent standard error.

To further study the effect of rotator cuff tears on tendon modulus, I analysed the data looking at each tear size category as separate groups. Tears were grouped into small, medium, large and massive (see Figure 2-9). Differences between the five groups were found to be statistically significant (p = 0.003, one-way ANOVA analysis). The five individual groups were compared to one another and the only significant paired-differences detected showed that the moduli of normal tendons were significantly higher than those of small and massive tears (p <0.01, Bonferroni's multiple comparison test). Hence normal healthy tendon samples possessed statistically greater mechanical integrity than those from tendons with small and massive tears. A negative trend was

apparent, with a decrease in the modulus as the size of the tendon tears increased, but this relationship was not significant at r = -0.698 (p = 0.189).

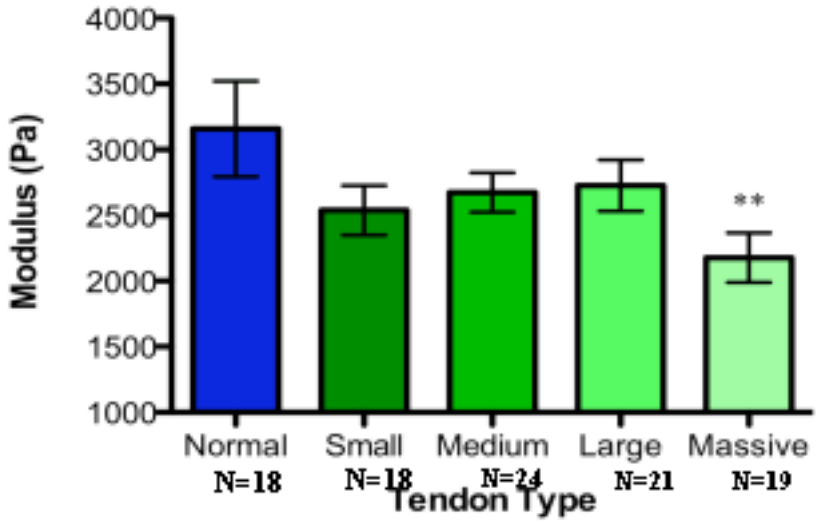

Figure 2-9: A graph looking at the specific effect of tendon tear size on storage modulus. There was a significant difference between the groups (p=0.003, one-way ANOVA). Small and massive tendons had a lower storage modulus (Pa) compared to normal tendons. **p < 0.01. Bars represent standard error.

2.3.4.2 Influence of Preoperative Factors

Looking at Table 2-1, there is no obvious difference between the four surgical groups for age, gender or hand dominance. The scatter of the data shows that there is no significant correlation between age and modulus (see Figure 2-10, r = 0.020, p = 0.846, alpha >0.05). However this study was not powered to detect an effect of age on modulus. Nor did gender have any obvious correlation with modulus (p = 0.651, unpaired t-test) as no difference was seen between the male

and female groups (see Figure 2-10). Interestingly, neither did hand dominance seem to have any effect on the mechanical integrity of rotator cuff tendons. For all patients it was determined whether the operated shoulder was on the same side as their dominant hand. A plot of average valid modulus versus dominant and non-dominant hand (see Figure 2-10) did not reveal any association ($p = 0.891$, unpaired t-test).

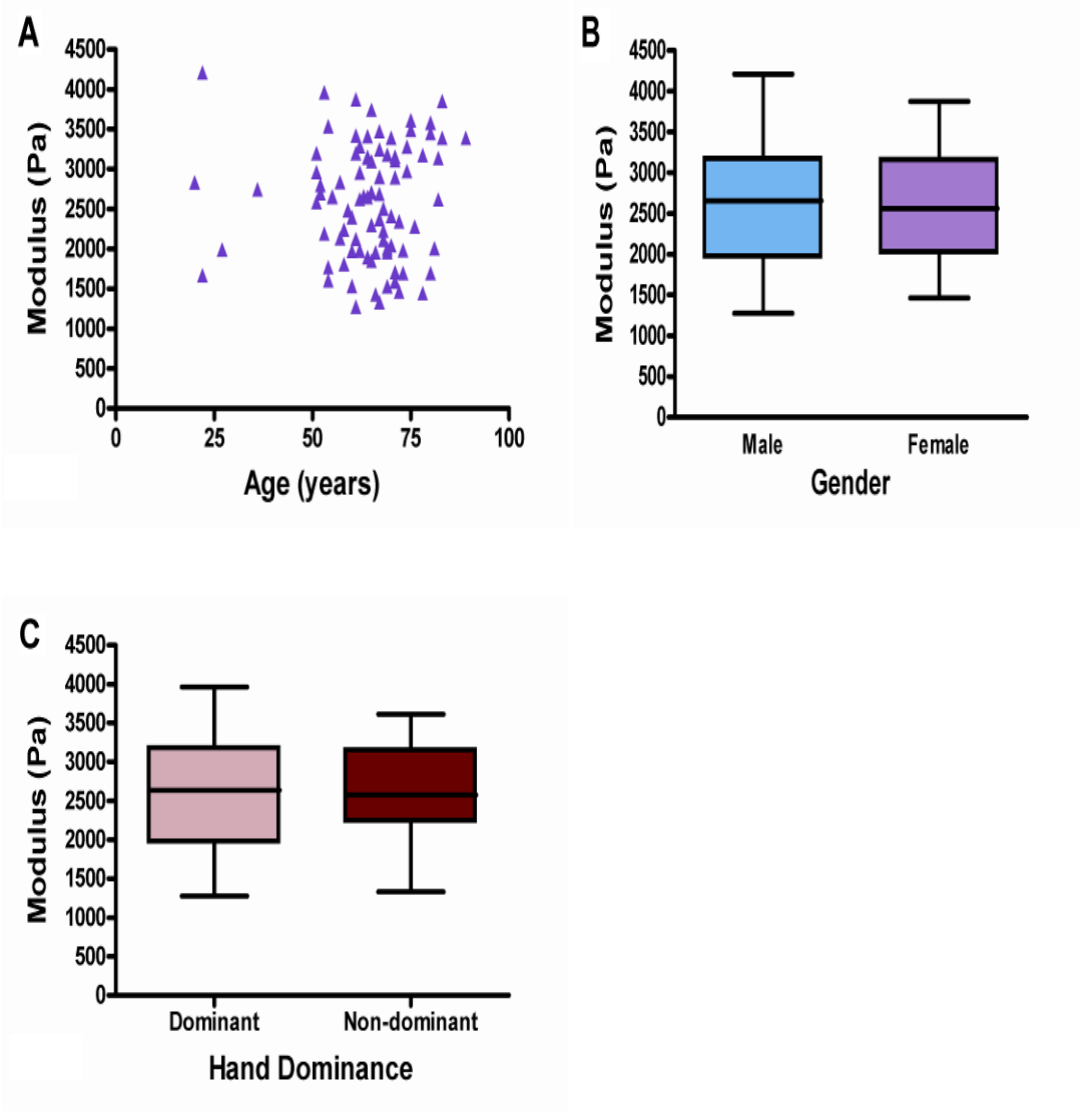

Figure 2-10:Influence of preoperative factors on modulus. A) Age, B) Gender, C) Hand Dominance. Rotator cuff tendon modulus was unaffected by age of patient (p=0.364, Pearson correlation), gender (p=0.493, unpaired t-test) or hand dominance (p=0.4116, unpaired t-test). Bars represent standard error.

2.3.4.3 Effect of formalin preservation

It was important to assess whether formalin preservation may have influenced the mechanical differences detected in this study. Specimens had been preserved in formalin for different periods of time, however no significant effect of length of formalin preservation on tendon modulus was seen ($p = 0.089$, see Figure 2-11). To determine the overall effect of formalin preservation, a separate study was performed on bovine flexor tendons to compare the shear modulus of fresh tendons and formalin preserved tendons. There was no significant difference between the shear modulus of fresh and formalin fixed specimens ($p = 0.38$, paired t-test, see Figure 2-11). There was good correlation between the modulus of the 2 groups (the correlation coefficient, $r = 0.75$, p-value = 0.03, and the error standard deviation was 1154.2 Pa).

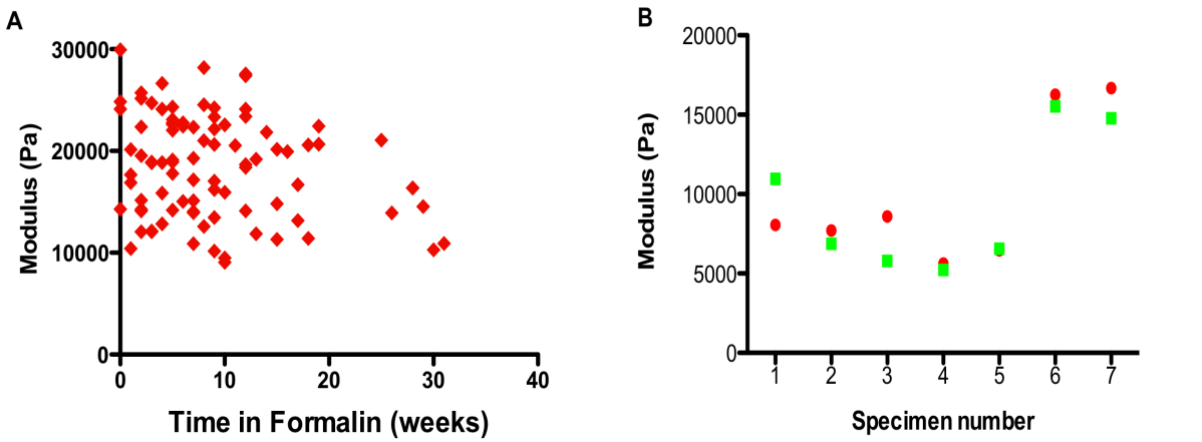

Figure 2-11: A) Graph showing that length of preservation in formalin has no effect on modulus (p=0.123, Pearson correlation). B) Graph comparing fresh tissue to formalin preserved tissue (p=0.279, paired t-test). There was no significant difference in the modulus of fresh (red circle) bovine tendons compared to the same specimens preserved in formalin (green square).

2.3.5 Comparison of DSA to Tensile Mechanical Properties

A positive correlation between the shear properties (as measured by the storage modulus) and Young's tensile modulus is apparent ($r = 0.6$, $p = 0.102$), but this was just outside of the significant range (see Figure 2-12).

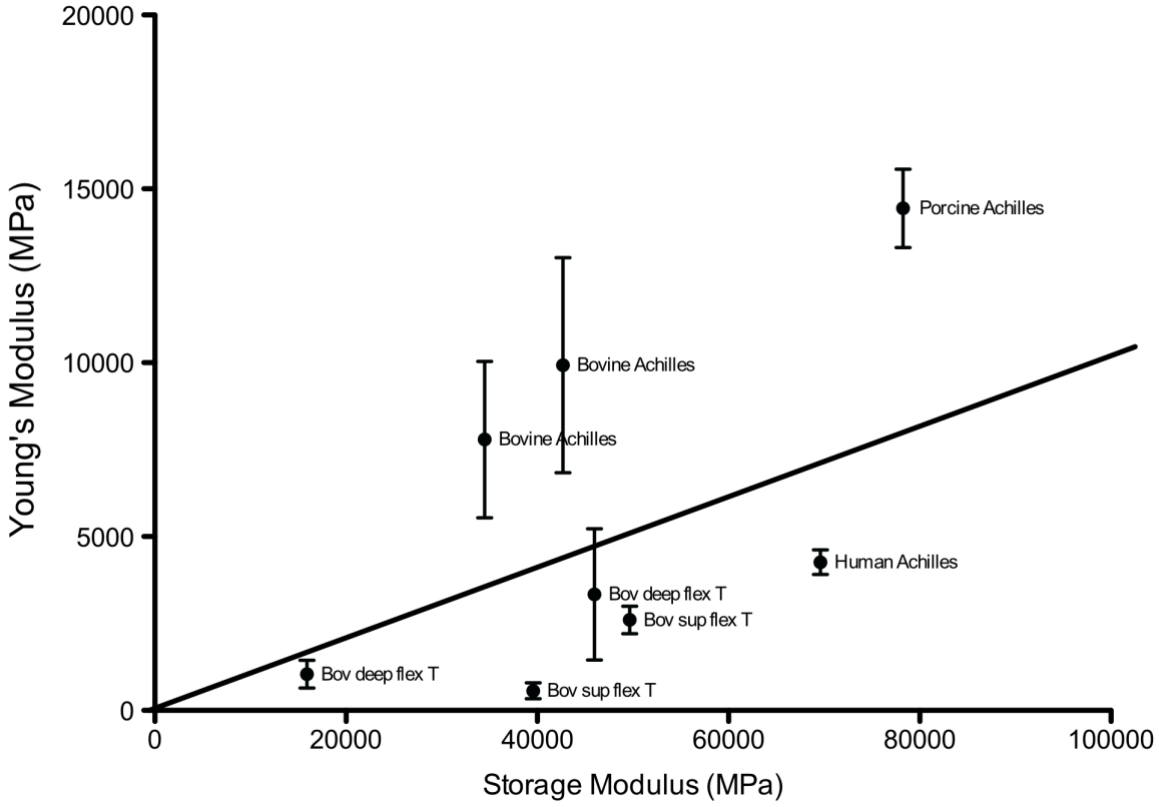

Figure 2-12: Graph comparing shear parameters (the storage modulus) to tensile parameters (Young's modulus). Repeated tendon measurements were taken from different sources: human Achilles, porcine Achilles, bovine superficial and deep flexors and bovine Achilles tendons. While there was a positive correlation between the two parameters (r = 0.6), but this was not significant (p > 0.05).

2.3.6 Discussion

This study demonstrated that normal rotator cuff tendons have a significantly higher shear modulus than torn rotator cuff tendons, indicating that torn tendons have lower mechanical integrity (unpaired t-test, p=0.0032). Ruptured tendons have been shown to have a very high proportion of degenerative change [61], which may translate to structural weakening of the

tendon tissue. The finding that torn tendons are have less mechanical integrity compared to normal tendons is important and offers potential insight into high post operative failure rates. Excessive compression of tissue has been shown to induce fibro-cartilagenous changes within supraspinatous tendon [74] which may not be able to withstand loading as well as intact tendons. Alternatively, tendon tears may heal via scar tissue formation [264] that is mechanically inferior to intact tendons. If the repair construct is formed amongst tissue at the edge of rotator cuff tears that has a lower modulus of elasticity, it is possible that this tissue may have a reduced capacity to withstand the strain and mechanical loading which may be placed upon the repair. There is limited literature confirming that naturally torn human rotator cuff tendons are in fact weaker.

This study further demonstrated a trend between increasing tear size and decreasing mechanical integrity, although it was not statistically significant ($r = -0.698$, $p = 0.189$). This is a novel observation as an effect of tear size has been previously seen in physiological and healing studies [125] but not in mechanical studies of rotator cuff tears. The only individual paired difference detected was that massive tears were found to be significantly less stiff than normal tendons ($p<0.01$, Bonferroni's multiple test). A number of studies have indicated that larger tears are more likely to re-rupture [35, 114, 205, 265, 266]. Cofield *et al.,* [267] have reported that tear size was the most important determinant of post-operative strength. Smaller tendon tear edges have higher reported metabolic rates and cellular activity compared to larger tears [125]. Higher healing rates have also been found is small tears, which could thus provide greater structural and mechanical integrity [208]. Interestingly, it was observed that a reduced storage modulus is apparent even in small tears, suggest that all torn tendons have reduced mechanical integrity, even though this did

not reach statistical significance with the small sample size. It is possible that any insult to the tendon occurs early, even with small tears, which is why the reduction in mechanical properties was apparent. Significant variability of modulus was found in all tear size groups. This may explain why some small and medium sized tears re-rupture after repair despite having better viability than massive tears [21]. Despite our large study size, by subdividing the tears into individual tear sized groups the sample numbers may have been inadequate to detect a difference between the different tear groups, and larger sample sizes may have revealed more mechanical differences between the various groups. The lack of detected difference may also be due to variability within this technique, although the repeatability of the test values was significantly high. While all 'normal' tendons were macroscopically normal, ideally preoperative radiographic imaging could have been employed to confirm the absence of any tears. More longitudinal data is needed to understand the rate of progression for different sized tears, however this study is cross sectional and only offers insight into one time point.

Although increasing age associated with higher failure rates post-operatively [194], an effect of age on the modulus of tendons was not demonstrated. No effect of age was also observed by Fukuda *et al.,* [268] but these findings contradict an earlier study by Reeves *et al.,* [269] suggesting that the tensile strength of anterior capsular structures weakens with age. This study was inadequately powered to detect any subtle effects of age or the other preoperative factors, as this was not the focus of this study. As the incidence of rotator cuff tendon tears increases with age [21], it is difficult to find tears or age-matched controls over a wide range of ages to accurately address this question. This study offers a unique assessment of human diseased tissue taken intra-

operatively from different stages of rotator cuff pathology. To date the majority of mechanical testing of rotator cuff tendons has relied on animal models or human cadavers, which may not directly transfer to human rotator cuff tendons. The anatomy, structure and mechanics are different in quadruped animals compared to bipedal humans. The degenerative and biological changes preceding the majority of tears, and the response following tears is a critical element in healing and tear propagation, and artificially created tears in *ex-vivo* tendons may not replicate these important parameters.

Developing an analytical technique that uses small tendon samples that are ethically imposed, is critical in achieving our stated aim of understanding human disease. Using a rheometer (instead of the traditional tensile-tester) minimised clamping effects by subjecting samples to oscillatory deformation under compression. Due to specimen size limitations, it is extremely difficult to test them under tension, which is why this type of study has so far never been performed on human intraoperative specimens. Indeed the supposed 'gold standard' of tensile testing can have surprisingly wide variation depending upon the method of gripping. This is due to the difficulty of achieving a uniform and effective grip on the collection of the partially independent sub-fibres, and any failure of gripping will result in a decrease of measured stiffness and strength [270]. DSA may be an answer to this problem. This is the first time, to my knowledge, that rheometry has been deployed in the characterisation of small tendon samples and hence DSA can be utilized as a novel and rapid method for assessing the shear mechanical properties of small tissue samples. DSA techniques could potentially be extended to study other soft tissue models. DSA provides data on relative differences in very small tendon specimens rather than absolute values. While the

type of shear used in this study is a relevant model, it cannot comprehensively simulate the complex biomechanics of the shoulder. However the aim of this study was to establish relative differences between different groups, which DSA permits.

Characterising the shear modulus of rotator cuff tendons is highly relevant as the shoulder is a complex joint subjected to multiple forces including shear. Rotator cuff tendons display anisotropy and region specific mechanical variations, with anterior supraspinatus strips demonstrating a higher ultimate load and stress [234, 271]. This study was designed only to test shear responses and does not quantify uniaxial tensile properties, which are the predominant strain pattern seen in shoulders. However shear properties are related to tensile properties and studies of numerous heterogenous anisotropic materials have demonstrated that tensile properties are related to shear mechcanical parameters such as shear modulus and bulk modulus [53]. Previous studies have also shown the importance of testing tendons in subfailure ranges which are consistent with *in-vivo* loading, as done in this study, rather than just focusing on the linear region of loading and at failure [262].

Importantly the collection of such a large number of human specimens for mechanical testing of rotator cuff tendons has never been performed before. To overcome logistical difficulties in collecting specimens from different locations and timepoints, it was necessary to immediately place specimens in formalin, in order to ensure that all specimens underwent the same handling and storage conditions, and hence could be tested in uniform conditions. It was assumed that any effect of formalin will be uniform across all specimens as all tendon samples were subjected to the same storage conditions, and hence any differences between samples will be inherent to their

material properties and not their preparation. While fixation of tissues prior to testing is not the standard, it has been shown there was no effect of the time spent in formalin ($P > 0.05$). All storage methods of human tissues are not without problems and even the commonly reported technique of freezing tendons has been shown to alter the mechanical properties of tendons and to reduce Young's modulus [237]. Future studies can build upon this important preliminary study by looking at tendons preserved in a more standard technique such as freeze-drying, although this technique is applicable to the testing of fresh samples.

While this pilot study has shown differences in the shear mechanical properties of rotator cuff tendons, further investigation is required to understand the clinical implication of differences in shear moduli. If differences in shear moduli correlate with failure rates, it may be clinically possible to apply DSA to rotator cuff biopsies for monitoring pre- and post-interventions, or for early identification of mechanically weakened tissue which may be unlikely to sustain over sewing with sutures and may warrant further augmentation of the surgical repair. Thus it is theoretically possible that DSA may assist surgeons to specifically match the properties of the repair technique to the patient's mechanical properties, and this will be an interesting avenue for future studies. In the future, if a threshold of "integrity' could be established, DSA could potentially help to delineate diseased tissue which appears to look normal, and to differentiate between which partial tears should be debrided and which partial tears need to be fixed.

This study has demonstrated that there are important differences in the mechanical properties of normal and torn rotator cuff tendons. This demonstration has only been possible through the successful application of a novel technique, DSA. Hence there is a strong argument for

streamlining treatments and surgical methods so that they better match the tissue that is being repaired. This novel technique provides opportunities for the investigation of other small musculoskeletal tissue samples obtained at surgery and could be developed as an intra-operative assessment of the mechanical properties of tissue.

3 CHAPTER 3: COMPARING THE CHEMICAL PROPERTIES OF NORMAL AND TORN ROTATOR CUFF TENDONS USING FOURIER TRANSFORM INFRARED SPECTROSCOPIC ANALYSIS

3.1 Abstract

3.1.1 Background

Rotator cuff tears may involve a multistage disease process, where small and large tears have different characteristics. This study uses Fourier transform infrared spectroscopy (FTIR) with the aim to (i) characterise the chemical and structural composition of rotator cuff tendons and to (ii) identify structural differences between anatomically distinct tears. Such information may help identify biomarkers of rotator cuff tear pathologies and provide insights into the healing rates of different tear sizes.

3.1.2 Methods

The chemical composition of 92 formalin-fixed rotator cuff tendons were measured from patients aged between 20 and 89. The infrared spectra of 81 partial, small, medium large and massive rotator cuff tendon tears were measured using FTIR and compared to 11 uninjured controls. A diamond attenuated total reflectance accessory was used with a FTIR spectrometer to collect spectra for each sample. The spectra were reduced and classified using standard multivariate

analysis techniques: principal component analysis, partial least square and discriminant function analysis.

3.1.3 Results

FTIR readily differentiated between normal and torn tendons, and different tear sizes. This study identified the key discriminating molecules and spectra altered in torn tendons as: (i) carbohydrates/phospholipids (1030-1200 cm^{-1}), (ii) collagen (1300-1700, 3000-3350 cm^{-1}) and (iii) lipids (2800-3000 cm^{-1}).

3.1.4 Conclusions

FTIR can clearly distinguish normal and different sized rotator cuff tendon tears. This prospective non-randomized study indicates that the onset of rotator cuff tendon tear pathology is mainly associated with altered collagen structural arrangements, with associated chemical changes in lipids and carbohydrates. The approach described is rapid and has the potential to be used intraoperatively to determine the quality of the tendon and extent of disease, and to determine treatment responses.

3.2 Introduction

A challenge to medical diagnostics is to accurately and reliably identify pathology and monitor its progression, such as rotator cuff tendon pathologies. The aetiology of tears is not a purely

mechanical problem, but involves underlying biochemical changes. The ECM of tendons helps to transmit tensile and shear strength and dictate its mechanical properties. Changes in the ECM of torn rotator cuff tendons have been demonstrated previously, including increased collagen I and III, altered matrix metalloproteinases (MMP) and an accumulation of glycosaminoglycans and lipids [140, 141]. Torn tendons have been shown to have altered chemical compositions with varying levels of proteoglycans [74], oxygen free radicals [169], atrophy [143] and chondrocyte markers [144]. There is increasing evidence to support the idea of a progressive multistage disease process where small tears have different characteristics to larger tears. Increased tear size has been shown to correlate with changes in the cellular and ECM composition, a reduction in metabolism and presumed viability [125] and an increase in apoptosis [272]. The implications of these cellular and ECM changes are unclear and require further understanding. In order to address this significant disease burden, there is a need for a better understanding of the pathophysiology underlying rotator cuff tears and its progression. It has been clearly demonstrated that larger tears are associated with higher failure rates [32, 35, 204, 206]. There is a strong need for identification of disease biomarkers which may help to (i) identify earlier stages of disease, (ii) monitor disease progression and (iii) possibly predict outcomes following therapeutic or surgical interventions.

This case-control study employed Fourier transform infrared spectroscopy (FTIR) to characterize the chemical properties of torn rotator tendon. FTIR of affected tissue can potentially reveal a wealth of information regarding the biochemical and biophysical basis of disease processes. Molecules are excited to higher vibrational states, using light at specific wavelengths which correspond with the frequency of excited vibration modes of molecules, such as bending or

stretching motions (see Figure 3-1) [273]. The structure of molecules, specifically the vibration of bonds or groups, determine the frequencies at which light is absorbed. This allows the absorption positions to be mapped and the chemical composition to be identified.

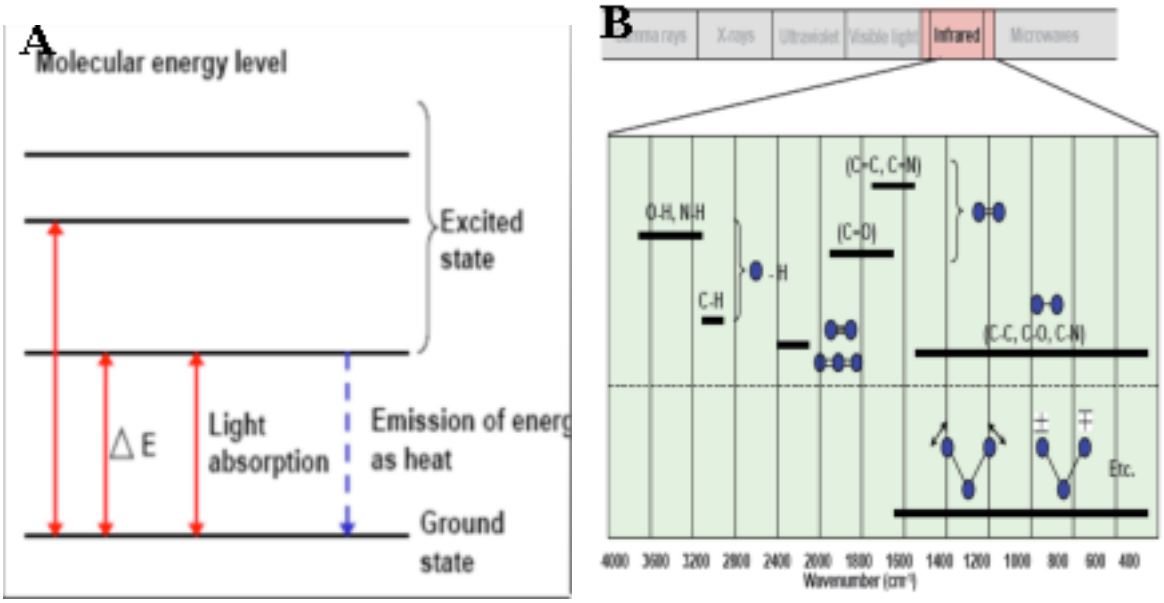

Figure 3-1: Explanation of Fourier Transform Infrared Spectroscopy (FTIR). A) Molecules can be excited to higher energy states at specific wavenumbers. As molecules return to ground state, they emit energy. B) The emitted energy can be detected and used to map the absorption position and thus identify chemical components within tissue.

As FTIR has the capacity to provide a sensitive infrared biochemical fingerprint of specimens, it was hoped that FTIR could be used to obtain a greater insight into compositional changes in different sized rotator cuff tendon tears than has previously been afforded by other currently available assays. A key advantage of FTIR is that it is a quick, non-manipulative and non-destructive test, which can identify a wide range of chemical targets and could possibly be used within the operating room with the use of a fibre-optic probe [274]. The biomedical applications of FTIR to date have been numerous, including mapping of cartilage collagen and proteoglycan

content, the study of brain, breast and cervical tumours, as well as bone and cartilage degeneration, heart, lung, spleen, skin and human mesenchymal stem cells [275-277]. FTIR has been able to differentiate between different grades of cartilage degeneration in the knee and map collagen and proteoglycan content [278, 279]. In order to overcome confounding variables of the thickness or lack of transparency of the specimens, surface attenuated total reflectance (ATR) FTIR was used.

3.2.1 Hypotheses

- It was hypothesized that tendon tears of varying sized will have different chemical compositions and thus altered FTIR spectra when compared to normal tendons.
- It was also hypothesized that smaller tendon tears and partial tears can be chemically differentiated from larger tendon tears using their infrared fingerprint.

3.3 Methods and Materials

3.3.1 Specimen Collection

95 specimens in total were studied. Specimens were collected from 81 patients undergoing surgical repair of a rotator cuff defect, which were identified preoperatively with an ultrasound scan. Patients were aged between 20 and 89 with a mean age of 65.7 years. All patients were aged 45 years or older, as most tears occur after this age, and indeed Nobuhara *et al*., found that 95% of their patients with rotator cuff tears were aged 45 years or over [107]. Specimens were obtained

from consecutive patients who had been recruited into the United Kingdom Rotator Cuff Trial (UKUFF), where patients were randomized into the operative repair arm for either open or arthroscopic tendon repair. The sizes of tears were measured intraoperatively by taking the widest diameter of any tear. Tendon specimens were taken from the edge of rotator cuff tendons torn on the articular side, and from the intact tendon edges of the controls. Rotator cuff tendons were categorized according to the classification suggested by Post *et al.*, [79]: partial (n=7), small (n=16), medium (n=23), large (n=17) and massive tears (n=18). There was no significant difference between the duration of symptoms between different tear size groups. 11 age and sex matched controls were used of normal intact tendons, which were obtained from patients undergoing other types of surgery with no evidence of rotator cuff tendon disease with an average age of 59 years. This type of study is not easily amenable to a power calculation. Specimens were immediately placed in formalin for preservation, or fresh frozen in liquid nitrogen and stored at -80^{o}C. Non-formalin treated tendons were included in the study to assess the effect of formalin and verify the robustness of the vibrational spectroscopy classification. Punch biopsies of 3mm diameters were taken to provide uniformity, with 2 separate samples collected from each specimen. Approval for the study was obtained from the local institutional review board. All patients gave informed consent.

3.3.2 FTIR

To collect the FTIR spectra, a Nicolet 6700 spectrometer (Thermo Fisher, Madison, WI) was used with an attenuated total reflectance (ATR) single bounce diamond accessory and a liquid nitrogen

cooled detector (MCTA) (see Figure 3-2). The main advantage of the ATR is that it circumvents the lack of transparency of the specimens. Each specimen was orientated along the long axis of the collagen fibres. Spectral information was collected using OMNIC 7.6 software in the spectral region ranging from 400-7000 cm^{-1}, at a resolution of 4 cm^{-1}. Each spectrum represented an average of 64 scans taken per specimen. Every patient's tendons were measured at least 4 times as 2 separate punch biopsies were taken from each patient, and 2 spectral readings were taken per sample and averaged.

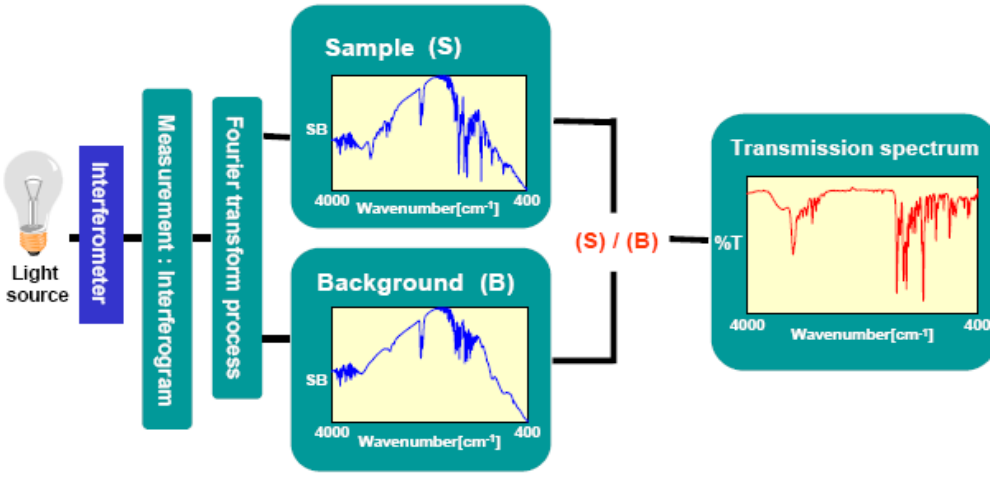

Figure 3-2: Collection of FTIR spectra. Light is shone through an interferometer which splits light into all component wavenumbers and an interferogram is generated. Using the Fourier transform process, spectral information from each separate wavenumber can be collected simultaneously, and the raw data is converted to absorbance which is represented by wavenumbers. A spectra is collected for the sample, and one for the background and then the two are subtracted to obtain a unique transmission spectra with spectral information regarding the specimen of interest only.

Prior to the collection of any data, the system was calibrated to try to remove background signals and to try to purge the CO_2 bands. The background air acted as a buffer and a background spectra was collected before each sample reading. Results from the pilot studies showed that formalin did

not significantly alter the FTIR readings (see Appendices). The formalin buffer was used as background spectrum, was collected before each sample reading and subtracted from each tendon spectra. Pure reference compounds of common ECM molecules were obtained, and included collagen I, II and III, chondroitin sulphate, decorin and elastin from Sigma Aldrich (St. Louis, Missouri, USA). FTIR spectra were collected for 6 samples of each pure specimen as outlined above and averaged to assist with vibrational band assignment. Chondroitin sulphate is the most common proteoglycan found in rotator cuff tendons and decorin is a common glycosaminoglycan [74].

Figure 3-3: Photograph of a Nicolet 6700 spectrometer (Thermo Fisher, Madison, WI).

3.3.3 Data Analysis

All data was run on Matlab [274] and Pychem [280] multivariate analysis software package, and the data and mathematical modelling were validated during the analysis process. The data window was reduced to 700-4000 cm^{-1} as the near infrared region (> 4000 cm^{-1}) is very weak and has

complex biologically relevant band assignments that are harder to interpret. In order to remove the atmospheric CO_2 contribution, the corresponding spectral region 2250-2420 cm^{-1} was replaced by a linear trend. Data pre-processing was applied to ensure accurate quantitative data analysis, using a similar approach to those described in previous studies using FTIR to differentiate human mesenchymal stem cells and brain tumours [274, 281, 282]. An ATR correction was applied to address the wavelength dependency of penetration. In order to ensure accurate quantitative analysis, the data was smoothed, normalized and variance-scaled, which are standard validated techniques for FTIR analysis. Smoothing reduces the data noise effects on the multivariate analysis. The spectrum were normalised to values between 0 and 1, as this allows for easy comparison of the various samples. The absolute concentrations are lost, but the relative ratio of component concentrations are retained which permits comparison. Variance scaling, scales the peak by their variance. This pre-processing prevents large peaks from dominating the analysis. Small peaks with associated large variation in amplitude may be as chemically important as a large peak, and this variance scaling corrects for this.

Every pure compound gives rise to a unique pattern of infrared absorptions, essentially a distinctive ‘‘fingerprint’’. For more complex mixtures, the spectrum is a combination of the component spectra weighted by the relative concentrations of those components. For tissue, there may be hundreds of components contributing to the absorption profile, and, in general, the spectra are far too complex to permit assignment of specific absorptions to individual constituents. However, it is often unnecessary to resolve all of the individual components from one another; useful insights can be drawn from the spectra by focusing on classes of biological macromolecules rather than

individual chemical species. For example, molecular structures such as long lipid (CH_2) chains or protein backbone groups (carbonyl and amine, N—H and C=O) provide characteristic absorptions of these classes of compounds. Difficulties can emerge when interpretation of very complex spectra on the basis of individual or group assignments is attempted. It is often the case that a potentially defining pattern that might distinguish among various groups of spectra is obscured by overlapping absorptions to such an extent that even the trained eye cannot discriminate the groupings. In this situation, automated pattern-recognition methods can be invaluable. Algorithms may be trained to recognize common patterns within subgroups of seemingly unrelated spectra and hence to distinguish the spectra within one group from those in a different group. Once trained, the same model may be used to classify the spectra of unknown ‘‘test’’ samples as belonging to specific groups.

Initial data analysis to detect differences between tear groups was performed using a multivariate approach in a blinded manner, before moving on to analysis where the tendon tear size was known. To determine which were the spectral features that differentiated between different diseased states, the spectra were reduced and classified using standard multivariate analysis; principal component analysis (PCA), partial least squares (PLS) and discriminant function analysis (DFA) [283]. As the wavenumbers relevant to biological materials are not all independent, PCA allowed reduction of data colinearity and dimensionality to observe whether the data naturally clustered. However PCA only highlights the most significant principal components in the raw data. PLS is a modelling approach where the data is stratified for tear size and highlights the most salient spectral features that can differentiate between normal and different tear types, and helps to predict the tendon tear

categories that the spectra would fall into. DFA of the principal components was used to train a supervised classification model [284]. For easier visualization the DFA were plotted using a hierarchical cluster analysis (HCA) to produce a classification tree. The multivariate analyses were cross-validated by randomly splitting the samples into train, test and validation sets and making sure that the data modelling was accurate. In order to identify the chemical components that optimally differentiated different tendon tears, a genetic algorithm (GA) was used. The obtained wavenumbers were then cross referenced with tables listing previously published wavenumbers for biologically relevant materials and with the spectra collected from the pure model compounds [53]. Finally, the multivariate results were statistically tested using a general linear model (GLM), which encompassed linear regression and analysis of variance (ANOVA). This approach provides a robust test for multivariate data [285]. A significance level of $p < 0.05$ was set for all of the above statistical tests.

3.3.4 Histology

Tendon samples used for FTIR analysis were embedded in paraffin and 10 μm sections were cut perpendicular to the long axis of collagen fibres using a Leica-LM microtome (Leica Microsystems, Wetzlar, Germany). Histological assessment of 2 random sections from each sample was performed following haematoxylin and eosin (H&E) and Alcian blue staining. The worst affected areas were selected to assess basic collagen structure and areas rich in glycosaminoglycans using the Alcian blue, as it is a glycosaminoglycan specific stain [286]. Each H&E stained section was classified using Riley's score, which describes the organization,

orientation and quality of collagen fibres [71] (see Appendices for an outline of Riley's classification). Grade 1 describes normal tendons, and grade 2 describes mild degeneration with patchy waviness of collagen fibres and shorter nuclei with an Indian file alignment. Increased collagen hyalinization and loss of collagen orientation is assigned as grade 3, moderate degeneration. Severe degeneration is designated as grade 4 and describes diffuse hyalinization with complete loss of collagen orientation. Glycosaminoglycans were assessed using the Movin score based on Alcian blue staining and classified as 0 (normal), 1 (slightly abnormal), 2 (abnormal) and 3 (markedly abnormal) [71]. Two separate reviewers examined and graded the specimens independently and were blinded to the type of tear. Data from both examiners were pooled, to calculate the means and standard deviations. The interobserver variation was calculated using the Kendall coefficient of variance for non-parametric data.

3.4 Results

It is possible to measure and characterize the properties of both normal and torn rotator cuff tendons using FTIR. The average spectrum of each tendon, in the mid-infrared region of interest, is shown in Figure **3-4**. Even without any data modelling, it is possible to see separation of normal and different sizes of rotator cuff tendon tears using FTIR, suggesting that they contain chemically distinguishable groups. Figure **3-4** indicates that the spectra show no peak shift, and that the main changes are in the relative intensity of the spectral peaks. This suggests a change in relative amounts of chemical groups between the different tendon tear types. More subtle differences between the groups can be visualised in Figure **3-5**.

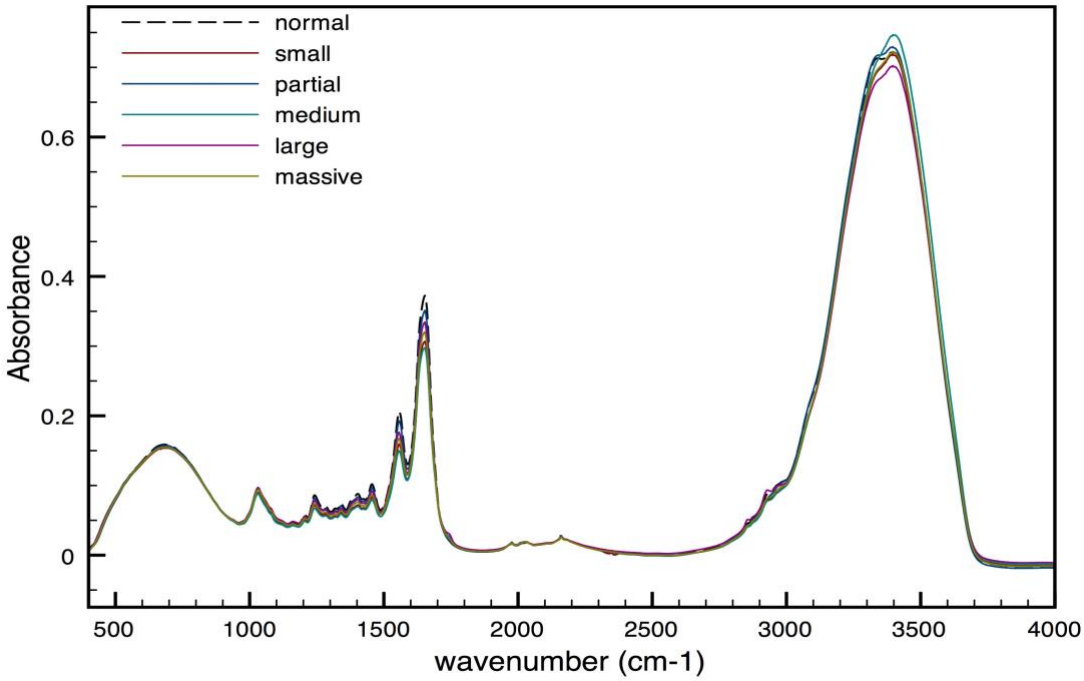

Figure 3-4: Mid-infrared (400-4000 cm^{-1}) average ATR-FTIR spectra of the different tendons in formalin. Without any data pre-processing, separation of the 6 different groups is visible, suggesting that chemical differences exist between these different disease groups.

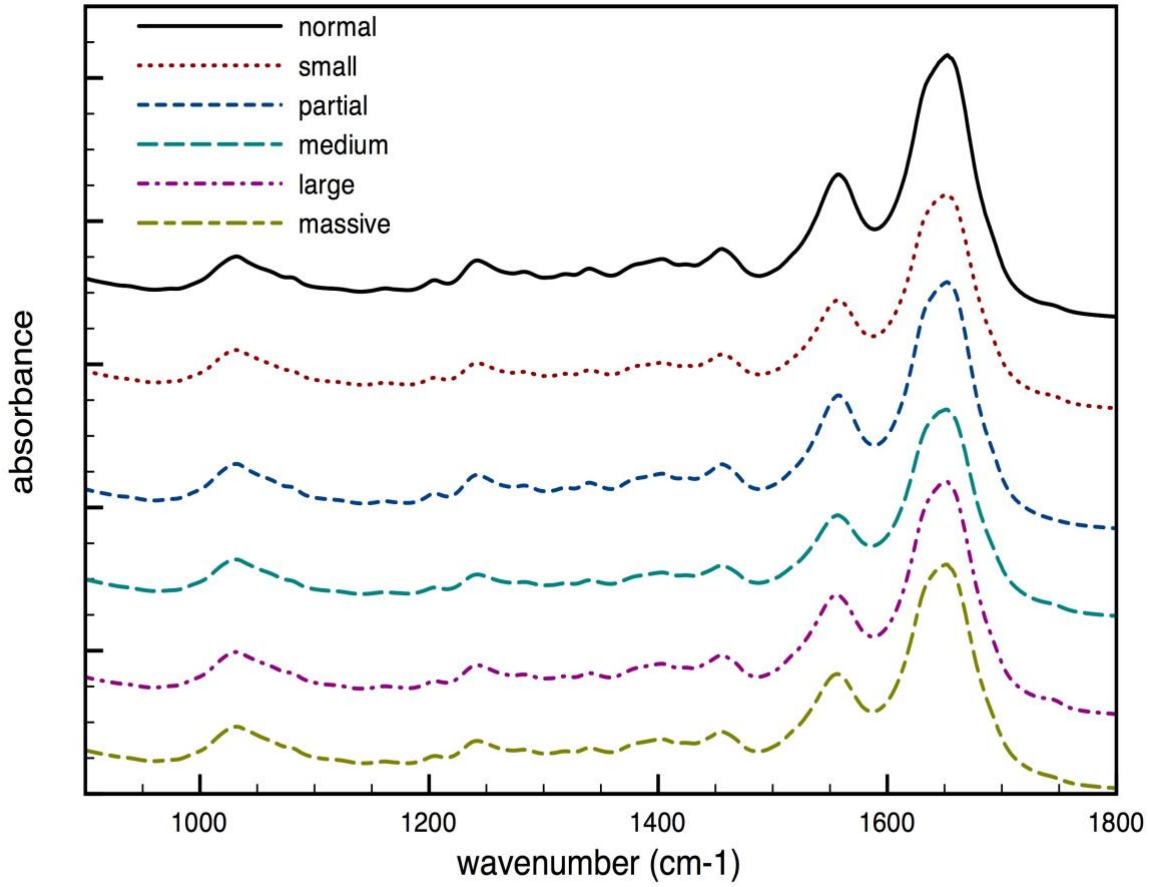

Figure 3-5: Representation of mid-infrared (400-4000 cm^{-1}) average ATR-FTIR spectra of the different tendons in formalin, shown in Figure 3-4. The spectra from each group had been shifted to allow identification of any differences between groups, revealing subtle spectral and hence chemical variations between the 6 groups.

3.4.1 Comparing Different Tear Sizes

Focusing specifically on normal and torn tendons, it is apparent that the two groups can be readily differentiated (see Figure 3-6).

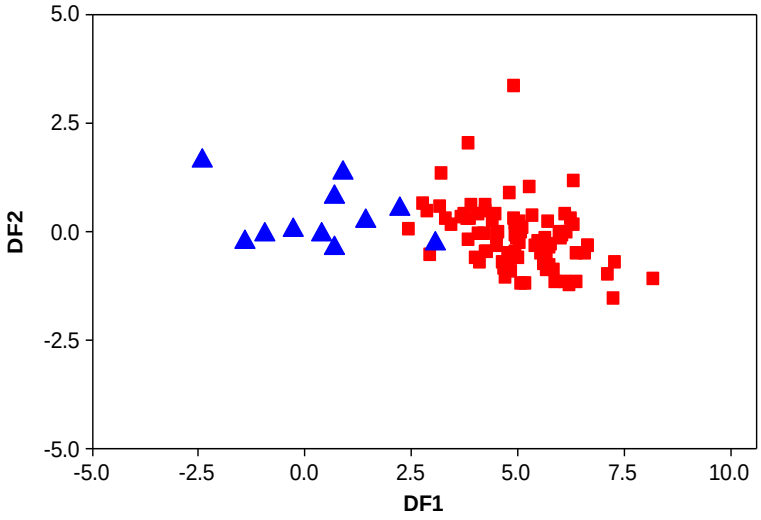

Figure 3-6: Discriminant Canonical plot of normal (triangles) vs. diseased tendons (squares).

The details, however, of the diseased tendons required more advanced analysis. Therefore DFA-HCA analysis was used to determine the degree of relatedness of the different diseased tendons. Figure 3-7 shows the results of the classification analysis in the form of a hierarchical tree. The Euclidean distance represents the degree of relatedness of the samples.

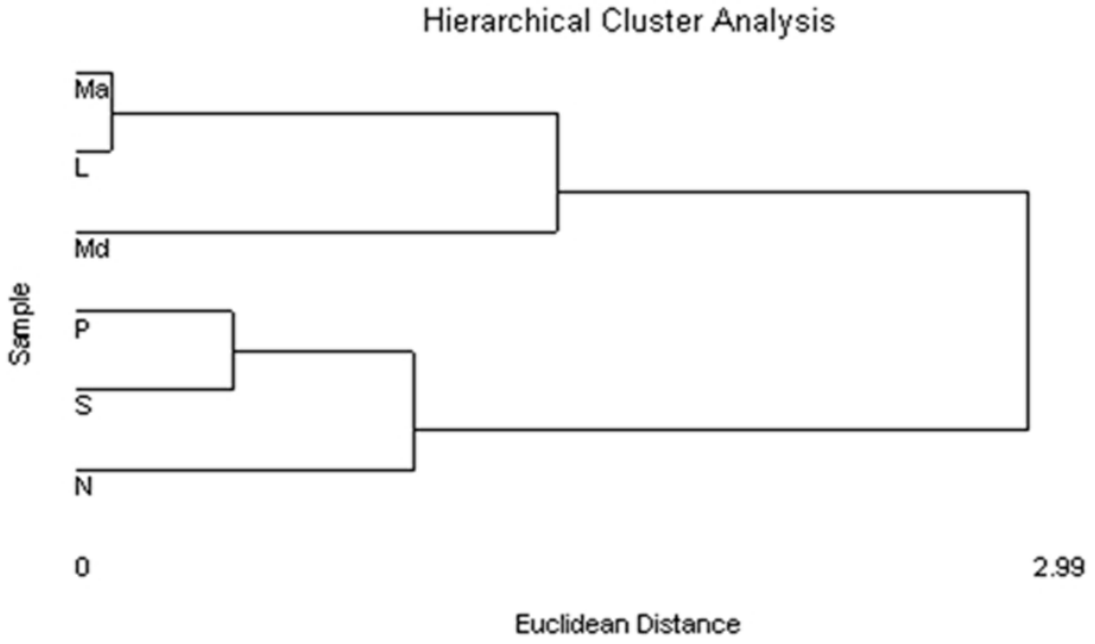

Figure 3-7: Hierarchical cluster analysis of different classes of rotator cuff tear types. Normal tendons are clearly distinguishable from torn tendons. Partial tendons are also distinct from small partial tears, but demonstrate some similarities. Legend: N, normal; S, small; P, partial; Md, medium; L, large; Ma, massive.

The classification within the tree shows that normal tendons are a separate chemical entity from torn tendons. Chemically the torn tendon groups can be classed into (i) partial and small tears and (ii) medium, large, massive tears. Partial tears are chemically distinguishable from normal and small torn tendons, confirming that they are a biologically separate entity, even though they do share more similar chemical features with small tears. Large and massive tears are more related than medium rotator cuff tears, and the high similarity suggests a large chemical overlap. Although informative, the tree does not however provide any information about the basis of the differences seen between the diseases types.

3.4.2 Identifying Chemical Differences Between Groups

PCA of each of the different tear groups revealed that the first two principal components could explain at least 87.4% of the variance. Changes between different tendon tear types were examined by comparing the difference spectra, where the spectrum of the normal tendon was subtracted from the spectra of the different tendon tear groups (see Figure **3-8**). Figure **3-8** shows the relevant spectral regions matching Figure **3-4**. Typically, if no changes are observed between groups then the difference spectrum would show a flat line at zero ΔAbs, as seen between 3700 and 4000 cm^{-1} wavelength. It is possible to observe from Figure **3-8**, a series of positive (dotted lines 1 and 11) and negative peaks (dotted lines 2-10), with the positive peaks accounting for the presence of new compounds, and negative peaks accounting for disappearing compounds.

summarises the peaks found from the difference analysis in Figure **3-8** with corresponding band assignments to indicate the chemical changes that are occurring. Negative peaks dominated below 1800 cm^{-1} (lines 2-6, Amide bands), suggesting a loss or change of chemical and structural composition compared to normal tendons. However one positive peak dominated the spectral region centred on 1000 cm^{-1} (peak 1). Most remarkably, peak 1 is strong only within the partial tendon (spectrum A in Figure **3-8**). On the contrary above 2700 cm^{-1} more random behaviour is seen with changes in lipids (peak 7 and 8), collagen (peak 9, Amide B band) and hydroxyl groups which reflect the formalin signal (peaks 10 and 11).

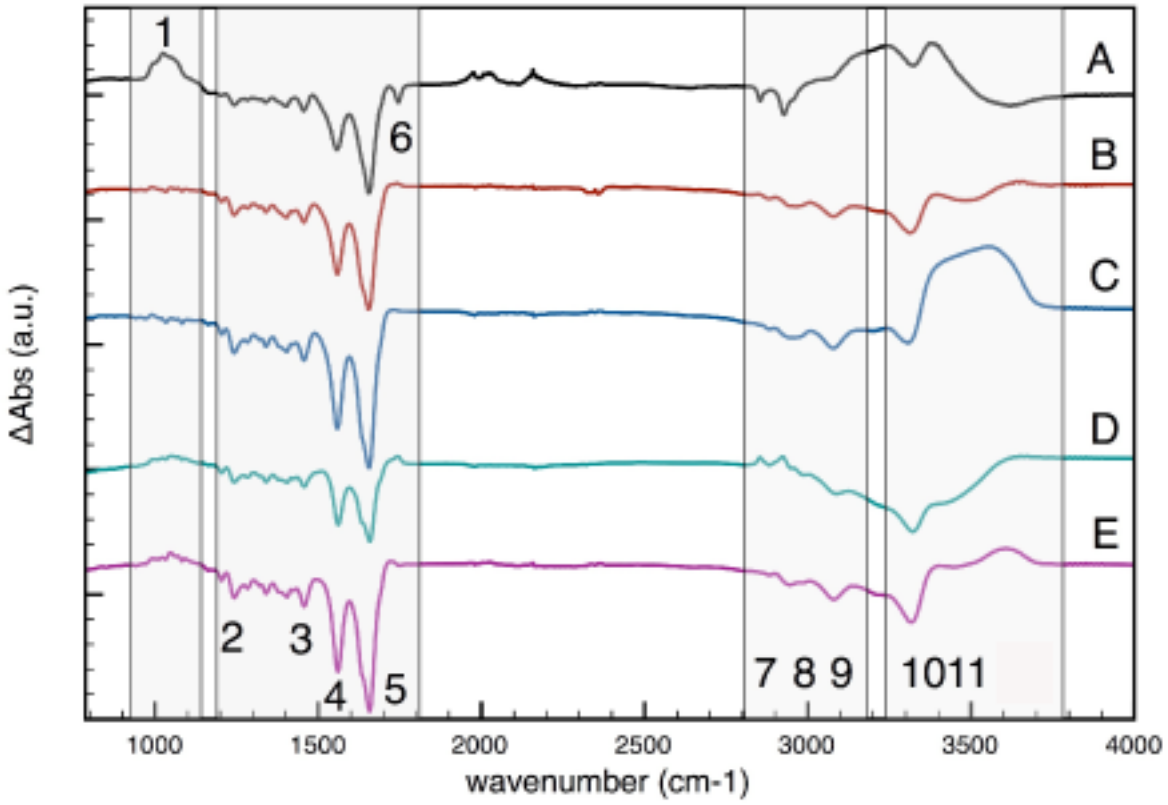

Figure 3-8: Difference spectra between diseased and normal tendons expressed in (ΔAbs), highlighting structural and chemical changes. The appearance of positive peaks (i.e. line 1 and 11) marks features absent from the normal spectrum, and negative peaks (i.e. lines 2-10) show features that have decreased in intensity relatively to the normal spectrum. A, Partial-Normal; B, Small-Normal; C, Medium-Normal; D, Large-Normal; E, Massive-Normal. Explanations of lines and spectral features is shown in

.

The wavenumbers corresponding to the identified spectral peaks were then cross-referenced to identify the chemical groups that they corresponded with **Table 3-1** summarises the peaks found from the difference analysis with corresponding band assignments suggested by previous studies for biologically relevant materials [287, 288].

Table 3-1: Vibrational band assignment in tendon tissues. Assignments are from spectrochemical analysis using Fourier transform infrared spectroscopy of biological tissues [287, 288].

Band position (cm^{-1})	Position in Figure 3.8	Chemical group
940		Trans Fat
970		Polysaccharides
1030	1	Carbohydrates/Proteins
1080		Phospholipids
1160		Lipids
1200		Collagen (Amide III)
1240	2	Phospholipids
1284		Collagen (Amide III)
1319		Collagen (Amide III)
1338		Collagen
1380		Collagen / Lipids
1400		Collagen
1424		Collagen
1456	3	Lipids / Collagen
1557	4	Collagen (Amide II)
1631	5	Collagen (Amide I)
1654		Collagen (Amide I)
1740	6	Lipids
2851	7	
2876		Complex carbohydrates
2928	8	Lipids
2962		
3080	9	Collagen (Amide B)
3200		Collagen
3315- 3325	10	Collagen (Amide A)
3400-3500	11	Hydroxyl group

A DFA analysis suggested that the following key spectral regions and their corresponding biological compounds accounted for most of the differences between normal and torn tendons:

1. Carbohydrates, Phospholipids (1030 - 1200 cm^{-1})
2. Protein, collagen structures (1300 - 1700 cm^{-1}, 3000 - 3350 cm^{-1})
3. Lipids (2800 – 3000 cm^{-1}).

Further testing of differences between tear groups was done using a GLM analysis, with age as a covariate and sex as a random factor. It was found that age or sex did not vary significantly between the tear size groups, and there was no spectral effect from age and sex. This study does encompass a reasonably wide age distribution of patients, but most importantly the age profile is similar and matched between the different groups and hence changes between the groups are unlikely to be age related.

To identify the specific chemical basis of discriminating variables and chemical evolution between different tear groups, a genetic algorithm was used to identify the significant wavenumbers that accounted for most variability between groups, and cross referenced them with known wave-numbers for biologically relevant materials and the wavenumbers obtained from imaging pure ECM compounds [53] (see

and Figure 3-9). Collagen I, II and III decreased in the torn tendons, most noticeably in collagen II and to the least extent in collagen III. There was a progressive decrease in collagen I and II, with a smaller decrease in collagen III moving from normal, to partial, to small and medium tears. The greatest decrease was evident in collagen II with higher levels in massive tears compared to

small tears. Large and massive tears had higher collagen I levels than small and medium tears. Elastin increased between small to massive tears, with no change in partial tears when compared to normals. The onset of partial tears only involves small collagen structural changes, particularly collagen II. Small tears involve mostly changes in lipids, and to some extent sugars such as proteoglycans. For medium tears, the chemical groups that appear most affected are collagen structure and sugars, suggesting a change in the proteoglycans. Most chemical groups are altered in large tears, whereas massive tears show the greatest change in collagen, with some proteoglycan. The exact proteoglycans involved are unclear as no significant difference in chondroitin sulphate or decorin was detected between groups.

Table 3-2. Significant spectral features differentiating normal from diseased tendons.

Normal-Partial (cm^{-1})	**Normal-Small (cm^{-1})**	**Normal-Medium (cm^{-1})**	**Normal-Large (cm^{-1})**	**Normal-Massive (cm^{-1})**	**Chemical structure group**
	730 – 770		730 – 770		Protein
			800 – 830	820 – 870	Sugars
			840 – 860		
985 – 989	960 – 1005		960 – 990	980 – 1020	
			1010 – 1030		Protein (N-C)
		1060 – 1098			Carbohydrates
	1140 – 1173		1135 – 1190		Carbohydrates
		1240 – 1270	1260 – 1280	1215 -1250	Protein, Collagen
		1300 – 1320			Protein (Amide III)
			1380 – 1400		Proteins
		1430 – 1470			Lipids fatty acids
1493 – 1585					Protein (Amide II)
			1540 – 1590		
1612 – 1643		1608 – 1640			Protein (Amide I)
1651 – 1701		1689 – 1700			
	1760 - 1790				Fatty acids

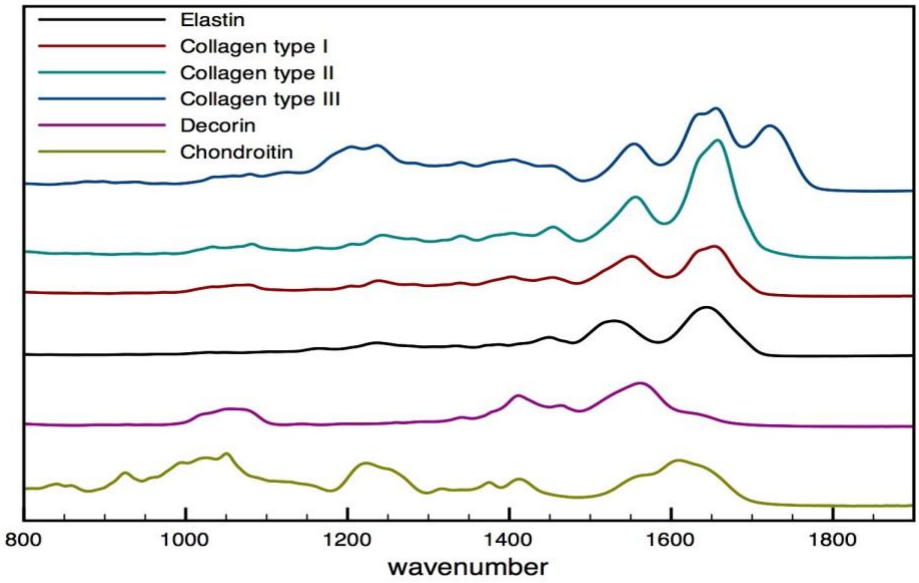

Figure 3-9: Spectra for pure chemical compounds that play important roles in the tendon extracellular matrix (elastin, collagen types I, II and III, decorin and chondroitin sulphate).

3.4.3 Characterizing Partial Tears

Partial tears are also chemically distinguishable from both normal tendons and small rotator cuff tendon tears, suggesting that they are a biologically separate entity (see Figure 3-10). However the HCA from Figure 3-7 reveals that partial tears do share similar chemical features with small tears. Partial tears were found to be primarily associated with changes in collagen type II.

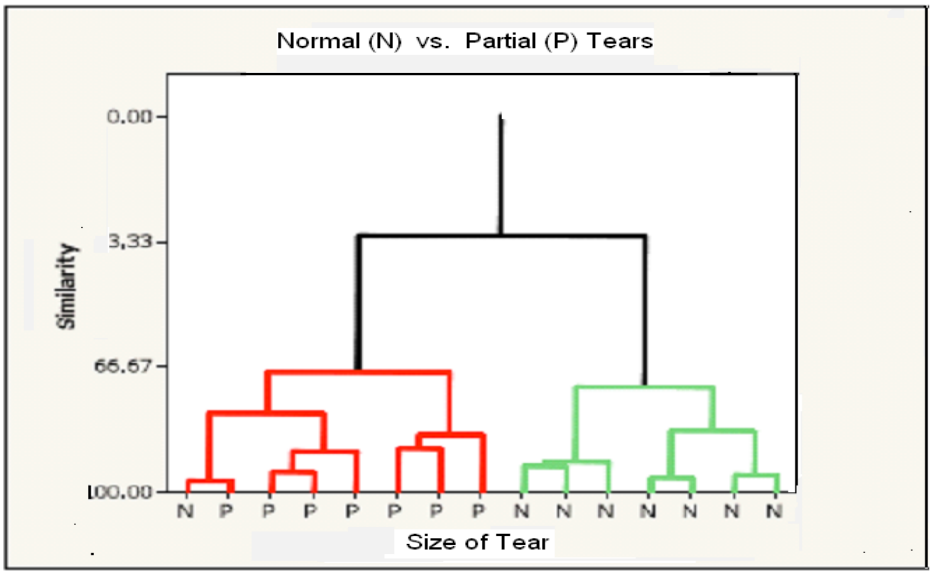

Figure 3-10: Hierarchical cluster analysis comparing normal and partial rotator cuff tendon tears. Partial tears are clearly chemically distinguishable from normal tendons.

3.4.4 Effect of formalin preservation

Before the onset of my main study, I undertook a pilot study to assess what mode of fixations would be possible to allow FTIR analysis of tendon specimens. The results of the pilot study showed that it was feasible to collect tendon specimens in formalin, and that there was still a large degree of overlap with fresh and glutaraldehyde preserved tendons, indicating that formalin fixation did not prevent or obscure FTIR analysis compared to other modes of fixation (see Appendices). As most of the tendon specimens were formalin fixed, it was necessary to assess the effect of formalin fixation on the spectral features. Prior to data processing or analysis, a spectral reading of tendon in formalin and pure 10% formalin was taken, and subtracted from the first tendon spectra.

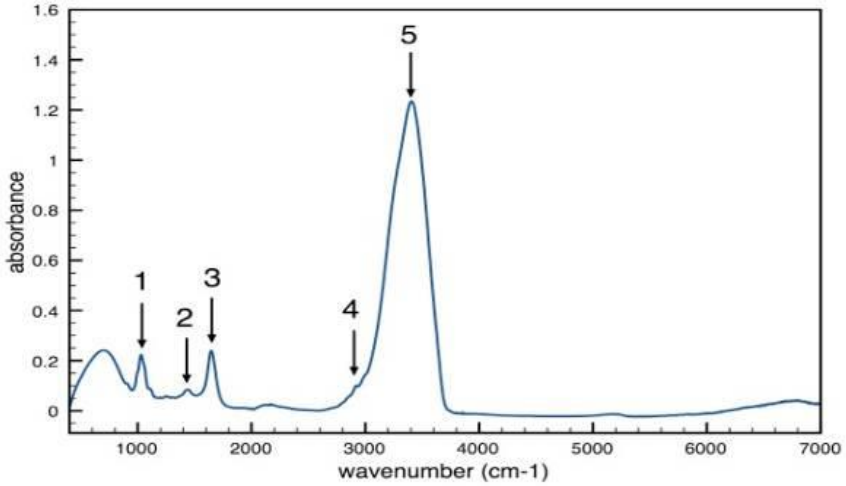

Figure 3-11. Spectra for formalin alone. Arrows indicate significant spectral peaks associated with formalin structures.

I also compared (i) Normal tendons without formalin to (ii) Normal tendons in 4% formalin and (ii) Normal tendons in 10% formalin. Even with preservation in formalin, all of the tendon peaks could still be detected, indicating that formalin preserved specimens can be used to assess tendon infrared spectroscopic features. No significant differences existed between 4 and 10% formalin, and thus 10% formalin was used, as this is the standard preparation available in most pathology departments. The spectral features (band positions) were not altered amongst the different groups. The major changes were found in the band amplitudes and the peaks are much more apparent without formalin. If it had been feasible, using fresh tendons would have been advantageous, but in order to obtain large numbers, specimens had to be collected from multiple sites and thus collection in formalin was easier.

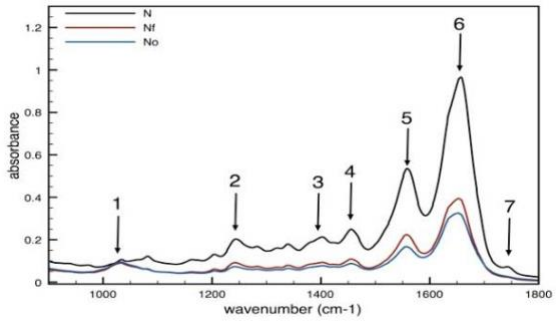

Figure 3-12. Spectra for wavenumbers 0 – 1800 cm^{-1} comparing Normal fresh tendons (N), Normal tendons in formalin (Nf and No). Nf represents 4% formalin and No represents 10% formalin.

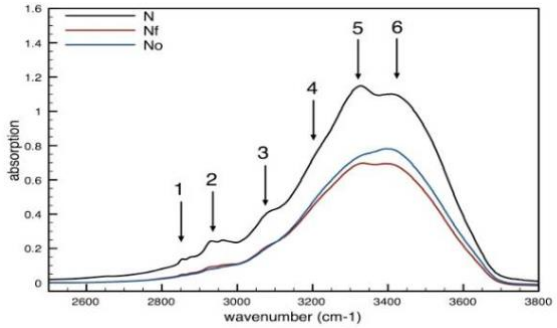

Figure 3-13. Spectra for wavenumbers 2500 – 3800 cm^{-1} comparing Normal fresh tendons (N), Normal tendons in formalin (Nf and No). Nf represents 4% formalin and No represents 10% formalin.

To obtain a more detailed assessment of how well the different groups could be distinguished, I compared normal fresh tendons (N), diseased fresh tendons (D), normal tendons in formalin (Nf) and diseased tendons in formalin (Df). Using formalin to preserve specimens did not prevent the ascertainment of differentiating chemical features. Figure **3-14** shows a discriminant canonical plot comparing fresh normal (N) and diseased (D) tendon, to formalin fixed normal (NF) and diseased (DF) tendon. While it is possible to differentiate between normal and diseased states in formalin fixed tendon, the two groups remain close. This differentiation is more apparent amongst the fresh tendon groups. A rapid analysis of the canonical discriminant function (DF) suggests that:

(i) Disease effects in tendon are mainly explained by discriminant function (DF) 1

(ii) Formalin effect is mainly explained by discriminant function (DF) 2

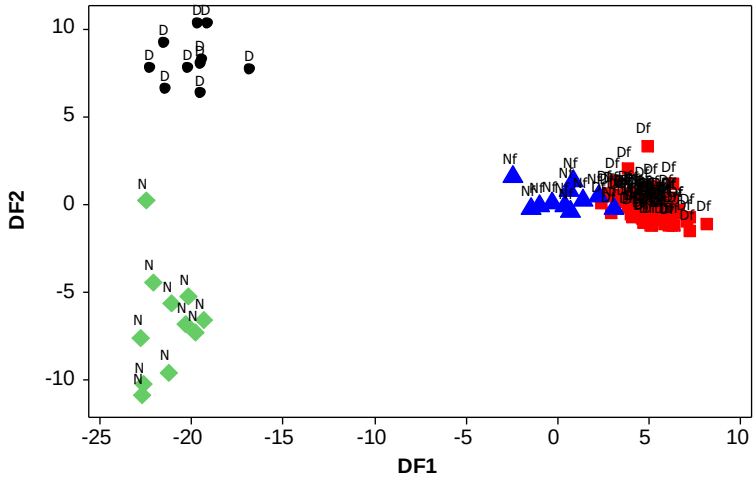

Figure 3-14. Discriminant canonical plot comparing normal (N, diamonds) and diseased (D, circles) fresh tendons versus normal (Nf, triangles) and diseased (Df, squares) formalin preserved tendons.

3.4.5 Accuracy of the FTIR Analysis

Attempts were made to validate the modelling and analysis techniques employed. A classification analysis was performed comparing how well the visual classification of tear sizes, reported by surgeons, correlated with the chemical classification suggested by FTIR analysis, to obtain insight into how accurately the infrared spectroscopy analysis model used here can predict tendon tear size. This analysis was performed using the PCA, which reduced data dimensions. Table 3-3 shows the results of the (mis-)classification table (also known as a confusion matrix).

Table 3-3: Classification table using a k-meloids cluster analysis. Based upon the spectral differences detected between the different groups, a comparison was made between the grade of tendon tear size based upon visual examination, and the classification that would have been predicted by the infrared spectroscopy analysis.

	Infrared Spectroscopy					
Visual examination	N	S	P	Md	L	Ma
Normal (N)	**9**	1	0	0	0	1
Small (S)	2	**12**	1	0	0	1
Partial (P)	0	6	**1**	0	0	0
Medium (Md)	0	0	10	**5**	5	3
Large (L)	1	1	0	0	**5**	7
Massive (Ma)	0	0	0	4	2	**11**

The table revealed that no group was fully accounted for, and strong group overlaps existed. Normal, small and massive tears presented the highest correct classification whereas 6 partial, 18 medium and 9 large tears were apparently misclassified based upon the chemical differentiation suggested by the FTIR analysis.

3.4.6 Histological Analysis

Examination of the H&E stained sections, revealed that the basophilic nuclei of tenocytes or fibroblast-derived cells were visible, as well as the homogen eosinophilic collagen bundles (see

Figure 3-15). The stained sections of normal tendons showed that collagen fibres and bundles were orientated in parallel and densely packed.

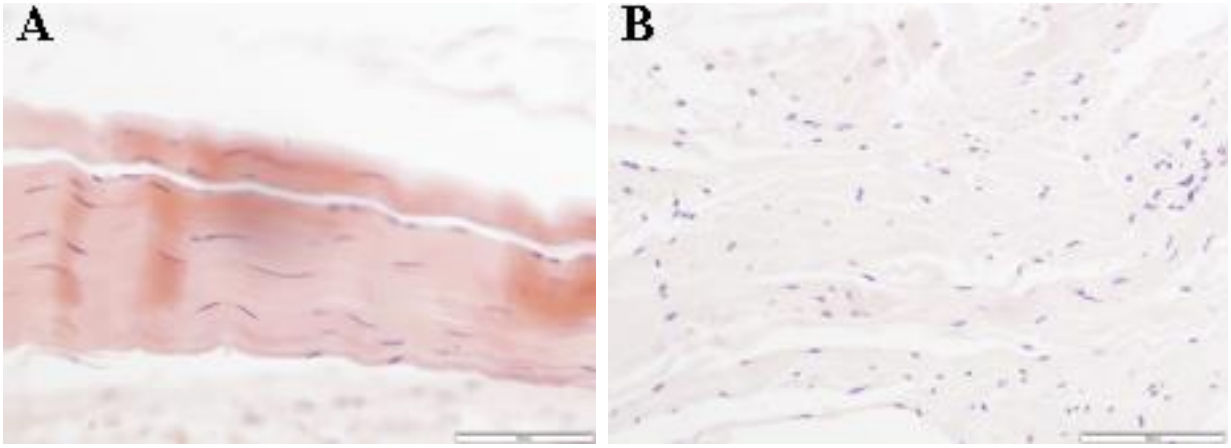

Figure 3-15: Sections of tendon stained with Haematoxylin and Eosin. A) Section through a normal tendon showing well organised collagen fibres with a crimp pattern. B) A tendon specimen with a large tear, demonstrating a more irregular, disorganised pattern of collagen fibres, with some loss of crimp. Scale bar represents 100µm.

Generally increased tear size resulted in higher Riley histological grades, indicating increased disruption of collagen fibre bundles and organization, with reduced regularity and loss of crimping patterns and abnormal nuclei appearances (see Table 3-4). The histology supported the FTIR findings that suggested disruption of collagen structures and organisation in torn tendons. Increasing tear size was also associated with higher Movin scores and showed increased proteoglycan abundance and decreased proteoglycan structural integrity. There was strong concordance between both examiners, as the interobserver coefficient of concordance for Riley's score was found to be 0.83 ($p = 0.001$).

Table 3-4. Histological analysis of different tear sizes. Average Riley grades and Movin scores are shown below for each tear category. Riley's histological grade describes collagen structure and the extent of degeneration, as grade I (normal), grade 2 (mid degeneration),

grade 3 (moderate) and grade 4 (severe). Movin's score here describes the glycosaminoglycan appearance only as 0 (normal), 1 (slightly abnormal), 2 (abnormal) and 3 (markedly abnormal).

	Normal	Partial	Small	Medium	Large	Massive
Riley's Grade	1.40	1.54	1.44	2.11	2.76	3
Movin Score	0.52	1.0	0.9	0.94	1.4	1.64

3.5 Discussion

The use of FTIR allowed the demonstration that normal and different sized rotator cuff tears have different and distinguishable chemical properties. This is the first study, to my knowledge, that uses FTIR to assess the chemical composition of normal and different sized rotator cuff tendons. The biological changes associated with tears are a critical element in both healing and tear propagation. Some insight is offered into the chemical alterations that may underlie structural and mechanical changes and predispose to tendon failure and the inability to withstand loads even after surgical repair. The results suggest that the onset and progression of rotator cuff tendon tear pathology primarily involves disruption and conformational alteration in collagen structural arrangements, with associated changes in proteoglycans and elastin. It is not possible to be certain whether the biological changes preceded the tear, or were a reactive change to the tears. However it is plausible that some of the ECM changes will have occurred in response to mechanical or biological insults, and thus weakened the integrity of the collagen-matrix lattice structure, making tendons more prone to rupture. The structural changes suggested by the FTIR correlated with the histological analysis showing a progressive alteration in collagen and proteoglycan structure and organization.

The collagen spectra primarily correlates with its peptide bond vibrations, which arise from Amide A, I, II and III [284]. This study has identified structural changes in these peptides in torn tendons. As collagen fibres are predominantly responsible for the tensile strength of tendons, and collagen structure correlates with mechanical parameters, the collagen structural changes identified here are likely to translate into decreased tensile strength [289]. The intermolecular cross-linkages contribute to various mechanical parameters such as tensile strength and viscoelasticity, thus alterations of collagen structures in torn rotator cuff tendons may disrupt these cross-linkages and thus impair tendon mechanics. This could account for weakness and inability to perform household tasks after development of rotator cuff tears [27] and the improvement in function and strength [38] seen following successful tendon repair.

Varying reductions in collagen type I, II and III were detected. FTIR has previously been used to differentiate between collagen I and collagen III [290]. Previous rotator cuff tendon studies have also described decreased collagen levels [67] and this may predispose to rupturing as a correlation between collagen density and tendon strength has been demonstrated [291]. Many studies looking at collagen subtypes have studied a much earlier time period since the tears, unlike this study where the average duration of symptoms was 18 months. Using a rabbit model, Hirose *et al*., demonstrated increased type I collagen in tear edges until 3 weeks only [235]. Increased mRNA levels of collagen I precursors were found in full thickness rotator cuff tendon tears for up to 4 months after injury [292]. These findings are supported by the observations of Riley *et al*., [67] who also detected a reduction in collagen III in torn human rotator cuffs. Increased collagen III has been detected in only the first week of healing in one study [235]. It has been proposed that

in scar tissue there is an initial increase in type III collagen, whereas a gradual increase in type I collagen is seen during maturation and healing [293, 294], and any reductions in torn tendons may reflect decreased healing and scar formation. Increased levels of collagen III have been identified at normal canine rotator cuff insertion sites which coincide with areas of greater stress and compression [295]. Collagen II is less commonly found but is associated with the fibrocartilage at the osseotendinous junction, and areas of the tendon undergoing compression [141]. The absence of load and compression in the chronic tears studied in this study may explain the reduction in collagen II and III. Despite changes in subtypes of collagen, an overall decrease in collagen was not found in this study, which is supported by similar findings by Riley *et al.* [74]. It can be postulated that early healing, and initiation of repair is therefore indicated by an increase in collagen III, whereas a later increase in collagen I indicates maturation, and a return to baseline ratio levels indicates completion of the attempted repair process.

Furthermore, this study demonstrated changes in proteoglycan structures, but not amounts between different tear groups. The proteoglycan changes were confirmed by histology. In contrast Riley *et al.*, reported an increase in glycosaminoglycans in chronic rotator cuff tendionpathy [74] and Frank *et al*., found a decrease in decorin at the edges of tendon tears [296]. It is possible that ECM changes may be the initial insult or event that reduces the ability of tendons to withstand tension and transmit loads at the collagen-matrix interface, thus predisposing to rupturing. It has previously been proposed that tendon degeneration occurs when the tendon's elastic capability is overcome by recurrent minor strains [297]. The matrix within which the collagen fibres are embedded allows one collagen subfibre to interact with another, and increases the stiffness against

bending and transmits shear forces at the fibre-matrix interface [270]. Alterations in proteoglycans are likely to have important consequences as they are thought to play a role in resisting compressive forces. Altered levels of MMPs and tissue inhibitors of matrix metalloproteinases (TIMPs) [141] have been demonstrated in torn tendons. Modulation of this pathway may have potential treatment implications, as inhibition of MMPs was shown to improve histological healing, but interestingly there was no difference in mechanical properties [158]. While supraspinatus tendons have high levels of chondroitin sulphate and decorin [74], no changes in either were detected between the tear groups. Thus changes to other chemical components may be more critical in the development and extension of tears. The findings of alterations in the lipid composition and increased elastin are supported by previous findings demonstrating fatty infiltration in rotator cuff degeneration, particularly in the larger tears [276].

Importantly, a number of previous studies have indicated that larger tears are more likely to re-rupture [35]. It is possible that the collagen and ECM structural changes suggested by this study may reflect an imbalance between synthesis and degradation. Smaller tears have been shown to have higher healing rates postoperatively than larger tears [21]. The edges of smaller tendon tears have been shown to have higher metabolic rates and presumed viability, as well as increased cellular activity in comparison to larger tears [125], thus smaller tears may have a better ability to repair any ECM structural damage [127].

Further investigation will be required to examine whether biochemical alterations might result in altered healing rates and/or higher failure rates. This study has provided extensive qualitative data but was limited in the ability to extract quantitative data. Another limitation is that FTIR lacks

specificity for many types of proteins due to the strong spectral overlap of some of their common features, such as proteoglycans and collagen, which can make differentiation between the two groups more difficult. Infrared has a limited penetration of only a few microns, limiting it to assessment of superficial surface tissue and possibly missing un-observed biochemical variations at greater depth. The spectra for each of the different tear sizes were not completely distinct and some overlap between the different groups was observed. It is possible that there is a continuum of underlying chemical changes and hence each tear size is not completely or reliably distinguishable chemically. One possible explanation for the lack of good agreement between the two classification systems could be the natural chemical variance that may occur within each tear group. Some error may have been introduced during classification of tear size, as tears are 3-dimensional entities, which are sometimes judged in a 2-dimensional plane when repaired arthroscopically. It is likely that extremes, such as normal, small and massive tears are much easier to visualise, and this may explain the strong crossover between partial, medium and large tear groups. Due to the relatively small number of surgical repairs of partial tears, there was a smaller sample size of 7 partial tears compared to the larger number in other categories. Formalin preservation was shown to have a levelling effect on spectral readings and differentiation of diseased tissue is much more apparent when using fresh tendons, but nonetheless formalin preservation did not prevent differentiation between different groups. Regardless of any effect of formalin, as all specimens were preserved in formalin it was assumed that formalin effects would have been uniform across all specimens. While attempts were made to find appropriate controls, the average age of normal tendons was slightly lower (59 years) than torn tendons and this may be a confounding variable. Age however did not significantly vary between the different tear groups,

and a specific analysis looking at age as an independent variable did not find any effects of age. A previous histological study also reported that even at an advanced age, significant difference in degeneration existed between ruptured and non-ruptured supraspinatus tendons [110].

This current cross sectional study provides insight into the disease process at a single time-point. Further longitudinal studies would provide some insight into disease progression, and underlying chemical changes. These changes may help to identify disease earlier and monitor response to treatment and disease progression, for example on biopsies taken in an out-patient setting. To date the earliest detection of rotator cuff tendon tears has relied upon imaging which show gross anatomical tears. There is currently no method for identifying early extracellular biochemical changes *in-situ*. As larger tears are associated with higher failure rates, one could argue there is a need for earlier diagnosis and intervention for rotator cuff tendon tear pathology. FTIR is advantageous as the approach is non-destructive, reagent-free and relatively quick and theoretically all chemical components of the tissue are assessed without presuppositions about likely chemical content. This study has focused on changes at the edge of the rotator cuff tendon, and it may be useful to see how far back within the tendon these biochemical changes extend using FTIR spectral mapping. FTIR probes have been developed, which means that this technique could be used to study tissue *in-vivo* [46], and potentially intraoperatively to demarcate the extent of diseased tissue. In the future a larger study combining unfixed biopsy samples and ideally, *in-vivo* measurements and outcome imaging would further help to delineate chemical changes involved in tendon tears and healing.

However this may be, understanding possible differences between different tear sizes is an important question to address, and this study has demonstrated significant chemical differences in tissues that surgeons are trying to treat and repair. Understanding these changes is important as they may play a role in the biological response to any form of treatment or intervention. This study is a useful preliminary study that establishes FTIR as a tool that can be used to differentiate chemical features of rotator cuff tears.

4 CHAPTER 4: CHARACTERISATION OF THE COLLAGEN THERMAL PROPERTIES OF NORMAL AND TORN ROTATOR CUFF TENDONS USING DIFFERENTIAL SCANNING CALORIMETRY

4.1 Abstract

4.1.1 Introduction

The pathophysiology of the high failure rates often observed following rotator cuff tendon repairs, particularly massive tears, is not fully understood. Rotator cuff tendons are predominantly formed of collagen, and conformational and structural changes in collagen have been shown to alter tendon thermal and mechanical properties. Increased cross-linking of collagen has also been shown to result in stronger mechanical properties. Differential scanning calorimetry allows the study of collagen structure and integrity, as collagen undergoes detectable conformational and chemical changes during heating. This study aimed to form a quantitative rather than qualitative assessment, of whether differences in collagen structure and integrity existed between small biopsies of normal, small and massive rotator cuff tears using differential scanning calorimetry.

4.1.2 Methods

Thermal properties were measured for 28 human biopsies taken intra-operatively from normal, small, and massive rotator cuff tendon tears in this powered study. Rotator cuff tendon biopsies

were taken from the edges of 8 small (< 1cm) and 9 massive tears (> 5cm) during surgical repairs and frozen. 11 normal control tendons were also obtained. 3 samples were taken from each patient, weighing 0.5 mg each. During the denaturation experiments the specimens were heated at a rate of 2°C per minute, between 20-80°C with 0.318°C amplitude. The modulation amplitude was 0.613. Denaturation temperatures are represented by T_{onset} (°C) and T_{peak} (°C). The T_{onset} is proposed to represent water-amide hydrogen bond breakage and resulting protein backbone mobility. T_{peak} reportedly corresponds to the temperature at which the majority of proteins fall out of solution. Denaturation enthalpy (ΔH) should correlate with the amount of triple helical structure that is denatured. Fluorescence and light microscopy allowed quantitative validation.

4.1.3 Results

Small and massive rotator cuff tears had significantly higher T_{onset}, T_{peak} and ΔH compared to controls ($P < 0.05$). Polarized light microscopy of torn tendons confirmed greater collagen structural disruption compared to controls.

4.1.4 Conclusion

These novel findings suggest greater quantifiable collagen structural disruption in rotator cuff tears, compared to controls. This study offers insight into possible mechanisms for the reduced strength of torn tendons and may explain why repaired tendons fail to heal.

4.2 Introduction

Repairs of massive rotator cuff tendon tears have higher failure rates than small tears [38]. A multistage model of rotator cuff tears has been suggested, wherein tear size has been shown to affect both the cellular and extracellular matrix composition of the torn tendon edge [125]. Further understanding of changes in the extracellular matrix composition of rotator cuff tendon tears may offer insight into differences in healing and failure rates, and help to guide research into treatment strategies. Characterising human rotator cuff tears can enhance our understanding of the complex degeneration occurring in chronic tears, which animal models cannot fully replicate.

As collagen is the primary constituent in rotator cuff tendons, and my FTIR studies have suggested that rotator cuff tears are associated with structural changes within collagen, I wanted to further investigate and try to quantify the potential effects of changes within collagen. Differential scanning calorimetry (DSC) is a useful technique to characterise structural properties of very small (0.5 mg, approximately 2 x 2 x2 mm) human tendon biopsies that are sampled intraoperatively as thermal properties are inherent to a material and hence much less affected by sample size or shape. DSC measures the thermal properties of materials and allows quantification of the thermal effects of local and global changes in complex protein structure and integrity, during heating [298, 299].

A differential scanning calorimeter measures the heat of a sample relative to a reference. This process if performed while the sample is heated with a linear temperature ramp. Practically, DSC measures the heat flow (endo or exotherms) associated with transitions in materials as a function of time and temperature, within a controlled atmosphere [298]. These measurements can provide

both quantitative and qualitative information about physical and chemical changes within specimens.

Quantitative analysis of composite materials using DSC has been traditionally used in a number of industries such as the pharmaceutical industry to assess purity, the food industry to characterise fats and oils, and the polymer industry to provide a structural fingerprint of materials such as minerals, clays and polymers. Many biological tissues, such as tendon, can be considered as heterogenous composite materials, which is why DSC is an interesting technique to apply to the study of tendons.

The thermal properties of materials are measured by DSC and it allows quantification of subtle conformational and chemical changes in structure and integrity as a function of temperature [298]. DSC can be used on small samples to understand tendon structure, where mechanical tensile testing cannot be reproducibly undertaken. As DSC is quantitative, it has an advantage over other qualitative tissue analysis techniques such as histology, which are subject to interpretation errors.

Understanding the temperature based denaturation of hydrated proteins in tendons is useful, as it serves as a theoretical analogue to denaturation which can also occur due to mechanical stresses and changes in the chemical environment [280]. As collagen is heated, its triple helix structure changes into amorphous random coils, which causes the collagen to contract by up to one third [300, 301]. This can be detected as it produces a sharp endothermic peak at a defined temperature. DSC has previously been used to examine connective tissue collagen changes such as additional

glucose mediated covalent cross-links and changes in triple helical content in collagen type IV [302].

Changes in mechanical strain and cross-linking have been shown to alter the thermal properties of collagen, suggesting that these are useful parameters to measure. As collagen is the primary component of rotator cuff tendons, accounting for 65-80% of its dry weight, it is possible that tendon structure and mechanical properties may be affected by any collagen conformational changes that occur in tears. It has been previously demonstrated that mechanical overloading of bovine tendon resulted in reduced collagen thermal stability [303]. The structure and mechanical properties of collagen are affected by the extent of collagen cross-linking. Zeeman *et al*., demonstrated that dermis which had increased collagen cross-linking was associated with increased tensile strength and strain modulus [304]. Proteolysis has also been shown to induce thermal changes in tendons [305] and denaturation of collagen fibers (due to damage) has previously been shown to result in a reduction in denaturation enthalpy (ΔH) [306].

Ruptured Achilles tendons from ten cadavers have been shown to have reduced thermal properties (denaturation and melting temperature, and denaturation enthalpy) compared to four controls [307]. DSC has been used to investigate muscle proteins, and is sensitive enough to clearly differentiate between different functional and structural states of different muscles [78, 308]. A significant reduction in the endotherm of the detached group was reported when compared to the controls, and attributed to unfolding of the myosin heads [202]. However many studies have investigated protein solutions, rather than investigating intact functional muscle proteins in their native state. Although no direct DSC study of human rotator cuff tendons has been reported to

date, DSC examination has been performed on 37 rat normal and detached rotator cuff muscles [202]. Szabo *et al.*, studied long head of biceps tendons from human cadavers with or without rotator cuff tears and reported that long head of biceps tendons with associated massive rotator cuff tears had a decrease in the onset of denaturation and an increase of denaturation enthalpy (ΔH) [309]. This was suggested to be due to increased amounts of collagen and increased secondary cross-linking between collagen fibres. DSC has also been used to investigate other orthopaedic problems such as cartilage [310] and vertebral discs [311].

Improved understanding of the structure of tendon at a molecular level is important as tendon function is determined by its structure and composition. It is hoped that a greater understanding of the structural changes and pathophysiology underlying different sized rotator cuff tears will help to identify effective and appropriate treatment strategies. This study aimed to quantify if differences in collagen structural integrity and thermal properties varied between different sized rotator cuff tears when compared to normal rotator cuffs.

4.2.1 Hypothesis

- It was hypothesized that massive rotator cuff tendon tears will have different collagen structural compositions and thus altered thermal properties compared to normal rotator cuff tendons.
- It was also hypothesized that using DSC massive tendon tears can also be differentiated from smaller tendon tears, and this may partly explain higher failure rates in repairs of

massive tears.

4.3 Methods and Materials

28 human rotator cuff tendon biopsies were taken intra-operatively from the edges of chronic rotator cuff tears during surgical repair. Specimens measuring approximately 2 x 2 x 2 mm were classified according to size and 8 small (< 1cm) and 9 massive tears (>5 cm) were obtained. All tears were chronic, with a minimum of 8 months duration, and no difference was found in duration since onset of symptoms amongst small and massive tear groups. There was no significant difference in the number of previous steroid injections between the two tear groups, and all patients had two or fewer injections, and the last injection was at least two months prior to surgery. 11 age and gender matched, normal control tendons were obtained from patients undergoing open shoulder operative procedures with no complaints of rotator cuff problems (e.g. stabilization) and in whom the tendons had a grossly normal macroscopic appearance. Approval for the study was obtained from the local research ethics review committee, and all patients gave informed consent. Specimens were immediately snap frozen by placing them in liquid nitrogen and stored at -80^{o}C. No preservative agents were used, such as formalin, as they can be flammable when heated to high temperatures.

All frozen tendon specimens were thawed for 15 minutes and gently dried. Three samples were taken from each patient, weighing 0.5 mg each (+/-0.01 mg). Careful attempts were made prepare all the samples uniformly, and they were kept as thin as possible to minimise thermal gradients,

and to cover as much of the pan as possible. Specimens were carefully cut to avoid crushing. Calorimetric measurements were taken using a differential scanning calorimeter TA Instruments Q2000, equipped with an intra-cooler (TA Instruments Inc., New Castle, DE). Tendon specimens were placed in hermetically sealed conventional Tzero™ DSC pans to prevent any liquid loss during heating to avoid changes in thermal behaviour.

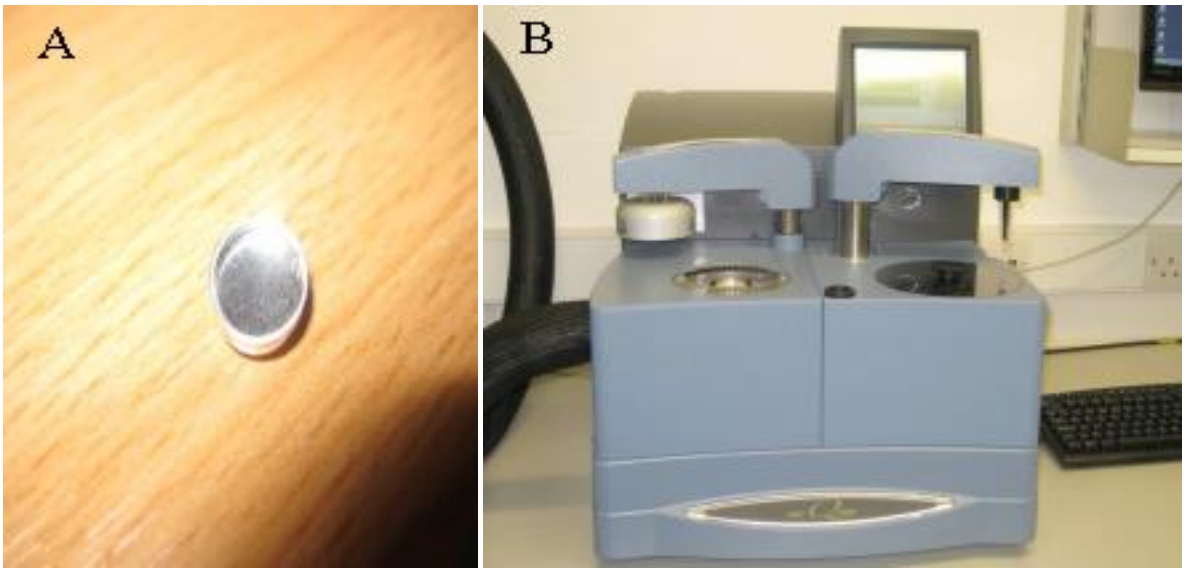

Figure 4-1: A) Photograph of a T0 aluminium pan, in which tendons are placed and heated. B) Photograph of a differential scanning calorimeter TA Instruments Q2000 DSC.

The heat capacity calibration was performed by heating the sample at the same time as heating an empty aluminum vessel, which was used as a reference point. The heat capacity calibration was performed with Tzero™ Sapphire standards, and Indium was used for temperature calibration due to its fixed melting temperatures. During the denaturation experiments, the samples were subjected to a modulated temperature ramp between 20-80^{o}C at a rate of 2^{o}C per minute with 0.318^{o}C amplitude of modulation. Modulated DSC allows a composite heating profile to be obtained. This allows determination of the heat capacity of the sample that is studies and any lag,

as well as separation of heat flow reversible and non-reversible components. Modulated heating is advantageous as it offers increased sensitivity by eliminating baseline curvature and drift, as well as increased resolution as two heating rates are applied so an average can be taken. Reversible transitions include melting, whereas evaporation of water is a non-reversible component.

All DSC related thermal parameters were obtained from thermograms (see Figure 4-2). The T_{onset} , T_{peak} and the denaturation enthalpy (ΔH) were measured, and are all related to denaturation [280].

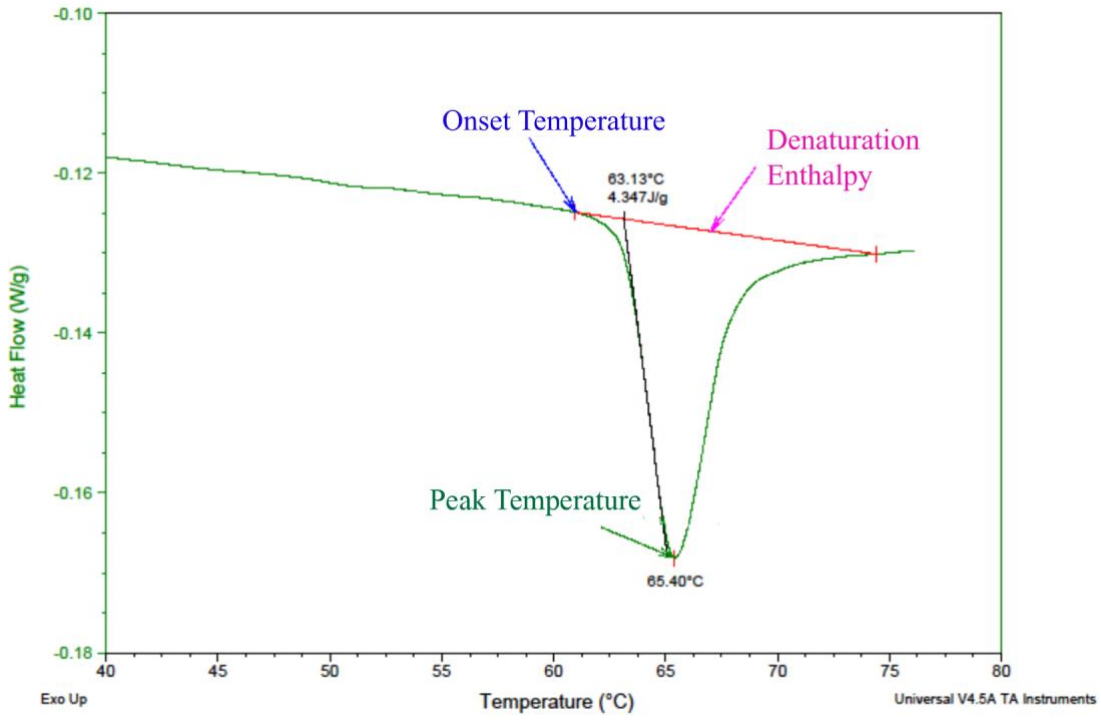

Figure 4-2: DSC themogram showing results from heating a supraspinatus tendon.

T_{onset} (^{o}C) is defined as the onset of the endotherm on the thermogram. This is proposed to represent breaking of the amide-amide hydrogen bonds, resulting in increased mobility of the

protein chain backbone and resulting in a ordered to disordered transition [280]. During heating the collagen molecules within tendon specimens undergo a sudden and specific helix to coil transition [300]. This can be detected as it produces a sharp endothermic peak at a defined temperature. The T_{peak} (^oC), is the peak of the endotherm, and reportedly corresponds to the temperature at which the majority of proteins fall out of solution i.e. when water is removed from hydrogen-amide bonds. The denaturation enthalpy, ΔH (J/g), was calculated as the area under the heat absorption curve by using two-point peak integration. ΔH is a measure of the energy required to fully denature all the collagen present and is thought to correspond to the relative amount and distribution of triple helical structure within the sample [312] and is independent of heating rate [298]. ΔH is independent of the scanning rate [298]. ΔH corresponds to the relative amount of triple helical structure in the samples [312, 313] and thus the mean triple helix content of torn tendons (T) can be calculated with respect to normal intact tendons (N); $\Delta H_T / \Delta H_N * 100$. To prove that the changes seen were due to heating, a heat-cool-heat experiment was performed.

4.3.1 Determining Experimental Conditions

Experimental settings were determined during a pilot study. To determine the test parameters human tendons taken from the elbow extensor common origin were used as these are similar to rotator cuff tendons, and avoided wastage of limited rotator cuff tendon specimens. I studied the effect on rotator cuff tendon thermal properties of varying some of the experimental parameters. Factors studied included changing the temperature range, type of seal used on the pan (single or double lid, and hermetically sealed or not), whether the specimens were heated in a modulated

manner or not, sample mass and the heating rate. I found that changes in the sample mass, type of heating (modulating or not) and type of seal affected the consistency of the results. Previous studies have supported my findings and also indicated that samples mass and type of heating both influence melting temperature [307]. Only a single lid was used, and the pans were hermetically sealed. Most of the interesting thermal changes occurred between 20-80^{o}C, which is why this temperature range was chosen. I decided to take 0.5 mg specimens, as this was a weight that I could consistently reproduce during my specimen sections. I also decided to heat the tendons in a modulated manner, at a rate of 2^{o}C per minute with 0.318^{o}C amplitude, as described above.

4.3.2 Statistics

Based upon a pre-study power calculation this study has 90% power to detect a 10% difference in the T_{onset} and T_{peak} temperature between groups, with a 5% level of error (alpha < 0.05). A Shapiro-Wilk normality test was performed and confirmed a Gaussian data distribution. Examinations to determine the effect of tear size on heat related parameters were performed using a one-way ANOVA test. A student's unpaired t-test with a Bonferroni correction was used to compare groups (small tears, massive tears and normal tendons). All tests were two tailed and a $p < 0.05$ was considered significant. All data analysis was run using the GraphPad Prism 5 software package (GraphPad Software Inc, La Holla, CA).

4.4 Histology

In order to confirm that changes were occurring in the collagen composition, polarised light microscopy was used to validate the DSC results. This allowed quantitative validation of changes in collagen organisation. Polarised light microscopy is a useful technique for tendon analysis as the alignment of collagen molecules means the fibres are birefringent, and this technique has previously been described for the assessment of tendon fibre orientation and structural integrity [314, 315]. Thus it is possible to visualise fibres, their arrangement and fibre angles.

One specimen per patients was taken, frozen and later cryosectioned for quantitative validation. 6-10 μm sections were cut. The collagen structural composition of tendon sections was determined using a fluorescent collagen binding probe 5-([4,6-dichlorotriazin-2-yl]amino)fluorescein (DTAF) for demonstration of collagen fiber integrity [316]. The sections were stained with 5-DTAF at a concentration of 20 ug/ml for 15 minutes. The specimens were then placed under a polarized light microscope and the number, alignment and integrity of the collagen fibres were determined [317]. Specifically, sections were mounted and imaged with Blue epifluorescence excitation using a EC Plan-Neofluar 10x/0.50 Ph2 M27 objective of a Zeiss Axio Imager M1 (Carl Zeiss MicroImaging, Thornwood, NY) coupled to AxioCam HR3 camera with exposure time of 50 ms. Images of DTAF labelled sections (1388 x 1040 pixels) were obtained (at fixed gain and off set and underwent 8 bit digitization with ImageJ software (National Institute of Health, Bethesda, Maryland). DTAF fluorescence associated with collagen was depicted by gray scales from 0 to 255. Higher gray scales signify more organised collagen. Within a give image 6 rectangular areas (25,000 um^2) were randomly chosen and the grey scales were measured (mean $\pm$ standard

deviation) with the ImageJ software. To minimize sampling error at least 6 to 12 sections of each specimen were examined. Representative DTAF labelled samples were also imaged using Zeiss LSM 710 (Carl Zeiss MicroImaging, Thornwood, NY) confocal/multiphoton microscope using 488 nm Argon laser.

4.4.1 Results

The T_{peak} temperatures of the three groups of normal, small and massive tears were significantly different ($p = 0.026$, 1-way ANOVA) (see Table 4-1).

Table 4-1: Table summarising the thermal properties of normal tendons, and small and massive rotator cuff tears.

Tendon Type	**Endotherm Peak (T_{peak}, ^oC)**	**Onset of Endotherm (T_{onset}, ^oC)**	**Denaturation Enthalpy (ΔH, J/g)**
Normal Tendons	$63.84 \pm 0.40^{b,c}$	$67.26 \pm 0.41^{b,c}$	$7.94 \pm 0.82^{b,c}$
Small Tears	62.13 ± 1.71^{a}	65.11 ± 0.55^{a}	3.27 ± 0.35^{a}
Massive Tears	62.10 ± 1.54^{a}	64.82 ± 0.47^{a}	4.12 ± 0.58^{a}

The T_{peak} was significantly lower in small and massive rotator cuff tears when compared to normal rotator cuff tendons ($p<0.001$) (see **Figure 4-3**). However there was no significant difference between the T_{peak} of small and massive tears ($p > 0.05$). All data was normally distributed.

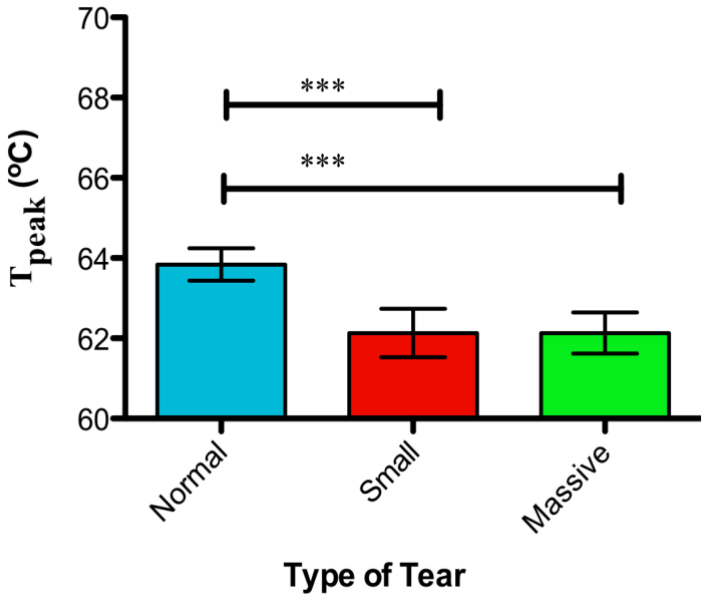

Figure 4-3: Graph showing the T_{peak} temperature of different tendons. Small and massive tears were found to have a significantly lower T_{peak} compared to normal tendons ($p<0.05$, unpaired t-test). **$p < 0.01$. ***$p < 0.001$. Bars represent standard error.

Analysis of the T_{onset} with a 1-way ANOVA revealed that the three groups were significantly different ($p = 0.0012$, see **Figure 4-4**). The T_{onset} was also significantly lower in small ($p=0.005$) and massive ($p =0.001$) rotator cuff tendon tears in comparison to normal tendons. Again, no differences were detected in the T_{onset} between the small and massive tear groups ($p = 0.34$).

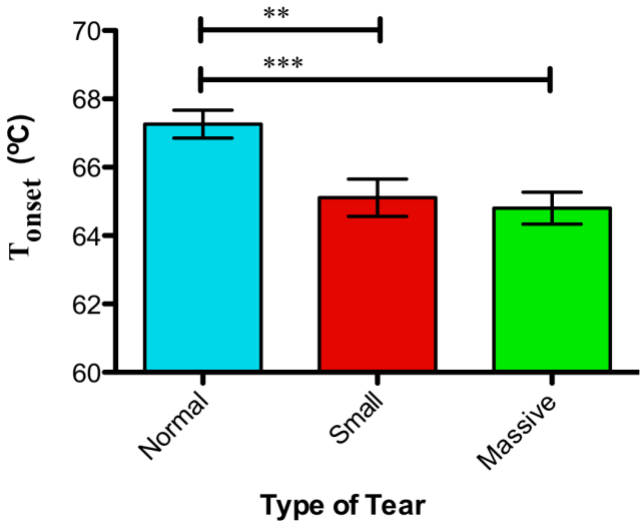

Figure 4-4: Graph showing the T_{onset} of different tendons. Small and massive tears were found to have a significantly lower T_{onset} compared to normal tendons ($p<0.05$, unpaired t-test). **$p < 0.01$. ***$p < 0.001$. Bars represent standard error.

The denaturation enthalpy, ΔH, varied significantly between the three groups ($p = 0.0001$, 1-way ANOVA, see **Figure 4-4**). ΔH of both small ($p=0.0003$) and massive rotator cuff tears ($p=0.0013$) were also significantly reduced when compared to normal rotator cuff tendons. No difference was detected between small and massive tears ($p = 0.168$).

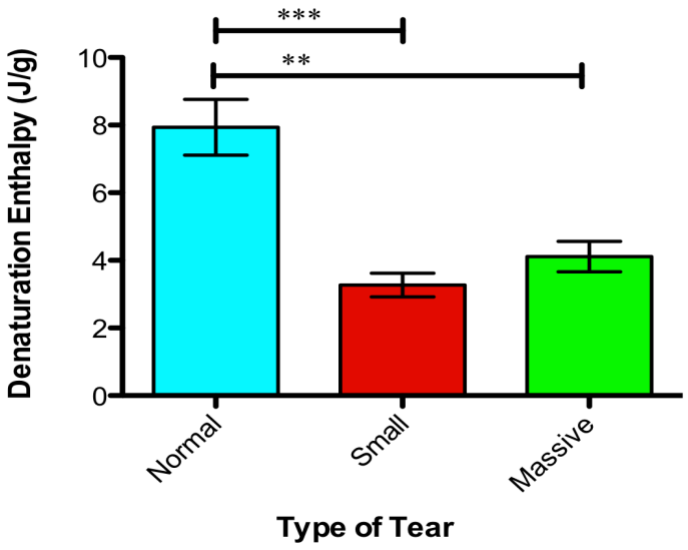

Figure 4-5: Graph showing the denaturation enthalpy of normal and torn tendons. Small and massive tears were found to have a significantly lower denaturation enthalpy compared to normal tendons ($p<0.05$, unpaired t-test). **$p < 0.01$. ***$p < 0.001$. Bars represent standard error.

4.4.2 Histology validation

The high-resolution fluorescence microscopy findings of DTAF stained tendon sections mirrored the DSC findings between normal and torn tendons. Small and massive tendon sections revealed increased disruption of collagen structure and integrity, disorganized collagen bundles and reduced collagen fiber thickness compared to normal tendons ($p < 0.001$, see Figure 4-6). A significant difference was also detected between small and massive tears ($p < 0.01$).

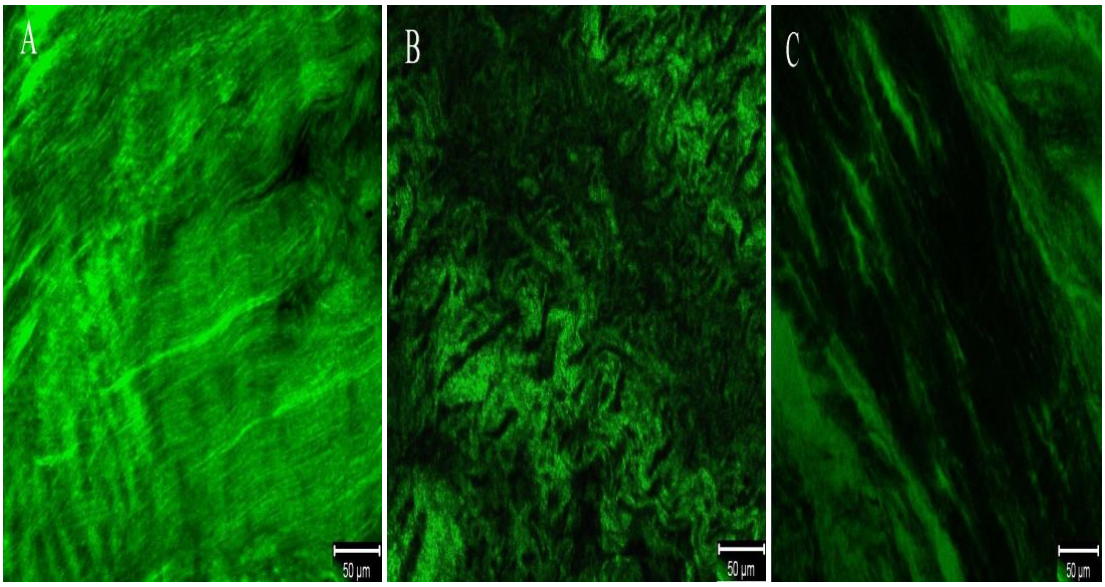

Figure 4-6: Images showing 5-([4,6-dichlorotriazin-2-yl]amino)fluorescein (DTAF) stained fluorescent images of A) normal, B) small and c) massive tendons. Scale bar represents 500µm. A) Normal tendons with collagen fibers and bundles, orientated in parallel and densely packed. Increased structural disruption is visible in B) small tears, with greater discontinuous fibers and spaces between fibers in C) massive tears.

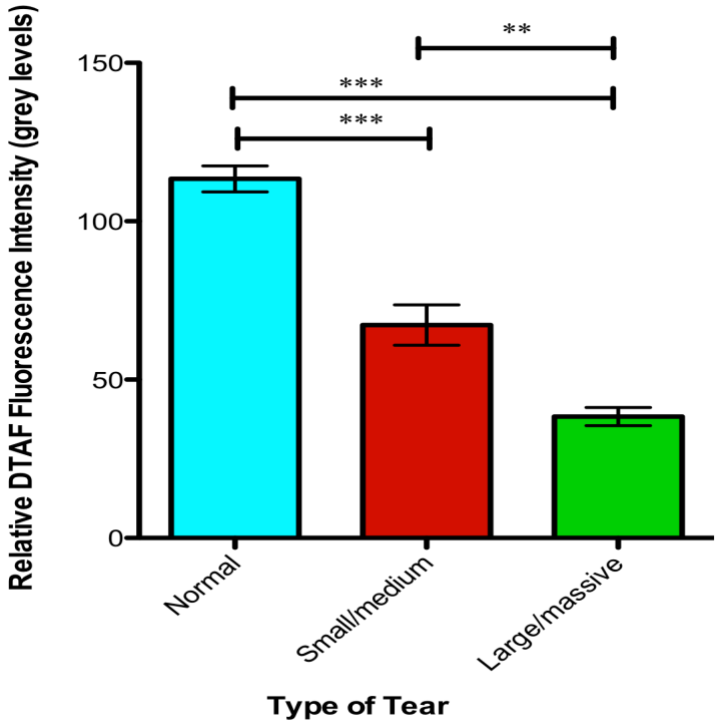

Figure 4-7: Graph showing the relative DTAF fluorescence intensity, measured as grey levels, of normal, small and massive tendons. Small and massive tears were found to have a significantly lower denaturation enthalpy compared to normal tendons. Massive tears had a significantly lower fluorescence intensity compared to small tears ($p<0.05$, unpaired t-test). **$p < 0.01$. ***$p < 0.001$. Bars represent standard error.

4.5 Discussion

This study has demonstrated greater collagen thermal instability and structural disruption in torn rotator cuff tendons, compared to intact healthy tendons. This prospective, non-randomized case control study indicates that the onset of rotator cuff tear pathology is primarily due to alterations in collagen thermal stability that reflect alterations in collagen structural arrangements. However it is possible that these changes may occur as a consequence of the tear, rather than precede the tear. This is the first study to my knowledge, comparing the thermal properties of collagen in

normal and different sized human rotator cuff tendons collected intraoperatively. The T_{peak} of collagen is 65ºC. A decrease in the T_{peak} of torn tendons, suggests that the material is intrinsically less stable. Collagen has a triple helical structure stabilized by 4-hydroxyproline that forms hydrogen bonded 'waterbridges' [298]. It has been proposed that damage to the collagen lattice structure within tendons produces gaps that allow increased collagen mobility, forming the basis of the "polymer in a box" theory [318]. Thus the disrupted tendon fibers have reduced conformational restrictions and require less energy to be denatured. The denaturation has been proposed to start in the less stable parts of collagen, termed the co-operative unit or themally labile-domain [318].

Changes in thermal properties manifest themselves in changes in either the structure or conformation of tendon collagen. As collagen is predominantly responsible for transmitting tensile forces in tendons, it is likely that torn tendons cannot withstand changes in temperature or stress as well as an intact tendon could [289]. Collagen cross-linkage had been previously demonstrated to have an effect on the T_{peak}. The intermolecular cross-linkages contribute to mechanical parameters such as tensile strength and viscoelasticity, and as such alterations of these cross-linkages may impair tendon mechanics. Dermal sheep collagen which had undergone increased epoxy and carbodiimide induced cross-linking, was found to have a higher T_{peak}, as well as increased tensile strength and elongation to breakage [304]. Lee *et al.*, proposed that the T_{peak} is affected by intrahelical cross-links formed between 2 polypeptide chains in the same helix, rather than interhelical cross-links [319]. Willett *et al.*, have demonstrated that the thermal stability of collagen is sensitive to mechanical forces, as stability is reduced simply by overextension rather

than rupture of tendons [320]. Increased initial supraspinatus collagen fiber alignment is important, and a correlation with higher mechanical stiffness has been reported [54].

The reduction detected in the denaturation enthalpy of small and massive tears suggests that the amount of collagen structures and intramolecular bonds varies between different sized tears and normal rotator cuff. As tendons are predominantly formed by collagen, other extracellular components which are present in much smaller proportions are unlikely to affect thermal properties. Willett *et al*., found no change in the denaturation enthalpy following mechanical overloading of bovine tail tendons [303]. Previous studies have proposed that the denaturation enthalpy is altered by breakage of water bonds that stabilize collagen [321]. Collagen density is an important parameter as a correlation between collagen density and tendon strength has been previously demonstrated [291]. However previous studies have reported both increased and decreased collagen levels in torn tendons [67]. In particular varying levels of collagen I and III have been reported, at different stages of healing, which can affect the number of cross links [235, 292]. Tears are often repaired by the formation of scar tissue, with an initial increase in collagen III rather collagen I, and this may contribute to why scar tissue is weaker than normal tendons [293]. As type III collagen consists of smaller, less organized fibrils [322] any increase may result in diminished ability to transmit loads and thus reduced mechanical properties. The disrupted collagen structure detected in torn tendons may be more susceptible to altered levels of matrix metalloproteinases (MMPs) and tissue inhibitors of matrix metalloproteinases (TIMPs) found in rotator cuff tears [141]. This technique allows unique perspective on the fact that tendon tears are associated with changes in collagen structure rather than the amount of collagen.

No differences were detected between the thermal properties of small and massive rotator cuff tears as had been expected, suggesting that collagen thermal stability does not significantly vary between these groups. The significant structural changes detected in small tears could explain previous evidence indicating that even repairs of small tears can have high failure rates [21]. The previously reported differences related to size, such as healing rates, post-operative strength, metabolic rates and cellular activity do not appear to affect tendon thermal properties and collagen structural integrity between small and massive rotator cuff tendon tears [125, 267]. Changes in the biological milieu rather than collagen structure, may make a greater contribution to the effect of tear size on outcomes.

Bank *et al.*, have demonstrated increased collagen turnover and remodelling in normal biceps brachii tendons compared to torn rotator cuffs, as well as changes in collagen cross-linkage [139]. This may result in rotator cuff tendons being more susceptible to alterations in its collagen conformation. The ECM of tendons helps to transmit tensile and shear strength and dictate its mechanical properties. This could account for weakness and inability to perform household tasks [27] after development of rotator cuff tears, and the improvement in function [205] and strength [38] seen following successful tendon repair.

A potential weakness of our study is that freezing the tendons prior to testing may have had an effect on the final thermal property results, although any effect should be uniform throughout all tendon specimens as they were all snap frozen prior to testing using a standardized protocol. However a previous study comparing frozen and thawed human posterior tibial tendons to unfrozen tendons found no significant difference between the T_{peak} or ΔH [237]. Thermal lag can

occur if there are variations in the heating/cooling rates, or for different sample masses, and thus it was hoped that careful standardization of the protocol would avoid such confounding variables.

Further investigation is required to determine the clinical and functional implications of the detected changes, to see if torn tendons with a lower T_{peak} or T_{onset} are more like to result in higher post-operative failure rates or strength. Due to ethical restrictions, small specimens could only be taken from the edge of tears, however it would be useful to examine how far back within the tendon these thermal changes exist. Future studies on cadavers could look for any correlations between thermal properties, and both clinical outcomes and mechanical properties.

This study has demonstrated reduced thermal properties and tendon structural integrity in rotator cuff tendon tears, and offers insight into a possible molecular mechanism for, or adaptation to, rotator cuff weakness and failure. These differences may have been present before the tears occurred as part of a progressive pathological process, or they may have occurred post-rupture in this group of chronic tears in response to altered mechanical loads.

5 CHAPTER 5: CHARACTERISING GENE EXPRESSION PROFILES OF NORMAL AND TORN ROTATOR CUFF TENDONS

5.1 Abstract

5.1.1 Introduction

There is increasing evidence for a progressive age related cellular and extra-cellular matrix change in rotator cuff tendons. Larger tendon tears demonstrate significant structural abnormalities that are likely to adversely influence healing potential. This study aimed to gain greater insight into the relationship of pathology to tear size by analyzing gene expression profiles from normal, small and massive rotator cuff tears.

5.1.2 Methods

The gene expression profiles of 28 human rotator cuff tendons were analyzed using microarrays representing the entire genome. 11 massive and 5 small torn rotator cuff tendon specimens were obtained from tear edges intraoperatively, and compared to 12 age matched normal controls. Real-time polymerase chain reaction (RT-PCR) and immunohistochemistry were performed for validation.

5.1.3 Results

Key gene changes included upregulation of aggrecan in massive tendon tears ($p < 0.05$ and > 2-fold change) but not in small tears. Matrix metallopeptidases (MMP)-3,-10,-12,-13,-15, -21,-25 and a disintegrin and metallopeptidase (ADAMs)-12,-15,-22 were significantly upregulated in tears. Amyloid was downregulated in both tear groups. Small tears also displayed upregulation of BMP-5. Chemokines and cytokines that may play a role in chemotaxis were altered, IL-3,-10,-13,-15,-18 were upregulated in tears, whereas downregulation of IL-1,-8,-11,-27, was seen.

5.1.4 Conclusion

The gene expression profiles of normal rotator cuff and small and massive rotator cuff tear groups differ significantly. This study has identified a number of novel pathways that suggest that rotator cuff tear pathogenesis is contributed to by ECM remodeling genes, chemotaxis genes, aggrecan and amyloid. These gene products may potentially have a role as biomarkers of failure. Modulating these ECM pathways may be a useful treatment strategy for improving clinical outcomes.

5.2 Introduction

Persistently high failure rates following repairs of rotator cuff tears implies a deficiency in biological healing mechanism following surgical repairs. The aetiology of rotator cuff tears is not

a purely mechanical phenomenon, but also involves underlying biochemical changes that are often classified as intrinsic degeneration. There is increasing evidence for progressive biological abnormality of rotator cuff tendons as tear size increases. Both healing and clinical outcome are affected by tear size. Larger tears are associated with poorer scores and function; they are also more likely to re-rupture after surgical repairs when compared to smaller tears [206]. Studies have suggested that the cellular and vascular composition, as well as the metabolism and viability of the torn tendon edge changes significantly as the tear size increases [125]. Recent evidence has highlighted chemical differences between different sized tears, and indicated that rotator cuff tear pathology involves alterations in pre-existing molecular components within tissues such as collagen and proteoglycans, rather than being due to completely new molecular players. However, the underlying pathophysiology and biological milieu of gene expression changes related to rotator cuff tears is not fully understood.

Greater understanding of changes in gene expression associated with rotator cuff tears may provide insight into the aetiology of tear pathogenesis, as well as differences in healing and failure rates. Regulatory changes in genes related to production and remodeling of the rotator cuff extracellular matrix (ECM) are likely to be important determinants of rotator cuff tendinopathy, as they affect structural integrity and the ability to transmit loads. Biomarkers of rotator cuff pathogenesis may assist in earlier disease detection, monitoring of disease and modification of pathology. By identifying modifiable targets related to failure, this important knowledge may help to guide treatment strategies and help to focus future research. Detection of biomarkers may potentially be achieved through microarray analysis of torn and normal rotator cuff tendons.

Microarray technology offers insight into alterations in mRNA transcript abundance, relevant gene expression and pathway involvement. Since it was first described in 1995 [323], microarray techniques have been applied to numerous medical conditions with reported success in classifying disease subtypes and predicting prognosis in breast cancer [324] and multiple myeloma [8]. A major advantage of using microarrays is that it can be used to analyze small intra-operative samples (ng of RNA or DNA) to obtain a wealth of information about large numbers of target genes.

Changes in a limited number of gene expression pathways following rotator cuff tears or tendon degeneration have been previously identified. Millar *et al*. analyzed torn rotator cuff tendon samples taken from rodents and humans and compared them to controls. Significant upregulation of expression was detected for cytokines and apoptosis markers [121, 218] as well as heat shock protein [325]. Schmutz *et al*. identified an increase in atrophy markers in tissue taken from human rotator cuff tears [143]. Microarray analysis of patients with concomitant subacromial bursitis and rotator cuff disease demonstrated increased expression of several cytokine genes (TNF, IL-1α, IL-1β, and IL-6), metalloproteases (MMP-1 and MMP-9) and cyclooxygenases (COX-1 and COX-2) [125]. Changes in MMPs have also been detected in other degenerative tendons; a small study comparing four degenerate human Achilles tendon samples to three normal controls found that MMP-3 was upregulated in the diseased samples [326].

This study aimed to gain greater insight into size related tear pathogenesis by analyzing whether differences exist in gene expression profiles from normal, small and massive rotator cuff tendons tears while performing the first human genome wide microarray analysis.

5.3 Hypothesis

- It was hypothesized that small and massive human rotator cuff tendon tears will have different gene expression profiles compared to normal rotator cuff tendons.
- A secondary hypothesis was that many of the altered genes would be related to the ECM composition, as the ECM plays a fundamental role in tendon structure and load transmission.

5.4 Methods and Materials

5.4.1 Sample Collection

28 human rotator cuff tendon specimens were obtained intraoperatively from the edges of chronic tears of more than 1 years duration, as well as intact controls. The 28 specimens were divided into 3 groups based upon their tear size: normal intact tendons, small/medium (<3 cm, n=5) tendon tears and large/massive (>3 cm, n=11) tendon tears. The torn specimens were divided into two groups to highlight potential differences between two the ends of the tear spectrum. 12 age and gender matched normal controls were obtained from hemiarthroplasties and stabilizations from patients with no history of rotator cuff problems, and normal tendon appearance intraoperatively. Tendon samples was obtained from the Oxford Musculoskeletal BioBank and were collected with informed donor consent in full compliance with national and institutional ethical requirements, as well as the UK Human Tissue Act.

5.4.2 RNA isolation

The specimens were immediately stored in RNAlater® (Qiagen, California, USA) for RNA preservation at room temperature for a few hours, then at 4°C overnight, as per the manufacturer's recommendation. Specimens were then stored at -80ºC until later analysis. RNA was extracted using the RNeasy® Lipid Tissue Mini Kit (Qiagen, California, USA), according to the manufacturer's instructions (see Appendices for detailed protocol). This mRNA isolation method has been previously described by Reno *et al.*, [327]. In brief, frozen tissue in RNAlater® was thawed and the RNAlater® liquid was removed. The tissue specimens were reduced to a powder using liquid nitrogen pre-cooled mortars (VWR, Leicestershire, UK). 1 mL of a tissue lyser, TRIzol® (Sigma-Aldrich, Dorset, UK) reagent was added to the tissue powder to homogenise it further. Tissue was incubated at room temperature and 200 µl of chloroform was added, vigorously shaken for 15 seconds, and centrifuged at 12,000 g for 15 minutes at 4°C. The upper aqueous phase (600 µl) was removed to another tube, then 600 µl of 70% ethanol was added and the sample was vortexed, washed and sequentially purified. Finally, the extracted RNA was dissolved in RNase-free water and eluted. All RNA samples were stored at -80ºC, until sufficient numbers were collected to run the microarrays.

5.4.3 Determining High Quality RNA Yields

The total RNA content was quantified fluorometrically using SYBR Green II fluorescent RNA dye and compared to standard calf liver ribosomal RNA concentrations using a fluorescence spectrofluorometer. As tendons are relatively acellular, it was a challenge to extract large quantities of high quality RNA from the small size of human tendon specimens that could be obtained intraoperatively due to ethical limitations. The quality of the extracted RNA was determined using a Nanodrop spectrometer and an Agilent (Berkshire, UK) bioanalyser [328]. RNA integrity number (RIN) was used as a measure of RNA quality [329]. A great challenge in this tendon study was that it is difficult to extract large quantities of high quality RNA from tendons, as it is relatively acellular. The issue was further been compounded by the small size of tendon specimens, due to ethical limitations when sampling human tissue. To ensure adequately high quality RNA, only specimens with an RNA integrity number of greater than 6.8 were used based upon recommendations by Schroeder et al. and the Agilent technologies RNA integrity database, although there is no universally accepted RIN number for tendon samples (http://www.chem.agilent.com/rin/_rinsearch.aspx) [329].

The initial quality control assessment of some samples revealed poor qualities, as some of the samples showed phenol contamination, which was detected by absorbance at 270 nm. Therefore ethanol precipitation was performed on all samples for continuity, and a repeat quality control was performed using the Nanodrop spectrophotometer and Agilent bioanalyser. This resulted in much higher yield and better quality RNA that was suitable for hybridisation (see Appendices). 64

samples were initially collected for this study, however finally RNA of sufficient quality for use with microarrays was only obtained from a total of 28 out of the 64 samples.

5.4.4 Microarray Technology

5.4.4.1 Microarray Sample Labelling and Hybridisation

This study represents the first reported genome wide gene expression profiles of human rotator cuff tendons. RNA was reverse transcribed into cDNA and then complementary RNA (cRNA) using biotin labelled ribonucleotides (see Figure 5-1). Fragmentation of the cRNA probes produced smaller RNA probes that were ready for hybridisation. All the samples were hybridised on 8 Agilent 4 x 44,000 human expression slides (AMADID 014850), as per Agilent's One-Colour Microarray Gene Expression Analysis (Quick Amp Labelling) protocol (version 5.7). The microarrays were prepared and processed by Sandra Lam, a technician from Oxford Gene Technology (Begbrooke, Oxford, UK). The RNA was then fragmented at 60°C for 30 minutes and the reaction was stopped by the addition of 2X Agilent revolutions per minute (RPM) hybridisation buffer. The samples were loaded onto the arrays and hybridised at 65°C for 17 hours at 10 RPM. The slides were then washed and scanned as per Agilent's protocol, using triton supplemented wash buffers.

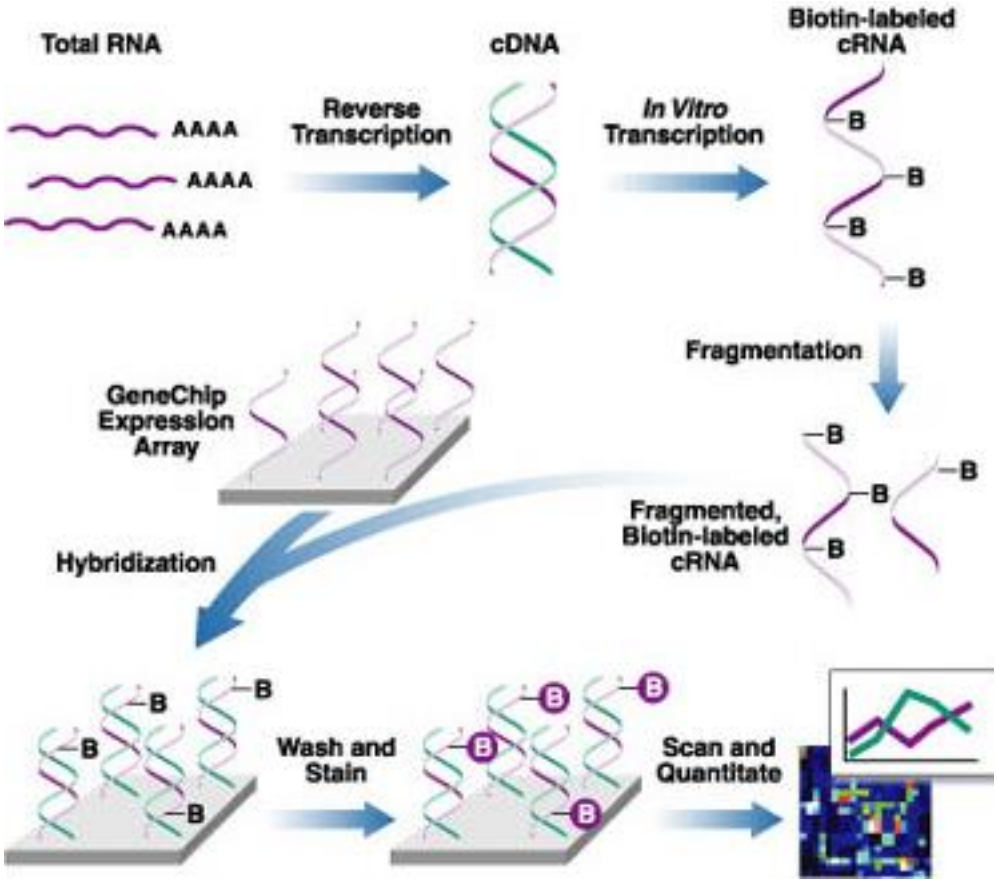

Figure 5-1: Diagram outlining the processes involved in microarray technologies. Total RNA is reverse transcribed. Eventually the fragmented cRNA hybridised to the gene chip arrays, and degree of binding is measured by fluorescence of each gene probe. Image taken from Centre for Functional Genomics website (http://www.cfgbiotech.com/microarray/genechip_expression.htm).

5.4.4.2 QC and Normalization

In order to process the microarray images representing different intensities, the microarray platforms were scanned. Fluorescent intensity data was read from the arrays using a scanner and the signals were converted using Agilent Feature Extraction software (version 10.5) (see Figure

5-2). The fluorescence data was then imported using Agilent's GeneSpring GX software (version 11.0.2).

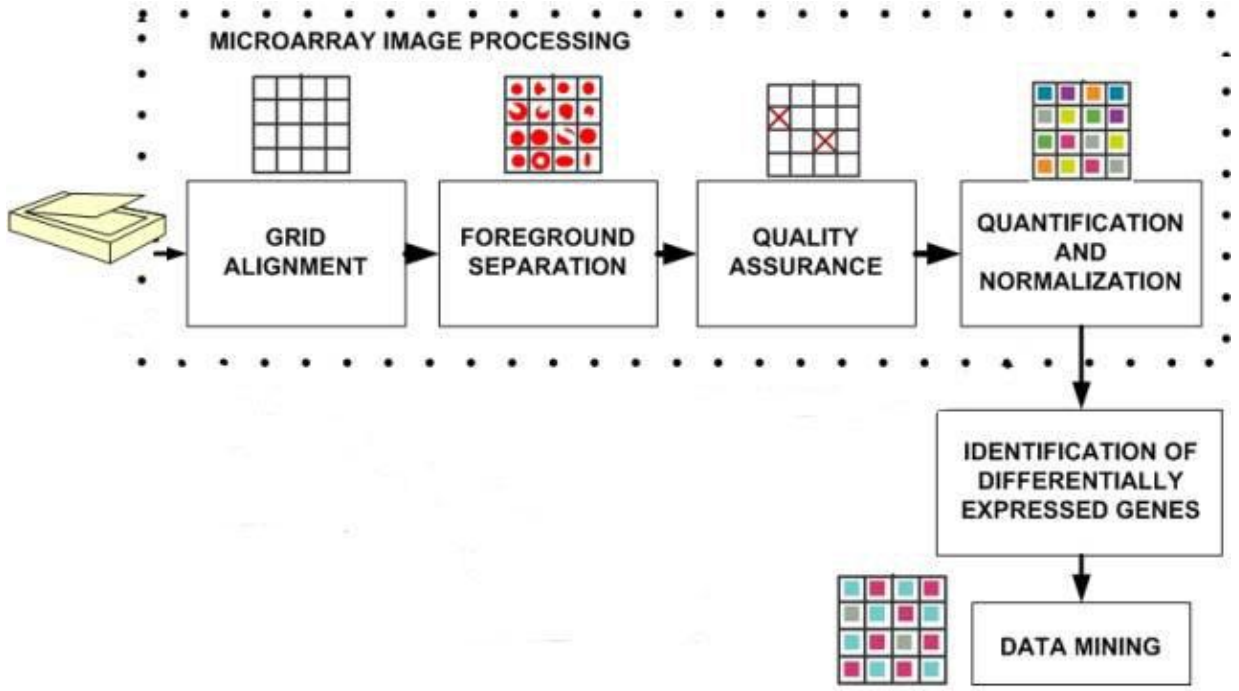

Figure 5-2: A schematic representation of the steps involved in analysing microarray images. These steps include (1) Grid Alignment Problems, (2) Foreground Separation, (3) Quality Assurance, (4) Quantification and (5) Normalization. This image was taken from the Image Spatial Data Analysis Group website (http://isda.ncsa.uiuc.edu/Microarrays/).

To correct for systematic differences in intensities across each array, a standard technique of 'spatial detrend' normalization was performed. Intensity values for all slides were centered to the 75th percentile of expression to correct for global intensity differences between arrays (pre-normalisation figures are shown in Figure 5-3, and figures following normalisation are shown in Figure 5-4). Probe data was converted to data at the gene level by taking the arithmetic mean of intensities across probes for the same gene. Quality filtering was applied to remove spots with

low signals. Only probes with readings of acceptable quality (intensity greater than 20 Relative Fluorescence Units) were deemed to pass this quality control. 28 microarrays were run with more than 44,000 probes that hybridised with fluorescent labelled cRNA, which were detected by scanning. A total of 18,688 of 41,076 unique probes passed this filter and were used in subsequent analysis. Of the unique probes, 26,227 were gene expression probes i.e. not control probes. Ultimately, gene expression profiles were generated for the three categories of tissue damage: normal, small/medium and large/massive.

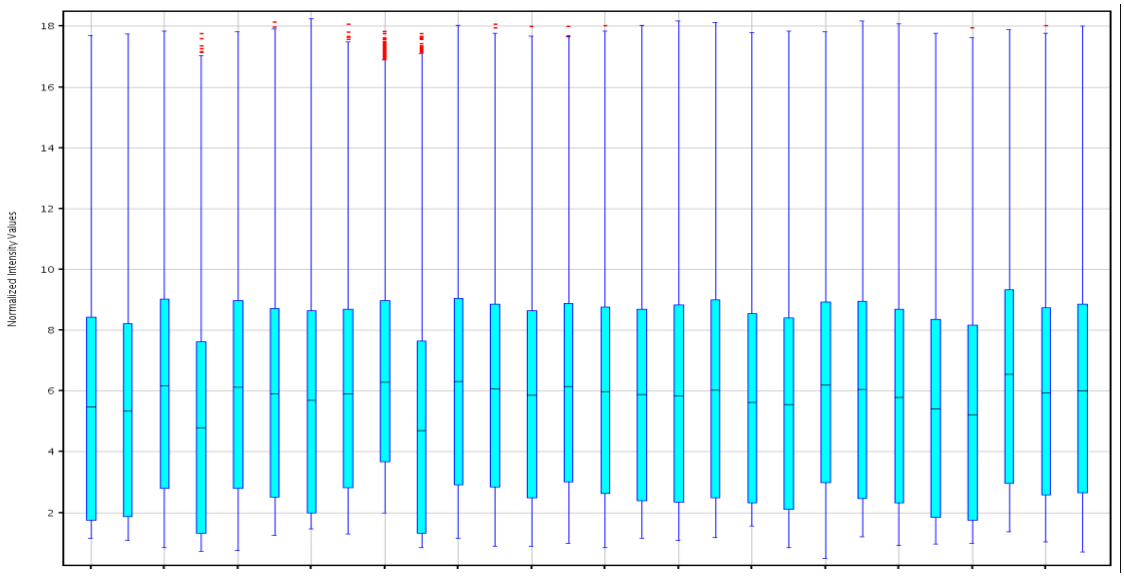

Figure 5-3: Pre-normalisation box plot showing the distribution of all probe intensity data for all QC passed arrays before normalisation. Y-axis is log2 of intensity, boxes cover the 25th to 75th percentile with horizontal line being the median. Vertical lines extend to 1.5 times the inter-quartile range. Outliers are plotted in red.

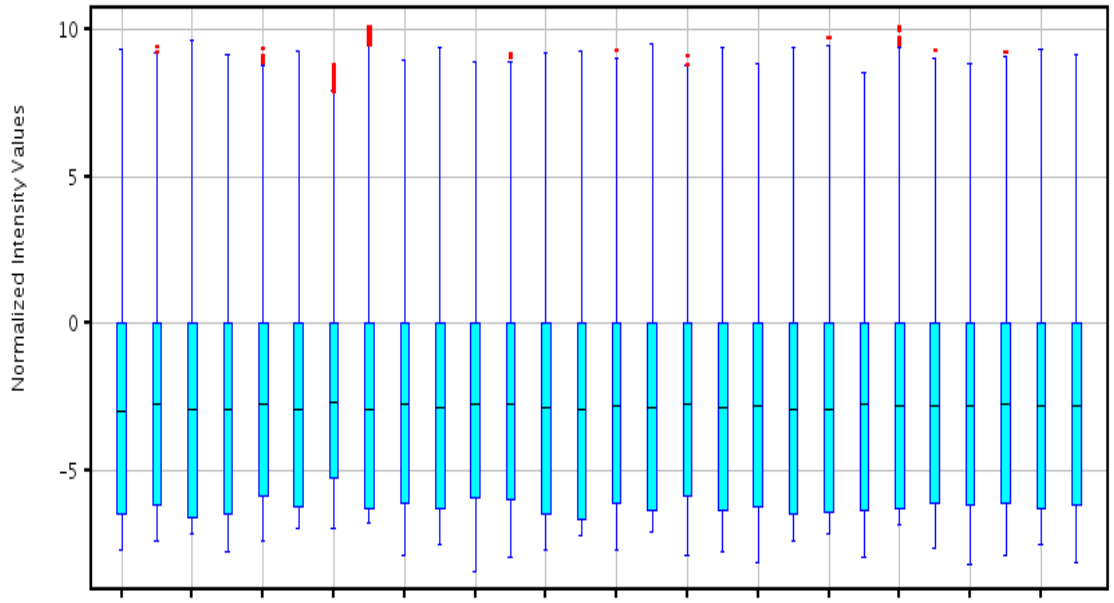

Figure 5-4: Boxplots showing the distribution of all probe intensity data for all QC passed arrays before and after normalisation. Y-axis is log2 of intensity, boxes cover the 25th to 75th percentile with horizontal line being the median. Vertical lines extend to 1.5 times the inter-quartile range. Outliers are plotted in red.

5.4.4.3 Data Analysis

To determine the number of specimens required to adequately power this study, a review of similar published microarray studies with reported pre-study power calculations suggested that a minimum of 6 [330] and 10 [218, 325] samples per group were needed; however no details of the calculation were available.

To identify differentially expressed genes between the three groups, a Mann-Whitney test was used with a greater than 2-fold change and a significance threshold of p-value of <0.05. Initially the data was analysed using unsupervised methods to determine whether there is an internal

structure to the data that indicates relationships within the data. Hierarchical clustering of the samples and mRNA expression was carried out using Euclidian distance, with distances calculated between cluster averages. To assess changes in specific pathways and functional groups, the microarray data was analysed using Gene Ontology (GO) terms and with Gene Set Enrichment Analysis (GSEA).

Further data analysis and maps of signalling pathways related to each of the gene groups were generated using Ingenuity Pathways Analysis software (version 4.0) (Ingenuity Systems, Redwood City, California, USA).

5.4.4.4 Validation with Reverse Transcription PCR (qRT-PCR)

To validate altered genes and tendinopathy related pathways suggested by the microarray, real-time quantitative polymerase chain reaction (qRT-PCR) was used to confirm changes in expression for a selected number of genes. Specifically, five genes related to ECM regulation were investigated: matrix metalloproteinase (MMP)-3, interleukin (IL)-8, a disintegrin and metalloproteinase (ADAM)-15, forkhead box (FOX)-F2 and aggrecan (ACAN). Validated human primers were purchased from Qiagen (Chatsworth, California, USA) that were designed to cross introns to decrease any nonspecific amplication due to potential genomic DNA contamination. In view of the limited RNA obtained from each specimen, validation studies were performed using RNA obtained from other disease and phenotypically matched patients. It was believed that this would increase the robustness of the validation, if it could be demonstrated that the gene changes

detected by the microarray are applicable to all patients with the same phenotypically matched disease patterns.

RNA was extracted from rotator cuff samples and reverse transcribed using the Qiagen QuantiTect SYBR green PCR kit, as per the manufacturer's instructions. Aliquots of cDNA were amplified in a total volume containing primers to detecting the target transcript in addition to the SYBR green master mix containing PCR buffer, dNTP mixture, and Taq DNA polymerase (see Appendices for protocol).

QPCR was performed using a Rotorgene 3000. Reactions were incubated at 25°C for 5 minutes, 50°C for 50 minutes then 70°C for 15 minutes. Samples were initially heated to 95°C for 15 minutes, then each sample was run for 35 cycles, with each cycle lasting for 15 seconds at 94°C, then 30 seconds for annealing. Finally the samples were heated for 30 seconds at 72°C. Duplicates of each sample were run. Quantitative comparison of expression levels was performed using Rotorgene software version 1.7 (Qiagen, Sussex, UK).

To ensure successful reverse transcription, the concentration of cDNA was normalized relative to a housekeeping gene. A panel of potential housekeeping gene candidates were run to find the most suitable candidate, and included TATA box binding protein (TBP1), hypoxanthine phosphoribosyl-transferase (HPRT), ß$_2$-macroglobulin, and glyceraldehyde-3-phosphate dehydrogenase (GAPDH) [326]. A minimal cycle threshold (C_T) method was used to ensure that accurate amplification had occurred. Reactions were quantified by calculating the average delta C_T (DC_T) value of the samples, and used as a calibrator to determine relative expression for each

individual samples. A student's t-test was used to calculate differences between the groups.

It was necessary to confirm with immunohistochemistry that the gene changes measured actually resulted in altered protein level expression, as it is possible that proteins may undergo post-translational modifications. Age, disease and gender matched intraoperative tendon samples were snap frozen and cryosectioned into 6-10 μm sections. Sections were stained specifically for MMP-3, bone morphogenetic protein 5 (BMP-5) and serum amyloid (SAA) antibodies purchased from Sigma-Aldrich (St Louis, MO, USA).

5.5 Results

5.5.1 Differences Between the Three Test Groups

Results are presented as a hierarchical cluster analysis (HCA), with each row corresponding to a probe set and each column representing a different patient (i.e. normal, small tear or massive tear) (see Figure 5-5). Each row represents a set of gene expression level and is coloured as red for upregulation and green for downregulation.

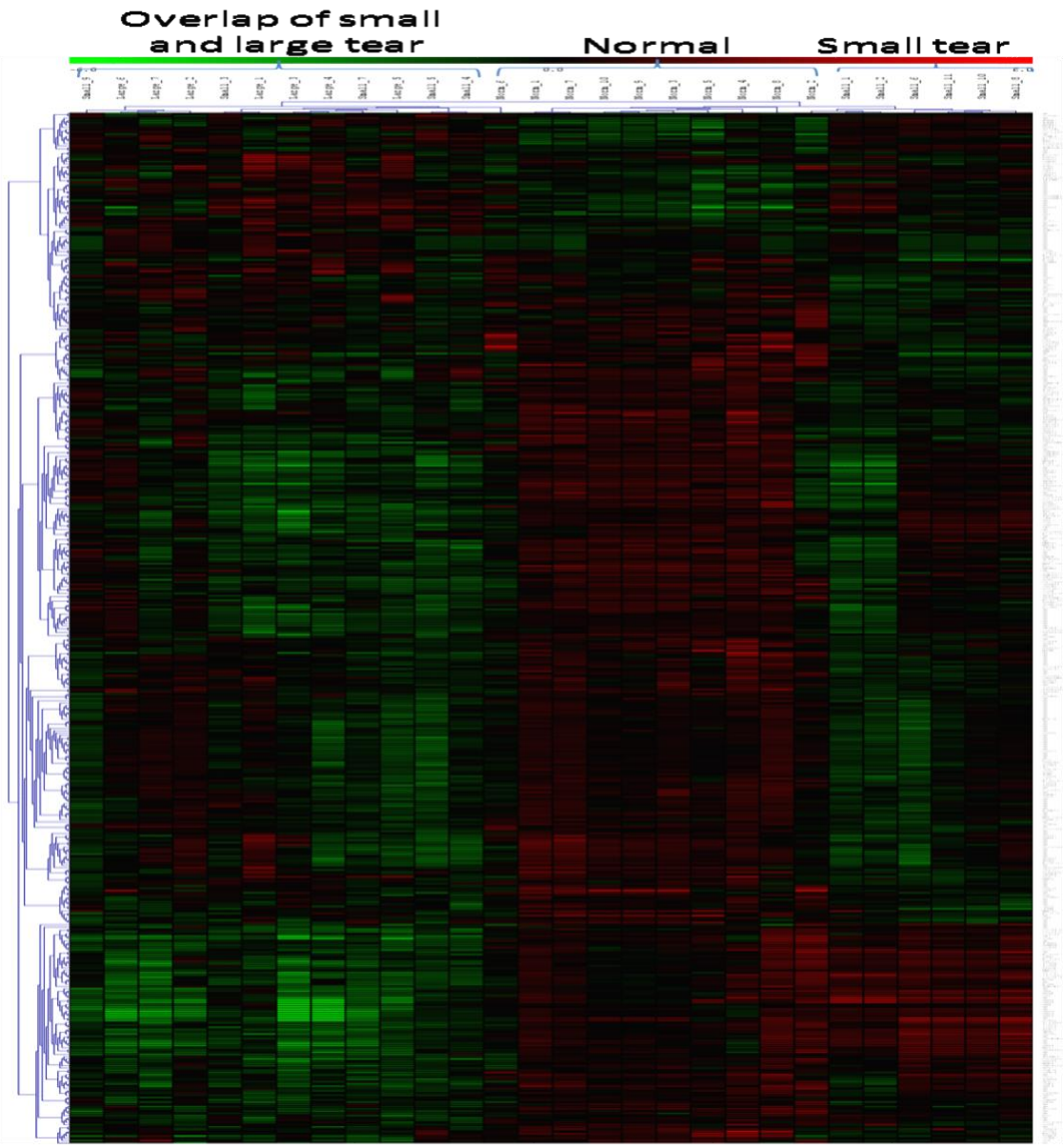

Figure 5-5: **Hierarchical cluster analysis expression profiles of normal, small and massive rotator cuff tendon samples displayed as a heat map. The columns show distinction between normal and all torn tendons, with a small degree of overlap between small and massive tears. Expression profiles are colour coded, with red indicating upregulation and green representing downregulation.**

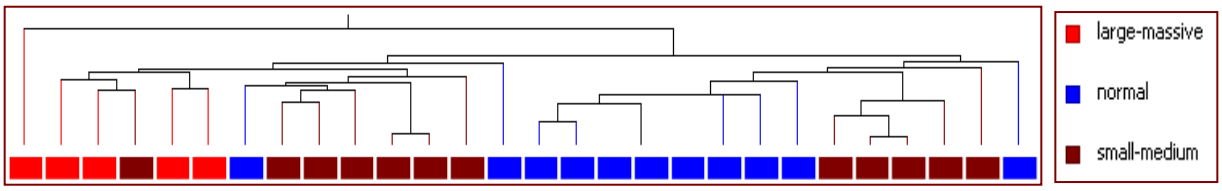

Figure 5-6: Dendrogram showing the clustering of all QC-passed samples, coloured by the tissue damage category. The clustering uses all probes identified as significantly different (uncorrected p<0.05) by a one-way ANOVA from the three sample groups.

Detailed examination of differences between the groups is achieved with the dendogram in Figure 5-6 which allows allow visualization of clustering between different expression profiles [331]. There is clear separation between normal tendons and large/massive tears. However the small/medium tears have clustered as two separate groups, suggesting some differences within this sample group.

Hierarchical clustering of the samples was carried out using Euclidian distance, with distances calculated between cluster averages Figure 5-7. Greater separation between groups correlates with biologically distinct groups. The normal tendons samples appear to be a very distinct group compared to the tear groups. The small/medium and large/massive tears are reasonably well separated, apart from small areas of overlap.

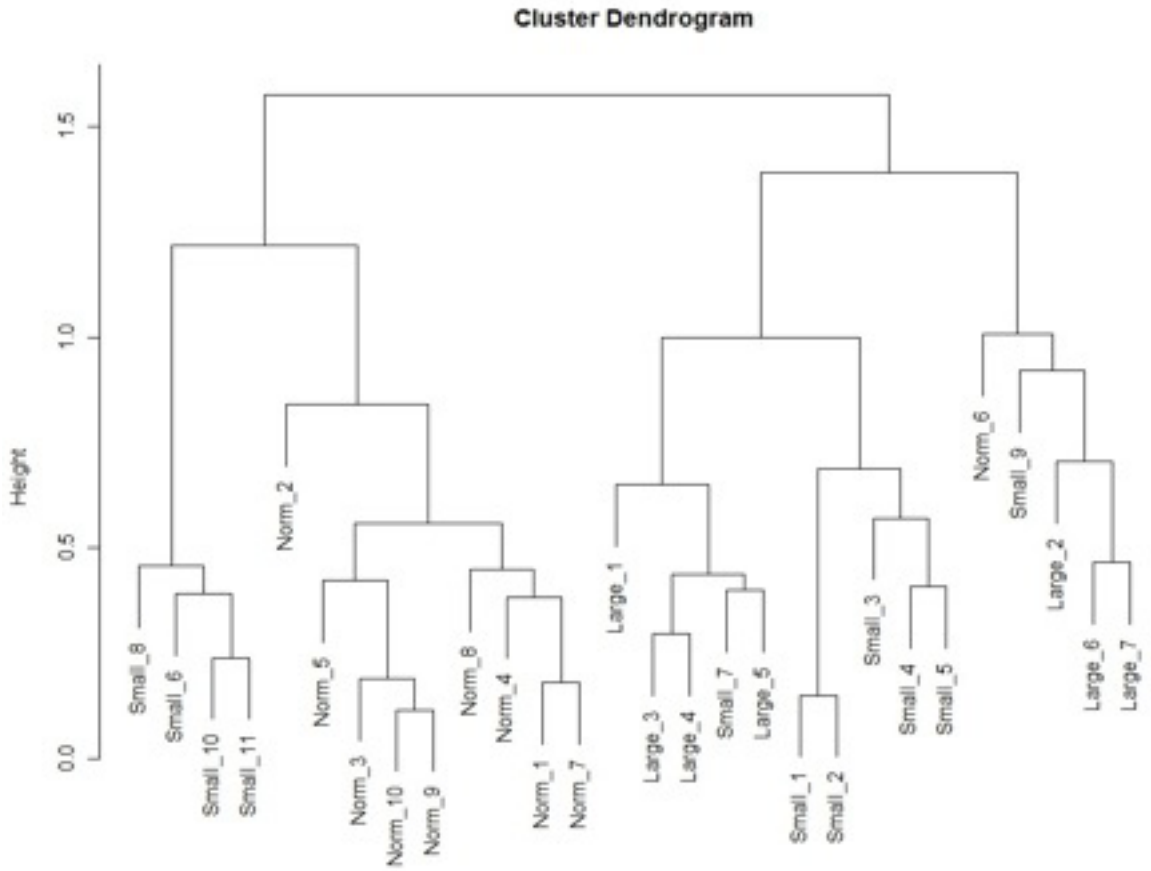

Figure 5-7: A more detailed dendogram displaying clustering of the different specimens, plotted against height to display the degree of relatedness between individual samples. The three groups examined include normal tendons (Norm), small/medium (Small) and large/massive (Large). Greater height indicates greater genetic differences between samples. Generally there is good separation between each of the three groups, although a small area of overlap is seen to the very right of the dendogram.

To further examine how distinct the diseased groups were, a principal component analysis (PCA) was run. The PCA algorithm reduces the dimensions of datasets by projecting samples in a high dimensional subspace to a lower dimensional subspace. This can be used to identify outlier samples and confirm expected experimental results. Looking at just the first two principal

components, the three groups can be clearly distinguished visually in the three-dimensional PCA (see Figure 5-8). The normal tendons are clearly distinct, with no overlap with the other two groups, whereas one of the small/medium and one of the large/massive tear samples appear to be close, although there is no direct overlap.

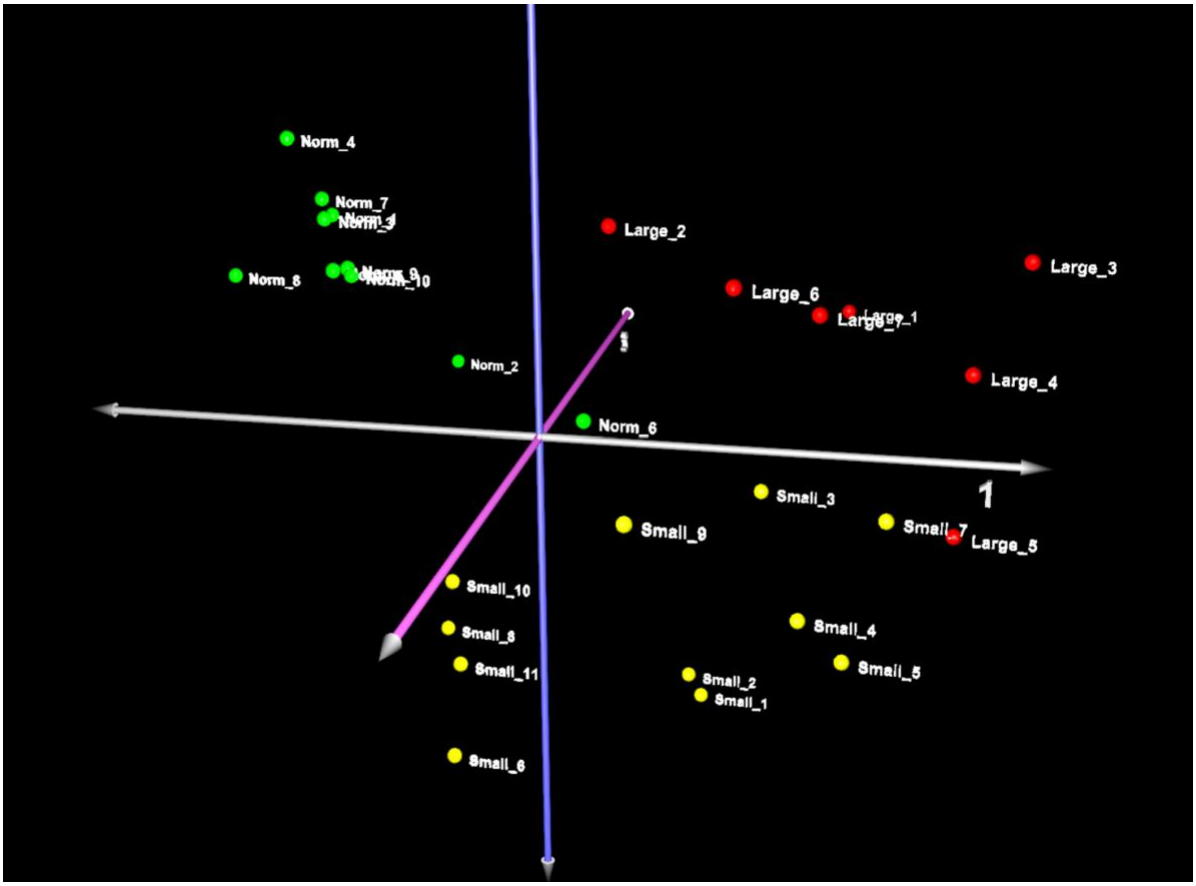

Figure 5-8: A Principal Component Analysis of normal tendons (green, labelled Norm), small/medium tears (yellow, labelled Small) and large/massive tears (red, labelled Large). There is clear separation of the different groups, most clearly seen for the normal tendons.

5.5.2 Differentially expressed genes

Numerous relevant gene changes were detected between normal, small and massive tears, and are represented in a Venn diagram (see Figure 5-9). 165 genes had altered expression between the normal and small tear group, 181 between small and massive tears, and the greatest number of 258 genes were changed in massive tears compared to normal tendons.

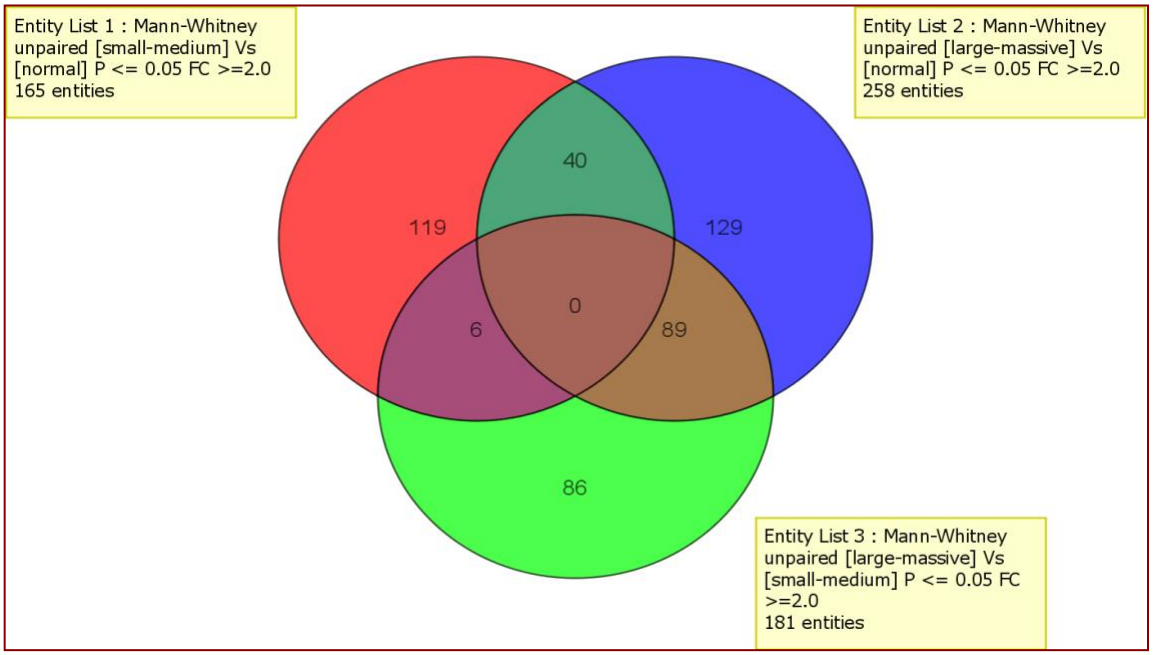

Figure 5-9: Venn diagram showing the numbers of genes common between the differential expression gene lists.

Paired analyses were performed between the subsets of the three groups. For each paired analysis, the most significant changes are represented below as tables, sorted by fold change (see Table 5-1, Table 5-2, **Table 5-3**). A complete list of all gene changes are available in the Appendices, sorted according to p-value.

Table 5-1: Comparison of Top Gene Changes for Small/Medium Tears compared to Normal Tendons, Sorted By Highest Fold Change (Mann-Whitney test). 165 genes were found to be significantly different (p<0.05 AND >2 fold change).

Gene Symbol	p-value	FCAbsolute	Regulation (versus Normal)
BARX1	0.01382302	7.523184	up
CSN1S1	0.031232242	7.1814184	down
SAA1	0.031232242	6.0489206	down
FOSB	0.005613233	5.6334887	down
TUBAL3	0.022774728	4.846784	down
HES5	0.01382302	4.6845655	down
LEP	0.016382353	4.4938235	up
BMP5	0.01382302	4.3528547	up
FLJ10232	5.68E-04	4.2661796	down
SEMA3G	0.01382302	4.1596146	down
CCL19	0.022774728	4.058556	down
MMP3	0.042254012	4.0383816	down
LOC338328	0.042254012	3.8756833	down
NPHS2	0.001106586	3.852058	down
TNNT3	7.12E-04	3.8335028	up
JAG2	0.008133745	3.721596	down
DARC	0.022774728	3.704794	down
KRT12	4.51E-04	3.5443099	up
BMPER	0.005613233	3.4946024	up
TEK	0.042254012	3.4668128	down
MAPK12	0.001372472	3.466109	down
RAMP3	0.008133745	3.4445832	down
GJA4	0.03638887	3.4228203	down
TCL1A	4.51E-04	3.4205365	down
FOS	0.016382353	3.3890395	down
ENST00000303979	0.002088939	3.3888443	down
LY6G5C	0.04889985	3.3603413	down
BP871540	0.026715705	3.3580577	down
DUSP27	0.003134851	3.357478	up
THEG	0.001106586	3.3055768	down
U85992	0.008133745	3.2752311	up
C10orf39	0.016382353	3.2665324	down
TIE1	0.016382353	3.2297635	down
AK092472	0.016382353	3.2287035	down
GNG13	0.001696221	3.185278	down
SNTG2	0.031232242	3.1261804	down
C20orf160	0.011623421	3.1197882	down
LOC728176	0.016382353	3.103184	down

Table 5-2: Comparison of Top Gene Changes for Large/Massive Tears compared to Normal Tendons, Sorted By Highest Fold Change (Mann-Whitney test). 258 genes were found to be significantly different (p<0.05 AND >2 fold change).

Gene Symbol	p-value	FCAbsolute	Regulation (versus Normal)
HBG1	0.001836791	56.466267	down
HBD	0.001836791	46.91802	down
HBA2	0.001836791	41.971424	down
HBA1	0.001836791	40.291943	down
ALAS2	0.002680903	39.97802	down
PPBP	0.001836791	37.239613	down
DEFA3	0.010803687	28.390078	down
PF4	0.001836791	21.017838	down
DQ655984	0.001836791	17.104618	down
CSN1S1	0.047418367	15.883066	down
FLJ22655	0.036097065	15.525827	down
AQP9	0.002680903	15.045649	down
HBQ1	0.001836791	14.857312	down
S100A12	0.001836791	14.062034	down
HBM	0.001836791	12.302959	down
HBB	0.001836791	12.194052	down
S100P	0.001836791	11.875064	down
RGR	0.001836791	11.717697	down
SAA1	0.02716626	11.459341	down
KRT1	0.020210927	9.900101	down
CIDEA	0.002680903	9.227827	down
THC2588392	0.001836791	9.062474	down
IL8RB	0.002680903	8.680703	down
MYH11	0.047418367	8.588229	down
CCL19	0.047418367	8.064544	down
ACTG2	0.02716626	8.047529	down
PPP1R1A	0.001836791	7.745518	down
GZMA	0.007761475	7.642209	down
LOC338328	0.036097065	7.558988	down
GPR109B	0.001836791	7.5222263	down
EPB42	0.002680903	7.2994637	down
PDZK1IP1	0.002680903	7.14159	down
SEMA3G	0.02716626	7.1173387	down
CA1	0.001836791	7.1082807	down
NFE2	0.002680903	7.0264273	down
FCN1	0.010803687	6.8642225	down
LGALS2	0.007761475	6.5456967	down
ITLN1	0.047418367	6.4442015	down
PROK2	0.005510642	6.406212	down
CCL18	0.02716626	6.297678	down
TRBV5-4	0.007761475	6.2009263	down
W60781	0.036097065	6.183622	down
TESC	0.020210927	6.0239167	down
LY6G5C	0.020210927	5.75123	down
IL18RAP	0.002680903	5.4690027	down

Table 5-3: Comparison of Top Gene Changes for Large/Massive Tears compared to Small/Medium Tears, Sorted By Highest Fold Change (Mann-Whitney test). 181 genes were found to be significantly different (p<0.05 AND >2 fold change).

Gene Symbol	p-value	FCAbsolute	Regulation (versus Normal)
HBG1	0.008407991	49.6046	down
ALAS2	0.004426527	34.845467	down
HBD	0.004426527	28.559492	down
HBA2	0.004426527	26.205135	down
HBA1	0.004426527	24.701893	down
DEFA3	0.015333158	21.994802	down
CIDEA	0.004426527	19.636786	down
PPBP	0.001565402	18.66491	down
S100A12	0.001565402	15.250143	down
AQP9	0.004426527	14.952919	down
HP	0.011412037	13.246728	down
PPP1R1A	0.008407991	11.990509	down
HBM	0.004426527	11.771764	down
ITLN1	0.020394841	10.847768	down
DQ655984	0.008407991	10.74847	down
RGR	0.003162764	10.644172	down
HBQ1	0.004426527	10.323473	down
KIAA1881	0.02685669	10.13279	down
KRT1	0.015333158	9.4804735	down
GPR109B	0.015333158	8.861405	down
PF4	0.004426527	8.702475	down
HBB	0.004426527	8.39701	down
CAMP	0.02685669	8.202233	down
PROK2	0.020394841	8.108908	down
EPB42	0.008407991	7.864664	down
S100P	0.008407991	7.6710525	down
S100A8	0.015333158	7.589171	down
IL8RB	0.006131953	7.0360126	down
NFE2	0.011412037	6.747375	down
BI026064	0.006131953	6.2789392	down
ADH1C	0.045201346	6.1649594	down
S100A9	0.008407991	6.089028	down
CA1	0.006131953	5.906948	down
CCL18	0.020394841	5.0003276	down
LMO3	0.045201346	4.85293	down
RGS18	0.001565402	4.7942243	down
S100B	0.045201346	4.773519	down
ALDH1A1	0.006131953	4.730658	down

Key Gene Changes

Given the importance of ECM composition suggested by findings in Chapters 3 and 4, genes related to ECM components were focused upon during the microarray analysis. A number of insightful gene changes were identified between the two groups. Some of the key findings included downregulated expression of genes encoding collagen 4, 12 and 14 in small tears rather than massive tears. In contrast the collagen 9 gene COL9A3 was downregulated in both small and massive tears. With regards to ECM remodelling, MMP-3,-10,-12,-13,-15, -21,-25 and ADAMs-12,-15,-22 were significantly upregulated in tears. Other major changes included upregulation of aggrecan in massive tendon tears compared to normal controls, but not in small tears ($p < 0.05$, > 2-fold change). Serum amyloid A was downregulated in the small and massive tear groups when compared to normals, but was unchanged between the tears groups. BMP-5 was upregulated in small tears only when compared to normals. Some genes related to the FOX family were both up and downregulated.

A number of genes related to the chemotaxis pathway were altered in rotator cuff tears. IL-3,-10,-13,-15,-18 were upregulated in tears, whereas downregulation of IL-1,-8,-11,-27 was noted. Previously reported gene expression changes in heat shock proteins, IL-1, MMP-3 and cyclooxygenase (COX-1) were also detected by this microarray analysis [125]. Common tendon markers such as scleraxis, decorin and tenascin-C were not altered between normal and torn rotator cuff groups. However, tenomodulin showed a >2-fold increase between normal and small tears, as well as between small and massive tears.

5.5.3 Gene Ontology Analysis

In order to identify patterns of gene function within the lists of differentially expressed genes. Gene Ontology (GO) analysis was carried out. GOs are descriptions of the known properties of related gene groups. These descriptions are structured in a complex hierarchy with each level of the hierarchy providing increasingly specific information. The GO analysis calculates a p-value for the 'enrichment' of a GO term within a gene. The output gives a p-value for each GO term found in at least one member of the gene list. This analysis was performed using probe annotations supplied by the array manufacturers. Full lists of the terms that were significantly enriched are found in Table **5-4**.

Table 5-4: Table listing top Gene Ontology Terms looking at specific comparisons between paired groups (normal tendons, small/medium and large/massive tears). Results are sorted by the lowest p-value.

Normal vs Sm/Med	P-value	Normal vs L/Mas	P-value	Sm/Med vs Lar/Mas	P-value
integral to membrane	0.01914922	defense response	4.15E-11	defense response	7.24E-13
				response to stimulus	1.96E-07
intrinsic to membrane	0.01914922	immune system process	4.15E-11	immune system process	3.12E-07
membrane part	0.01914922	multicellular organismal process	6.06E-09	hemoglobin complex	3.80E-07
plasma membrane part	0.020095672	immune response	4.60E-08	oxygen transport	1.61E-06
multicellular organismal development	0.020095672	response to stimulus	4.60E-08	oxygen transporter activity	1.61E-06
membrane	0.020095672	inflammatory response	1.43E-07	inflammatory response	2.01E-06
multicellular organismal process	0.08573657	taxis	3.96E-07	gas transport	3.17E-06
calcium-activated potassium channel activity	0.087526545	chemotaxis	3.96E-07	immune response	4.76E-06
developmental process	0.087526545	response to wounding	5.67E-07	response to wounding	6.81E-06
integral to plasma membrane	0.087526545	locomotory behavior	5.67E-07	response to external stimulus	1.30E-04
intrinsic to plasma membrane	0.093878895	hemoglobin complex	6.58E-07	receptor activity	3.80E-04

An analysis was performed looking at the specific genes associated with the gene ontology pathways. Full results have been included in the Appendices, but a few examples of genes associated with gene ontology pathways of interest, are shown below in Table 5-5. For example a specific focus looked at genes that were altered between large/massive and normal tendons.

Table 5-5: Table examining genes associated with gene ontology terms.

List Name	Gene Ontology term	Gene Symbol	Description	p-value	Absolute fold change	Regulation (versus Normal)
smlMedVsNorm	integralToMembrane	CDH15	cadherin 15, M-cadherin (myotubule)	0.010	2.731	up
smlMedVsNorm	integralToMembrane	ACVR1C	activin A receptor, type IC	0.049	2.215	up
smlMedVsNorm	integralToMembrane	ADORA3	adenosine A3 receptor	0.001	2.884	up
smlMedVsNorm	integralToMembrane	GPR155	G protein-coupled receptor 155	0.012	2.033	up
smlMedVsNorm	integralToMembrane	DCAL1	dendritic cell-associated lectin-1	0.023	2.453	up
smlMedVsNorm	integralToMembrane	NLGN1	neuroligin 1	0.019	2.305	up
smlMedVsNorm	integralToMembrane	PTGIS	prostaglandin I2 (prostacyclin) synthase	0.004	2.009	up
smlMedVsNorm	integralToMembrane	SCD	stearoyl-CoA desaturase (delta-9-desaturase)	0.012	2.780	up
smlMedVsNorm	integralToMembrane	SYT12	synaptotagmin XII	0.049	2.508	up
smlMedVsNorm	integralToMembrane	HS3ST2	heparan sulfate (glucosamine) 3-O-sulfotransferase 2	0.002	2.335	up
smlMedVsNorm	intrinsicToMembrane	CDH15	cadherin 15, M-cadherin (myotubule)	0.010	2.731	up
smlMedVsNorm	intrinsicToMembrane	ACVR1C	activin A receptor, type IC	0.049	2.215	up
smlMedVsNorm	intrinsicToMembrane	ADORA3	adenosine A3 receptor	0.001	2.884	up
smlMedVsNorm	intrinsicToMembrane	GPR155	G protein-coupled receptor 155	0.012	2.033	up
smlMedVsNorm	intrinsicToMembrane	DCAL1	dendritic cell-associated lectin-1	0.023	2.453	up
smlMedVsNorm	intrinsicToMembrane	NLGN1	neuroligin 1	0.019	2.305	up
smlMedVsNorm	intrinsicToMembrane	PTGIS	prostaglandin I2 (prostacyclin) synthase	0.004	2.009	up
smlMedVsNorm	intrinsicToMembrane	SCD	stearoyl-CoA desaturase (delta-9-desaturase)	0.012	2.780	up
smlMedVsNorm	intrinsicToMembrane	SYT12	synaptotagmin XII	0.049	2.508	up
smlMedVsNorm	intrinsicToMembrane	HS3ST2	heparan sulfate (glucosamine) 3-O-sulfotransferase 2	0.002	2.335	up
smlMedVsNorm	membranePart	CDH15	cadherin 15, M-cadherin (myotubule)	0.010	2.731	up
smlMedVsNorm	membranePart	ACVR1C	activin A receptor, type IC	0.049	2.215	up
smlMedVsNorm	membranePart	ADORA3	adenosine A3 receptor	0.001	2.884	up
smlMedVsNorm	membranePart	GPR155	G protein-coupled receptor 155	0.012	2.033	up
smlMedVsNorm	membranePart	DCAL1	dendritic cell-associated lectin-1	0.023	2.453	up
smlMedVsNorm	membranePart	NLGN1	neuroligin 1	0.019	2.305	up
smlMedVsNorm	membranePart	HK2	hexokinase 2	0.027	2.393	up
smlMedVsNorm	membranePart	PTGIS	prostaglandin I2 (prostacyclin) synthase	0.004	2.009	up

smlMedVsNorm	membranePart	SCD	stearoyl-CoA desaturase (delta-9-desaturase)	0.012	2.780	up
smlMedVsNorm	membranePart	SYT12	synaptotagmin XII	0.049	2.508	up
smlMedVsNorm	membranePart	HS3ST2	heparan sulfate (glucosamine) 3-O-sulfotransferase 2	0.002	2.335	up
smlMedVsNorm	membrane	CDH15	cadherin 15, M-cadherin (myotubule)	0.010	2.731	up
smlMedVsNorm	membrane	ACVR1C	activin A receptor, type IC	0.049	2.215	up
smlMedVsNorm	membrane	ADORA3	adenosine A3 receptor	0.001	2.884	up
smlMedVsNorm	membrane	GPR155	G protein-coupled receptor 155	0.012	2.033	up
smlMedVsNorm	membrane	NLGN1	neuroligin 1	0.019	2.305	up
smlMedVsNorm	membrane	NBEA	neurobeachin	0.007	2.021	up
smlMedVsNorm	membrane	HK2	hexokinase 2	0.027	2.393	up
smlMedVsNorm	membrane	LPL	lipoprotein lipase	0.036	2.193	up
smlMedVsNorm	membrane	PTGIS	prostaglandin I2 (prostacyclin) synthase	0.004	2.009	up
smlMedVsNorm	membrane	SCD	stearoyl-CoA desaturase (delta-9-desaturase)	0.012	2.780	up
smlMedVsNorm	membrane	SYT12	synaptotagmin XII	0.049	2.508	up
smlMedVsNorm	membrane	HS3ST2	heparan sulfate (glucosamine) 3-O-sulfotransferase 2	0.002	2.335	up
smlMedVsNorm	multicellularOrganismalDevelopment	DLX5	distal-less homeobox 5	0.019	2.229	up
smlMedVsNorm	multicellularOrganismalDevelopment	BARX1	BarH-like homeobox 1	0.014	7.523	up
smlMedVsNorm	multicellularOrganismalProcess	DLX5	distal-less homeobox 5	0.019	2.229	up
smlMedVsNorm	multicellularOrganismalProcess	KRT12	keratin 12 (Meesmann corneal dystrophy)	0.000	3.544	up
smlMedVsNorm	multicellularOrganismalProcess	LPL	lipoprotein lipase	0.036	2.193	up
smlMedVsNorm	multicellularOrganismalProcess	BARX1	BarH-like homeobox 1	0.014	7.523	up

5.5.4 Gene Set Enrichment Analysis

Gene Set Enrichment Analysis (GSEA) was used as an alternative method of identifying gene functions demonstrating differential expression between the different disease categories. GSEA uses an *a priori* set of lists of genes with associated functions, such as members of a certain pathway, and then calculates for each of these lists the enrichment of genes that are significantly different between the two groups (see Table 5-6).

Table 5-6: Gene Set Enrichment Analysis Terms most altered between normal, small and massive tear groups. The gene count indicates the fraction of genes associated with each GO term that are actually altered between the different groups tested.

Gene Set Enrichment Analysis Term	Gene Count
INFLAMMATORY_RESPONSE	91/130
REGULATION_OF_BODY_FLUID_LEVELS	36/57
LATE_ENDOSOME	11/12
DEFENSE_RESPONSE	176/271
IDX_TSA_UP_CLUSTER6	149/166
DEFENSE_RESPONSE	176/271
POSITIVE_REGULATION_OF_RESPONSE_TO_STIMULUS	27/41
HSA04640_HEMATOPOIETIC_CELL_LINEAGE	59/88
ISOPRENOID_METABOLIC_PROCESS	10/12
STEMCELL_COMMON_DN	53/63

5.5.5 Pathways

Separate pathway maps highlighting the potential relationships between genes involved in normal rotator cuff tendons, small/medium tears and large/massive tears were generated (see Figure 5-10, Figure 5-11, Figure 5-12).

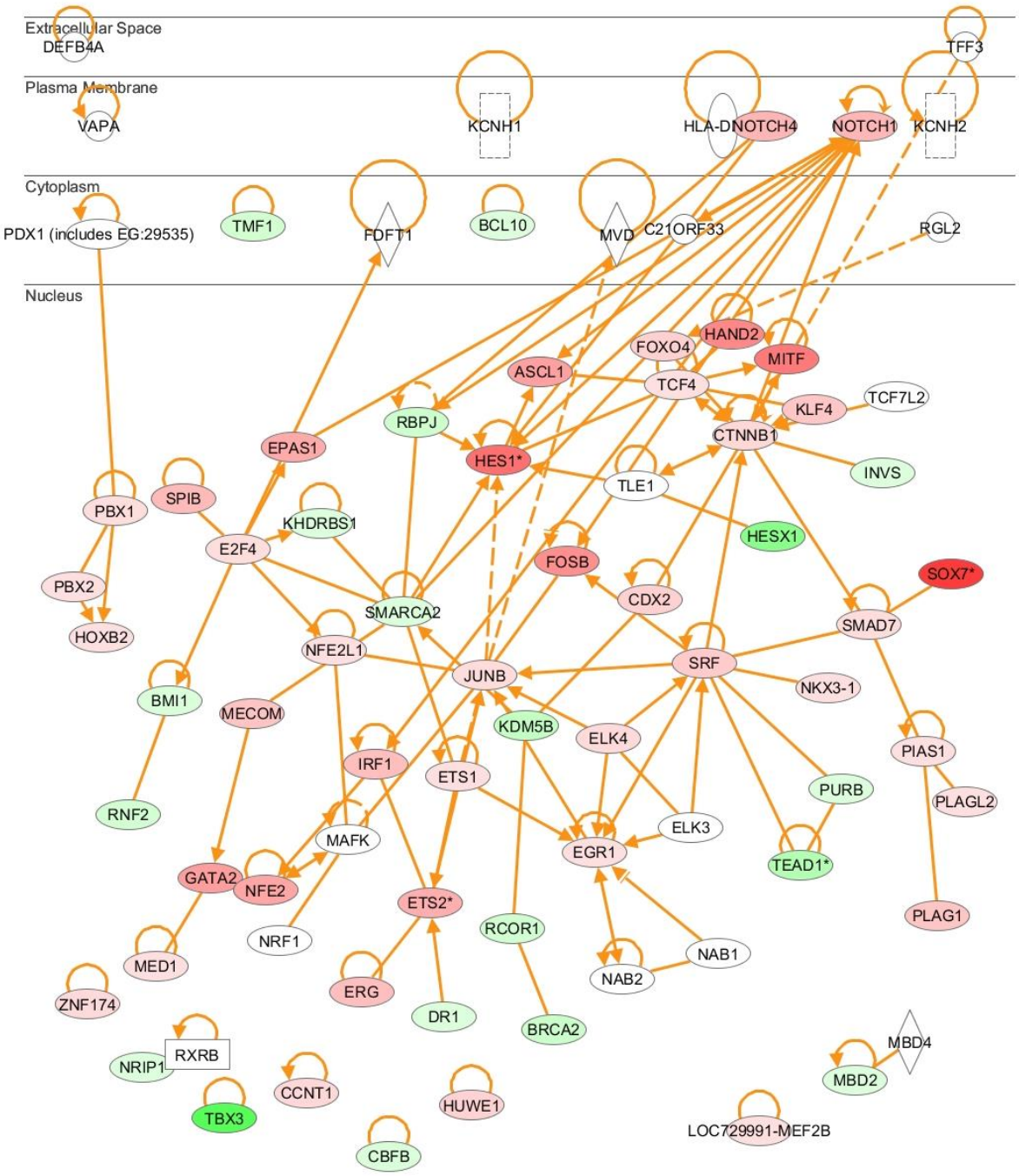

Figure 5-10: Gene expression pathways related to normal tendons. Expression profiles are colour coded, with red indicating upregulation and green representing downregulation.

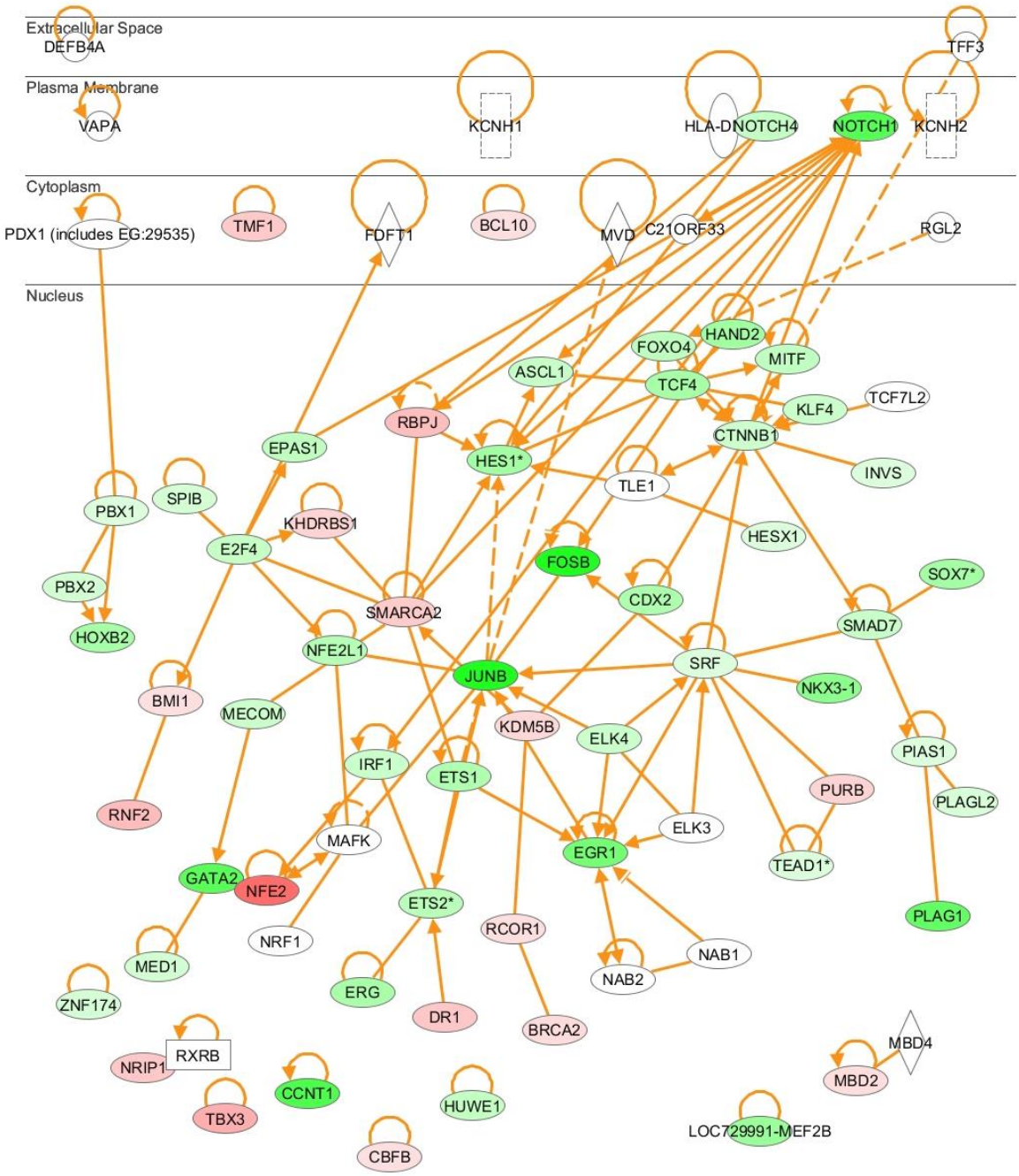

Figure 5-11: Gene expression pathways related to small tears. Expression profiles are colour coded, with red indicating upregulation and green representing downregulation.

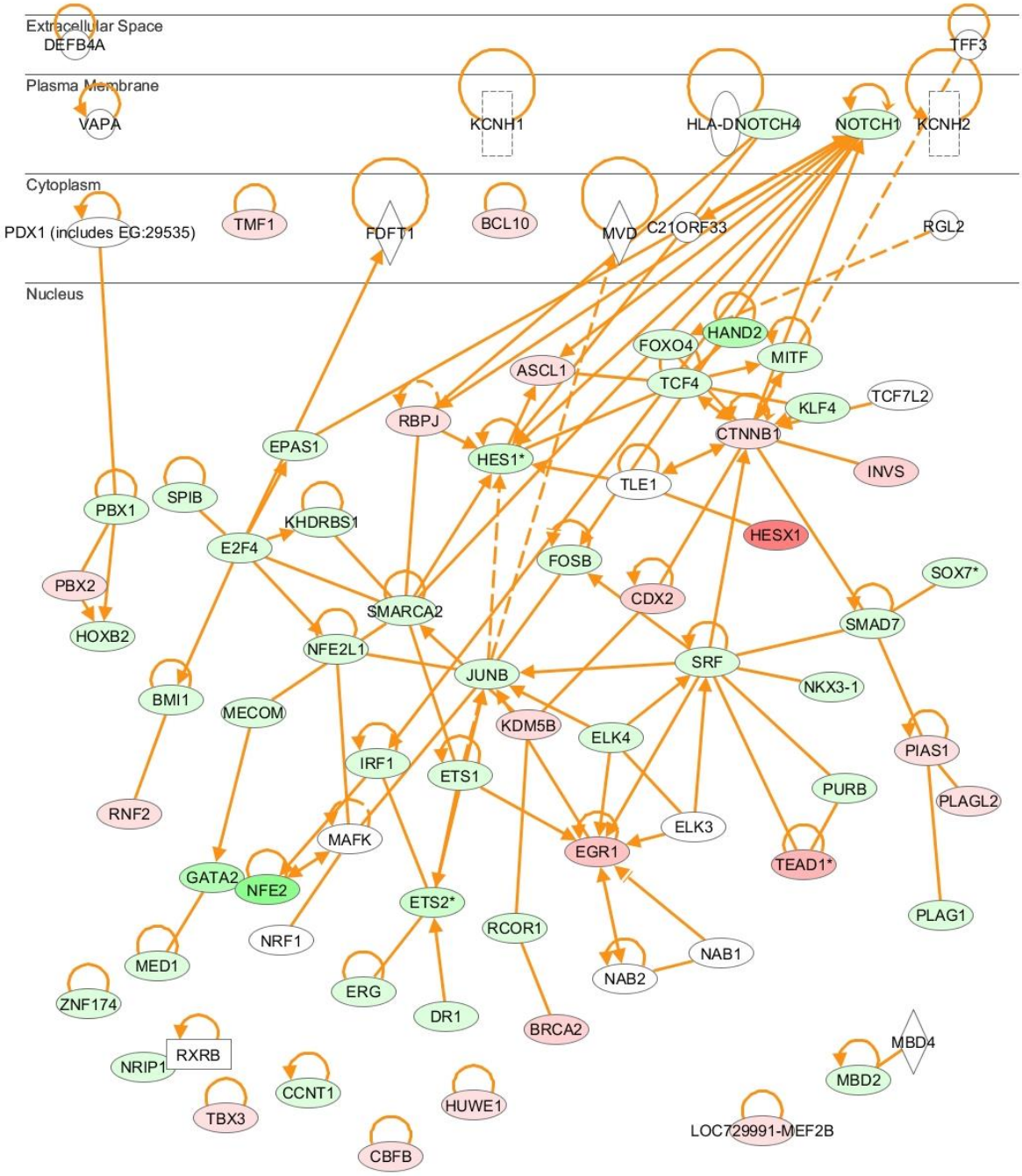

Figure 5-12: Pathways related to large tears. Expression profiles are colour coded, with red indicating upregulation and green representing downregulation.

5.5.6 PCR Validation

To assess the accuracy of the PCR technique, housekeeper gene candidates for comparison were analysed to confirm stable expression levels. The two most commonly used housekeeper genes for tendon research are GAPDH and ß-actin [326]. ß-actin was ineligible as a housekeeper candidate as the microarray results indicated that ß-actin significantly varied between the groups ($p > 0.05$). A panel of potential housekeeping gene candidates was run, and included tata box binding protein (TBP1), hypoxanthine phosphoribosyl-transferase (HPRT), $ß_2$-macroglobulin, and GAPDH. The QPCR results indicated that apart from GAPDH, all of the other primers varied significantly between the three tested groups, confirming that GAPDH was the most suitable housekeeping candidate. Changes in the relative gene expression levels measured using qRT-PCR agreed with gene changes suggested by the microarray (see Figure 5-13).

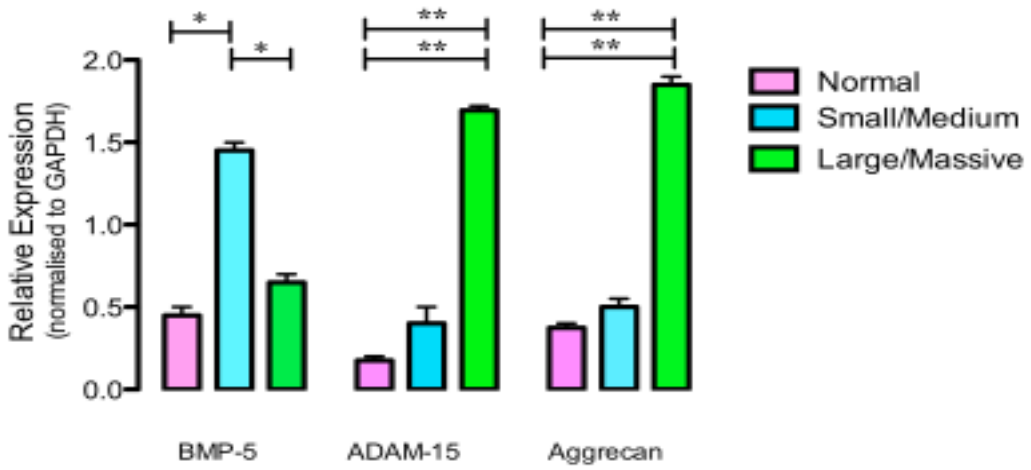

Figure 5-13: PCR results. BMP-5 is significantly upregulated in small/medium tears, compared to large/massive tears and normal tendons. ADAM-15 and Aggrecan are both significantly upregulated in large/massive tears compared to small/medium tears and normal tendons. * $p< 0.05$ ** $p<0.01$

5.5.7 Validation with Immunohistochemistry

Altered protein expression was confirmed using immunohistochemistry. specifically for MMP-3, bone morphogenetic protein-5 (BMP-5) and serum amyloid (SAA). Immunohistochemistry confirmed increased BMP-5 expression in small tears, and increased MMP-3 expression in both small and massive tears compared to normal tendons (see Figure 5-14). Increased SAA expression was detected in massive tears only.

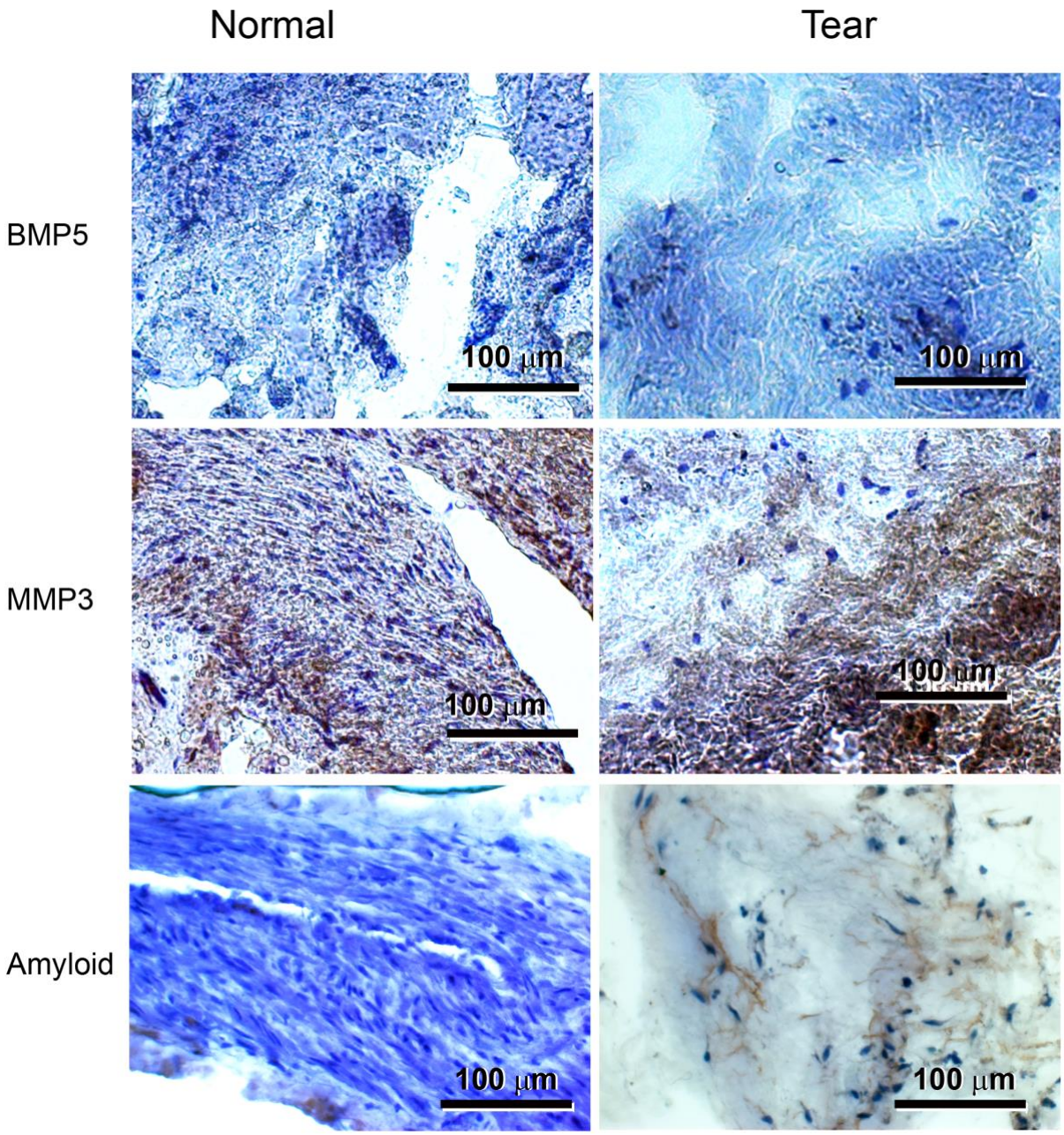

Figure 5-14: Immunohistochemistry results. The torn rotator cuff tear samples all demonstrate increased expression of BMP5, MMP3 and amyloid compared to the normal controls.

5.6 Discussion

This study is the first genome wide analysis of rotator cuff tears, to my knowledge. The gene expression profiles of normal, small and massive rotator cuff tear groups suggest that they are biologically distinct groups. This study also confirmed altered gene expression in pathways reported in previous studies, and has identified a number of novel pathways that are affected between the different tendon groups studied.

A significant role for ECM related genes, such as MMPs and ADAMs, have been identified by this study. The potential importance of such genes in contributing to rotator cuff tears has been recognized by a number of studies [150, 332]. The findings of increased MMP-13 expression were mirrored by previous studies examining patients with rotator cuff tears, from both tendon and synovial fluid samples [141, 151]. However this study did not detect an increase in MMP-1 as reported by both of these studies. This study suggests that upregulation of the reported ECM genes may play key roles in the development of tears, as they may reflect a disruption between ECM synthesis and degradation. A fine balance is likely to exist between MMPs and TIMPs, as they normally play a role in remodeling of the tendon and an imbalance may result in excessive degradation and degeneration, which outweighs collagen synthesis and healing. MMPs are also critical for healing and cell migration. The highlighted changes in MMPs in either the pathogenesis or adaptation to tears, encourage further studies about the suggested role of MMP inhibitors in the treatment of rotator cuff tendon tears [333]. Modulating these ECM pathways may be a useful treatment strategy for improving clinical outcomes.

Both collagenases and inflammatory mediators are also likely to play important roles in cell-mediated pathogenesis of rotator cuff tears, and some collagenase and cytokine pathways are related. IL-1β has been shown to upregulate MMPs -1, -9 and -13, in addition to its recognised pro-inflammatory effects [334]. The interaction of MMP-13 and IL-1β is also sensitive to mechanical strain, with lower strain shown to produce downregulation of both MMP-13 and IL-1β, and higher strain causing upregulation of both molecules. By specifically blocking IL-1β in tenocyte cultures, MMP-13 expression was actually induced. However, there is evidence to suggest that MMP-13 is regulated by both IL-1β dependent, and IL-1β independent pathways.

Aggrecan was specifically upregulated in massive tears, suggesting a potentially important role for chondroplasia in the pathogenesis of massive tears. Amyloidogenesis appears to contribute to massive tears, as increased expression was measured in massive tears only and not in small tears. Increased amyloid expression in torn rotator cuff specimens have been measured [335]. BMP-5 upregulation may contribute to the development or healing response to small tears.

Potential limitations of microarray technologies are that vast volumes of data are produced, and data mining can be challenging and subject to interpretive bias. Microarray studies can be limited by the sensitivity and design of the probes, the efficiency of complementary RNA labeling, hybridisation conditions, as well as the decreased sensitivity to measuring low gene expression levels. A particular concern with microarrays is that genes can be subjected to post-translational modifications at multiple levels, and as such upregulated gene expression may not result in protein translation which is why validation is necessary. The immunohistochemical profile of a select number of genes did confirm protein translation. In this particular study it is possible that some

of the changes detected were related to age rather than tear type, however all three study groups were age and gender matched to overcome this potential confounding variable. All tears were taken from supraspinatus tendons, whereas the control group involved a mix of 6 supraspinatus and 6 subscapularis specimens. As subscapularis has some functional and structural differences compared to supraspinatus, this may have affected the gene profile. However, a separate analysis of the controls only did not show significant differences in the dendograms between the two rotator cuff tendon groups. The results only represent gene changes at the tear edge and it is not possible to be certain that these changes are occurring throughout the entire tendon. Additionally the gene profiles represent a snapshot of gene changes occurring at a single time point, and gene expression may have altered at different time points in the healing process. To try to address this, all of the study specimens have been taken from chronic tears and the average duration of symptoms were matched between the groups.

In conclusion, this study has demonstrated that the gene profiles of normal, small and massive RC tear groups suggested they are biologically distinct groups. This study identified that pathogenesis of different sized rotator cuff tendon tears is associated with varying expression patterns of ECM remodelling genes, chemotaxis genes, aggrecan and amyloid. In addition to confirming altered gene expression in pathways reported in previous studies, this study has identified a number of novel pathways which are affected between the different tendon tear and normal groups. This may offer an insight into the molecular pathogenesis of different sized rotator cuff tears, and ultimately different healing rates both with and without surgery.

The highlighted changes in MMPs in either pathogenesis or adaptation to tears, encourage further studies about the suggested role of MMP inhibitors in the treatment of RC tendon tears as MMPs are critical for healing and cell migration. Further investigation is required to determine whether some of these genes may potentially have a role as biomarkers of failure. Modulating these ECM pathways may be a useful treatment strategy for improving clinical outcomes.

6 CHAPTER 6: MECHANICAL CHARACTERISATION OF ROTATOR CUFF REPAIR PATCHES, AND COMPARISON WITH HUMAN ROTATOR CUFF TENDON

6.1 Abstract

6.1.1 Background:

Augmentation of rotator cuff tears aims to strengthen the repair and reduce re-rupture, yet studies still report high failure rates. This study determines key mechanical properties of rotator cuff repair patches including establishing values for toughness, as well as measuring the shear properties of repair patches and human rotator cuff tendons. It was hypothesized that different repair grafts would a) have varying material parameters, and b) not all have similar mechanical properties to human rotator cuff tendons.

6.1.2 Methods:

Eight specimens each from repair patches Restore, GraftJacket, Zimmer Collagen Repair and SportsMesh were tested to failure in tension, and for suture pull-out. The ultimate tensile strength, tensile (Young's) modulus and failure strain were assessed. This study also established toughness values and shear data. Storage modulus was calculated using dynamic shear analysis, for the patches and compared to the results for the 18 normal rotator cuff tendon samples that were analysed in Chapter 3.

6.1.3 Results:

This study reports important mechanical properties of repair patches, with the mechanical parameters of the patches diverting variously (and often significantly), from those of human rotator cuff tendon values.

6.1.4 Conclusion:

All of the repair grafts tested displayed significant variation in their mechanical properties and had at least some reduced parameters compared to human rotator cuff tendons. This study offers experimentally derived information of value to surgeons when selecting rotator cuff repair grafts. A better understanding of the mechanical suitability of repair grafts for supporting human rotator cuffs is needed if repair patches are to provide a solution for the clinical problem of failure of rotator cuff repairs.

6.2 Introduction

This thesis thus far, has demonstrated clear mechanical and biochemical changes within rotator cuff tendon tears, and apparent progressive abnormalities as tear size increases. In addition to understanding the mechanical and chemical properties of rotator cuff tendons, it is useful to consider the translational relevance of these changes during surgical management.

High failure rates associated with traditional surgical repair of rotator cuff tears have encouraged the search for new methods to improve surgical repair. Assuming that optimal surgical techniques are being employed, then it is possible that surgical repairs may require augmentation either mechanically or biologically. Regenerated tendon often cannot recapitulate the complex structure, composition and organization of the native rotator cuff enthesis. Torn tendons often repair by forming fibrovascular scar tissue at the tendon insertion. Scar tissue usually contains a higher proportion of type III collagen and is often weaker and more prone to failure compared to normal tendon tissue [100].

An effective modality of encouraging healing may be to encourage regeneration of pre-existing native tendon tissue. Attempts to improve post-operative outcomes have resulted in the increased use of repair grafts to augment repairs. It is hoped that repair grafts will act as highly inductive temporary scaffolds, which can support and enhance tendon healing. Ideally a patch will facilitate biological healing to allow tissue remodelling and provide mechanical support during a critical period of healing, and then be reabsorbed before further mechanical failure takes place. Patches can be inserted as augmentation devices by overlaying them over the tear, or used as interpositional devices.

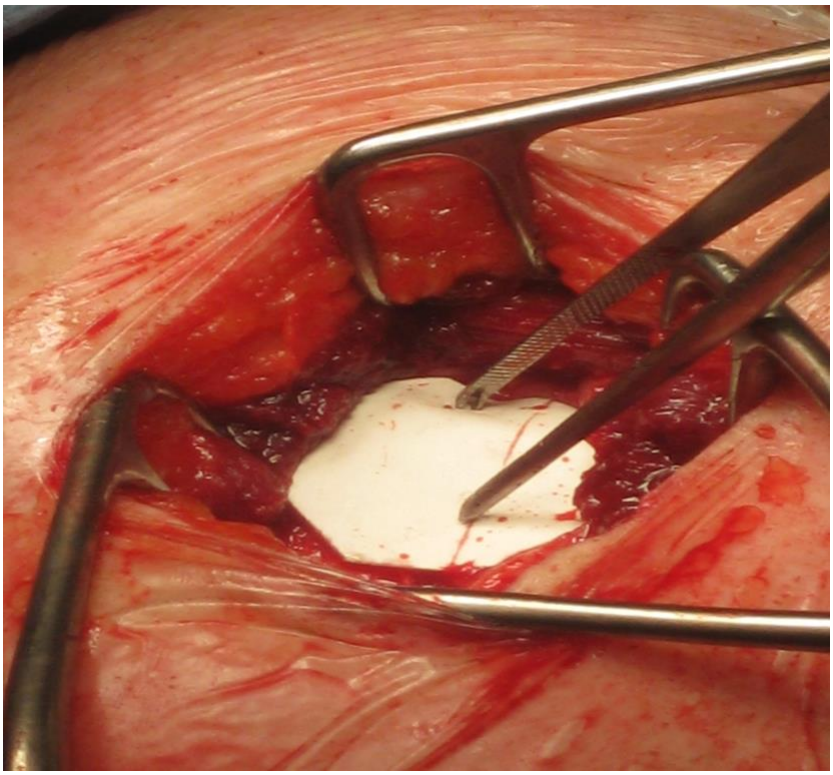

Figure 6-1: showing demonstrating the potential use of a repair patch for reinforcement of a rotator cuff tendon tear, using an overlay technique. Image taken at Nuffield Orthopaedic Centre, Oxford, with full permission.

It has been estimated that thousands of extracellular matrix repair grafts are used annually to augment surgical repair of rotator cuff tears [336]. However the clinical uptake of rotator cuff repair patches has been limited by concerns about effectiveness, safety and cost [337]. A possible explanation for the high failure rates of repairs using patches is that the material properties of rotator cuff repair patches may not be ideally matched to those of human rotator cuff tendons.

6.2.1 Types of Repair Patches

Various broad categories of tendon repair patches exist, and are listed below with examples:

1. Biological
    a. Human (autograft)
        i. Tendon e.g. Achilles tendon
    b. Human (allograft)
        i. Dermis e.g GraftJacket (*Wright medical*)
        ii. Fascia lata e.g. AlloPatch (*Musculoskeletal Transplant Foundation*)
    c. Animal (xenograft)
        i. Bovine dermis e.g Tissuemend (*Stryker*)
        ii. Porcine dermis e.g. Zimmer Collagen Repair (*Zimmer*) – cross linked
        iii. Porcine small intestine submucosa e.g. CuffPatch (*Arthrotek*) – multilayered, Restore (*DePuy*) – multilayered
        iv. Equine pericardium e.g. OrthADAPT (*Pegasus Biologics*)
2. Biopolymers
    a. Collagen – in the form of fibres, gels, sponges [338-340]
    b. Silks [341, 342]
3. Synthetic
    a. Polyethylene (Mersilene Mesh)
    b. Polyglycolic acid (PLGA)
    c. Polylactic acid
    d. Poly-N-acetyl-D-glucosamine (i.e. chitin)
    e. Polyhydroxyalkanoates [343]
    f. Dacron
    g. Nanofibrous and electrospun structures

6.2.2 Clinical Studies Using Repair Patches

Only limited clinical trial results exist examining the efficacy of repair patches. More than 800,000 GraftJacket repair patches are estimated to have been implanted into humans to augment deficient or damaged tissues with no documentation of transmission of diseases [344]. GraftJacket studies have suggested an overall improvement in the majority of cases. Snyder *et al*., implanted GraftJacket patches into 24 patients but only presented follow-up data on eighteen of these patients [344]. Only two of these repairs had failed and the patients reported improvements in pain and function. MRI scans at one year showed full incorporation of the patches into native tendon tissue. Another similar retrospective study found that GraftJacket patches had failed to incorporate into three out of sixteen patients with massive rotator cuff tears [345]. Again patients from the failed repairs reported improved pain and clinical outcome scores. GraftJacket was used as an interpositional graft to repair 16 massive, irreparable rotator cuffs in a retrospective study [345]. 3 of the repairs demonstrated failure by 1 year assessed by MRI, but reported improved pain. Slightly less favourable results were reported after a prospective study using GraftJacket to repair seventeen massive rotator cuff tears presented follow-up in only twelve patients, of whom three had failed surgical repairs [346]. An improvement in post-operative outcome scores was reported. None of these studies had control groups, and they were all limited by their small sample sizes.

Human studies using the Restore patch have reported less favourable outcomes. Eleven large and massive tears were repaired with the Restore patch, and MRI scans at six months post-operatively showed that ten out of the eleven repairs had failed [347]. Ianotti *et al*., carried out a randomized control trial involving thirty patients with large tears involving two or more tendon tears. The control

group without the Restore patch was found to be 7% more likely to heal than those repaired with the patch, and the control group also had significantly better shoulder outcome scores [348]. A small study of twelve patients found that only one out of twelve patches failed, and reabsorption was otherwise detected by twelve weeks. Repair with the Restore patch was associated with improved mean post-operative outcome scores, strength and function [349]. Post-operative non-infectious oedema and significant pain have been reported following the use of Restore patches and remnants of porcine DNA were detected [337], highlighting concerns about its safety. Another study using Restore patches involved nineteen augmented rotator cuff repairs [350]. Four of the xenograft patients had severe reactions postoperatively that required surgical debridement and removal of the xenograft. Ten augmented repairs and twelve standard repairs were assessed at two years with MRI showing six retears in the xenograft group and seven retears in the standard group. The xenograft group took longer for pain to settle postoperatively, had lower strength and lower participation in sports than the control group.

The Zimmer Collagen Repair patch has been marketed for use in urological treatments, hernia repairs and plastic and reconstructive surgery of the head and face. There is a paucity of data about its use for the repair of human rotator cuff defects, and Zimmer Collagen Repair has been used in 2 small studies. A small, prospective observational study followed ten patients for up to five years, having had augmented rotator cuff repair [351]. There were positive results in terms of pain reduction, abduction power and range of motion and, at final follow up, ultrasound revealed that eight of the ten repairs remained intact. A case series of four patients with Zimmer Collagen Repair patch augmented rotator cuff repairs reports that, despite a promising period of recovery after surgery, the

repairs failed between three and six months [352]. The series also describes inflammatory changes, bursal fluid collection and necrotic fibrous material on histological analysis.

SportMesh has been studied in a small series of 10 patients, and a significant reduction in pain, shoulder scores and range of motion was detected [353].

6.2.3 Mechanical Properties of Patches

Maximizing the material properties and clinical efficacy of patches is important, as there is a need for an effective augmentation product. Rotator cuff repair patches need appropriate mechanical properties to be able to withstand loads from tension of the repair, and the mechanical loads applied by shoulder movement. Mechanical assessment of some rotator cuff tendon repair grafts to-date has been limited and only involved tensile testing only [336]. Derwin *et al*., measured the mechanical parameters of five commercially available patches and compared grafts to canine infraspinatus, and found that while GraftJacket had a lower modulus of elasticity than Restore or CuffPatch, it was stiffer than the latter two patches and TissueMend [336]. All of the repair patches had a lower linear moduli than canine infraspinatus tendon, and reported stiffness values for human infraspinatus [354].

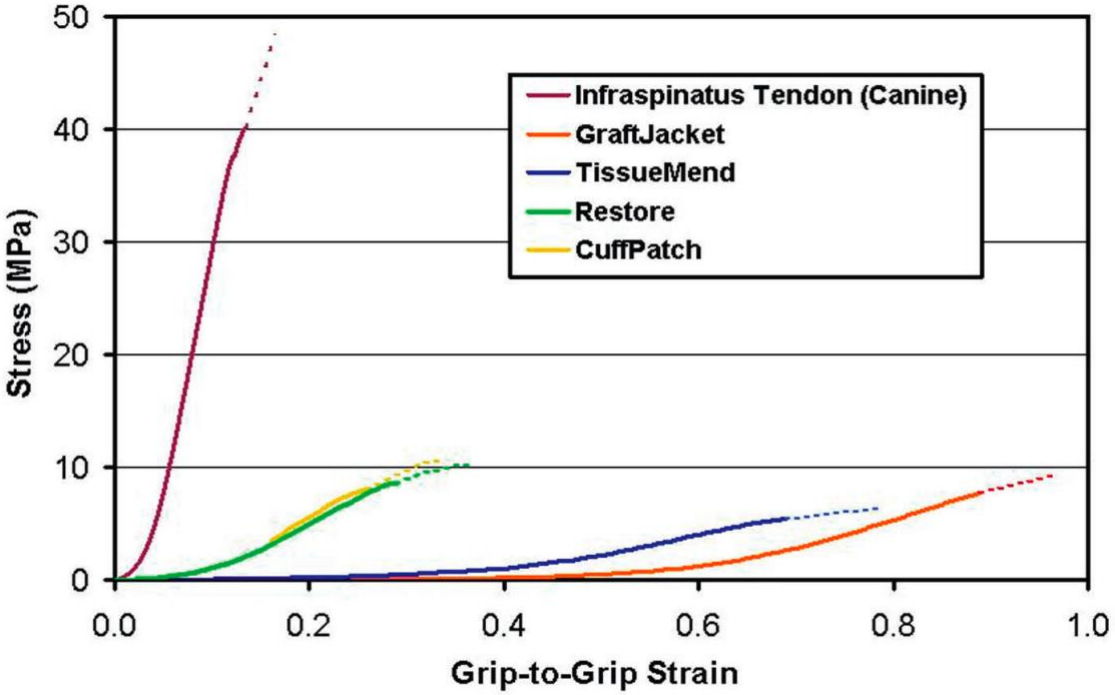

Figure 6-2: Graph comparing mechanical properties of some commercially available rotator cuff repair patches, and canine infraspinatus tendon. Results and graph taken from study by Derwin *et al* [336].

Table 6-1: Comparison of mechanical properties of rotator cuff tendon repair patches. Results and table taken from study by Derwin *et al* [336].

Table II Biomechanical properties of commercially available ECMs

Graft material	Linear region strain* (%)	Linear modulus† (MPa) (mean ± SD)	Linear stiffness‡ (N/mm) (mean ± SD)	Suture failure load (N) (mean ± SD)
Infraspinatus tendon (canine)[22]	5-12	405 ± 86	–	–
AlloPatch[21]	3-11	304 ± 52	98.2 ± 16.2	–
Restore[8,22]	22-25	35.5 ± 9.1	7.0 ± 1.5	38.2 ± 2.8
CuffPatch[8,22]	20-22	40.1 ± 15	6.8 ± 2.3	32 ± 4.1
GraftJacket[8,22]	53-93	22.5 ± 5.3	16.4 ± 5.9	229 ± 72§
TissueMend[8,22]	37-53	15.2 ± 3.5	7.4 ± 1.4	76 ± 21.5§
Zimmer Collagen Repair Patch[8]	–	–	–	128 ± 26.3

Previous studies have indicated that the forces applied to rotator cuff tendons, and therefore their repairs, are multi-directional, resulting in shear and compression in additional to uniaxial tensile

loading [93, 245, 247, 248]. Therefore, a more comprehensive assessment of the material properties of repair patches is warranted and shear data provides additional data of value to orthopaedic surgeons, particularly when it can directly be compared to the shear data values of the tissue they are designed to reinforce, human rotator cuff tendon specimens. It is also paramount to determine the comparability of repair patches to human rotator cuff tendons, as gross mismatching of material properties will result in stress concentrations, increasing the likelihood of post-operative failure of the repair.

6.3 Aims of this Study

This study has investigated a number of mechanical properties of rotator cuff patches, including tensile properties, suture pull out strength and response to shear. Previous studies have reported slippage at the patch-grip interface, which can result in an underestimation of tensile properties of tendons [231, 232, 336]. The aim of this study was to overcome reported problems of patch-grip slipping and failure, in the hope of providing more accurate material values. Since rotator cuff tendons are exposed to substantial shear loading in addition to tensile load, and the shear properties of repair patches have not previously been reported, the shear properties of repair grafts and human rotator cuff tendons were compared using dynamic shear analysis (DSA). This material characterization technique has been used here for the first time to study the material deformation of repair patches. This study also presents for the first time the key material property of toughness, which provides an estimate of the amount of mechanical energy per unit volume that a material can absorb before rupturing. This study focused on four commercially available patches that are

marketed for augmentation of rotator cuff tendon repair. The patches included Restore (DePuy Orthopaedics, Indiana), GraftJacket (Wright Medical Technology, Tennessee), Zimmer Collagen Repair (ZCR, also known as Permacol, Zimmer, Indiana) and SportMesh (Biomet, Indiana).

The aims of this study were to determine whether there were significant differences between the tensile and shear mechanical properties of four rotator cuff repair patches, and how well they were matched to measured shear values for human rotator cuff tendon and reported tensile rotator cuff tendon properties.

6.4 Hypothesis:

The null hypotheses were that there will be:

- no difference between the mechanical properties of different patches, and
- no difference between the shear properties of human rotator cuff tendons and different patches.

6.5 Methods and Materials

Four commercially available rotator cuff repair patches were obtained, which included Restore, GraftJacket, Zimmer Collagen Repair and SportMesh. Their properties are outlined in **Table 6-2**, with further details in the Appendices.

Table 6-2: Properties of four commercially available rotator cuff repair patches characterised in this study.

Patch	Company	Source	Type	Cost as of 2009 (in the United Kingdom)
Zimmer Collagen Repair/ Permacol	Zimmer	Porcine	Dermis	£940
Restore	Depuy	Porcine	Small Intestine Submucosa	£1,946
GraftJacket	Wright Medical	Human	Dermis	£1,025
SportMesh	Biomet	Synthetic	Artelon (polyurethane urea)	£840

In order to visualise the material organisation of the four rotator cuff tendon repair patches, scanning electron miscroscopy (SEM) images of the four patches were taken. Samples from each patch were subjected to sputter coating, and then SEM images were taken.

6.5.1 Failure Testing under Tension

The tensile, shear and suture pull out properties of four rotator cuff tendon repair grafts were measured. Eight specimens from the repair grafts Restore, GraftJacket, Zimmer Collagen Repair (ZCR) and SportMesh were tested to failure under tension and for suture pull-out.

For each type of repair graft, eight separate specimens were used, measuring 45 mm in length and 2 mm in width. Material testing dumbbell shapes were created. These 2 mm strips were 1 mm at their narrowest point to ensure mid-patch failure was unaffected by stress-risers occurring at the

patch-grip interface. The thickness of the grafts was measured at four separate point using automated callipers with an accuracy of +/- 0.001 mm, and averaged. The testing protocol was based upon a modified version of a previously published study of patch mechanical properties [336]. Specimens were tested to failure under tension using an Instron 5542 machine with a 500-N load cell (Instron, Canton, Massachusetts) at room temperature. Specimens were loaded to failure at a displacement rate of 10 mm/min until failure. Failure was defined as a decrease in load of more than 20% during tensile testing. Soft tissue clamps were used to grip the ends of the grafts, leaving a nominal grip-to-grip gauge length of 30 mm.

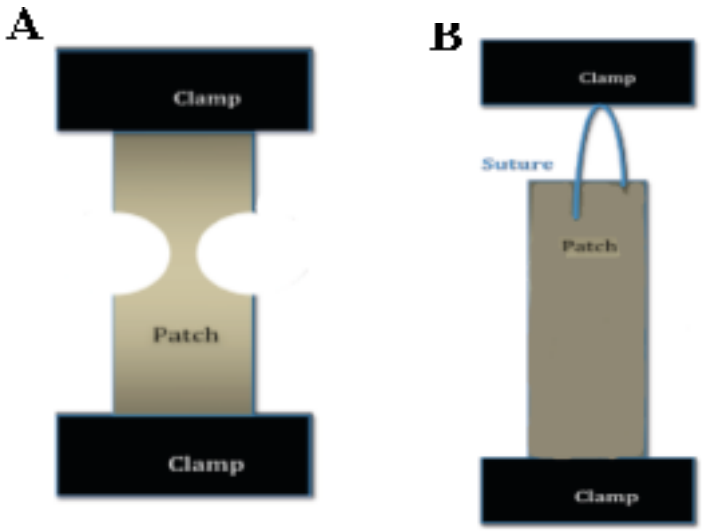

Figure 6-3: A) Dumbbell shaped specimens were clamped and tested to failure. B) Figure represents testing of suture pull-through testing, with a 3.0 Ethibond suture passed through one end of the patch, and gripped using a clamp on the other end.

Maximum tensile stress (MPa), tensile modulus (MPa), breaking strain and toughness (J/cm^3) were assessed at the location of patch failure, as these values are independent of specimen shape, and

thus could be compared to published human rotator cuff tendon data and other tendons [355]. Stress, σ, is measured in Pascals and is calculated as:

$$\sigma = \frac{F}{A}$$

where F is force (in Newtons) and A is the cross sectional area of the sample at the gauge section. Strain, ϵ, is an indicator of the extent to which a material is being stretched, or changed in length, and as such is calculated as:

$$\epsilon = \frac{L - l}{l} = \frac{\Delta l}{l}$$

L is the final length, and Δl is the change in tissue length, and l is the original tissue length.

The tensile modulus (also termed Young's modulus) was calculated from the steepest pre-yield slope of the stress-strain curve. The tensile modulus, E, is derived by dividing the stress (σ) by the strain (ϵ) using the following formula:

$$E = \frac{\sigma}{\epsilon}$$

The modulus was also measured at a physiological level of strain of 2%, as reported by Bey *et al*, [251]. Higher modulus values have been previously reported to correspond with the linear region for canine infraspinatus, but macroscopic failure occurs in human rotator cuff tendons before

reaching 8% strain [56, 336]. Some studies suggest that human tendons fail by microdamage at strains above 6% [251, 253].

Toughness (J/cm^3) was calculated as the integral of the stress strain curve to failure for each sample, and failure was defined as a decrease in load of more than 20% during tensile testing. This measure indicates the deformation energy absorbed before failure.

6.5.2 Tensile Suture Pull-Through Testing

Functional patch data rather than specific material characteristics were determined by testing suture pull-through. Another eight rectangular strips from the four repair patches were taken, measuring 45 mm in length and 2 mm in width throughout and tested for suture pull out. 3.0 Ethibond (Ethicon, Somerville, NJ, USA) sutures were used as this is a common suture type used for rotator cuff tendon repairs, and is used in my hospital. Dumbbell shapes were not required for the suture retention tests, due to stress concentrations being at the suture point.

One end of the strip was gripped using soft tissue grips, and a looped suture was placed 2.5 mm from the other end, and the suture was gripped. A simple suture configuration was used. The suture was left untied and both ends of the free suture were gripped in a soft tissue clamp and the construct was tested to failure and mechanical properties were measured as above. Prior to testing, it was verified that using 2 mm wide strips gave the same information for suture pull through as 1 cm wide strips, when both sutures were placed 2.5 mm from the end of the patch strip.

6.5.3 Shear Testing

Five separate 3 mm diameter punch biopsies were taken from each repair patch. These samples were compressed to 0.2 N between two parallel plates and compressed in a Bohlin Gemini 200 HR Nano rheometer (Malvern Instruments, Worcestershire, UK). Dynamic shear analysis (DSA) of the samples from the repair grafts was performed as described in Chapter 3. The storage modulus (G′) was calculated as an indicator of the mechanical integrity of the patches. In order to assess how well the repair grafts were matched to normal human rotator cuff tendons, the results were compared to similar measurements of storage modulus using DSA that were taken from 18 normal human rotator cuff tendons with no history of shoulder problems in Chapter 3 (aged 20-89 years, mean age 58.8 years, 9 males and 9 females).

6.5.4 Statistics

A pre-study power calculation indicated that the DSA experiments had an 80% power to detect a 20% difference in maximum stress between groups with alpha = 0.05. A Kruskal-Wallis 1-way ANOVA of all of the groups was performed to compare the shear properties of the different commercially available repair grafts and human rotator cuff tendons. Specific comparison between the different repair grafts and normal rotator cuff tendons was performed using Dunn's multiple comparison tests. All tests were two-tailed and a significance level of $p < 0.05$ was set for all statistical tests.

6.6 Results

6.6.1 Scanning Electron Microscopy Properties

The SEM results of the patch surfaces are shown below (see Figure 6-4). While Restore has a relatively smooth surface, the two dermal patches (ZCR and GraftJacket) have very similar appearances. SportMesh has a braided fiber appearance, which is clearly demonstrated.

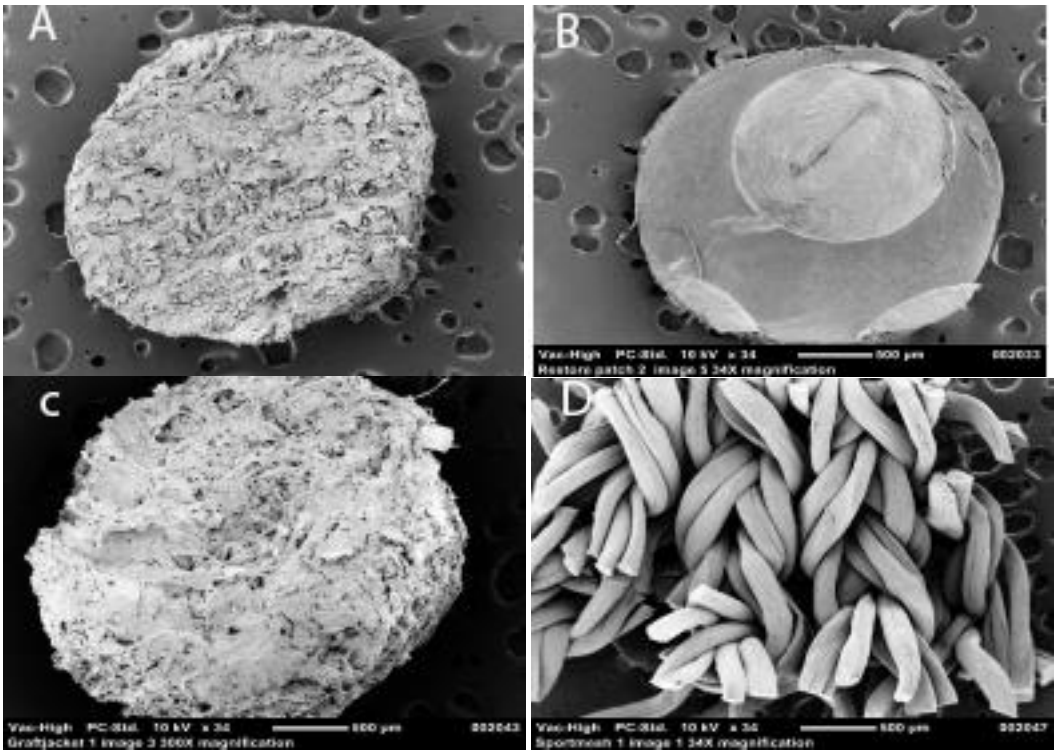

Figure 6-4: **Scanning Electron Microscopy images of A) Zimmer Collagen Repair B) Restore C) GraftJacket and D) SportMesh. Scale bar represents 500µm.**

6.6.2 Tensile Properties

The thicknesses of the different strips varied significantly, with a mean thickness of 1.48 mm for GraftJacket, 0.82 mm for SportMesh, 0.78 mm for Restore and 1.53 mm for the ZCR patch ($p <$

0.05). The maximum stress values were significantly different between two of the four repair patches (p = 0.0056, see Figure **6-5**). ZCR had a significantly higher mean maximum stress of 32.65 ± 7.43 than the lowest maximum stress values measured for SportMesh (11.86 ± 4.64, p < 0.01).

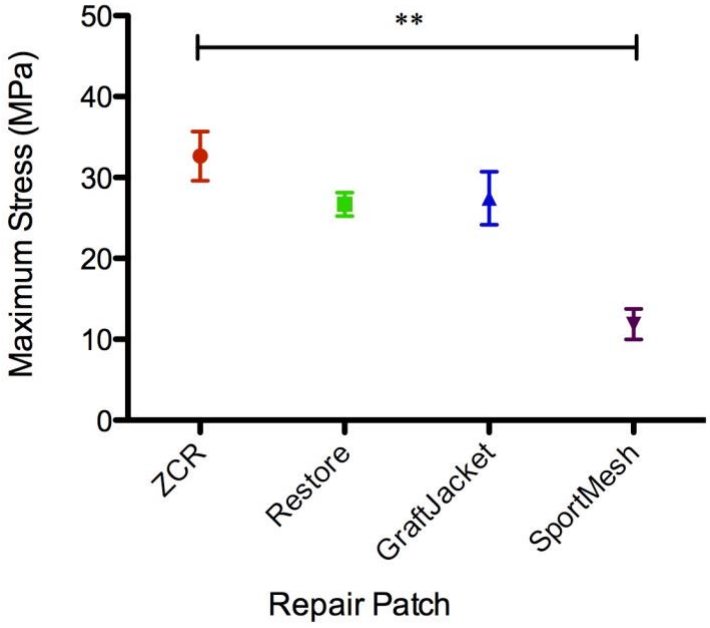

Figure 6-5: A graph demonstrating the maximum stress (MPa) of different patches. ZCR has a significantly greater maximum stress (MPa) than SportMesh patches. Bars represent standard error. ** represents p < 0.01.

SportMesh had a significantly lower mean tensile modulus (14.25 ± 2.41 MPa at 2-5% strain) compared to ZCR (68.85 ± 7.99 MPa at 29-37% strain) and Restore 71.34 ± 19.2 MPa at 19-27% strain, p < 0.01, see Figure **6-6**). The tensile or Young's modulus of all grafts varied significantly, and occurred at different strains (p = 0.0064). The modulus at a more physiologically relevant 0.1-

2% strain revealed that ZCR had the lowest modulus of 6.883 ± 0.797, which was significantly lower than GraftJacket (19.2 ± 6) and SportMesh (13.39 ± 3.415) ($p < 0.01$, see

Table 6-3).

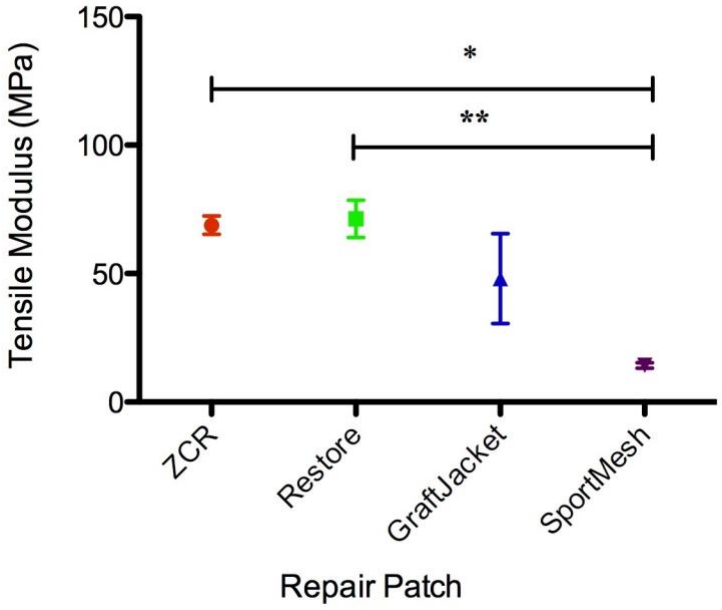

Figure 6-6: A graph representing tensile (Young's) Modulus (MPa) of different patches. ZCR has a significantly higher tensile modulus than SportMesh patches. Bars represent standard error. * represents $p < 0.05$. ** represents $p < 0.01$.

The highest mean failure strain of 0.82 ± 0.1 was measured for SportMesh, and this was significantly greater than the failure strain of 0.35 ± 0.03 for Restore and 0.36 ± 0.07 for ZCR ($p < 0.01$, see Figure 6-7). A mean strain value of 0.72 ± 0.1 was measured for GraftJacket.

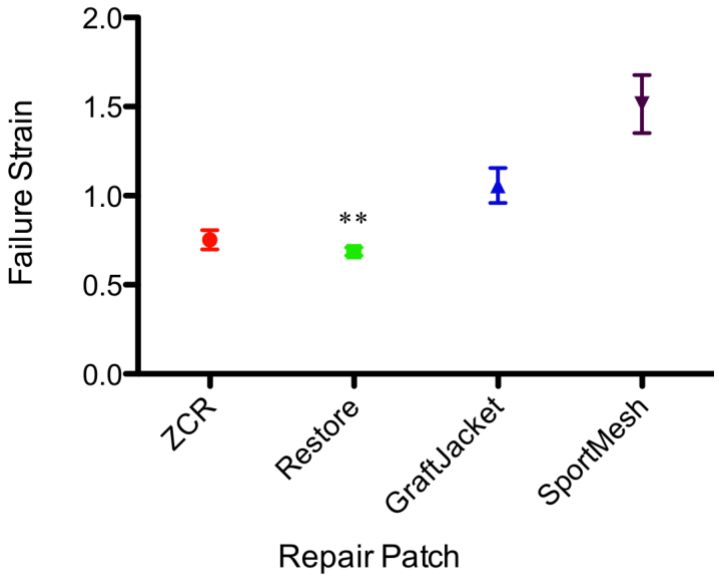

Figure 6-7: A comparison of the failure strain of different patches. SportMesh and GraftJacket have significantly higher toughness than Restore patches. Bars represent standard error. ** represents p < 0.01, * represents p < 0.001.**

While SportMesh displayed the largest toughness values of 503.8 ± 185.3 J/cm^3, no difference was detected compared to other patches (see Figure 6-8A). Restore exhibited the lowest toughness properties (mean 341.3 ± 35.67 J/cm^3).

The suture pull-through data for toughness reveals a similar trend between the patches, but lower toughness values were mostly measured compared to similar toughness values derived from tensile testing to failure (see Figure 6-8B). ZCR, Restore and GraftJacket all had significantly lower suture pull-through toughness values compared to SportMesh ($p<0.001$). The largest maximum suture

retention load was measured for ZCR patches at 30.22 ± 7.88 N, which was significantly greater than Restore with a suture retention load of 7.09 ± 1.5 N.

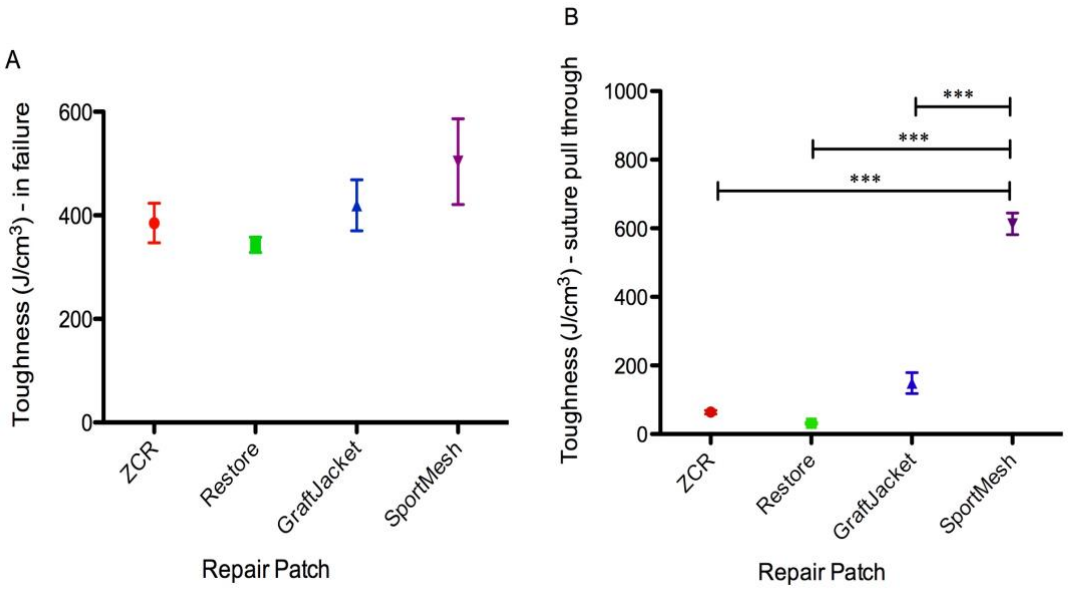

Figure 6-8: A) Comparison of the toughness (J/cm^3) of different patches, as measured by failure in tension. No significant difference was detected between the patches. B) Comparison of the toughness (J/cm^3) of suture pull through from different patches. SportMesh has significantly higher toughness than ZCR, Restore and GraftJacket patches. Bars represent standard error. * represents p < 0.001.**

6.6.3 Shear Storage Modulus

A significant difference in the shear moduli of all four rotator cuff repair grafts was detected ($P<0.0001$, 1 way ANOVA) (see Figure 6-9). ZCR had the highest storage modulus (mean 10,759 MPa, $P<0.05$), followed by SportMesh, with Restore patches demonstrating the lowest shear values. Both Restore and GraftJacket had significantly lower shear values than normal human rotator cuff tendon (mean 22,764 MPa, $p<0.05$, Dunn's multiple comparison test).

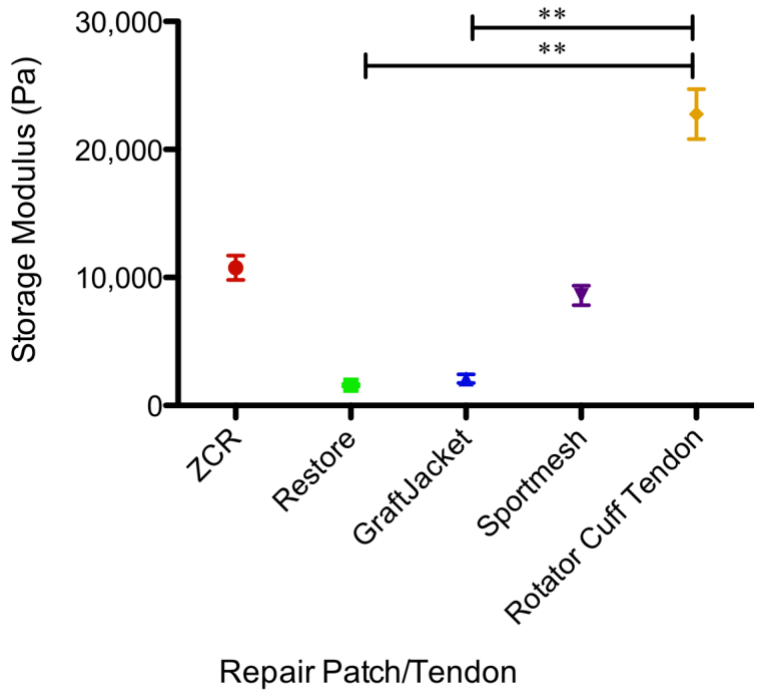

Figure 6-9: A comparison of the shear storage modulus (Pa) of different commercially available rotator cuff repair grafts, and human rotator cuff tendons. GraftJacket and Restore patches have a significantly lower modulus than rotator cuff tendons. Bars represent standard error. **p < 0.05.

In summary, wide variations were measured in the mechanical properties (tensile properties, shear modulus and suture pull-out properties) of different repair patches. All of the various mechanical parameters related to each patch have been summarised in

Table 6-3.

Table 6-3: Summary table listing the mean values for the different mechanical properties measured. * indicates highest value in each category, ^ indicates lowest value per category.

Patch	Maximum Stress (MPa)	Failure strain	Tensile/Young's Modulus (MPa) (+ corresponding strain)	Modulus at 0.1-2% strain (MPa)	Maximum Failure Load (N)	Toughness - in failure (J/cm^3)	Toughness - suture pull through (J/cm^3)	Maximum Suture Retention Load (N)	Storage Modulus (Pa)
Zimmer Collagen Repair/ Permacol	32.65 ± 7.43 *	0.36 ± 0.07	68.85 ± 7.99 (29-37%)	6.883 ± 0.797 ^	50.26 ± 12.21 *	385.2 ± 85.48	63.98 ± 10.6	30.22 ± 7.88 *	10,759 ± 1,894 *
Restore	26.7 ± 3.8	0.35 ± 0.03 ^	71.34 ± 19.2 (19-27%) *	7.905 ± 1.46	13.04 ± 0.90 ^	343.1 ± 35.67^	31.21 ± 5.97^	7.09 ± 1.5^	1,584 ± 183.1^
GraftJacket	27.45 ± 6.55	0.72 ± 0.10	48.09 ± 49.56 (27-36%)	19.2 ± 6 *	27.85 ± 6.77	419.4 ± 85.23	148.8 ± 53.04	21.84 ± 9.3	2,097 ± 667.8
SportMesh	11.86 ± 4.64 ^	0.82 ± 0.10 *	14.25 ± 2.41 (2-5%) ^	13.39 ± 3.415	17.66 ± 7.55	503.8 ± 185.3 *	512.9 ± 53.29 *	16.38 ± 1.58	8,600 ± 1,531

6.7 Discussion

Reduced mechanical properties have been previously demonstrated in torn rotator cuff tendons, encouraging the augmentation of repairs with patches to provide adequate mechanical support [356, 357]. There is a need to understand the mechanical properties of repair grafts, and compare how well they correlate with human rotator cuff tendons; if the patches are too weak they may fail prematurely, and if too strong they may prevent tissue in-growth due to stress-shielding [358]. This study shows that repair grafts vary significantly in mechanical properties between each other, and also display wide variations when compared to human rotator cuff tendon.

Maximum stress at failure based upon a study of 8 supraspinatus tendons has been reported as 11.5 ± 5 MPa, and 16.5 ± 7.1 MPa based upon a study of 11 cadavers, whereas a lower estimate of 8 MPa was measured by Sano et al [50, 61, 234]. ZCR, Restore and GraftJacket all have greater

maximum stress values when compared to a range of published values for human supraspinatus tendons.

Despite similar trends, this study measured greater tensile modulus values for Restore (71.34 MPa) and GraftJacket (48.09 MPa) than a previous study by Derwin et al. which measured values of 35.5 MPa for Restore and 22.5 MPa for GraftJacket (ZCR and SportMesh were not included in their study). This difference may be accounted for by differences in sample shape [336]. By testing dumbbell shaped specimens in this study, failure was encouraged at the neck of specimens rather than at the grip-patch interface, which meant that material properties were less likely to be underestimated. Tensile modulus values for human rotator cuff tendons as high as 50 to 170 MPa have been reported [50, 359]. Apart from lower modulus values seen with SportMesh, the other patches have maximum tensile modulus values that are well matched to human rotator cuff tendons.

At physiologically relevant strains of 2%, SportMesh and Graftjacket had significantly greater moduli than ZCR [251, 253]. It is difficult to interpret our data in a clinically relevant context, as many studies investigating the mechanical properties of human rotator cuff tendons do not report values corresponding to physiologically relevant strains at 8% or less. Human tendon failure strain values have been reported between 1.11 to 4.87, although lower values of 0.07 to 0.225 have also been measured, reflecting varying rotator cuff tendon properties in different anatomical locations [52, 102, 234, 249]. All patches failed at strains lower than some published human rotator cuff tendon failure strains [52, 234, 249]. This implies that the patches may fail at physiologically relevant strains before failure of the rotator cuff tendons. The ultimate load for human rotator cuff

tendon strips has been previously reported between 88 to 411 N according to the location, however it is not possible to make direct comparisons to our study due to the use of different specimen proportions [50]. No published human rotator cuff tendon toughness values are available for comparison with our measured values.

Barber et al. also measured suture pull-through of rotator cuff patches, but due to differences between the two studies in clamping and sample preparation, it is not possible to undertake a quantitative comparison [360]. However they observed similar trends in the properties of the patches tested as shown by our study. The suture pull-through data provides both a measure relevant to the clinical setting *in-vivo* as patches are sutured in place during the repair, as well as *in-situ* failure which is a common mechanism for failure of rotator cuff repairs [78].

Interestingly, most specimen toughness values were lower when sutures were pulled through the patches, compared to values measured from failure of the patch under tension alone. This indicates that patches are more likely to fail clinically by stress concentration surrounding suture pull-though than complete material failure by direct tensile loading. Two of the patches, Restore and GraftJacket, also had reduced shear modulus values compared to human tendons.

The mechanical performances of the patches are likely be linked to their base material and microstructure as shown in the SEM images (Figure 6-4). SportMesh demonstrated low stress, high strain and high toughness, all of which may be due to the woven synthetic fabric "uncrimping" under increasing load. The fiber diameter in SportMesh is approximately 50 μm, and thus a 2 mm width strip aligned to the fiber direction will include 4 or 5 braids of the material, each composed

of 8 fibers. Restore on the other hand has a continuous, smooth, low defect appearance that could account for the relatively higher storage modulus and tensile modulus compared to SportMesh. The two dermal patches (ZCR and GraftJacket) have some comparable properties such as maximum stress, tensile modulus and toughness, yet ZCR has a higher failure strain and storage modulus compared to GraftJacket. Mechanical variations could be due to differences in material processing; ZCR is cross-linked, subjected to enzymatic extractions and packaged hydrated, unlike GraftJacket which is not cross-linked, freeze dried and packaged dry.

In addition to mechanical properties, concerns about clinical efficacy, cost-effectiveness and safety of patches also need to be addressed. Even though the patches are marketed as acellular, traces of DNA have been detected on Restore and GraftJacket patches [336, 337]. Limited clinical trial data exist for all patches. GraftJacket studies have suggested an improvement in the majority of cases, without reports of serious complications [344-346]. Human studies using the Restore patch have reported less favorable outcomes and increased complications [337, 347-349]. ZCR has been used in 2 small studies, with 1 study reporting 100% failure and signs of inflammation [351, 352]. SportMesh was studied in 10 patients, and a significant reduction in pain, shoulder scores and range of motion was detected [353].

A significant limitation of this study was that entire, intact patches were not tested; instead sample specimens were taken from a single patch. While patches are marketed as uniform, variations may exist between individual patches. Material properties of patches were only characterized at one time point, which was pre-implantation. Ideally this study should be extended to see how different repair constructs, suture configurations and the shoulder's physiological environment may interact

with and alter patch mechanical properties. The degradation rate differs between the four patches, which could result in different mechanical behaviors *in-situ*. Another limitation of this study is that human rotator cuff tendons could not be subjected to the same tensile testing protocols as patches. It was not possible to accurately and reproducibly perform tensile tests on diseased human tendons obtained intraoperatively, due to ethical limitations that restrict the amount of tissue sampled. Slippage problems and stress-risers at the clamp tendon interface are a well-recognized and reported problem, and can affect the measured tensile properties of tendons [231, 232, 336]. Therefore DSA was used in this study to overcome some clamping issues and allows testing of small samples to produce quantitative and comparable results [361].

Achieving a reconstruction that is immediately strong and has comparable mechanical properties to native rotator cuff tendons may be more pertinent than with other tendons, such as the Achilles tendon. Supraspinatus tendons are more prone to injury, and a rat study found that supraspinatus tendons sustained significantly more injury than Achilles tendons subjected to the same exercise loading protocol [362]. The greater sensitivity to load may be reflected by the fact that human supraspinatus tendons usually function at only 25-30% of its ultimate tensile strength, unlike Achilles tendons for example which function between 50-100% [363]. Exactly how closely matched repair grafts need to be to human rotator cuff tendons remains undefined.

Our study provides a useful baseline comparator of different repair patches and their mechanical similarities with the gold standard of human rotator cuff tendons, which patches should ideally emulate. It is difficult to conclusively state which of the mechanical parameters measured is most relevant to tendon healing and function. It is likely that a combination of the different factors

measured in this study are all likely to play important roles. In the future patches may be increasingly used to deliver appropriate cells, growth factors and cytokines to provide both a mechanical and biological stimulus for healing.

7 CHAPTER 7: DISCUSSION

This thesis has demonstrated that the edges of torn rotator cuff tendons have complex altered mechanical, chemical and gene expression properties compared to normal intact tissue. Intraoperative tissue samples provide a snapshot of the biological milieu surrounding rotator cuff tears, with potential insight into the pathophysiology of failure and the healing potential of tendon.

7.1 Summary of Findings

Mechanical changes between different tear sizes have been shown by this study. Torn tendons were shown to have a reduced storage modulus indicating decreased mechanical integrity, which may reflect a decreased ability to withstand mechanical loads. Mechanical testing of small tendon samples using DSA is an interesting technique that avoids clamping the ends of tissue, and may have wider applications in the future. This DSA technique avoids the cellular and collagen fibre collapse that would occur with clamp closure, which could irreparably damage the material and weaken the ends and lead to spuriously low force readings.

Biochemical differences in torn tendons have also been measured using FTIR and were shown to vary between different tear sizes. These differences occur in the composition of tendons affecting collagen, proteoglycans, glycosaminoglycans and lipids. Tendon degeneration and tears are most likely to occur when there is an imbalance between the synthesis and degradation of collagen and ECM materials. The potential use of FTIR intraoperatively with a fibreoptic probe is an exciting possibility, but in view of the expense and complicated analysis, this technique is likely to remain a research tool rather than a main-stream clinical test. Reduced collagen structural integrity was measured in torn tendons using DSC, which is another interesting and specialist research

technique. This approach provided a greater understanding of subtle but important compositional changes in collagen. Some of the tendon differences measured in varying sized rotator cuff tendons may reflect the reported effect of tear size on repair outcomes [267, 364-366]. However, an effect of tear size on outcome is not universally accepted and Essman *et al*., did not report any effect of tear size on clinical outcome or duration of symptoms [367].

Table 7-1: Summary of key experimental findings from each chapter.

Chapter Number	Chapter Description	Key Findings
2	**Dynamic Shear Analysis**	• Healthy tendons had a significantly higher modulus than torn tendons, indicating that torn tendons are mechanically weaker • Normal tendons had a significantly higher mean shear modulus than tendons with massive tears
3	**Fourier Transform Infrared Spectroscopy**	• FTIR readily differentiated between normal and torn tendons, and different tear sizes. • The key discriminating molecules and spectra altered in torn tendons are (i) carbohydrates/phospholipids (1030-1200 cm^{-1}), (ii) collagen (1300-1700, 3000-3350 cm^{-1}) and (iii) lipids (2800-3000 cm^{-1}).
4	**Differential Scanning Calorimetry**	• Small and massive rotator cuff tears had significantly higher T_{onset}, T_{peak} and ΔH compared to controls. • There was no difference in thermal properties between small and massive tears. • Polarized light microscopy of torn tendons confirmed greater collagen structural disruption compared to controls.
5	**Microarray Gene Analysis**	• Upregulation of aggrecan was seen in massive tendon tears but not in small tears. • Matrix metallopeptidases (MMP)-3,-10,-12,-13,-15, -21,-25 and a disintegrin and metallopeptidase (ADAMs)-12,-15,-22 were significantly upregulated in tears. • Amyloid was downregulated in both tear groups. • Small tears also displayed upregulation of BMP-5.

		• Chemokines and cytokines that play a role in chemotaxis were altered in teras: IL-3,-10,-13,-15,-18 were upregulated whereas downregulation of IL-1,-8,-11,-27, were detected.
6	**Mechanical Testing of Repair Patches**	• All repair grafts displayed significant variation in their mechanical properties • All repair grafts had at least some reduced parameters compared to human rotator cuff tendons.

7.2 Clinical Implications of Findings

The mechanical and chemical changes noted in torn rotator cuff tendons are likely to be related. A significant correlation has been previously reported between increasing supraspinatus degeneration and decreasing ultimate tensile stress [112]. Biochemical changes have been shown to ensue following the loss of mechanical stimulus from torn rotator cuff tears. Changes in mechanical loads specifically affect rotator cuff biology and tendon healing through modulation of ECM related components such as MMPs, collagen organization and cell signalling [368]. Riley *et al.*, [71] have proposed higher rates of collagen turnover and remodelling in intact tendons compared to ruptured tendons, which may be part of the tendon's normal adaptive response to mechanical loading [74, 75]. *In-vitro* stress deprivation has been shown to increase the length of tendon cell cilia whereas cyclical loading can reverse this effect and decrease the length of cilia from rat tail tendon cells [369]. As cyclical strain has been shown to upregulate collagen synthesis in tendon fascicles, the absence of strain in disrupted collagen fibrils following tears may conversely downregulate collagen synthesis [370]. This could compound pre-existing collagen

structural irregularities and result in a further reduction in the tendon's ability to transmit loads along its collagen axis.

While this thesis has highlighted a number mechanical, chemical, structural and gene profile changes that occur in different sized rotator cuff tendon tears, the relationship between these changes is uncertain. It is possible that some of the mechanical changes addressed in Chapter 2 may be the initial insult to tendons. Some of the chemical ECM changes highlighted in Chapter 3 and the collagen structural damage measured in Chapter 4 may occur in response to differences in mechanical loads, and result in further microstructural damage. When these changes are combined with superimposed degeneration, it may result in an altered tendon structure that is less able to withstand and transmit mechanical loads. This will ultimately result in macroscopic damage and tendon rupturing which may clinically manifest as functional weakening. The chemical and gene changes may both predispose and occur as a result of changes in the mechanical environment.

Mechanical insults may translate to cellular insults and changes at a gene transcription level, which may further propagate damage within the tendon. Collagen damage or failure may expose local cells to decreased load and stress deprivation. Following either mechanical or cellular stresses, changes to cytokine pathways may occur as discussed in Chapter 5. Such changes involve interleukin-1, stress-activated protein kinases, oxygen free radicals and apoptosis mediators, all of which have the potential to cause tenocyte apoptosis. Some insights into both ECM changes have also been offered by the microarray analysis in Chapter 5. A key role for ECM remodelling pathways has been suggested by changes related to MMPs, ADAMTs and TIMPs. Macroscopic changes to the ECM may also be mediated through chondrogenic changes

with increased collagen II, as well as increased amyloid deposition. Xu *et al.,* have proposed that multi-factorial pathways contributes to tendinopathy [371]. A complex balance between these multivariate factors is likely to exist. In particular, changes in the ECM are likely to contribute to both cellular and mechanical factors. Based upon the findings of this thesis, I am proposing my own mechanism for tendinopathy (see **Error! Reference source not found.**). Areas which require increased investigation are Importantly, the full potential implications of these detected changes for surgical repair remain undetermined. It is likely that modulation of rotator cuff tendinopathy may be achieved by targeting extracellular matrix related pathways, as they play a key role in regulating the ability of tendons to transmit loads.

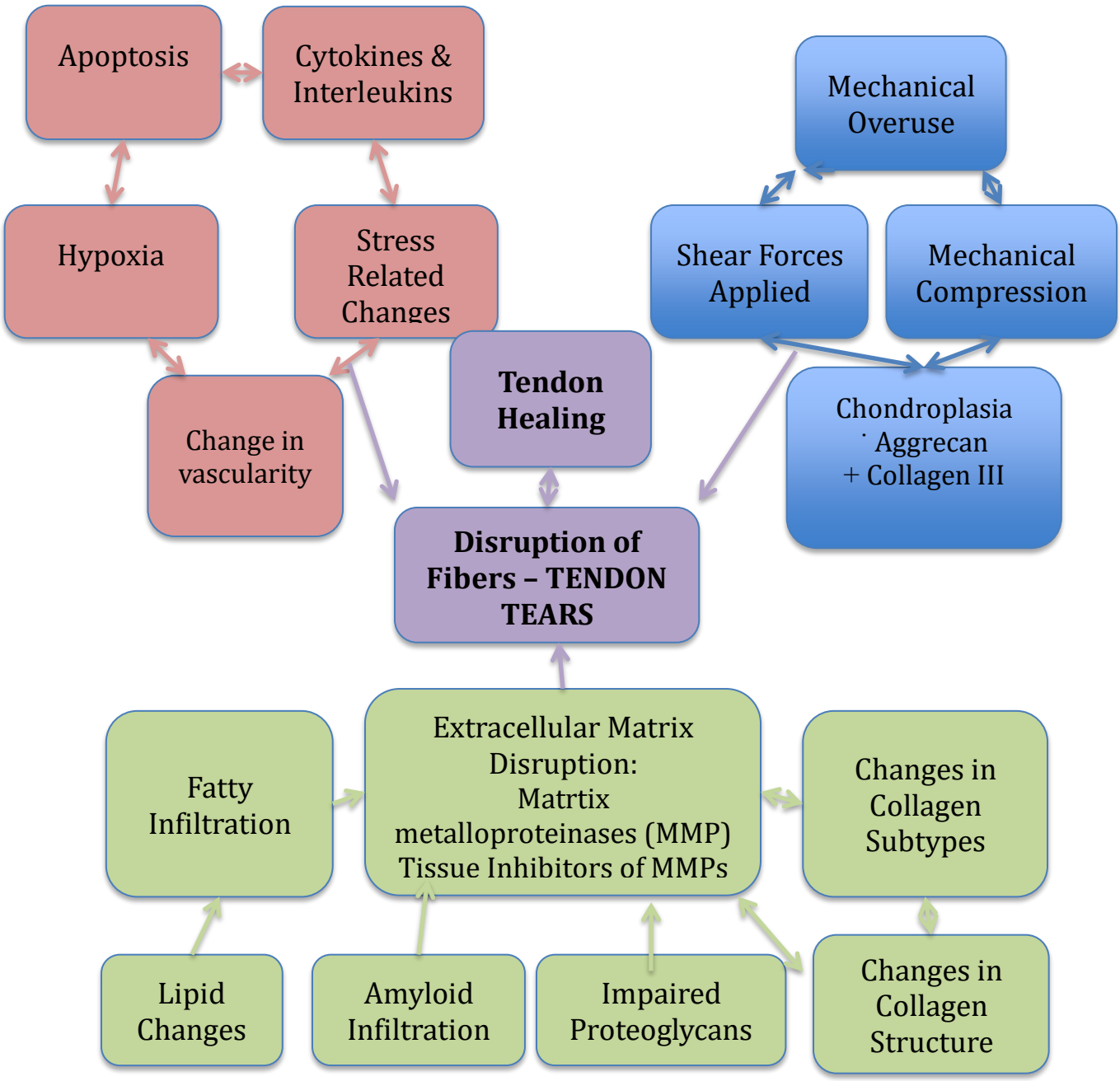

Figure 7-1: A proposed mechanism of tendinopathy, incorporating mechanical, biochemical and gene expression changes identified by this thesis. Mechanical factors are indicated in blue, viability related factors are highlighted in pink and extracellular matrix related factors are indicated in green. Increased understanding is required of viability related factors that may determine the healing potential. Therapeutic targets are likely to be achieved by targeting extracellular matrix pathways.

Factors favouring structural and chemical disruption appear to be more predominant in larger tears, compared to smaller tears and may underlie failure of tendon healing. The complex biology of torn tendons is contributed to by degeneration, and reflected by the fact that traumatic tears are more likely to have successful post-operative outcomes than degenerative tears [116]. While the mechanics and biology of tears correlates to some extent with tear size, there is undoubtedly a close relationship with age that needs to be recognised. Age is an important factor and affects the incidence of tears and potential healing thereafter. The effect of age on rotator cuff tears could not be addressed by this thesis, as none of the studies were adequately powered to investigate this important variable. A limitation of many studies looking into rotator cuff tendon pathologies is the difficulty in finding age matched normal controls; I attempted to avoid this potential confounding variable by examining age and gender matched groups in this thesis. Another limitation of this study is that all patients from whom 'normal' tendon samples were obtained, did not undergo preoperative radiographic imaging to confirm the absence of any tears or abnormal tendon morphology. However, as all 'normal' tendons were consistently distinguishable from torn tendons, I am confident that this group did not include grossly abnormal rotator cuff tendons. Some of the changes identified as part of the rotator cuff 'disease' process by this study and many others, may in fact represent tissue senescence or normal ageing. Thus, delineating between normal age related degenerative changes and pathological changes is difficult, but it is important to realise that both factors are likely to be contribute to rotator cuff tendinopathies.

7.3 Modulating Rotator Cuff Healing

Some of the knowledge offered by this thesis can potentially be used to guide attempts to modulate healing through the identification of mechanical, chemical, gene or structural targets that are altered in torn rotator cuff tendons. Insight into the characteristics of torn rotator cuff tendons can have direct translational effects on surgical management of tears. Following some histological studies of tendon edges, some surgeons recommended resection of edges or the "falciform edge of new tissue" to expose more healthy tissue further back [1]. However further understanding that tissue at the edges of tendons are in fact viable, with good vascularity and ability to produce collagen, has prevented this approach from being routinely undertaken [66, 184]. In order to improve high post-operative failure rates, repairs need to address both the mechanical and the biological properties of abnormal tissue at the edges of torn tendons, as this tissue will have to support any attempted surgical repairs.

There is increasing understanding that it may be possible to modulate rotator cuff healing by altering the surrounding mechanical environment. Tendons respond to mechanical stimulation by altering MMPs, TIMP and cell signalling pathways. Tensile loading has been shown to increase collagen fiber organization, collagenous and non-collagenous matrix proteins synthesis and to decrease matrix degradation [150, 153, 368]. Botulinum toxin A was injected into supraspinatus tendons to induce muscle paralysis and reduce any excessive tension that may be placed on the rotator cuff repair in a rat model [372]. Botulinum injections improved collagen fiber organization at 4 weeks, but resulted in inferior mechanical properties, bone volume and mineral content. This study suggests that total removal of load has a negative effect on rotator cuff healing and is thus

inadvisable. Thomopoulos *et al.,* reported that rotator cuff tendon healing to bone was impaired by early exercise and the best healing was found in rats that were immobilized post-operatively [373]. While mechanical load is important for maintenance of tendon homeostasis, excessive loading can lead to microscopic and macroscopic damage [84]. At present the ideal amount, timing and duration of mechanical load to be applied during the rehabilitation period is still undetermined. It is possible that the formation of scar and fibrotic tissue following many rotator cuff repairs is exacerbated by excessive early motion that may induce inflammation.

Understanding the biology of rotator cuff tendon failure is important as it can help to identify some important parameters to look at when assessing treatments for rotator cuff tendinopathies and tears. For example corticosteroid injections are probably the most common treatment employed for the treatment of rotator cuff tendinopathies. Even though it undoubtedly reduces the symptoms of pain in some patients, a greater understanding of its biological effects on tendons is required. Previous studies have shown that dexamethasone induces a reduction in collagen synthesis, cell proliferation and proteoglycan synthesis in cultured tenocytes. As this thesis has shown that larger tears are associated with changes in collagen structure and proteoglycans, it is possible that despite improving pain symptoms, glucocorticoid treatments may be exacerbating or worsening structural and chemical changes seen in rotator cuff tendon tears [194, 195]. The findings from this thesis could help to identify modifiable targets for accelerating tendon healing. Another potentially interesting avenue of research are MMP inhibitors, such as doxycycline, which have been shown to result in accelerated healing, improved collagen organisation and mechanical strength in rat models [374].

In addition to tear size, all factors that affect tendon healing need to be considered in conjunction. The behaviour of the tear and its subsequent healing outcomes may be influenced by factors relating to the type of tear, e.g. whether the tear is acute or chronic, the tear pattern, any tissue loss and the size of the subacromial space. Even if the inherent biomechanical ability of the tendon to heal is the key determinant of successful repair, it must be remembered that outcome is also influenced by the mechanical construct and other surgical factors such as whether there was adequate footprint coverage, stability of the cuff repair construct, repair technique employed, adequate mobilisation of the tendon, avoidance of tension mismatch or tension overload in addition to the post-operative rehabilitation programme.

In view of the biomechanical alterations seen at the edges of rotator cuff tendons tears, the tissue present at the edges of tears, particularly larger tears, may lack the capability to repair and recapitulate the complex structure, composition and organization of the native rotator cuff enthesis. Simply suturing the repair may be inadequate as this is only addressing the mechanical element of the repair and not the underlying biology. The future of rotator cuff tendon repair, is already seeing a move towards mechanical augmentation of repairs, for example with repair patches, or through the use of biological augmentation, for example with stem cells and growth factors. None of the four commercially available rotator cuff repair patches tested closely matched the mechanical properties of human rotator cuffs, so a great deal of work is needed to find better, more suitable treatment options to improve rotator cuff tendon healing. Fortunately, there is a lot of exciting potential for furthering understanding of rotator cuff failure, and developing novel surgical and therapeutic treatments.

8 CHAPTER 8: FUTURE WORK

It would be useful to build upon some of the findings from this thesis to investigate whether any of the detected altered parameters could predict higher rerupture rates. As well as the investigating modalities employed by this thesis, simultaneous clinical follow of patients would help to investigate whether the detected chemical or mechanical changes correlate with poorer clinical outcomes. Ideally patients would be investigated by clinical outcome scores, functional assessment and imaging of tendons. Such information is available for the subset of intraoperative specimens that were collected from patients enrolled in the UKUFF trial as these patients were followed up by clinical assessment and MRI scans at one year following theur surgery. I am specifically investigating whether a reduced storage modulus or a particular FTIR signal corresponds with higher post-operative MRI retear rates.

To be able to delineate whether chemical changes in tendon specimens translate to altered mechanical properties, I am completing another study performing DSA and FTIR on the same tendon samples. I hypothesise that disruption of collagen structural arrangements with reduced proteoglycan and elastin content that is seen in chronic rotator cuff tendinopathies will directly correlate with a lower storage modulus, as the extracellular matrix will have a reduced ability to transmit forces through and between collagen fibrils.

8.1 Spectral FTIR Mapping of Changes

In the future, FTIR could be used on serial tendon samples to analyse chemical effects of various treatments, such as corticosteroids or vitamin C. To improve the resolution and reliability of the spectral data, I am intending on using a FTIR spectral mapping system. I have already performed a small pilot study using this technique, which allow three-dimensional mapping of the FTIR signal. The resolution and amount of chemical information available is vastly improved compared to the standard FTIR that was used in Chapter 3, as readings are taken over a wider area and the spectra can be correlated directly with histology. This should help to overcome difficulties with spectral overlaps between areas of interest e.g. overlapping amide bands from collagen and proteoglycans. To prepare the specimens for mapping, cryosections of snap frozen tendons without any fixation agents were taken to avoid any formalin interference within the tendon spectral maps. This technique allows high resolution mapping of subtle changes between different tear sizes, as exemplified by images of normal tendons and massive tendon tears (see Figure 8-1 and Figure 8-2).

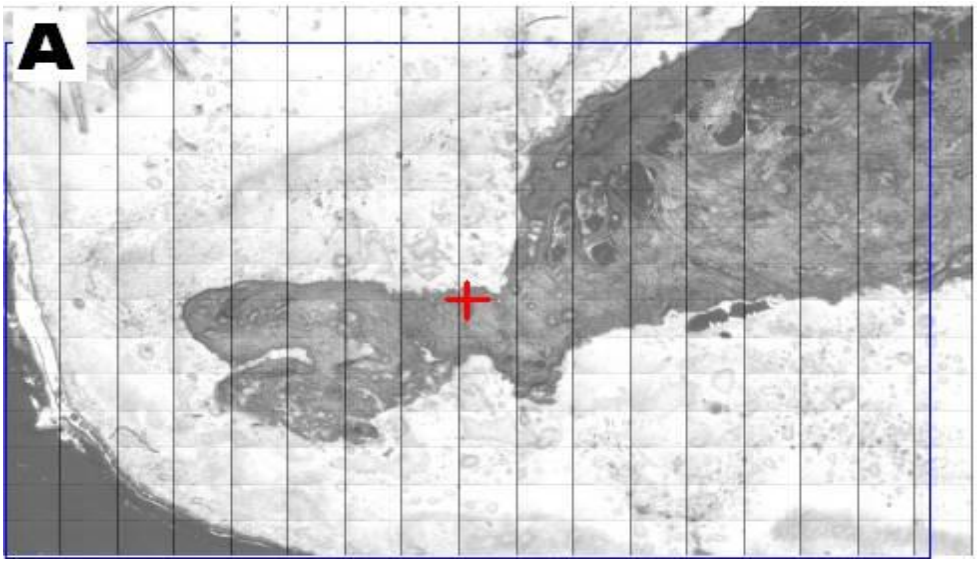

Figure 8-1: FTIR spectral map of normal tendon.

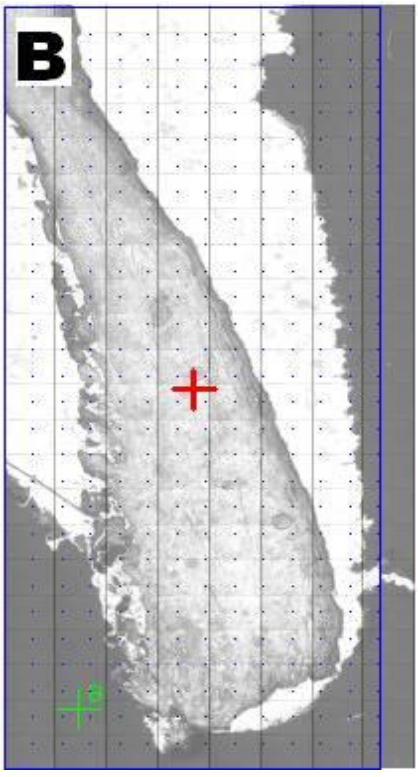

Figure 8-2: FTIR spectral map of a tendon with a massive tear.

8.2 Further Chemical and Gene Profile Analysis

Further studies could artificially cross-link the collagen in tendon tissue using one of numerous chemical treatments [304] and study whether this would increase the thermal properties of tendon, as I would predict from the results of my study.

It would also be useful to characterise the mechanical properties and the thermal properties from the same tendon specimens, to establish whether there is a relationship between the two. Unfortunately the small sample sizes of tissues that I was able to obtain meant that I was unable to perform this study myself.

In the future it may be useful to extend my study to analyse the chemical and gene profile of samples taken from bursal and synovial tissue. Inflammatory and ECM changes seen in rotator cuff tendons have also been reflected in changes in synovial fluid, and may be particularly relevant as the synovial bursa is accepted to be the main source of pain in shoulder disease and it is also vulnerable to mechanical friction [375]. Also, it would be very interesting to compare the gene profiles of tissue specimens collected at least six weeks or longer after rotator cuff repairs, to assess whether gene expression varies over time and if there are specific pathways which mau correlate to healing.

8.3 Further Patches Work

A clearer understanding is required of the physiology of the postoperative environment as this is likely to influence durability of repair and the ultimate success of healing. Seeding cells onto repair patches has been proposed as a superior approach by providing both mechanical support and a biological stimulus for healing. It will be useful to assess whether the three-dimensional bioactive and degradable scaffolds facilitates the anchorage and growth of cells, but also provides a suitable cellular micro-environment through increased cell differentiation, metabolic activity, and cell–cell signalling [376, 377]. Tenocytes could be tracked and an assessment made of cell number, shape and whether cells migrate and penetrate the patch, or whether they remain on the surface. A greater understanding is also required of how the mechanical properties of scaffolds may alter *in-vivo* due to the interaction with cells and the ECM over the critical time period of three to six weeks surgical repair when healing takes place. A hyaluron-chitosan scaffold seeded with fibroblasts has been used to augment the repair of a large infraspinatus defect, resulting in improved tensile and tangent modulus compared to the scaffold without cells [378]. Tenocytes were seeded onto Restore™ patches and a collagen type I/III based ACI-Maix™ scaffold, and used to repair massive rotator cuff defects in rabbits [379]. This resulted in some initial inflammation, but produced an improved histological appearance compared to the control group without cells. These studies support the idea that the addition of cells to scaffolds results in superior tendon healing.

Future approaches may utilize scaffolds that are coated with growth factors to achieve localized and sustained delivery of factors that are proposed to speed up healing.

8.4 Conclusion

In the future, it may be possible that a matrix of a number of predictors of failure could be assessed in each patient to try to predict outcomes following therapies or surgical repairs. Such information may help to tailor treatments to each individual patient. Unfortunately a much deeper understanding of tendon healing is required before this can be achieved. This thesis did not focus on whether changes in tears had any potential correlation with treatment outcomes and this would be the next area to explore. I have identified numerous potential candidates that could be modulated to encourage healing in further studies.

This body of work has highlighted that rotator cuff tendon tears are associated with significant changes in both the mechanics and the biology of tendon tear. In order to successfully overcome high post-operative failure rates, treatments will most likely have to address both the biology of the failing tendon and restore the appropriate mechanics. However it is possible that torn tendons, particularly for larger tears, may never regain normal mechanical and chemical properties and adjunct treatments or approaches may be necessary.

9 CHAPTER 9: PRESENTATIONS

9.1 Oral Presentations:

1. ‘Genetic Profiling of Normal and Different Sized Rotator Cuff Tears Using Microarrays’. Orthopaedic Research Society (ORS), California, USA, 2011.

2. ‘Genetic Profiling of Normal and Different Sized Rotator Cuff Tears Using Microarrays’. SECEC, Nice, Paris, 2011.

3. ‘Identification of Novel Collagen Structural Appearances in Rotator Cuff Tendon Tears Using Transmission Electron Microscopy’. European Federation of National Associations of Orthopaedics and Traumatology (EFORT), Copenhagen, Denmark, 2011.

4. ‘Torn Human Rotator Cuff Tendons Have Reduced Collagen Structural Properties Which Are Quantifiable Using Differential Scanning Calorimetry’. European Federation of National Associations of Orthopaedics and Traumatology (EFORT), Copenhagen, Denmark, 2011.

5. ‘Genetic Profiling of Normal and Different Sized Rotator Cuff Tears Using Microarrays’. European Federation of National Associations of Orthopaedics and Traumatology (EFORT), Copenhagen, Denmark, 2011.

6. ‘Genetic Profiling of Normal and Different Sized Rotator Cuff Tears Using Microarrays’. European Society for Surgery of the Shoulder and the Elbow (SECEC), Lyons, France, 2011.

7. ‘Investigating The Mechanical Properties Of Normal And Torn Rotator Cuff Tendons Using Dynamic Shear Analysis’. American Academy of Orthopaedic Surgeons (AAOS) Scientific Meeting; New Orleans, USA, 2010.

8. ‘Fourier Transform Infrared Analysis of Rotator Cuff Tears’. American Academy of Orthopaedic Surgeons (AAOS) Scientific Meeting; New Orleans, USA, 2010.

9. ‘Dynamic Shear Analysis: A Novel Technique For Comparing Normal And Torn Rotator Cuff Tendons’. International Congress for Shoulder and Elbow Surgery (ICSES), Edinburgh, UK, 2010.

10. ‘Identifying Differentiating Features Between Normal And Torn Rotator Cuff Tendons Using Fourier Transform Infrared Spectroscopy’. Combined Orthopaedic Meeting (COMOC), Glasgow, UK, 2010.

11. ‘Identifying Differentiating Features Between Normal And Torn Rotator Cuff Tendons Using Fourier Transform Infrared Spectroscopy’. European Federation of National Associations of Orthopaedics and Traumatology (EFORT), Madrid 2010.

12. ‘Microarray Analysis of Normal, Small and Massive Rotator Cuff Tendon Tears’. Tendinopathy Symposium, Umea, Sweden, 2010.

13. ‘Mechanical Suitability Of Extracellular Matrix Grafts To Augment Repairs of Rotator Cuff Tears’. European Society of Traumatology (ESTES), Brussels, Belgium, 2010.

14. ‘Determining Mechanical Differences Between Normal and Torn Rotator Cuff Tendons Using Dynamic Shear Analysis’. British Elbow & Shoulder Society Scientific Meeting; London, UK, 2009. **Awarded 1st Prize for best presentation.**

15. ‘Using Fourier Transform Infrared Spectroscopy to Differentiate Between Normal and Torn Rotator Cuff Tendons’. British Elbow & Shoulder Society Scientific Meeting; London, UK, 2009.

9.2 Poster Presentations:

1. ‘Characterizing Differences In The Collagen Structural Composition Between Normal And Torn Rotator Cuff Tendons Using Differential Scanning Calorimetry’. Orthopaedic Research Society (ORS), California, USA, 2011.

2. ‘Genetic Profiling of Normal and Different Sized Rotator Cuff Tears Using Microarrays’. Orthopaedic Research Society (ORS), California, USA, 2011.

3. ‘Fourier Transform Infrared Analysis of Rotator Cuff Tears’. Orthopaedic Research Society Scientific Meeting; New Orleans, USA, 2010.

4. ‘Using FTIR To Differentiate Rotator Cuff Tears And Identify Treatment Biomarkers’. International Congress for Shoulder and Elbow Surgery (ICSES), Edinburgh, UK, 2010

5. ‘Dynamic Shear Analysis: A Novel Technique For Comparing Normal And Torn Rotator Cuff Tendons’. European Federation of National Associations of Orthopaedics and Traumatology (EFORT), Madrid, Spain, 2010

6. ‘Biochemical Differentiation Between Normal And Torn Rotator Cuff Tendons Using Fourier Transform Infrared Spectroscopy’. Société Internationale de Chirurgie Orthopédique et de Traumatologie (SICOT), Gothenburg, Sweden, 2010.

7. ‘Too Weak Or Too Tough? A Study To Investigate The Tensile, Shear And Suture Pull Out Mechanical Properties Of Rotator Cuff Repair Patches And Assess How Well They Match To Normal And Torn Rotator Cuff Tendons’. Société Internationale de Chirurgie Orthopédique et de Traumatologie (SICOT), Gothenburg, Sweden, 2010.

8. ‘Dynamic Shear Analysis: A Novel Technique For Comparing Normal And Torn Rotator Cuff Tendons’. Société Internationale de Chirurgie Orthopédique et de Traumatologie (SICOT), Gothenburg, Sweden, 2010.

9. ‘Characterizing Differences In The Collagen Structural Composition Between Normal And Torn Rotator Cuff Tendons Using Differential Scanning Calorimetry’. Société Internationale de Chirurgie Orthopédique et de Traumatologie (SICOT), Gothenburg, Sweden, 2010.

10. ‘Using Fourier Transform Infrared Spectroscopy to Differentiate Between Normal and Torn Rotator Cuff Tendons’. British Orthopaedic Research Society Scientific Meeting; Newcastle, UK, 2009.

10 APPENDICES

<u>APPENDIX 1: Diagram outlining some common conditions affecting the shoulder, their potential diagnosis and treatment</u>. Reproduced with permission from Andrew J Carr.

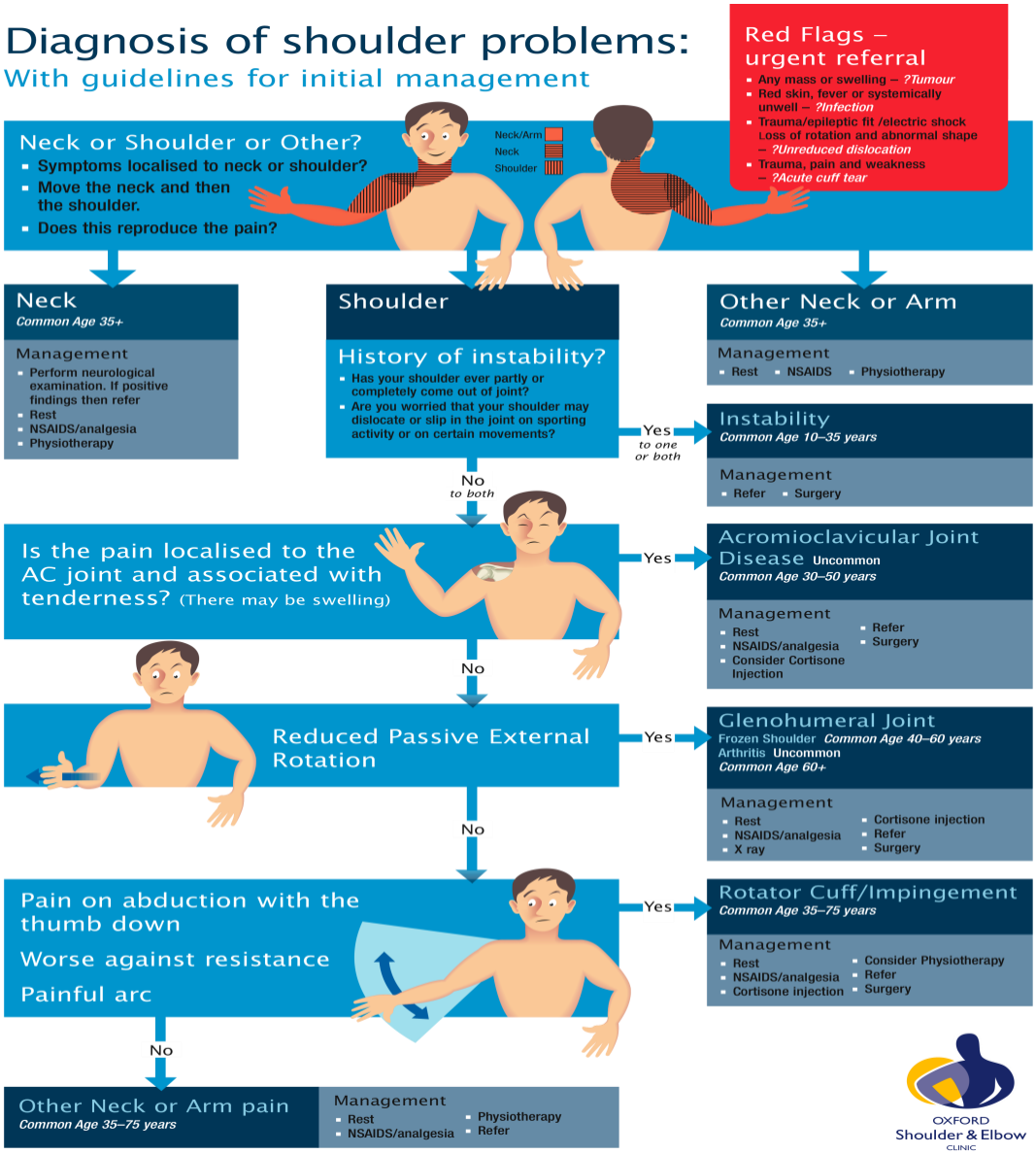

APPENDIX 2 - The United Kingdom Rotator Cuff Trial (UKUFF)

The UKUFF Trial (funded by the Department of Health's Health Technology Assessment Programme) is a multi-centre randomised controlled trial to measure the clinical and cost effectiveness of different types of rotator cuff repairs. The Nuffield Department of Orthopaedic Surgery (NDOS) at the University of Oxford will co-ordinate the trial in collaboration with the Health Services Research Unit at the University of Aberdeen.

Background

The clinical evidence available regarding the natural history and the treatment of rotator cuff tears is limited and conflicting. Different methods of rotator cuff tear management are practiced throughout the United Kingdom. These include:

- Arthroscopic Repair – where the tear is repaired through key-hole surgery
- Open Repair – involving a longer skin incision to undertake the procedure under direct vision
- Non-Surgical Treatment – where a programme of Rest then Exercise is practiced

Aims

This study was designed to assess these three methods of treatment.

Method

Over 600 patients, from 70 centres throughout the United Kingdom will be investigated. Information to be collected and analysed includes:

- Patient focused questionnaires regarding shoulder pain and function
- Patient focused questionnaires regarding the economic cost of the treatment
- Health care resources used (i.e. hospital stays, operating theatre equipment)
- MRI scans 12 months after the surgical repairs (to see if the repair is intact)
- Histological findings from tissue samples harvested during surgical repairs (to see if tissue quality influences success)

Recruitment of Patients

Those who consent to participate will be randomised to undergo an arthroscopic repair or an open repair, or to complete the rest then exercise programme. All participating patients will be placed on the NHS waiting list for surgery. Those allocated to the Rest then Exercise programme will still be placed on the waiting list and will not be at any disadvantage if surgery is required. However if they feel their shoulder has improved after completing the programme, they can decline surgery.

UKUFF Inclusion Criteria:

- Degenerative Rotator Cuff Tear
- Full thickness Rotator Cuff Tear
- Diagnosed using MRI or Ultrasound
- Patient able to consent

UKUFF Exclusion Criteria:

- Previous surgery on affected shoulder
- Dual shoulder pathology
- Rheumatoid arthritis/systemic disease
- Significant osteoarthritis problems
- Significant neck problems
- Cognitive impairment or language issues

APPENDIX 3: Variance Of Dynamic Shear Testing Of Tendons

To measure the variance of the test-retest of tendons, I repeated dynamic shear testing of human tendon specimens preserved in formalin. The modulus of tendon specimens were measured, and then measured again 6 weeks later to assess the variability of the tendon rheology data. The correlation coefficient was 0.69 and the error standard deviation was 3202.8 Pa.

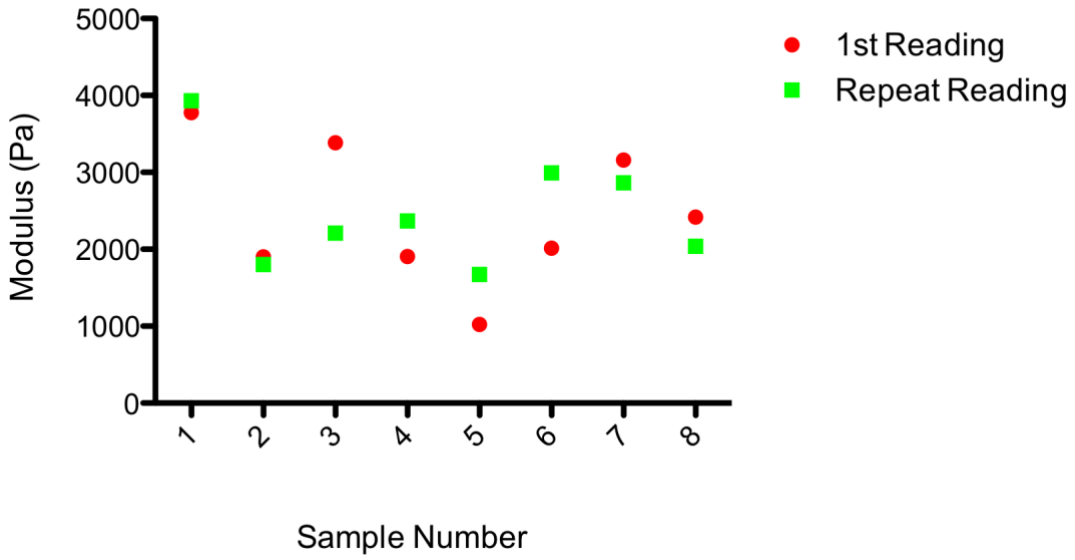

Graph showing the variance of testing and then retesting the same human supraspinatus tendon samples at a later date.

APPENDIX 4: FTIR Pilot Data Looking At Effects Of Sample Preparation

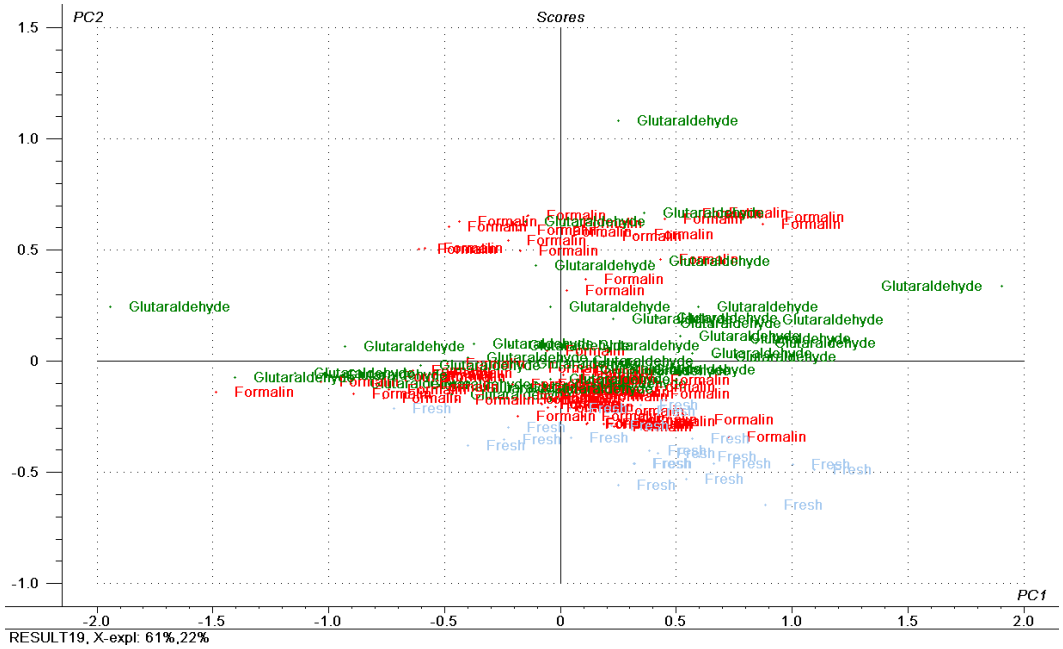

Graph showing results from the pilot study to assess the effect of different types of preservation modalities on FTIR results. Data reduction using performed using principal component analysis. Legends refer to the type of buffer: Formalin (red), Glutaraldehyde (green), and Fresh (light blue). Overlap is shown between fresh and formalin preserved tendons, indicating that it is possible to use formalin preserved tendons without a substantial effect on the results.

APPENDIX 5 – Vibrational Assignment Of Biologically Relevant Functional Groups

Functional group	Frequency (cm^{-1})	Compound class
ν(OH)	3300	Water, carbohydrate
ν(NH)	3250	Protein
ν(=C-H)	3010	Unsaturated lipids
νx(CH3)	2960	Lipids, proteins
νx(CH2)	2925	
νx(CH2)	2870	
νx(CH3)	2855	
ν(CH)	2930 2890	Complex carbohydrates and amorphous fully hydrated sugars
(OH)	2150	Water
ν(C=O)	1740	Lipids
ν(C=O)	1650	Proteins
δ(OH)	1630	Water
$\nu x(CO_3^{2-})$	1460	Carbohydrates
$\nu x(CO_2^{-})$	1560	Fatty acids salts
δ(NH)	1550	Proteins
δ(CH2)	1470	Lipids
δ(CH3)	1375	Lipids
ν(PO2)	1240	Phospholipids
ν(C-O)	1000	Carbohydrates
δ(=C-H)cis	720	Cis Fat
δ(=C-H)trans	956	Trans Fat
δ(OH)lib	700	Water
ν: stretching, δ: deformation data from Spectrochemical Analysis Detectors ((Bargahava and Levin)		

APPENDIX 6: Vibrational Band Assignment For Collagen Rich Tissues, As Well As Their Associated Chemical Group

Table 1. Vibrational band assignment in tendon tissues

Band position (cm^{-1})	Group frequency	Vibrational assignment	Chemical group
940			
970			
1030		C-O stretching	Carbohydrates
1080		Symmetric PO^{2-}	Phospholipids
1160		NH3	Lipids
1200			
1240			
1284	Amide III		
1319			
1338			
1380			
1400			
1424			
1456	Amide II		
1557			
1631			
1654	Amide I		
1740			
2851			
2876			
2928			
2962			
3080	Amide B		
3200			
3315- 3325	Amide A		
3420			

APPENDIX 7: Differentiating Different Sized Rotator Cuff Tears

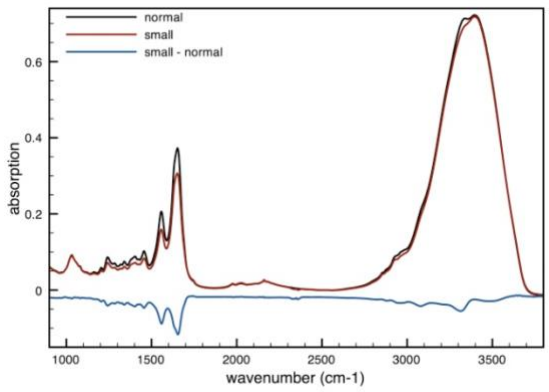

Normal vs. Small

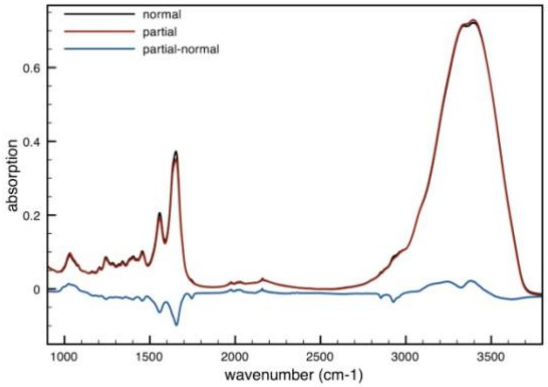

Normal vs. Partial

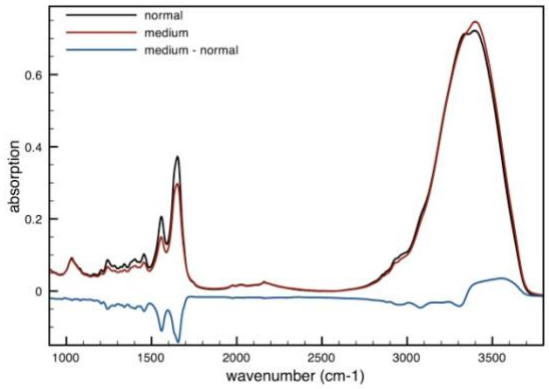

Normal vs. Medium

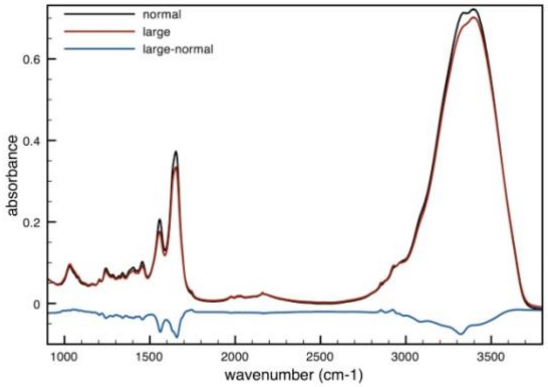

Normal vs. Large

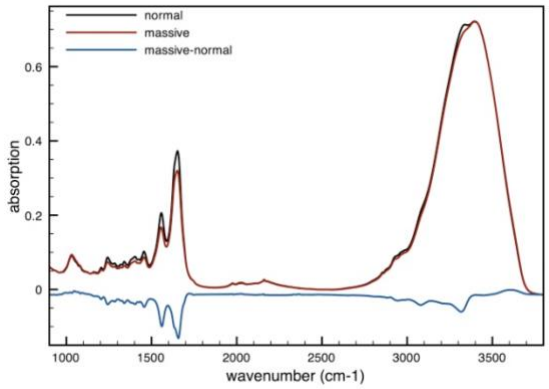

Normal vs. Massive

Principal component analysis (PCA) was used to obtain further details about tendon characteristics and discriminating variables by allocating a prior class aperture of tear size.

Principal Component Analysis (PCA) comparison of paired tendons samples:

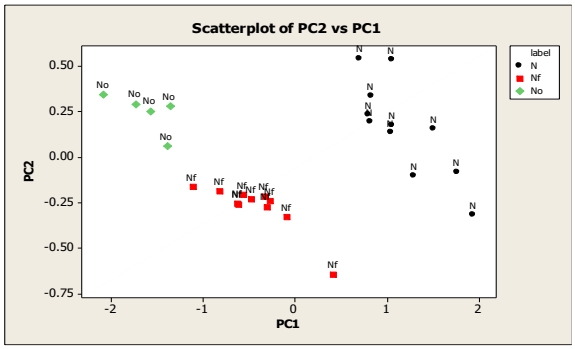

Normal vs. Normal Formalin

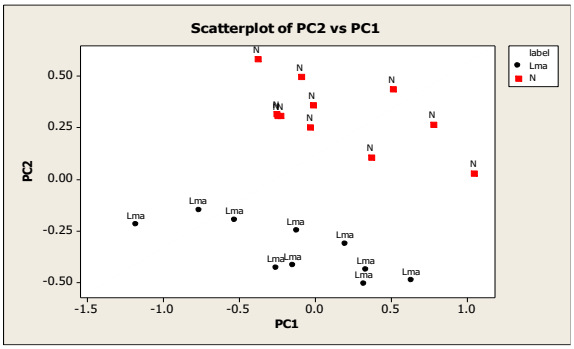

Normal vs. Large/Massive

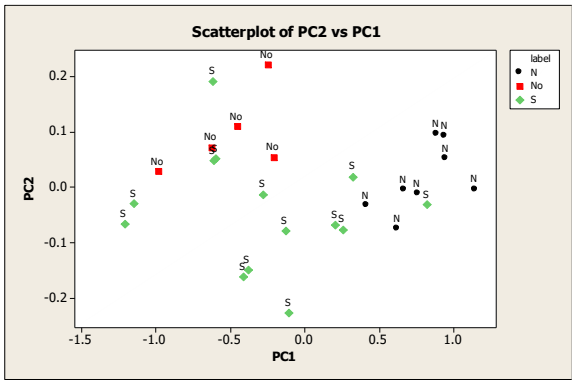

Normal vs. Small

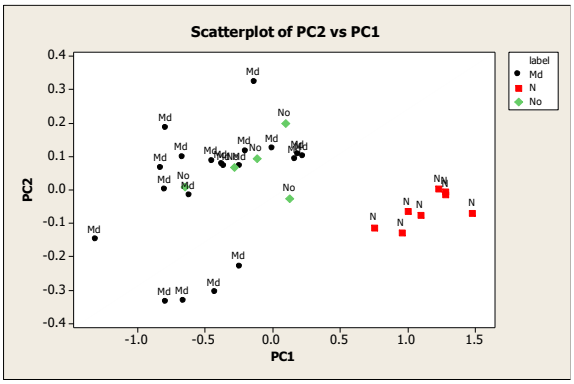

Normal vs. Medium

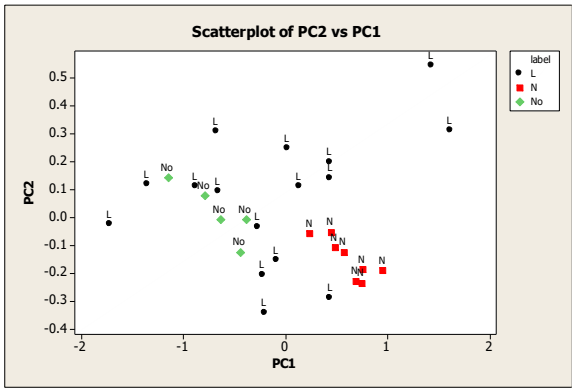

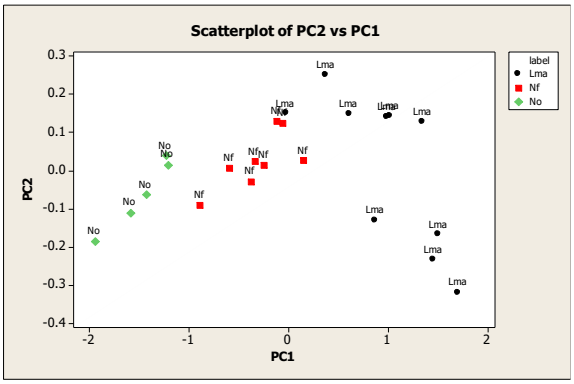

Normal formalin vs. Large/Massive fresh

Normal vs. Large

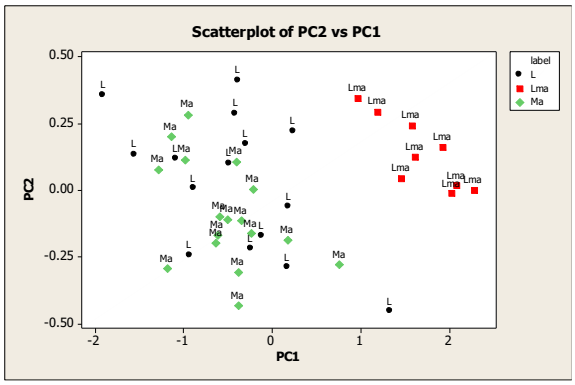

Large/massive fresh vs. Large and Massive formalin

Using discriminant function analysis (DFA), sub-differentiation is possible for different sized tears, with very minimal overlap between the different sized tears.

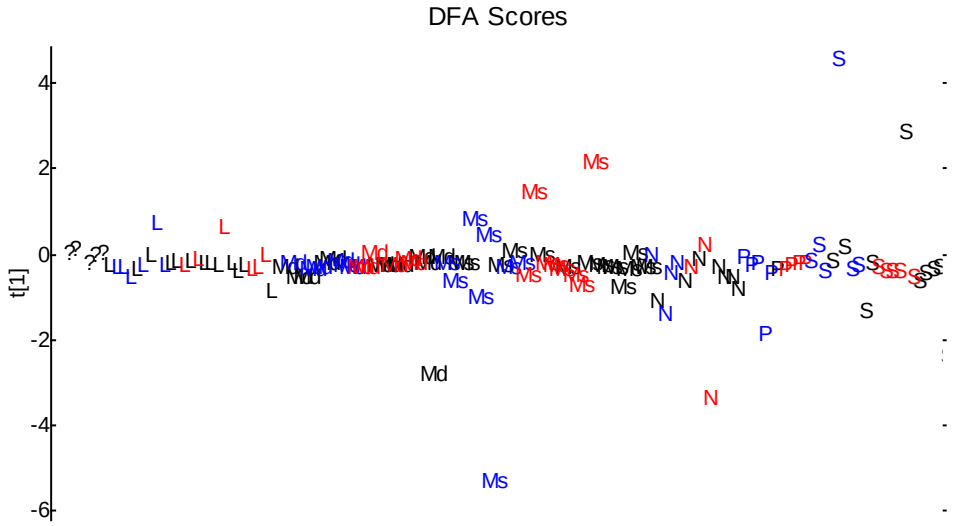

Discriminant function analysis scores show clear separation between different tear size groups, with minimal overlap.

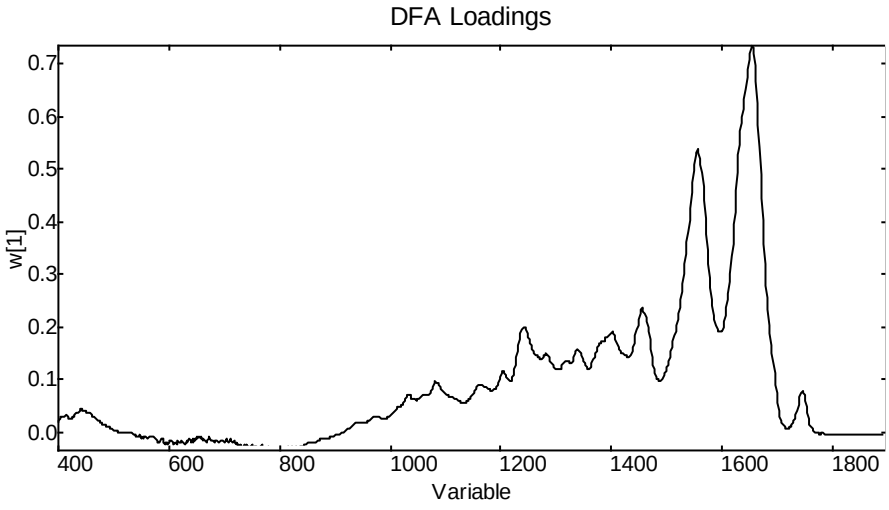

Discriminant function analysis of the loadings helped to highlight key spectral wavenumbers where most spectral variability occurred.

APPENDIX 8a - Paraffin Embedding

- Fix the tendon sample by submerging it in 10% formalin for 24 hours
- Decalcify tendon in nitric acid for 12 hours
- Embed in paraffin was blocks.
- Cut into 5 micron sections using Leica RM2135 microtome (Leica Microsystems, Germany)
- Heat adhere to Snow coat X-tra per-cleaned micro slides (Surgipath Winnipeg, Manitoba, Canada)

APPENDIX 8b: H&E (Haematoxylin and Eosin) Staining protocol

1. DeParafinise for 10 minutes in Xylene
2. Rehydrate for 2 minutes in Alcohol 100% (x2) then,
   1 minute Alcohol 90% then
   1 minute Alcohol 70%
3. Rinse for 1 minute in distilled water
4. Stain for 5 minutes with Haematoxylin
5. Rinse for 2 minutes in the water bath
6. Stain blue for 15 seconds with 2% Sodium Bicarbonate
7. Rinse for 1 minute under running water
8. Stain for 5 minutes with 1% eosin
9. Rinse for 1 minute in the water bath
10. Dehydrate for 1 minute with 70% alcohol, followed by
    1 minute in 90% alcohol
    1 minute in 100% alcohol
11. Clear for 3 minutes with Xylene
12. Mount with DPX glue and coverslips

APPENDIX 8c: Alcian Blue Staining protocol

1. DeParafinise for 10 minutes in Xylene
2. Rehydrate for 2 minutes in Alcohol 100% (x2) then,
   1 minute Alcohol 90% then
   1 minute Alcohol 70%
3. Rinse for 1 minute in distilled water
4. Incubate for 3 minutes with 3% acetic acid
5. Rinse for 1 minute in distilled water
6. Stain blue for 1 hour with 0.1% Alcian blue 8GX in 3% acetic acid, pH 2.5
7. Rinse for 10 minutes under running water
8. Counterstain for 1 minute with 1% eosin
9. Rinse for 1 minute in the water bath

10. Dehydrate for 1 minute with 70% alcohol, followed by
    1 minute in 95% alcohol
    1 minute in 100% alcohol
11. Clear for 3 minutes with Xylene (repeat twice)
12. Mount with DPX glue and coverslips

APPENDIX 9a – Supraspinatus Histological Grading System Described By Riley *et al.* [71]

Grade	Tendon description	Collagen fibre appearance	Ability to distinguish collagen fibres	Tenocyte nucleus appearance
1	**Normal**	wavy fibres	easy to discern individually	nuclei elongated + parallel to collagen
2	**Mild degeneration**	well aligned fibres, irregular waviness	individual fibres not easily identified	shorter nuclei, displayed in Indian file
3	**Moderate degeneration**	collagen hyalinisation - fragments in ECM	loss of fiber orientation	less orientated, increased nuclei density
4	**Severe degeneration**	diffuse homogenous appearance hyalinisation	complete loss of fiber orientation	rounded tenocytes, reduced number of nuclei

APPENDIX 9b – Supraspinatus histological grading system to describe glycosaminoglycan (GAG) content following alcian blue staining

Grade	Tendon description	Presence in between collagen fibres
0	**Normal**	No stainable GAG
1	**Mild accumulation**	Stainable GAG between fibers but bundles still discrete
2	**Moderate accumulation**	Stainable GAG between fibers with loss of clear demarcation of bundles
3	**Severe accumulation**	Abundant GAG throughout

APPENDIX 10 - RNA Extraction

Equipment and reagents required:

- RNeasy Lipid Tissue mini kit (Qiagen)
- RNAZap (Sigma)
- Pestles and Mortars
- Liquid Nitrogen
- Chloroform (Sigma)
- Ethanol
- RNAse-free water

Grinding protocol:

1. Tendon samples are stored in RNA later at – 80
2. Prepare all surfaces and equipment with RNA zap
3. Thaw samples on the benchside while preparing the required equipment.
4. Pour liquid nitrogen into mortar, and submerge pestle end. Repeat x3, until minimal bubbling.
5. Using a pipette, remove RNA later from ependorph and use tip to aid moving tendon from ependorph to mortar.
6. Allow volume of liquid nitrogen to reduce to half the mortar depth and begin grinding the tendon.
7. When liquid nitrogen empties, immediately refill.
8. Repeat cycle 3 times, or more, until fine powder consistency is achieved.
9. Move immediately to RNA extraction

RNA extraction

1. Add 1ml of tissue lyser (Qiazol) from RNA easy kit to the ground tissue. It will freeze on contact with the mortar.
2. Allow to thaw (approx 10mins) until it reaches an ice cream like texture and homogenise further using the pestle.
3. Leave until it becomes clear (approx 10mins) and then pipette the lysate into an ependorph tube.
4. Leave at room temperature on the benchtop for 5mins to allow dissociation of the nucleoprotein complexes.
5. Add 200ul chloroform and shake vigorously for 15 seconds.
6. Leave for 5 minutes at room temperature.
7. Centrifuge at 12000g for 15 mins at 4 degrees.
8. Transfer the upper aqueous phase to a new tube and add equal volume of 70% Ethanol.
9. Vortex (do not centrifuge).

10. Transfer 700ul to RNeasy column and centrifuge at 8000g for 15 seconds at room temperature. Discard the flow through – continue discarding flow through until step 17.
11. Repeat with the remainder of the sample.
12. Add 700ul of buffer RW1 to RNeasy column. Centrifuge for 15 seconds at 8000g
13. Add 500ul of buffer RPE and centrifuge for 15 seconds at 8000g
14. Repeat step 13
15. Place the RNeasy column into a new 1.5ml collection tube. Add 50ul RNase free water to directly onto the column membrane. Leave for 5 mins.
16. Elute RNA by centrifuging for 1min at 8000g.
17. Transfer the eluent on ice to nanodrop for quantification.
18. Store at -80 degrees.

APPENDIX 11 – RNA Extraction And Hybridisation Results

Sample ID	Conc (ng/ul)	260/280	260/230	Nano RIN	Array	Tendon type
59	134	2.05	1.69	6.80	1_1	Normal
67	124	2.06	1.63	6.80	1_2	Normal
54	306.8	1.98	2.1	6	1_3	Medium
45	118.8	1.93	1.66	N/A	1_1	Small
62	26.49	1.96	1.3	5	1_2	Massive
68	80	2.04	1.92	6.40	1_3	Medium
46	55.28	1.81	1.22	5.7	1_4	Massive
12b	117	2.04	1.78	7.30	1_1	Medium
42	104.6	1.9	1.72	N/A	1_2	Small
61	51.85	1.93	1.67	5.3	1_3	Small
24b	98	2.05	1.82	7.30	1_4	Medium
66	27.45	2.01	1.62	6	1_1	Normal
11	105.78	2.04	1.93	6.40	1_2	Normal
35	316.4	1.88	1.75	6.6	1_3	Large
60	69.83	1.91	1.58	6.1	1_4	Normal
18	430.2	1.91	2.1	6.2	1_1	Normal
58	184.8	1.99	1.95	7.2	1_2	Small
5	25.23	1.84	1.51	6.20	1_3	Medium
20	60.91	1.87	1.56	6.2	1_4	Large
15	33.89	2.16	1.53	6.9	1_1	Normal
17	85.83	1.94	1.97	6.8	1_2	Normal
57	61.89	1.92	1.57	5.4	1_3	Medium
19	38.26	2.06	1.55	6.6	1_4	Small
56a	199.3	1.97	1.8	7.1	1_1	Large
21A	66.60	2.14	1.84	6.2	1_2	Normal
9	100.3	1.91	1.78	N/A	1_3	Normal
36b	195.6	1.94	1.95	7.1	1_4	Large
39b	123	2.08	1.55	6.80	1_1	Normal
7b	111.3	1.96	1.78	6.9	1_2	Small
6	62.68	2.01	1.54	6.80	1_3	Massive
47	85	2.05	1.49	7.20	1_4	Normal

APPENDIX 12 - cDNA Synthesis

cDNA synthesis was conducted using SuperScript™ III First-Strand Synthesis System for RT-PCR (Invitrogen™ life technologies)

- Mix and briefly centrifuge each component before use
- Combine the following:
    - up to 5 µg total RNA *n* µl
    - Primer (50 µM oligo(dT)20) 1 µl
    - 10 mM dNTP mix 1 µl
    - DEPC-treated water to 10 µl
- Incubate at 65 for 5 mins then place on ice for 1min
- Prepare the following cDNA synthesis Mix adding each component in the indicated order:
    - 10X RT buffer 2 µl
    - 25 mM MgCl2 4 µl
    - 0.1 M DTT 2 µl
    - SuperScript III RT (200 U/µl) 1 µl
- Add 9ul of cDNA Synthesis Mix to each RNA/primer mixture, mix gently, and collect by brief centrifugation.
- Incubate at 50ºC for 50 mins
- Terminate the reaction at 85ºC for 5 mins and chill on ice
- Conduct PCR reaction or store at -80

APPENDIX 13: Reagents Used For Microarray Experiments:

- Quick Amp Labelling Kit, One-Color Agilent p/n 5190-0442
- RNA Spike-In Kit, One-Color Agilent p/n 5188-5282
- Gene Expression Hybridization Kit Agilent p/n 5188-5242
- Gene Expression Wash Buffer 1 Agilent p/n 5188-5325
- Gene Expression Wash Buffer 2 Agilent p/n 5188-5326
- RNeasy Mini Kits (50 columns or 250 columns) Qiagen p/n 74104 or 74106

APPENDIX 14a: Comparison of All Gene Changes for Small/Medium Tears compared to Normal Tendons, Sorted By Lowest p-value (Mann-Whitney test). 165 genes were found to be significantly different (p<0.05 AND >2 fold change).

MANN WHITNEY OF SMALL/MEDIUM VERSUS NORMAL			
Gene Symbol	**p-value**	**FCAbsolute**	**Regulation (versus Normal)**
AJ243810	3.57E-04	2.0213826	down
KRT12	4.51E-04	3.5443099	up
MUC5B	4.51E-04	2.0928762	down
TCL1A	4.51E-04	3.4205365	down
THC2686110	5.68E-04	2.5199444	down
DHDH	5.68E-04	2.0849197	up
FLJ10232	5.68E-04	4.2661796	down
ADORA3	7.12E-04	2.8841317	up
TNNT3	7.12E-04	3.8335028	up
CH25H	8.89E-04	2.3296266	down
BC013171	8.89E-04	2.4330635	down
THEG	0.001106586	3.3055768	down
NPHS2	0.001106586	3.852058	down
LY6D	0.001106586	2.696003	down
GPR56	0.001106586	2.1597612	down
LOC728044	0.001372472	2.3533123	down
THC2617409	0.001372472	2.0291924	up
MAPK12	0.001372472	3.466109	down
GNG13	0.001696221	3.185278	down
PTX3	0.001696221	2.3981462	up
KIAA1957	0.001696221	2.8901734	down
IER2	0.001696221	2.0253294	down
BC042517	0.001696221	2.507509	down
MUC3A	0.002088939	2.081487	down
C20orf82	0.002088939	2.3494902	up
ENST00000303979	0.002088939	3.3888443	down
ENST00000260303	0.002088939	2.0964592	down
NOV	0.002088939	2.0207224	up
LOC402665	0.002088939	2.0118883	down
TCF23	0.002088939	2.1420774	down
HS3ST2	0.002088939	2.3351665	up
U92981	0.002088939	2.910282	up
AF289562	0.002088939	2.9229188	down
THC2550202	0.002563516	2.022629	up
KCNN3	0.002563516	2.624046	down
LOC730589	0.002563516	2.18189	down
THC2536817	0.002563516	2.2851357	up

THC2678812	0.002563516	2.4653516	down
ENST00000360758	0.002563516	2.2264595	down
DUSP27	0.003134851	3.357478	up
KIAA1922	0.003134851	2.5065458	down
PTGIS	0.003820066	2.0087817	up
MAGEC1	0.003820066	2.3221846	down
NOS3	0.003820066	2.005517	down
THC2647276	0.003820066	2.7822435	down
COL9A3	0.004638759	2.513975	down
PLAT	0.004638759	2.3931181	down
C1QTNF7	0.005613233	2.0922952	up
OSR1	0.005613233	2.088144	up
BMPER	0.005613233	3.4946024	up
FOSB	0.005613233	5.6334887	down
NBEA	0.006768741	2.0214725	up
GRRP1	0.006768741	2.5173025	down
THC2655842	0.006768741	2.652682	down
JAG2	0.008133745	3.721596	down
RAMP3	0.008133745	3.4445832	down
IRX2	0.008133745	2.7822368	down
U85992	0.008133745	3.2752311	up
CN479126	0.009740121	2.066742	down
CDH15	0.009740121	2.731331	up
MTTP	0.009740121	2.0200777	up
ADCY4	0.009740121	2.291886	down
ITGB4	0.009740121	2.6232805	down
RP5-821D11.2	0.011623421	2.0557728	down
C20orf160	0.011623421	3.1197882	down
MMP15	0.011623421	2.0471463	down
SCD	0.011623421	2.7800212	up
PLAG1	0.011623421	2.4222245	down
THC2603732	0.011623421	2.3971696	up
HOXD11	0.011623421	2.3667338	down
GPR155	0.011623421	2.033137	up
PPAP2C	0.011623421	2.0017629	down
SHANK3	0.01382302	2.760705	down
AK027294	0.01382302	2.4463553	up
BARX1	0.01382302	7.523184	up
HES5	0.01382302	4.6845655	down
BMP5	0.01382302	4.3528547	up
TCF15	0.01382302	2.4608576	down
SEMA3G	0.01382302	4.1596146	down
FOS	0.016382353	3.3890395	down
LEP	0.016382353	4.4938235	up

NBLA00301	0.016382353	2.287577	down
ANKRD47	0.016382353	2.5005555	down
FGFBP2	0.016382353	2.291938	up
TIE1	0.016382353	3.2297635	down
LOC728176	0.016382353	3.103184	down
TBX2	0.016382353	2.5998597	down
AK125361	0.016382353	2.2495477	down
C10orf39	0.016382353	3.2665324	down
CLU	0.016382353	2.0219817	down
AK092472	0.016382353	3.2287035	down
PRPF19	0.016382353	2.2041397	down
SH2D3C	0.016382353	2.1377413	down
NLGN1	0.019348975	2.3049786	up
ATP1B2	0.019348975	2.085189	down
CDH5	0.019348975	2.5300994	down
DLX5	0.019348975	2.2290714	up
BC030083	0.019348975	2.4975328	down
AF132203	0.019348975	2.246057	up
EFNA1	0.022774728	2.0687246	down
ZNF366	0.022774728	2.2742445	down
TUBAL3	0.022774728	4.846784	down
CYYR1	0.022774728	3.088857	down
CCL19	0.022774728	4.058556	down
C3orf32	0.022774728	2.0030596	down
DCAL1	0.022774728	2.4531379	up
DARC	0.022774728	3.704794	down
EPHA2	0.026715705	2.124932	down
KDR	0.026715705	2.5333495	down
FUT1	0.026715705	2.1174073	down
LOC728215	0.026715705	2.7746751	down
RASIP1	0.026715705	2.6923313	down
HK2	0.026715705	2.3928413	up
KCNN2	0.026715705	2.025721	down
LOC389831	0.026715705	2.5921137	up
BP871540	0.026715705	3.3580577	down
FAM74A4	0.026715705	2.061623	down
EDNRB	0.031232242	2.2161424	down
CARD10	0.031232242	2.2094743	down
HAND2	0.031232242	2.0505998	down
ELOVL7	0.031232242	2.6440904	down
SSTR2	0.031232242	2.1200528	down
PLVAP	0.031232242	2.9651325	down
SAA1	0.031232242	6.0489206	down
CSN1S1	0.031232242	7.1814184	down

ECSM2	0.031232242	3.0436447	down
ADAM15	0.031232242	2.1678782	down
TSPAN13	0.031232242	2.5136383	down
HSPB7	0.031232242	2.147788	up
SNTG2	0.031232242	3.1261804	down
EFNB2	0.03638887	2.1913612	down
LOC728371	0.03638887	2.1054626	down
ESAM	0.03638887	2.6291225	down
GJA4	0.03638887	3.4228203	down
LPL	0.03638887	2.192669	up
DKFZP761M1511	0.03638887	2.3872993	down
FAM101A	0.042254012	2.7435944	down
TEK	0.042254012	3.4668128	down
PCDH17	0.042254012	2.17992	down
C20orf103	0.042254012	2.3666701	down
MMP3	0.042254012	4.0383816	down
TINAGL1	0.042254012	2.1334333	down
IL3RA	0.042254012	2.1557012	down
DDIT4	0.042254012	2.6136918	up
LOC338328	0.042254012	3.8756833	down
TSPAN18	0.042254012	2.2450306	down
CLEC14A	0.042254012	2.3720603	down
SEMA5B	0.042254012	2.067221	down
LY6G5C	0.04889985	3.3603413	down
SYT12	0.04889985	2.5081584	up
CCDC48	0.04889985	2.012573	down
SCN4B	0.04889985	2.1303086	down
LOC199800	0.04889985	2.8202534	down
ACVR1C	0.04889985	2.2149432	up
MOXD1	0.04889985	2.042774	up
RPIB9	0.04889985	2.7339478	down

APPENDIX 14b: Comparison of Top Gene Changes for Large/Massive Tears compared to Normal Tendons, Sorted By Lowest p-value (Mann-Whitney test). 258 genes were found to be significantly different (p<0.05 AND >2 fold change).

MANN WHITNEY LARGE/MASSIVE VERSUS NORMAL			
Gene Symbol	**p-value**	**FCAbsolute**	**Regulation (versus Normal)**
PLAC8	0.001836791	5.107482	down
IL8RBP	0.001836791	3.9233077	down
C21orf7	0.001836791	4.0060754	down
HBQ1	0.001836791	14.857312	down
THC2588392	0.001836791	9.062474	down
HBG1	0.001836791	56.466267	down
BF217859	0.001836791	2.1060963	up
S100A12	0.001836791	14.062034	down
HBB	0.001836791	12.194052	down
S100P	0.001836791	11.875064	down
PPBP	0.001836791	37.239613	down
HBM	0.001836791	12.302959	down
PPP1R1A	0.001836791	7.745518	down
RGR	0.001836791	11.717697	down
DQ655984	0.001836791	17.104618	down
HBD	0.001836791	46.91802	down
HBA2	0.001836791	41.971424	down
CA1	0.001836791	7.1082807	down
HBA1	0.001836791	40.291943	down
PF4	0.001836791	21.017838	down
MAPK10	0.001836791	4.913889	down
BI026064	0.001836791	5.6391387	down
GPR109B	0.001836791	7.5222263	down
EPB42	0.002680903	7.2994637	down
TCL1A	0.002680903	5.1437225	down
CD6	0.002680903	2.0371537	down
ALAS2	0.002680903	39.97802	down
PDZK1IP1	0.002680903	7.14159	down
NFE2	0.002680903	7.0264273	down
IL18RAP	0.002680903	5.4690027	down
PTHLH	0.002680903	2.1746132	down
CIDEA	0.002680903	9.227827	down
S100A9	0.002680903	5.208879	down
MYL4	0.002680903	4.335158	down
AQP9	0.002680903	15.045649	down
IL8RB	0.002680903	8.680703	down
CCL5	0.003866535	4.0732584	down

VNN2	0.003866535	3.8883176	down
CORO1A	0.003866535	2.2561374	down
PHYHIP	0.003866535	2.071697	down
DA572835	0.003866535	2.6845243	down
FLJ10232	0.003866535	3.5286226	down
MIAT	0.005510642	4.336427	up
GABRP	0.005510642	2.1998892	down
LTB	0.005510642	4.8166423	down
ZNF683	0.005510642	4.5030413	down
EDG6	0.005510642	4.7601595	down
MEG3	0.005510642	2.2999473	up
TBC1D10C	0.005510642	4.414287	down
CSF3R	0.005510642	3.3707745	down
THC2721275	0.005510642	3.1664858	up
AL581048	0.005510642	2.7207017	up
RTN4R	0.005510642	2.0985005	down
PROK2	0.005510642	6.406212	down
APOBEC3B	0.007761475	4.262176	down
CIDEC	0.007761475	2.2192204	down
FLJ10781	0.007761475	2.063639	up
FLJ20160	0.007761475	2.2845504	down
IL1B	0.007761475	3.350815	down
TNFRSF10C	0.007761475	2.2270656	down
BC015370	0.007761475	2.2303016	up
RBM38	0.007761475	2.2710738	down
UBXD3	0.007761475	2.4830446	down
CD244	0.007761475	2.1017804	down
LCK	0.007761475	4.5323033	down
GZMB	0.007761475	3.2414255	down
CD3G	0.007761475	2.9325738	down
RGS18	0.007761475	5.194849	down
TRBV5-4	0.007761475	6.2009263	down
STX11	0.007761475	2.2291894	down
LGALS2	0.007761475	6.5456967	down
GZMA	0.007761475	7.642209	down
THC2657612	0.007761475	2.7235754	up
TM4SF1	0.007761475	2.0684469	down
THC2650457	0.007761475	2.8718278	down
THC2729213	0.010803687	2.0089376	down
KRT12	0.010803687	3.5504806	up
FCN1	0.010803687	6.8642225	down
THC2702250	0.010803687	2.834884	up
CD52	0.010803687	3.5385692	down
CCR7	0.010803687	3.8919113	down

IL1R2	0.010803687	2.1157775	down
FPR1	0.010803687	2.4747682	down
GBP5	0.010803687	2.295319	down
MNDA	0.010803687	2.4337516	down
TGM2	0.010803687	3.6785452	down
IRX2	0.010803687	2.2535188	down
DEFA3	0.010803687	28.390078	down
DLG4	0.010803687	2.210205	up
BC030813	0.010803687	4.2865815	down
THC2543840	0.010803687	2.2493267	up
THC2516687	0.010803687	2.316776	up
MMP25	0.010803687	2.6263905	down
BX111257	0.010803687	2.147033	up
TMEM88	0.010803687	3.298262	down
SLAMF7	0.010803687	3.6909194	down
NRGN	0.010803687	2.0835128	down
CD8A	0.014863126	4.501723	down
HOXC8	0.014863126	2.0925193	up
COL9A3	0.014863126	2.7696722	down
M31157	0.014863126	2.0804079	down
CCR2	0.014863126	3.451809	down
ACRBP	0.014863126	2.628357	down
NLRP12	0.014863126	2.073274	down
NPHS2	0.014863126	3.3410163	down
LIPE	0.014863126	2.68696	down
EN1	0.014863126	3.8209822	up
LOC730857	0.014863126	2.0077624	down
DNM3	0.014863126	2.0820143	up
ZDHHC2	0.014863126	2.0507798	down
EFNB3	0.014863126	2.1421816	down
A_24_P746044	0.014863126	2.765249	down
HSH2D	0.014863126	3.2017844	down
CD2	0.014863126	3.7376356	down
CEACAM4	0.014863126	2.518246	down
P2RY12	0.014863126	3.7605681	down
THC2655842	0.014863126	3.8699577	down
LOC402125	0.014863126	2.6637266	down
RASGRP2	0.014863126	2.451658	down
NKG7	0.020210927	3.48787	down
LY6G5C	0.020210927	5.75123	down
F11R	0.020210927	2.1705043	down
RP11-138L21.1	0.020210927	2.7862053	down
THC2667205	0.020210927	2.5174925	up
CD48	0.020210927	5.1872005	down

LGALS12	0.020210927	2.1385524	down
C2orf55	0.020210927	2.1466653	down
TESC	0.020210927	6.0239167	down
PRKAG3	0.020210927	2.324261	up
HOP	0.020210927	2.1777487	down
BX537432	0.020210927	2.7612436	down
KRT1	0.020210927	9.900101	down
CNTNAP3	0.020210927	3.8084192	down
AFAP1L2	0.020210927	2.161522	down
SKAP1	0.020210927	2.0998836	down
A_32_P14737	0.020210927	2.0591402	down
S100A8	0.020210927	4.9198694	down
CXCL1	0.020210927	2.476729	down
CFP	0.020210927	3.2785559	down
CYSLTR1	0.020210927	2.0743825	down
RASGEF1A	0.020210927	2.2763414	up
COL27A1	0.020210927	2.249714	up
THC2656802	0.020210927	2.0866904	up
U92981	0.020210927	3.1576731	up
BC063506	0.020210927	2.107393	down
BC073935	0.020210927	2.0083327	down
C21orf96	0.020210927	2.452238	up
DSP	0.02716626	2.8658512	down
USHBP1	0.02716626	3.3370667	down
GNG13	0.02716626	2.5145545	down
ACTG2	0.02716626	8.047529	down
STAC2	0.02716626	2.4871452	up
ENST00000303979	0.02716626	3.5021694	down
LEP	0.02716626	2.6420126	up
HAND2	0.02716626	3.509202	down
LOC652370	0.02716626	2.0033298	down
THC2709909	0.02716626	2.0392056	up
ABCG1	0.02716626	2.2235804	down
C10orf81	0.02716626	4.5430794	up
ASB2	0.02716626	3.2619874	down
SPRR2C	0.02716626	2.124223	down
MMP3	0.02716626	3.7817664	down
ANK1	0.02716626	2.4498155	down
GLT1D1	0.02716626	3.9045584	down
BM544548	0.02716626	2.2035248	up
AK021531	0.02716626	2.1841264	up
KLRB1	0.02716626	3.1565013	down
SAA1	0.02716626	11.459341	down
AK027315	0.02716626	2.3420112	down

SEMA3G	0.02716626	7.1173387	down
BC013171	0.02716626	2.308546	down
AF088076	0.02716626	3.396872	down
SLC14A1	0.02716626	3.3048675	down
BE644757	0.02716626	3.6262977	down
C19orf33	0.02716626	3.8220606	down
SNAI3	0.02716626	2.472063	down
AY172962	0.02716626	2.5058594	down
NLF1	0.02716626	2.0735574	up
WFDC1	0.02716626	2.5217578	down
COL24A1	0.02716626	2.4164326	up
CCL18	0.02716626	6.297678	down
LYZ	0.02716626	2.0560374	down
NAPSB	0.02716626	2.3455675	down
JAG2	0.036097065	3.2308795	down
TMEM35	0.036097065	3.1073024	down
GRRP1	0.036097065	3.4010556	down
PLAT	0.036097065	2.7214897	down
TMCC3	0.036097065	2.0524466	down
FAM135B	0.036097065	3.2153747	down
RAMP3	0.036097065	4.383028	down
GRIN2C	0.036097065	2.4434857	down
A_24_P916853	0.036097065	2.0341375	up
NCF4	0.036097065	2.0364053	down
SNCA	0.036097065	2.2897089	down
CCDC48	0.036097065	2.454321	down
BG542103	0.036097065	2.113173	up
AMIGO2	0.036097065	2.3075771	down
CCL3L3	0.036097065	2.613626	down
ATP2A3	0.036097065	2.1683626	down

APPENDIX 14c: Comparison of All Gene Changes for Large/Massive Tears compared to Small/Medium Tears, Sorted By Lowest p-value (Mann-Whitney test). 181 genes were found to be significantly different (p<0.05 AND >2 fold change).

MANN WHITNEY LARGE/MASSIVE VERSUS NORMAL			
Gene Symbol	**p-value**	**FCAbsolute**	**Regulation (versus Normal)**
PPBP	0.001565402	18.66491	down
S100A12	0.001565402	15.250143	down
RGS18	0.001565402	4.7942243	down
THC2650457	0.001565402	3.0761282	down
RNASE6	0.001565402	2.104212	down
LYZ	0.002236625	3.122502	down
NCF2	0.002236625	2.2476308	down
RAB11FIP1	0.002236625	2.1536262	down
TRIM14	0.002236625	2.0619018	down
RGR	0.003162764	10.644172	down
MYL4	0.003162764	4.1265006	down
IGSF6	0.003162764	2.744006	down
THC2729213	0.003162764	2.0405393	down
ACIN1	0.003162764	2.0301914	up
PTPRC	0.003162764	2.0005028	down
ALAS2	0.004426527	34.845467	down
HBD	0.004426527	28.559492	down
HBA2	0.004426527	26.205135	down
HBA1	0.004426527	24.701893	down
CIDEA	0.004426527	19.636786	down
AQP9	0.004426527	14.952919	down
HBM	0.004426527	11.771764	down
HBQ1	0.004426527	10.323473	down
PF4	0.004426527	8.702475	down
HBB	0.004426527	8.39701	down
MS4A4A	0.004426527	3.0091286	down
THC2586092	0.004426527	2.2265952	down
TAS2R44	0.004426527	2.1596658	up
CD163	0.004426527	2.1381443	down
A_24_P147849	0.006131953	15.854507	down
IL8RB	0.006131953	7.0360126	down
BI026064	0.006131953	6.2789392	down
CA1	0.006131953	5.906948	down
ALDH1A1	0.006131953	4.730658	down
VNN2	0.006131953	4.5122895	down
MARCO	0.006131953	2.9984658	down
NLRP12	0.006131953	2.9196022	down
ADORA3	0.006131953	2.7460275	down
F13A1	0.006131953	2.6380663	down
ACRBP	0.006131953	2.617167	down
MNDA	0.006131953	2.5516195	down
NCF4	0.006131953	2.3806093	down
AIF1	0.006131953	2.0689895	down
GPR34	0.006131953	2.0111294	down

HBG1	0.008407991	49.6046	down
PPP1R1A	0.008407991	11.990509	down
DQ655984	0.008407991	10.74847	down
EPB42	0.008407991	7.864664	down
S100P	0.008407991	7.6710525	down
S100A9	0.008407991	6.089028	down
PDZK1IP1	0.008407991	5.561162	down
TKTL1	0.008407991	4.558156	down
APOBEC3B	0.008407991	3.4950292	down
BX537432	0.008407991	3.4586399	down
MAPK10	0.008407991	2.784008	down
ABCG1	0.008407991	2.5612786	down
GABRP	0.008407991	2.484155	down
TNFRSF21	0.008407991	2.4634938	down
THC2666070	0.008407991	2.2938285	down
BC015370	0.008407991	2.1067278	up
ALOX5AP	0.008407991	2.092842	down
NPL	0.008407991	2.0564368	down
HP	0.011412037	13.246728	down
NFE2	0.011412037	6.747375	down
FCN1	0.011412037	4.7076926	down
A_32_P208713	0.011412037	3.661148	down
CCL13	0.011412037	3.203188	down
SLC1A7	0.011412037	2.4535127	down
LONRF2	0.011412037	2.4394667	down
THC2543840	0.011412037	2.411545	up
NCF1	0.011412037	2.3735137	down
SNCA	0.011412037	2.3690062	down
HRASLS2	0.011412037	2.2696671	down
DEFA3	0.015333158	21.994802	down
KRT1	0.015333158	9.4804735	down
GPR109B	0.015333158	8.861405	down
S100A8	0.015333158	7.589171	down
THC2588392	0.015333158	6.6938686	down
C20orf26	0.015333158	4.160302	down
SCD	0.015333158	3.8762531	down
CFP	0.015333158	3.5786362	down
CIDEC	0.015333158	3.5225637	down
PLAC8	0.015333158	3.2910085	down
TBC1D10C	0.015333158	3.1345837	down
TGM2	0.015333158	2.8490493	down
CSF3R	0.015333158	2.757103	down
FLJ20581	0.015333158	2.3994234	down
LILRA3	0.015333158	2.2990687	down
FLJ36032	0.015333158	2.1834757	up
TLR8	0.015333158	2.1178548	down
CD244	0.015333158	2.0715344	down
PTPRO	0.015333158	2.0364661	down
ITLN1	0.020394841	10.847768	down
PROK2	0.020394841	8.108908	down
CCL18	0.020394841	5.0003276	down
GLT1D1	0.020394841	4.6162705	down

TSLP	0.020394841	3.9111528	down
ZNF683	0.020394841	3.282716	down
LOC732215	0.020394841	2.9134126	down
A_32_P131583	0.020394841	2.8379605	down
ENST00000327591	0.020394841	2.449672	up
LZTS1	0.020394841	2.4431489	up
LOC646753	0.020394841	2.421535	up
FBP1	0.020394841	2.3536434	down
THC2721275	0.020394841	2.2740347	up
PGDS	0.020394841	2.2617943	down
HSPB7	0.020394841	2.244565	down
C21orf7	0.020394841	2.2227015	down
Gcom1	0.020394841	2.2084408	down
SAMSN1	0.020394841	2.153433	down
CTSS	0.020394841	2.1334655	down
LOC642123	0.020394841	2.1332092	down
U52054	0.020394841	2.1151886	down
CORO1A	0.020394841	2.061805	down
GNA15	0.020394841	2.056424	down
NLF1	0.020394841	2.0404692	up
KIAA1881	0.02685669	10.13279	down
CAMP	0.02685669	8.202233	down
IL18RAP	0.02685669	4.4722104	down
LGALS2	0.02685669	4.2707186	down
LTB	0.02685669	3.3230674	down
LOC728783	0.02685669	3.2660928	up
IL20RB	0.02685669	3.1099443	down
MAB21L2	0.02685669	3.1029186	down
CH25H	0.02685669	3.0285707	up
DCAL1	0.02685669	3.0006151	down
GCHFR	0.02685669	2.7962523	down
A_32_P101799	0.02685669	2.7414813	up
A_23_P21907	0.02685669	2.426122	down
CEACAM4	0.02685669	2.3093042	down
GRIN2C	0.02685669	2.0901425	down
TNFRSF11A	0.02685669	2.0881803	down
MRC1L1	0.02685669	2.0582302	down
BC033829	0.02685669	2.0562127	down
HSPC157	0.02685669	2.0421443	down
GMFG	0.02685669	2.016805	down
CLEC4E	0.035014987	4.564257	down
FIGF	0.035014987	4.2623277	down
EDG6	0.035014987	3.8099751	down
AF132203	0.035014987	3.249724	down
CCR7	0.035014987	3.2334247	down
IL8RBP	0.035014987	3.1283133	down
AMICA1	0.035014987	2.876333	down
FGFR2	0.035014987	2.8097463	up
DA572835	0.035014987	2.5812862	down
HSH2D	0.035014987	2.379496	down
CSTA	0.035014987	2.294256	down
LOC441377	0.035014987	2.1994853	up

ENST00000299756	0.035014987	2.1734965	up
LILRA2	0.035014987	2.1671202	down
EGR1	0.035014987	2.1534288	up
REPS2	0.035014987	2.1101253	down
C10orf58	0.035014987	2.0831301	down
FCGR3A	0.035014987	2.0209105	down
GLIS1	0.035014987	2.0173123	up
RPS26	0.035014987	2.0059867	up
ADH1C	0.045201346	6.1649594	down
LMO3	0.045201346	4.85293	down
S100B	0.045201346	4.773519	down
CLEC4G	0.045201346	4.247946	down
GAL	0.045201346	3.6942275	down
BE644757	0.045201346	3.2915318	down
GPD1	0.045201346	3.2878487	down
LGALS12	0.045201346	3.2001286	down
KRTAP5-8	0.045201346	3.162942	down
P2RY12	0.045201346	3.0797317	down
GPT	0.045201346	2.9633677	down
FGL2	0.045201346	2.9501297	down
FAM124B	0.045201346	2.887269	down
ENST00000370599	0.045201346	2.463271	down
LOC441245	0.045201346	2.39163	down
PLA2G5	0.045201346	2.3704472	down
P2RY13	0.045201346	2.3531594	down
SNAI3	0.045201346	2.329691	down
ACAN	0.045201346	2.3103306	up
GPBAR1	0.045201346	2.2495408	down
C17orf81	0.045201346	2.1525776	down
THC2677796	0.045201346	2.1384072	up
VSNL1	0.045201346	2.1048281	up
CD163L1	0.045201346	2.0470166	down
CPVL	0.045201346	2.0458374	down

APPENDIX 15 – Gene Ontology (GO) Terms Altered in Rotator Cuff Tears.
The gene count indicates the proportion or actual number of relevant genes which are changed from each GO group.

GO Term	Gene Count
INFLAMMATORY_RESPONSE	91/130
REGULATION_OF_BODY_FLUID_LEVELS	36/57
LATE_ENDOSOME	39/97
DEFENSE_RESPONSE	176/271
IDX_TSA_UP_CLUSTER6	149/166
DEFENSE_RESPONSE	176/271
POSITIVE_REGULATION_OF_RESPONSE_TO_STIMULUS	27/41
HSA04640_HEMATOPOIETIC_CELL_LINEAGE	59/88
ISOPRENOID_METABOLIC_PROCESS	39/66
STEMCELL_COMMON_DN	53/63
HSC_MATURE_ADULT	287/339
HSC_MATURE_FETAL	264/331
CREBPATHWAY	22/27
WELCH_GATA1	19/24
SIG_PIP3_SIGNALING_IN_B_LYMPHOCYTES	31/36
CARIES_PULP_UP	182/212
ELECTRON_TRANSPORTER_ACTIVITY	86/128
HSA00620_PYRUVATE_METABOLISM	34/42
POSITIVE_REGULATION_OF_TRANSLATION	22/35
CARIES_PULP_HIGH_UP	77/96
AGED_MOUSE_CORTEX_UP	28/31
REGULATION_OF_TRANSLATION	63/93
LEUKOCYTE_ACTIVATION	44/69
POSITIVE_REGULATION_OF_CYTOKINE_BIOSYNTHETIC_PROCESS	25
HSA04060_CYTOKINE_CYTOKINE_RECEPTOR_INTERACTION	257
CYTOKINE_PRODUCTION	73
LOCOMOTORY_BEHAVIOR	97
LIPID_RAFT	29
IMMUNE_RESPONSE	237
POSITIVE_REGULATION_OF_LYMPHOCYTE_ACTIVATION	24
POSITIVE_REGULATION_OF_IMMUNE_SYSTEM_PROCESS	51
REGULATION_OF_RESPONSE_TO_STIMULUS	59
POSITIVE_REGULATION_OF_IMMUNE_RESPONSE	29
LYMPHOCYTE_DIFFERENTIATION	26
HSA00071_FATTY_ACID_METABOLISM	47

INFLAMMATORY_RESPONSE	130
B_CELL_ACTIVATION	20
CELL_ACTIVATION	77
SIG_BCR_SIGNALING_PATHWAY	46
CYTOKINE_METABOLIC_PROCESS	42
RESPONSE_TO_OTHER_ORGANISM	83
IFNALPHA_RESIST_DN	19
POSITIVE_REGULATION_OF_T_CELL_ACTIVATION	21
ADAPTIVE_IMMUNE_RESPONSE	25
REGULATION_OF_CYTOKINE_SECRETION	16
SA_MMP_CYTOKINE_CONNECTION	15
LEUKOCYTE_CHEMOTAXIS	13

APPENDIX 16 - Immunohistochemistry Protocol for Frozen Tendon Sections

1. Peroxidase block – 10 minutes
2. Wash
    a. PBS 3 x 2min
3. Permeabilzation in Triton X (0.5%) – 10 mins
4. Wash
5. Blocking stage with Horse Serum (3%) – 1 hour (do not wash – drain only)
6. Primary antibody – Over night @ 4degrees
7. Wash
8. Secondary antibody – 30 mins
9. Make up AB reagent (30 mins prior to use)
10. Wash
11. AB reagent – 30 mins
12. Wash
13. DAB – 8 minutes
14. Wash
15. PI (1:500) – 10 minutes
16. Wash
17. Mount with fluorosave

Solutions:

Peroxidase block = hydrogen peroxide + methanol (20 + 180)/slide
Triton X = Triton X + PBS (50 + 950) 200/slide
Horse Serum = Horse serum + PBS (6 + 194)/slide
Primary antibody = fot 3-NT, active bax, caspase-3, cytochrome C 1:100
Secondary antibody = II + HS + PBS (4 + 4 + 192)/slide
AB reagent = A + B + PBS (4 + 4 + 192)/side
DAB = DAB concentrate + DAB diluent (1 drop + 1ml) 200/slide
PI = PI + PBS (2 + 998) 200/slide

APPENDIX 17a – Desirable Properties for Rotator Cuff Repair Patches

- Biodegradable
    - 'tunable degradation', provide mechanical support during a critical period of healing, and then be reabsorbed
- Biocompatible
    - Non-toxic degradation products
    - Porous 3-dimensional structure to allow cell-in growth and permeable to chemicals and nutrients
- Promotes tissue regeneration
    - The matrix skeleton should support tendon, fibroblasts and/or stem cells
    - Allows cell-cell connectivity for intercellular communications
    - Wide variation is seen amongst the interaction with growth factors, and the potential ability to deliver growth factors
- Synthetic ECM produced can mimic tendon biomechanics
- Similar biomechanical properties of native tissue
    - Needs appropriate balance between stiffness and compliance
    - Natural scaffolds often have reduced mechanical parameters compared to synthetic material based constructs
    - Ease of incorporation into 3-dimensional structures of both bone and tendon

APPENDIX 17b – Limitations of Rotator Cuff Repair Patches

- Few published results with very few randomised trials.
- Published studies often have very small sample sizes
- Indications for the use of patches has not been clearly defined
- Primary indication for chronic tendon tears or revision/salvage procedures.
- Often put into tendons which are likely to fail e.g. massive tears.
- Chance patch may alter properties of repaired tendon.
- Decreased strength and integrity over time.
- Limited tendon growth and incorporation
- Increased inflammatory response, particularly with synthetic patches
- Cost is an important consideration, with many patches retailing at approximately one to two thousand pounds, significant clinical outcomes need to be proven to justify the additional expense of inserting these patches.
- Optimal mechanical and biological properties required of repair patches have not been fully defined
- FDA approval has only been granted for augmentation rather than interpositioning
- Use of organic solvents to prepare patches may inhibit cell and growth factor infiltration and attachment.

APPENDIX 18 – Details of 4 Commercially Available Rotator Cuff Tendon Repair Patches

Patch Name	Type	Source	Company	Properties	Mean Load To Failure [380]	Chemically Cross Linked	Details	ECM composition
GraftJacket MAX Force	Dermis	Human allograft (epidermis, cells and cell remnants removed)	Wright Medical, Tennessee	Acellular, After freeze drying extracellular architecture and vascular channels intact	229N	No	Packaged dry. Thickness 0.5-2mm. Varying sizes.	Collagen types I, III, IV VII, elastin, proteoglycans, laminin, tenacin, fibroblast growth factor and blood vessel channels
Restore	Small Intestine	Porcine	DePuy, Orthopaedics, Indiana	Acellular. Disinfected with peracetic acid and ethanol.	38N	No	Packaged dry. Thickness 0.8-1mm. Disc. 10 layers thick. Layaers orientated at 20º relative to each other and laminated together using a vacuum press.	Type 1 col, fibronectin, chondroitin sulphate, heparin, heparin sulphate, hyalurinane, FGF-2, TGF-B2, VEGF.
Zimmer collagen repair patch (Permacol)	Dermis	Porcine	Tissue Science Labs (licensed to Zimmer, Warsaw, IN)	Acellular. Organic and enzymatic extractions to remove fat, cellular material and soluble proteins.	128N	Yes (diisocyanate), thus resistant to enzymatic degradation	Packaged hydrated. 1.5mm thick.	Collagen/elastin. Fat, cellular material and soluble proteins are removed.
SportMesh	Artelon fibres – porous material. Poly(urethaneurea)	Synthetic	Biomet	NO collagen	N/A	No	Packaged dry. 0.2 mm thick	Nil

APPENDIX 19 - Previously published mechanical parameters for human rotator cuff (supraspinatus) tendons

Type of Tendon	Highest Tensile (Young's) Modulus [MPa]	Highest Ultimate Tensile Stress [MPa]	Highest Strain to Failure	Reference
Anterior	170	16.5		[50]
Middle	70	6		[50]
Posterior	50	4.1		[50]
Articular		11.5 ± 5	0.145	[234]
Bursal (insertion site)		11.5 ± 5	0.259	[234]
Bursal (anterior portion)			0.225	[234]
Articular side			0.075	[249]
Bursal side			0.106	[249]
Articular side			0.07	[253]
Bursal side			0.15	[253]
Articular (anterior)	70			[54]
Articular (middle)	180			[54]
Articular (posterior)	20			[54]
Bursal (anterior)	70			[54]
Bursal (middle)	220			[54]
Bursal (posterior)	40			[54]
Central portion		8		[61]

11 REFERENCES

1. Codman, E.A., *The Shoulder: Rupture of the Supraspinatus Tendon and other lesions in or about the Subacromial Bursa*1934.

2. Urwin, M., et al., *Estimating the burden of musculoskeletal disorders in the community: the comparative prevalence of symptoms at different anatomical sites, and the relation to social deprivation.* Annals of the Rheumatic Diseases, 1998. **57**(11): p. 649-655.

3. Van Der Heijden, G.J.M.G., *Shoulder disorders: A state-of-the-art review.* Bailliere's Best Practice and Research in Clinical Rheumatology, 1999. **13**(2): p. 287-309.

4. Yamamoto, A., et al., *Prevalence and risk factors of a rotator cuff tear in the general population.* Journal of Shoulder and Elbow Surgery, 2010. **19**(1): p. 116-120.

5. Bongers, P.M., *The cost of shoulder pain at work.* British Medical Journal, 2001. **322**(7278): p. 64-65.

6. Bunker, T., *Rotator cuff disease.* Current Orthopaedics, 2002. **16**(3): p. 223-233.

7. Linsell, L., et al., *Prevalence and incidence of adults consulting for shoulder conditions in UK primary care; patterns of diagnosis and referral.* Rheumatology, 2006. **45**(2): p. 215-221.

8. Oh, L.S., et al., *Indications for rotator cuff repair: A systematic review.* Clinical Orthopaedics and Related Research, 2007(455): p. 52-63.

9. Gottlieb, N.L. and W.G. Riskin, *Complications of local corticosteroid injections.* Journal of the American Medical Association, 1980. **243**(15): p. 1547-1548.

10. Van Der Windt, D.A.W.M., et al., *Shoulder disorders in general practice: Prognostic indicators of outcome.* British Journal of General Practice, 1996. **46**(410): p. 519-523.

11. Lashgari, C.J. and K. Yamaguchi, *Natural history and nonsurgical treatment of rotator cuff disorders.* Orthopaedic knowledge update: Shoulder and elbow 2, 2002.

12. Mitchell, C., et al., *Shoulder pain: Diagnosis and management in primary care.* British Medical Journal, 2005. **331**(7525): p. 1124-1128.

13. Macfarlane, G.J., I.M. Hunt, and A.J. Silman, *Predictors of chronic shoulder pain: A population based prospective study.* Journal of Rheumatology, 1998. **25**(8): p. 1612-1615.

14. Lehman, C., et al., *The incidence of full thickness rotator cuff tears in a large cadaveric population.* Bulletin: Hospital for Joint Diseases, 1995. **54**(1): p. 30-31.

15. Neer Ii, C.S., et al., *The anatomy and potential effects of contracture of the coracohumeral ligament.* Clinical Orthopaedics and Related Research, 1992(280): p. 182-185.

16. Tempelhof, S., S. Rupp, and R. Seil, *Age-related prevalence of rotator cuff tears in asymptomatic shoulders.* Journal of Shoulder and Elbow Surgery, 1999. **8**(4): p. 296-299.

17. Kennedy, J.C. and R.B. Willis, *The effects of local steroid injections on tendons: a biomechanical and microscopic correlative study.* Amer.J.Sports Med., 1976. **4**(1): p. 11-21.

18. Worland, R.L., et al., *Correlation of age, acromial morphology, and rotator cuff tear pathology diagnosed by ultrasound in asymptomatic patients.* Journal of the Southern Orthopaedic Association, 2003. **12**(1): p. 23-26.

19. Yamaguchi, K., et al., *Natural history of asymptomatic rotator cuff tears: A longitudinal analysis of asymptomatic tears detected sonographically.* Journal of Shoulder and Elbow Surgery, 2001. **10**(3): p. 199-203.

20. Fehringer, E.V., et al., *Full-thickness rotator cuff tear prevalence and correlation with function and co-morbidities in patients sixty-five years and older.* Journal of Shoulder and Elbow Surgery, 2008. **17**(6): p. 881-885.

21. Yamaguchi, K., et al., *The demographic and morphological features of rotator cuff disease: A comparison of asymptomatic and symptomatic shoulders.* Journal of Bone and Joint Surgery - Series A, 2006. **88**(8): p. 1699-1704.

22. Sher, J.S., et al., *Abnormal findings on magnetic resonance images of asymptomatic shoulders.* Journal of Bone and Joint Surgery - Series A, 1995. **77**(1): p. 10-15.

23. Van De Sande, M.A.J., J.H. De Groot, and P.M. Rozing, *Clinical implications of rotator cuff degeneration in the rheumatic shoulder.* Arthritis Care and Research, 2008. **59**(3): p. 317-324.

24. Pisan, M. and C. Gerber, *Clinical examination of the rotator cuff.* Current Orthopaedics, 2000. **14**(3): p. 155-160.

25. Rozing, P.M. and R. Brand, *Rotator cuff repair during shoulder arthroplasty in rheumatoid arthritis.* Journal of Arthroplasty, 1998. **13**(3): p. 311-319.

26. Bongers, P.M., et al., *Psychosocial factors at work and musculoskeletal disease.* Scandinavian Journal of Work, Environment and Health, 1993. **19**(5): p. 297-312.

27. Harkness, E.F., et al., *Mechanical and psychosocial factors predict new onset shoulder pain: A prospective cohort study of newly employed workers.* Occupational and Environmental Medicine, 2003. **60**(11): p. 850-857.

28. van der Windt, D., et al., *Occupational risk factors for shoulder pain: a systematic review.* Occupational and Environmental Medicine, 2000. **57**(7): p. 433-442.

29. Nygren, A., A. Berglund, and M. Vonkoch, *NECK-AND-SHOULDER PAIN, AN INCREASING PROBLEM - STRATEGIES FOR USING INSURANCE MATERIAL TO FOLLOW TRENDS.* Scandinavian Journal of Rehabilitation Medicine, 1995: p. 107-112.

30. Van Der Windt, D.A.W.M., et al., *Occupational risk factors for shoulder pain: A systematic review.* Occupational and Environmental Medicine, 2000. **57**(7): p. 433-442.

31. Aurora, A., et al., *Commercially available extracellular matrix materials for rotator cuff repairs: State of the art and future trends.* Journal of Shoulder and Elbow Surgery, 2007. **16**(5 SUPPL.).

32. Galatz, L.M., et al., *The outcome and repair integrity of completely arthroscopically repaired large and massive rotator cuff tears.* Journal of Bone and Joint Surgery-American Volume, 2004. **86A**(2): p. 219-224.

33. Jost, B., C.W.A. Pfirrmann, and C. Gerber, *Clinical outcome after structural failure of rotator cuff repairs.* Journal of Bone and Joint Surgery - Series A, 2000. **82**(3): p. 304-314.

34. Klepps, S., et al., *Prospective evaluation of the effect of rotator cuff integrity on the outcome of open rotator cuff repairs.* American Journal of Sports Medicine, 2004. **32**(7): p. 1716-1722.

35. Bishop, J., et al., *Cuff integrity after arthroscopic versus open rotator cuff repair: A prospective study.* Journal of Shoulder and Elbow Surgery, 2006. **15**(3): p. 290-299.

36. Galatz, L.M., et al., *The Outcome and Repair Integrity of Completely Arthroscopically Repaired Large and Massive Rotator Cuff Tears.* Journal of Bone and Joint Surgery - Series A, 2004. **86**(2): p. 219-224.

37. Sugaya, H., et al., *Repair integrity and functional outcome after arthroscopic double-row rotator cuff repair: A prospective outcome study.* Journal of Bone and Joint Surgery - Series A, 2007. **89**(5): p. 953-960.

38. Huijsmans, P.E., et al., *Arthroscopic rotator cuff repair with double-row fixation.* Journal of Bone and Joint Surgery-American Volume, 2007. **89A**(6): p. 1248-1257.

39. Sharkey, N.A., R.A. Marder, and P.B. Hanson, *The entire rotator cuff contributes to elevation of the arm.* Journal of Orthopaedic Research, 1994. **12**(5): p. 699-708.

40. Clark, J.M. and D.T. Harryman Ii, *Tendons, ligaments, and capsule of the rotator cuff. Gross and microscopic anatomy.* Journal of Bone and Joint Surgery - Series A, 1992. **74**(5): p. 713-725.

41. Wilk, K.E., C.A. Arrigo, and J.R. Andrews, *Current concepts: The stabilizing structures of the glenohumeral joint.* Journal of Orthopaedic and Sports Physical Therapy, 1997. **25**(6): p. 364-379.

42. Sharkey, N.A. and R.A. Marder, *The rotator cuff opposes superior translation of the humeral head.* American Journal of Sports Medicine, 1995. **23**(3): p. 270-275.

43. Burkhart, S.S., J.C. Esch, and R.S. Jolson, *The rotator crescent and rotator cable: An anatomic description of the shoulder's 'suspension bridge'.* Arthroscopy, 1993. **9**(6): p. 611-616.

44. Thibeault, S.L., et al., *Histologic and rheologic characterization of vocal fold scarring.* Journal of Voice, 2002. **16**(1): p. 96-104.

45. Schicker, M., et al., *Biomaterials as scaffold for bone tissue engineering.* European Journal of Trauma, 2006. **32**(2): p. 114-124.

46. West, P.A., et al., *Fourier transform infrared spectral analysis of degenerative cartilage: An infrared fiber optic probe and imaging study.* Applied Spectroscopy, 2004. **58**(4): p. 376-381.

47. Jarvis, R.M., et al., *PYCHEM: A multivariate analysis package for python.* Bioinformatics, 2006. **22**(20): p. 2565-2566.

48. West, P.A., et al., *Fourier transform infrared imaging spectroscopy analysis of collagenase-induced cartilage degradation.* Journal of biomedical optics, 2005. **10**(1): p. 14015.

49. Keating, J.F., et al., *THE RELATIVE STRENGTHS OF THE ROTATOR CUFF MUSCLES - A CADAVER STUDY.* Journal of Bone and Joint Surgery-British Volume, 1993. **75**(1): p. 137-140.

50. Itoi, E., et al., *Tensile properties of the supraspinatus tendon.* Journal of Orthopaedic Research, 1995. **13**(4): p. 578-584.

51. Sano, H., I. Wakabayashi, and E. Itoi, *Stress distribution in the supraspinatus tendon with partial-thickness tears: An analysis using two-dimensional finite element model.* Journal of Shoulder and Elbow Surgery, 2006. **15**(1): p. 100-105.

52. Nakajima, T., et al., *Histologic and biomechanical characteristics of the supraspinatus tendon: Reference to rotator cuff tearing.* J Shoulder Elbow Surg, 1994. **3**: p. 79-87.

53. Vincent, J., *Structural Biomaterials Revised Edition*1990, New Jersey: Princeton University Press. XII + 244P.

54. Lake, S.P., et al., *Effect of fiber distribution and realignment on the nonlinear and inhomogeneous mechanical properties of human supraspinatus tendon under longitudinal tensile loading.* Journal of Orthopaedic Research, 2009. **27**(12): p. 1596-1602.

55. Andarawis-Puri, N., E.T. Ricchetti, and L.J. Soslowsky, *Rotator cuff tendon strain correlates with tear propagation.* Journal of Biomechanics, 2009. **42**(2): p. 158-163.

56. Sharma, P. and N. Maffulli, *Basic biology of tendon injury and healing.* Surgeon, 2005. **3**(5): p. 309-316.

57. Wang, J.H.C., *Mechanobiology of tendon.* Journal of Biomechanics, 2006. **39**(9): p. 1563-1582.

58. Fallon, J., et al., *Functional morphology of the supraspinatus tendon.* Journal of Orthopaedic Research, 2002. **20**(5): p. 920-926.

59. Silver, F.H., J.W. Freeman, and G.P. Seehra, *Collagen self-assembly and the development of tendon mechanical properties.* Journal of Biomechanics, 2003. **36**(10): p. 1529-1553.

60. Sharma, P. and N. Maffulli, *Tendon injury and tendinopathy: Healing and repair.* Journal of Bone and Joint Surgery - Series A, 2005. **87**(1): p. 187-202.

61. Sano, H., et al., *Degeneration at the insertion weakens the tensile strength of the supraspinatus tendon: A comparative mechanical and histologic study of the bone-tendon complex.* Journal of Orthopaedic Research, 1997. **15**(5): p. 719-726.

62. Blevins, F.T., *Rotator cuff pathology in athletes.* Sports Medicine, 1997. **24**(3): p. 205-220.

63. Vogel, K.G. and J.A. Peters, *Histochemistry defines a proteogylcan-rich layer in bovine flexor tendon subjected to bending.* Journal of Musculoskeletal Neuronal Interactions, 2005. **5**(1): p. 64-69.

64. Riley, G.P., et al., *Matrix metalloproteinase activities and their relationship with collagen remodelling in tendon pathology.* Matrix Biology, 2002. **21**(2): p. 185-195.

65. Kannus, P., *Structure of the tendon connective tissue.* Scandinavian Journal of Medicine and Science in Sports, 2000. **10**(6): p. 312-320.

66. Goodmurphy, C.W., et al., *An immunocytochemical analysis of torn rotator cuff tendon taken at the time of repair.* Journal of Shoulder and Elbow Surgery, 2003. **12**(4): p. 368-374.

67. Riley, G.P., et al., *Tendon degeneration and chronic shoulder pain: Changes in the collagen composition of the human rotator cuff tendons in rotator cuff tendinitis.* Annals of the Rheumatic Diseases, 1994. **53**(6): p. 359-366.

68. Jackson, D.W., et al., *The effects of in situ freezing on the anterior cruciate ligament: An experimental study in goats.* Journal of Bone and Joint Surgery - Series A, 1991. **73**(2): p. 201-213.

69. Ohno, K., et al., *Effects of complete stress-shielding on the mechanical properties and histology of in situ frozen patellar tendon.* Journal of Orthopaedic Research, 1993. **11**(4): p. 592-602.

70. Blevins, F.T., et al., *Biology of the rotator cuff tendon.* Orthop Clin North Am, 1997. **28**(1): p. 1-16.

71. Riley, G.P., M.J. Goddard, and B.L. Hazleman, *Histopathological assessment and pathological significance of matrix degeneration in supraspinatus tendons [4].* Rheumatology, 2001. **40**(2): p. 229-230.

72. Siebold, R., et al., *Primary ACL reconstruction with fresh-frozen patellar versus Achilles tendon allografts.* Archives of Orthopaedic and Trauma Surgery, 2003. **123**(4): p. 180-185.

73. Giannini, S., et al., *Effects of freezing on the biomechanical and structural properties of human posterior tibial tendons.* International Orthopaedics, 2008. **32**(2): p. 145-151.

74. Riley, G.P., et al., *Glycosaminoglycans of human rotator cuff tendons: Changes with age and in chronic rotator cuff tendinitis.* Annals of the Rheumatic Diseases, 1994. **53**(6): p. 367-376.

75. Berenson, M.C., et al., *Proteoglycans of human rotator cuff tendons.* Journal of Orthopaedic Research, 1996. **14**(4): p. 518-525.

76. Screen, H.R.C., et al., *The influence of noncollagenous matrix components on the micromechanical environment of tendon fascicles.* Annals of Biomedical Engineering, 2005. **33**(8): p. 1090-1099.

77. Gosline, J., et al., *Elastic proteins: biological roles and mechanical properties.* Philos Trans R Soc Lond B Biol Sci, 2002. **357**(1418): p. 121-32.

78. MacGillivray, J.D. and C.B. Ma, *An arthroscopic stitch for massive rotator cuff tears: The Mac stitch.* Arthroscopy-the Journal of Arthroscopic and Related Surgery, 2004. **20**(6): p. 669-671.

79. Post, M., R. Silver, and M. Singh, *Rotator cuff tear. Diagnosis and treatment.* Clinical Orthopaedics and Related Research, 1983. **No. 173**: p. 78-91.

80. Ellman, H., *Diagnosis and treatment of incomplete rotator cuff tears.* Clinical Orthopaedics and Related Research, 1990(254): p. 64-74.

81. Neer, C.S., E.V. Craig, and H. Fukuda, *Cuff-tear arthropathy.* Journal of Bone and Joint Surgery-American Volume, 1983. **65**(9): p. 1232-1244.

82. Riley, G., *Tendinopathy - From basic science to treatment.* Nature Clinical Practice Rheumatology, 2008. **4**(2): p. 82-89.

83. Bigliani, L.U. and W.N. Levine, *Current concepts review. Subacromial impingement syndrome.* Journal of Bone and Joint Surgery - Series A, 1997. **79**(12 79A): p. 1854-1868.

84. Benazzo, F., G. Zanon, and N. Maffulli, *An Operative Approach to Achilles Tendinopathy.* Sports Medicine and Arthroscopy Review, 2000. **8**(1): p. 96-101.

85. Ker, R.F., *The implications of the adaptable fatigue quality of tendons for their construction, repair and function.* Comparative Biochemistry and Physiology - A Molecular and Integrative Physiology, 2002. **133**(4): p. 987-1000.

86. Harryman Ii, D.T., et al., *A prospective multipractice investigation of patients with full-thickness rotator cuff tears: The importance of comorbidities, practice, and other covariables on self-assessed shoulder function and health status.* Journal of Bone and Joint Surgery - Series A, 2003. **85**(4): p. 690-696.

87. Gerber, C., O. Hersche, and A. Farron, *Isolated rupture of the subscapularis tendon - Results of operative repair.* Journal of Bone and Joint Surgery-American Volume, 1996. **78A**(7): p. 1015-1023.

88. Goutallier, D., et al., *Histological lesions of supraspinatus tendons in full thickness tears of the rotator cuff.* Les lésions histologiques des tendons des supraspinatus dans les ruptures transfixiantes de la coiffe des rotateurs, 2005. **91**(2): p. 109-113.

89. Lewis, J.S., *Rotator cuff tendinopathy.* British Journal of Sports Medicine, 2009. **43**(4): p. 236-241.

90. Neer Ii, C.S., *Impingement lesions.* Clinical Orthopaedics and Related Research, 1983. **No. 173**: p. 70-77.

91. Luo, Z.P., et al., *Mechanical environment associated with rotator cuff tears.* Journal of Shoulder and Elbow Surgery, 1998. **7**(6): p. 616-620.

92. Bigliani, L.U., et al., *The relationship of acromial architecture to rotator cuff disease.* Clinics in Sports Medicine, 1991. **10**(4): p. 823-838.

93. Tokgoz, N., et al., *The relationship of glenoid and humeral version with supraspinatus tendon tears.* Skeletal Radiology, 2007. **36**(6): p. 509-514.

94. Budoff, J.E., R.P. Nirschl, and E.J. Guidi, *Debridement of partial-thickness tears of the rotator cuff without acromioplasty - Long-term follow-up and review of the literature.* Journal of Bone and Joint Surgery-American Volume, 1998. **80A**(5): p. 733-748.

95. Ozaki, J., et al., *Tears of the rotator cuff of the shoulder associated with pathological changes in the acromion. A study in cadavera.* Journal of Bone and Joint Surgery - Series A, 1988. **70**(8): p. 1224-1230.

96. Fukuda, H., et al., *Partial-thickness tears of the rotator cuff - A clinicopathological review based on 66 surgically verified cases.* International Orthopaedics, 1996. **20**(4): p. 257-265.

97. Tetreault, P., et al., *Glenoid version and rotator cuff tears.* Journal of Orthopaedic Research, 2004. **22**(1): p. 202-207.

98. Hughes, R.E., et al., *Glenoid inclination is associated with full-thickness rotator cuff tears.* Clinical Orthopaedics and Related Research, 2003(407): p. 86-91.

99. Cohen, D.B., et al., *Indomethacin and celecoxib impair rotator cuff tendon-to-bone healing.* American Journal of Sports Medicine, 2006. **34**(3): p. 362-369.

100. Koike, Y., et al., *Delay of supraspinatus repair by up to 12 weeks does not impair enthesis formation: A quantitative histologic study in rabbits.* Journal of Orthopaedic Research, 2006. **24**(2): p. 202-210.

101. Krafft, C., et al., *Identification of primary tumors of brain metastases by infrared spectroscopic imaging and linear discriminant analysis.* Technology in Cancer Research and Treatment, 2006. **5**(3): p. 291-298.

102. Reilly, P., et al., *Supraspinatus tears: Propagation and strain alteration.* Journal of Shoulder and Elbow Surgery, 2003. **12**(2): p. 134-138.

103. Perry, S.M., C.L. Getz, and L.J. Soslowsky, *After rotator cuff tears, the remaining (intact) tendons are mechanically altered.* Journal of Shoulder and Elbow Surgery, 2009. **18**(1): p. 52-57.

104. Krafft, C., et al., *Classification of malignant gliomas by infrared spectroscopic imaging and linear discriminant analysis.* Analytical and Bioanalytical Chemistry, 2007. **387**(5): p. 1669-1677.

105. Galatz, L.M., et al., *Nicotine delays tendon-to-bone healing in a rat shoulder model.* Journal of Bone and Joint Surgery - Series A, 2006. **88**(9): p. 2027-2034.

106. Mallon, W.J., et al., *The impact of preoperative smoking habits on the results of rotator cuff repair.* Journal of Shoulder and Elbow Surgery, 2004. **13**(2): p. 129-132.

107. Nobuhara, K., Y. Hata, and M. Komai, *Surgical procedure and results of repair of massive tears of the rotator cuff.* Clinical Orthopaedics and Related Research, 1994(304): p. 54-59.

108. Sano, H., et al., *Structural disorders at the insertion of the supraspinatus tendon. Relation to tensile strength.* J Bone Joint Surg Br, 1998. **80**(4): p. 720-5.

109. Kannus, P. and L. Jozsa, *Histopathological changes preceding spontaneous rupture of a tendon: A controlled study of 891 patients.* Journal of Bone and Joint Surgery - Series A, 1991. **73**(10): p. 1507-1525.

110. Longo, U.G., et al., *Histopathology of the supraspinatus tendon in rotator cuff tears.* Am J Sports Med, 2008. **36**(3): p. 533-8.

111. Kannus, P. and A. Natri, *Etiology and pathophysiology of tendon ruptures in sports.* Scandinavian Journal of Medicine and Science in Sports, 1997. **7**(2): p. 107-112.

112. Uhthoff, H.K. and H. Sano, *Pathology of failure of the rotator cuff tendon.* Orthopedic Clinics of North America, 1997. **28**(1): p. 31-41.

113. Sperling, J.W., R.H. Cofield, and C. Schleck, *Rotator cuff repair in patients fifty years of age and younger.* Journal of Bone and Joint Surgery-American Volume, 2004. **86A**(10): p. 2212-2215.

114. Boileau, P., et al., *Arthroscopic repair of full-thickness tears of the supraspinatus: Does the tendon really heal?* Journal of Bone and Joint Surgery-American Volume, 2005. **87A**(6): p. 1229-1240.

115. Adamson, G.J. and J.E. Tibone, *Ten-year assessment of primary rotator cuff repairs.* Journal of Shoulder and Elbow Surgery, 1993. **2**(2): p. 57-63.

116. Watson, E.M. and D.H. Sonnabend, *Outcome of rotator cuff repair.* Journal of Shoulder and Elbow Surgery, 2002. **11**(3): p. 201-211.

117. Grauer, J.D., L.E. Paulos, and W.P. Smutz, *Biceps tendon and superior labral injuries.* Arthroscopy, 1992. **8**(4): p. 488-497.

118. Tashjian, R.Z., et al., *Evidence for an Inherited Predisposition Contributing to the Risk for Rotator Cuff Disease.* Journal of Bone and Joint Surgery-American Volume, 2009. **91A**(5): p. 1136-1142.

119. Harvie, P., et al., *Genetic influences in the aetiology of tears of the rotator cuff. Sibling risk of a full-thickness tear.* Journal of Bone and Joint Surgery - Series B, 2004. **86**(5): p. 696-700.

120. Gwilym, S.E., et al., *Genetic influences in the progression of tears of the rotator cuff.* Journal of Bone and Joint Surgery-British Volume, 2009. **91B**(7): p. 915-917.

121. Millar, N.L., et al., *Cytokines and apoptosis in supraspinatus tendinopathy.* Journal of Bone and Joint Surgery - Series B, 2009. **91**(3): p. 417-424.

122. Szomor, Z.L., et al., *Differential expression of cytokines and nitric oxide synthase isoforms in human rotator cuff bursae [4].* Annals of the Rheumatic Diseases, 2001. **60**(4): p. 431-432.

123. Murrell, G.A.C., et al., *Modulation of tendon healing by nitric oxide.* Inflammation Research, 1997. **46**(1): p. 19-27.

124. Fenwick, S.A., et al., *Expression of transforming growth factor-beta isoforms and their receptors in chronic tendinosis.* Journal of Anatomy, 2001. **199**(3): p. 231-240.

125. Matthews, T.J.W., et al., *Pathology of the torn rotator cuff tendon.* Journal of Bone and Joint Surgery - Series B, 2006. **88**(4): p. 489-495.

126. Tuoheti, Y., et al., *Apoptosis in the supraspinatus tendon with stage II subacromial impingement.* Journal of Shoulder and Elbow Surgery, 2005. **14**(5): p. 535-541.

127. Samiric, T., M.Z. Ilic, and C.J. Handley, *Characterisation of proteoglycans and their catabolic products in tendon and explant cultures of tendon.* Matrix Biology, 2004. **23**(2): p. 127-140.

128. Soslowsky, L.J., et al., *Rotator cuff tendinosis in an animal model: Role of extrinsic and overuse factors.* Annals of Biomedical Engineering, 2002. **30**(8): p. 1057-1063.

129. Scott, A., et al., *Tenocyte responses to mechanical loading in vivo: A role for local insulin-like growth factor 1 signaling in early tendinosis in rats.* Arthritis and Rheumatism, 2007. **56**(3): p. 871-881.

130. Fukuda, H., K. Hamada, and K. Yamanaka, *Pathology and pathogenesis of bursal-side rotator cuff tears viewed from en bloc histologic sections.* Clinical Orthopaedics and Related Research, 1990(254): p. 75-80.

131. Archambault, J.M., et al., *Rat supraspinatus tendon expresses cartilage markers with overuse.* Journal of Orthopaedic Research, 2007. **25**(5): p. 617-624.

132. Almekinders, L.C. and G. Deol, *The effects of aging, antiinflammatory drugs, and ultrasound on the in vitro response of tendon tissue.* American Journal of Sports Medicine, 1999. **27**(4): p. 417-421.

133. Ippolito, E., P.G. Natali, and F. Postacchini, *Morphological, immunochemical, and biochemical study of rabbit Achilles tendon at various ages.* Journal of Bone and Joint Surgery - Series A, 1980. **62**(4): p. 583-598.

134. Riley, G., *Chronic tendon pathology: Molecular basis and therapeutic implications.* Expert Reviews in Molecular Medicine, 2005. **7**(5).

135. Hirose, K., et al., *Spontaneous healing process of a supraspinatus tendon tear in rabbits.* Archives of Orthopaedic and Trauma Surgery, 2004. **124**(6): p. 374-377.

136. Rodeo, S.A., et al., *Tendon-healing in a bone tunnel. A biomechanical and histological study in the dog.* J Bone Joint Surg Am, 1993. **75**(12): p. 1795-803.

137. Bishop, J., et al., *Cuff integrity after arthroscopic versus open rotator cuff repair: a prospective study.* J Shoulder Elbow Surg, 2006. **15**(3): p. 290-9.

138. Carpenter, J.E., et al., *Rotator cuff defect healing: a biomechanical and histologic analysis in an animal model.* J Shoulder Elbow Surg, 1998. **7**(6): p. 599-605.

139. Bank, R.A., et al., *Lysylhydroxylation and non-reducible crosslinking of human supraspinatus tendon collagen: Changes with age and in chronic rotator cuff tendinitis.* Annals of the Rheumatic Diseases, 1999. **58**(1): p. 35-41.

140. Riley, G., *The pathogenesis of tendinopathy. A molecular perspective.* Rheumatology, 2004. **43**(2): p. 131-142.

141. Lo, I.K.Y., et al., *Matrix metalloproteinase and tissue inhibitor of matrix metalloproteinase mRNA levels are specifically altered in torn rotator cuff tendons.* American Journal of Sports Medicine, 2004. **32**(5): p. 1223-1229.

142. Riley, G.P., et al., *Tenascin-C and human tendon degeneration.* American Journal of Pathology, 1996. **149**(3): p. 933-943.

143. Schmutz, S., et al., *Expression of atrophy mRNA relates to tendon tear size in supraspinatus muscle.* Clinical Orthopaedics and Related Research, 2009. **467**(2): p. 457-464.

144. Muehleman, C., et al., *Association between crystals and cartilage degeneration in the ankle.* Journal of Rheumatology, 2008. **35**(6): p. 1108-1117.

145. Magra, M. and N. Maffulli, *Matrix metalloproteases: A role in overuse tendinopathies.* British Journal of Sports Medicine, 2005. **39**(11): p. 789-791.

146. Kuno, K., et al., *Molecular cloning of a gene encoding a new type of metalloproteinase-disintegrin family protein with thrombospondin motifs as an inflammation associated gene.* Journal of Biological Chemistry, 1997. **272**(1): p. 556-562.

147. Alfredson, H., et al., *cDNA-arrays and real-time quantitative PCR techniques in the investigation of chronic achilles tendinosis.* Journal of Orthopaedic Research, 2003. **21**(6): p. 970-975.

148. Choi, H.R., et al., *Expression and enzymatic activity of MMP-2 during healing process of the acute supraspinatus tendon tear in rabbits.* Journal of Orthopaedic Research, 2002. **20**(5): p. 927-933.

149. Lo, I.K., et al., *Matrix metalloproteinase and tissue inhibitor of matrix metalloproteinase mRNA levels are specifically altered in torn rotator cuff tendons.* Am J Sports Med, 2004. **32**(5): p. 1223-9.

150. Thornton, G.M., et al., *Changes in mechanical loading lead to tendonspecific alterations in MMP and TIMP expression: influence of stress deprivation and intermittent cyclic hydrostatic compression on rat supraspinatus and Achilles tendons.* Br J Sports Med, 2008. **44**(10): p. 698-703.

151. Osawa, T., T. Shinozaki, and K. Takagishi, *Multivariate analysis of biochemical markers in synovial fluid from the shoulder joint for diagnosis of rotator cuff tears.* Rheumatology International, 2005. **25**(6): p. 436-441.

152. Smith, M.M., et al., *Modulation of aggrecan and ADAMTS expression in ovine tendinopathy induced by altered strain.* Arthritis and Rheumatism, 2008. **58**(4): p. 1055-1066.

153. Sun, H.B., et al., *Coordinate regulation of IL-1Œ≤ and MMP-13 in rat tendons following subrupture fatigue damage.* Clinical Orthopaedics and Related Research, 2008. **466**(7): p. 1555-1561.

154. Bedi, A., et al., *The effect of matrix metalloproteinase inhibition on tendon-to-bone healing in a rotator cuff repair model.* J Shoulder Elbow Surg, 2010. **19**(3): p. 384-91.

155. Bedi, A., et al., *Doxycycline-mediated inhibition of matrix metalloproteinases improves healing after rotator cuff repair*, in *The American Journal of Sports Medicine*2010. p. 308-17.

156. Corps, A.N., et al., *Ciprofloxacin reduces the stimulation of prostaglandin E₂ output by interleukin-1Œ≤ in human tendon-derived cells.* Rheumatology, 2003. **42**(11): p. 1306-1310.

157. Corps, A.N., et al., *Contrasting effects of fluoroquinolone antibiotics on the expression of the collagenases, matrix metalloproteinases (MMP)-1 and -13, in human tendon-derived cells.* Rheumatology, 2005. **44**(12): p. 1514-1517.

158. Bedi, A., et al., *The effect of matrix metalloproteinase inhibition on tendon-to-bone healing in a rotator cuff repair model.* Journal of Shoulder and Elbow Surgery. **19**(3): p. 384-391.

159. Cole, A.S., et al., *Localised deposition of amyloid in tears of the rotator cuff.* J Bone Joint Surg Br, 2001. **83**(4): p. 561-4.

160. Coleman, S.H., et al., *Chronic Rotator Cuff Injury and Repair Model in Sheep.* Journal of Bone and Joint Surgery - Series A, 2003. **85**(12): p. 2391-2402.

161. Barton, E.R., et al., *Rat supraspinatus muscle atrophy after tendon detachment.* Journal of Orthopaedic Research, 2005. **23**(2): p. 259-265.

162. Cole, A.S., et al., *Localised deposition of amyloid in tears of the rotator cuff.* Journal of Bone and Joint Surgery - Series B, 2001. **83**(4): p. 561-564.

163. Murrell, G.A.C., *Oxygen free radicals and tendon healing.* Journal of Shoulder and Elbow Surgery, 2007. **16**(5 SUPPL.).

164. Yuan, J., et al., *Apoptosis in rotator cuff tendonopathy.* Journal of Orthopaedic Research, 2002. **20**(6): p. 1372-1379.

165. Arnoczky, S.P., et al., *Activation of stress-activated protein kinases (SAPK) in tendon cells following cyclic strain: The effects of strain frequency, strain magnitude, and cytosolic calcium.* Journal of Orthopaedic Research, 2002. **20**(5): p. 947-952.

166. Skutek, M., et al., *Cyclic mechanical stretching of human patellar tendon fibroblasts: Activation of JNK and modulation of apoptosis.* Knee Surgery, Sports Traumatology, Arthroscopy, 2003. **11**(2): p. 122-129.

167. Millar, N.L., et al., *Heat shock protein and apoptosis in supraspinatus tendinopathy.* Clinical Orthopaedics and Related Research, 2008. **466**(7): p. 1569-1576.

168. Helliwell, T.R., et al., *Ape/Ref-1 expression in torn rotator cuff.* Journal of Pathology, 2005. **205**: p. 4-4.

169. Derfus, B.A., et al., *Comparison of matrix vesicles derived from normal and osteoarthritic human articular cartilage.* Connective Tissue Research, 1996. **35**(1-4): p. 337-342.

170. Wang, M.X., et al., *Antioxidant enzyme peroxiredoxin 5 is upregulated in degenerative human tendon.* Biochemical and Biophysical Research Communications, 2001. **284**(3): p. 667-673.

171. Hoffmeister, B.K., et al., *Ultrasonic determination of the anisotropy of Young's modulus of fixed tendon and fixed myocardium.* Journal of the Acoustical Society of America, 1996. **100**(6): p. 3933-3940.

172. Koshima, H., et al., *Expression of interleukin-1 beta, cyclooxygenase-2, and prostaglandin E2 in a rotator cuff tear in rabbits.* Journal of Orthopaedic Research, 2007. **25**(1): p. 92-97.

173. Yadav, H., et al., *Rotator cuff tears: pathology and repair.* Knee Surgery, Sports Traumatology, Arthroscopy, 2008: p. 1-13.

174. Codman, E.A., *The shoulder: Rupture of the supraspinatus tendon and other lesions in or about the subacromial bursa.* The Shoulder: Rupture of the Supraspinatus Tendon and Other Lesions in or About the Subacromial Bursa, 1934.

175. Rathbun, J.B. and I. Macnab, *The microvascular pattern of the rotator cuff.* Journal of Bone and Joint Surgery - Series B, 1970. **52**(3): p. 540-553.

176. Lindblom, K., *On pathogenesis of ruptures of the tendon aponeurosis of the shoulder joint.* Acta Radiol, 1939. **20**: p. 563-577.

177. Moseley, H.F. and I. Goldie, *The arterial pattern of the rotator cuff of the shoulder.* J Bone Joint Surg, 1963. **45**: p. 780-789.

178. Lohr, J.F. and H.K. Uhthoff, *The microvascular pattern of the supraspinatus tendon.* Clinical Orthopaedics and Related Research, 1990(254): p. 35-38.

179. Ling, S.C., C.F. Chen, and R.X. Wan, *A study on the vascular supply of the supraspinatus tendon.* Surgical and Radiologic Anatomy, 1990. **12**(3): p. 161-165.

180. Paoloni, J.A., *Topical glyceryl trinitrate treatment in chronic tendinopathies.* International SportMed Journal, 2006. **7**(4): p. 238-254.

181. Swiontkowski, M.F., et al., *Intraoperative assessment of rotator cuff vascularity using laser Doppler flowmetry.* Surgery of the Shoulder, 1990: p. 208-212.

182. Dinnes, J., et al., *The effectiveness of diagnostic tests for the assessment of shoulder pain due to soft tissue disorders: a systematic review.* Health Technol Assess, 2003. **7**(29): p. iii, 1-166.

183. Charousset, C., et al., *Accuracy of CT arthrography in the assessment of tears of the rotator cuff.* Journal of Bone and Joint Surgery - Series B, 2005. **87**(6): p. 824-828.

184. Teefey, S.A., et al., *Detection and Quantification of Rotator Cuff Tears: Comparison of Ultrasonographic, Magnetic Resonance Imaging, and Arthroscopic Findings in Seventy-*

One Consecutive Cases. Journal of Bone and Joint Surgery - Series A, 2004. **86**(4): p. 708-716.

185. Gilbert, T.W., T.L. Sellaro, and S.F. Badylak, *Decellularization of tissues and organs.* Biomaterials, 2006. **27**(19): p. 3675-3683.

186. De Jesus, J.O., et al., *Accuracy of MRI, MR arthrography, and ultrasound in the diagnosis of rotator cuff tears: A meta-analysis.* American Journal of Roentgenology, 2009. **192**(6): p. 1701-1707.

187. Sahin, G. and M. Demirtas, *An overview of MR arthrography with emphasis on the current technique and applicational hints and tips.* European Journal of Radiology, 2006. **58**(3): p. 416-430.

188. Torstensen, E.T. and R.M. Hollinshead, *Comparison of magnetic resonance imaging and arthroscopy in the evaluation of shoulder pathology.* Journal of Shoulder and Elbow Surgery, 1999. **8**(1): p. 42-45.

189. Wnorowski, D.C., et al., *Magnetic resonance imaging assessment of the rotator cuff: Is it really accurate?* Arthroscopy, 1997. **13**(6): p. 710-719.

190. Ainsworth, R. and J.S. Lewis, *Exercise therapy for the conservative management of full thickness tears of the rotator cuff: A systematic review.* British Journal of Sports Medicine, 2007. **41**(4): p. 200-210.

191. Frost, P., J.H. Andersen, and E. Lundorf, *Is supraspinatus pathology as defined by magnetic resonance imaging associated with clinical sign of shoulder impingement?* Journal of Shoulder and Elbow Surgery, 1999. **8**(6): p. 565-568.

192. Green, S., et al., *Systematic review of randomised controlled trials of interventions for painful shoulder: selection criteria, outcome assessment, and efficacy.* British Medical Journal, 1998. **316**(7128): p. 354-360.

193. Green, S., et al., *Interventions for shoulder pain.* Cochrane database of systematic reviews (Online : Update Software), 2000(2).

194. Nho, S.J., et al., *Prospective analysis of arthroscopic rotator cuff repair: Prognostic factors affecting clinical and ultrasound outcome.* Journal of Shoulder and Elbow Surgery, 2009. **18**(1): p. 13-20.

195. Wolf, B.R. and D.W. Altchek, *Elbow Problems in Elite Tennis Players.* Techniques in Shoulder & Elbow Surgery, 2003. **4**(2): p. 55-68.

196. Adams, J.E., et al., *Rotator Cuff Repair Using an Acellular Dermal Matrix Graft: An In Vivo Study in a Canine Model.* Arthroscopy - Journal of Arthroscopic and Related Surgery, 2006. **22**(7): p. 700-709.

197. Welsh, R.P., I. Macnab, and V. Riley, *Biomechanical studies of rabbit tendon.* Clinical Orthopaedics and Related Research, 1971. **81**: p. 171-177.

198. Corps, A.N., et al., *Increased expression of aggrecan and biglycan mRNA in Achilles tendinopathy.* Rheumatology, 2006. **45**(3): p. 291-294.

199. Riley, G.P., et al., *Prevalence and possible pathological significance of calcium phosphate salt accumulation in tendon matrix degeneration.* Annals of the Rheumatic Diseases, 1996. **55**(2): p. 109-115.

200. Szabó, I., et al., *Differential scanning calorimetric and histological examinations of the long head of the biceps in cadavers.* Journal of Thermal Analysis and Calorimetry, 2007. **88**(2): p. 343-349.

201. Aluisio, F.V., D.C. Osbahr, and K.P. Speer, *Analysis of rotator cuff muscles in adult human cadaveric specimens.* American journal of orthopedics (Belle Mead, N.J.), 2003. **32**(3): p. 124-129.

202. Szabó, I., et al., *DSC examination of the rotator cuff muscles in rabbits.* Thermochimica Acta, 2006. **445**(2): p. 179-184.

203. Ozaki, J., S. Fujimoto, and K. Masuhara, *Reconstruction of chronic massive rotator cuff tears with synthetic materials.* Clinical Orthopaedics and Related Research, 1986. **NO. 202**: p. 173-183.

204. Huijsmans, P.E., et al., *Arthroscopic rotator cuff repair with double-row fixation.* Journal of Bone and Joint Surgery - Series A, 2007. **89**(6): p. 1248-1257.

205. Harryman, D.T., et al., *Repairs of the rotator cuff - correlation of functional results with integrity of the cuff.* Journal of Bone and Joint Surgery-American Volume, 1991. **73A**(7): p. 982-989.

206. Sugaya, H., et al., *Repair integrity and functional outcome after arthroscopic double-row rotator cuff repair - A prospective outcome study.* Journal of Bone and Joint Surgery-American Volume, 2007. **89A**(5): p. 953-960.

207. Bigiliani, L.U., et al., *Repair of rotator cuff tears in tennis players.* American Journal of Sports Medicine, 1992. **20**(2): p. 112-117.

208. Fuchs, B., et al., *Clinical and structural results of open repair of an isolated one jendon tear of the rotator cuff.* Journal of Bone and Joint Surgery-American Volume, 2006. **88A**(2): p. 309-316.

209. Brown, J.N., et al., *Shoulder pathology associated with symptomatic acromioclavicular joint degeneration.* Journal of Shoulder and Elbow Surgery, 2000. **9**(3): p. 173-176.

210. Wright, T., C. Yoon, and B.P. Schmit, *Shoulder MRI refinements: Differentiation of rotator cuff tear from artifacts and tendonosis, and reassessment of normal findings.* Seminars in Ultrasound CT and MRI, 2001. **22**(4): p. 383-395.

211. Yamaguchi, K., et al., *Glenohumeral motion in patients with rotator cuff tears: A comparison of asymptomatic and symptomatic shoulders.* Journal of Shoulder and Elbow Surgery, 2000. **9**(1): p. 6-11.

212. Galatz, L.M., et al., *Delayed repair of tendon to bone injuries leads to decreased biomechanical properties and bone loss.* Journal of Orthopaedic Research, 2005. **23**(6): p. 1441-1447.

213. Magra, M. and N. Maffulli, *Molecular events in tendinopathy: A role for metalloproteases.* Foot and Ankle Clinics, 2005. **10**(2): p. 267-277.

214. Goldberg, B.A., S.B. Lippitt, and F.A. Matsen, *Improvement in comfort and function after cuff repair without acromioplasty.* Clinical Orthopaedics and Related Research, 2001(390): p. 142-150.

215. Rockwood, C.A., G.R. Williams, and W.Z. Burkhead, *Debridement of degenerative, irreparable lesions of the rotator cuff.* Journal of Bone and Joint Surgery-American Volume, 1995. **77A**(6): p. 857-866.

216. Hyvonen, P., S. Lohi, and P. Jalovaara, *Open acromioptasty does not prevent the progression of an impingement syndrome to a tear - Nine-year follow-up of 96 cases.* Journal of Bone and Joint Surgery-British Volume, 1998. **80B**(5): p. 813-816.

217. Magra, M. and N. Maffulli, *Genetics: Does it play a role in tendinopathy?* Clinical Journal of Sport Medicine, 2007. **17**(4): p. 231-233.

218. Rees, J.L., *The pathogenesis and surgical treatment of tears of the rotator cuff.* Journal of Bone and Joint Surgery - Series B, 2008. **90**(7): p. 827-832.

219. Dunn, W.R., et al., *Variation in orthopaedic surgeons' perceptions about the indications for rotator cuff surgery.* Journal of Bone and Joint Surgery-American Volume, 2005. **87A**(9): p. 1978-1984.

220. Fukuda, H., M. Mikasa, and K. Yamanaka, *Incomplete thickness rotator cuff tears diagnosed by subacromial bursography.* Clinical Orthopaedics and Related Research, 1987(223): p. 51-58.

221. Cordasco, F.A., et al., *The partial-thickness rotator cuff tear: Is acromioplasty without repair sufficient?* American Journal of Sports Medicine, 2002. **30**(2): p. 257-260.

222. Snyder, S.J., et al., *Partial thickness rotator cuff tears results of arthroscopic treatment.* Arthroscopy, 1991. **7**(1): p. 1-7.

223. Weber, S.C., *Arthroscopic debridement and acromioplasty versus mini-open repair in the treatment of significant partial-thickness rotator cuff tears.* Arthroscopy-the Journal of Arthroscopic and Related Surgery, 1999. **15**(2): p. 126-131.

224. Kamath, G., et al., *Tendon Integrity and Functional Outcome After Arthroscopic Repair of High-Grade Partial-Thickness Supraspinatus Tears.* Journal of Bone and Joint Surgery-American Volume, 2009. **91A**(5): p. 1055-1062.

225. Corps, A.N., et al., *The regulation of aggrecanase ADAMTS-4 expression in human Achilles tendon and tendon-derived cells.* Matrix Biology, 2008. **27**(5): p. 393-401.

226. Gartsman, G.M., *Massive, irreparable tears of the rotator cuff - Results of operative debridement and subacromial decompression.* Journal of Bone and Joint Surgery-American Volume, 1997. **79A**(5): p. 715-721.

227. Rokito, A.S., et al., *Strength after surgical repair of the rotator cuff.* Journal of shoulder and elbow surgery / American Shoulder and Elbow Surgeons ... [et al.], 1996. **5**(1): p. 12-17.

228. Rokito, A.S., et al., *Long-term functional outcome of repair of large and massive chronic tears of the rotator cuff.* Journal of Bone and Joint Surgery - Series A, 1999. **81**(7): p. 991-997.

229. Matthews, T.J.W., et al., *In vivo measurement of tissue metabolism in tendons of the rotator cuff: Implications for surgical management.* Journal of Bone and Joint Surgery - Series B, 2007. **89**(5): p. 633-638.

230. Benson, R.T., et al., *The morphological and immunocytochemical features of impingement syndrome and partial-thickness rotator-cuff tear in relation to outcome after subacromial decompression.* J Bone Joint Surg Br, 2009. **91**(1): p. 119-23.

231. Erhard, L., et al., *Treatment of partial lacerations in flexor tendons by trimming - A biomechanical in vitro study.* Journal of Bone and Joint Surgery-American Volume, 2002. **84A**(6): p. 1006-1012.

232. Ng, B.H., S.M. Chou, and V. Krishna, *The influence of gripping techniques on the tensile properties of tendons.* Proceedings of the Institution of Mechanical Engineers, Part H: Journal of Engineering in Medicine, 2005. **219**(5): p. 349-354.

233. Itoi, E., et al., *Morphology of the torn rotator cuff.* Journal of Anatomy, 1995. **186**(2): p. 429-434.

234. Huang, C.Y., et al., *Inhomogeneous mechanical behavior of the human supraspinatus tendon under uniaxial loading.* Journal of Orthopaedic Research, 2005. **23**(4): p. 924-930.

235. Haut, R.C., *Age-dependent influence of strain rate on the tensile failure of rat-tail tendon.* Journal of Biomechanical Engineering, 1983. **105**(3): p. 296-299.

236. Clavert, P., et al., *Effects of freezing/thawing on the biomechanical properties of human tendons.* Surgical and Radiologic Anatomy, 2001. **23**(4): p. 259-262.

237. Mankin, H.J. and K.A. Conger, *The effect of cortisol on articular cartilage of rabbits. I. Effect of a single dose of cortisol on glycine-C-14 incorporation.* Laboratory Investigation, 1966. **15**(4): p. 794-800.

238. Barnett, N.D., R.D.D. Duncan, and G.R. Johnson, *The measurement of three dimensional scapulohumeral kinematics - A study of reliability.* Clinical Biomechanics, 1999. **14**(4): p. 287-290.

239. Spitzer, V.M. and D.G. Whitlock, *The visible human dataset: The anatomical platform for human simulation.* Anatomical Record, 1998. **253**(2): p. 49-57.

240. Ezura, Y., et al., *Differential expression of lumican and fibromodulin regulate collagen fibrillogenesis in developing mouse tendons.* Journal of Cell Biology, 2000. **151**(4): p. 779-787.

241. Keene, D.R., et al., *Decorin binds near the C terminus of type I collagen.* Journal of Biological Chemistry, 2000. **275**(29): p. 21801-21804.

242. Scott, J.E., C.R. Orford, and E.W. Hughes, *Proteoglycan-collagen arrangements in developing rat tail tendon. An electron-microscopical and biochemical investigation.* Biochemical Journal, 1981. **195**(3): p. 573-581.

243. Cooper, D.E., *Biomechanical properties of the central third patellar tendon graft: effect of rotation.* Knee Surg Sports Traumatol Arthrosc, 1998. **6 Suppl 1**: p. S16-9.

244. Sigholm, G., et al., *Pressure recording in the subacromial bursa.* Journal of Orthopaedic Research, 1988. **6**(1): p. 123-128.

245. Lee, S.B., et al., *Dynamic glenohumeral stability provided by the rotator cuff muscles in the mid-range and end-range of motion: A study in cadavera.* Journal of Bone and Joint Surgery - Series A, 2000. **82**(6): p. 849-857.

246. Lee, S.B. and K.N. An, *Dynamic glenohumeral stability provided by three heads of the deltoid muscle.* Clinical Orthopaedics and Related Research, 2002(400): p. 40-47.

247. Labriola, J.E., et al., *Stability and instability of the glenohumeral joint: The role of shoulder muscles.* Journal of Shoulder and Elbow Surgery, 2005. **14**(1 SUPPL.).

248. Ackland, D.C. and M.G. Pandy, *Lines of action and stabilizing potential of the shoulder musculature.* Journal of Anatomy, 2009. **215**(2): p. 184-197.

249. Reilly, P., et al., *Mechanical factors in the initiation and propagation of tears of the rotator cuff.* Journal of Bone and Joint Surgery - Series B, 2003. **85**(4): p. 594-599.

250. Lee, S.B., et al., *The bursal and articular sides of the supraspinatus tendon have a different compressive stiffness.* Clinical Biomechanics, 2000. **15**(4): p. 241-247.

251. Bey, M.J., et al., *Intratendinous strain fields of the intact supraspinatus tendon: The effect of glenohumeral joint position and tendon region.* Journal of Orthopaedic Research, 2002. **20**(4): p. 869-874.

252. Zuckerman, J.D., et al., *The effect of arm position and capsular release on rotator cuff repair. A biomechanical study.* Journal of Bone and Joint Surgery - Series B, 1991. **73**(3): p. 402-405.

253. Bey, M.J., M.L. Ramsey, and L.J. Soslowsky, *Intratendinous strain fields of the supraspinatus tendon: Effect of a surgically created articular-surface rotator cuff tear.* Journal of Shoulder and Elbow Surgery, 2002. **11**(6): p. 562-569.

254. Zhu, J., et al., *Effects of probe pollutants on morphological and mechanical measurements of muscle and collagen fibers using atomic force microscopy.* Scanning, 2010. **32**(3): p. 113-21.

255. Hauch, K., et al., *Nanoindentation of the insertional zones of human meniscal attachments into underlying bone.* J Mech Behav Biomed Mater, 2009. **2**(4): p. 339-47.

256. Duenwald, S., et al., *Ultrasound echo is related to stress and strain in tendon.* J Biomech, 2010.

257. Wikepedia. *Rheology*. 2010; Available from: http://en.wikipedia.org/wiki/Rheology.

258. Janmey, P.A., P.C. Georges, and S. Hvidt, *Basic Rheology for Biologists*, in *Methods in Cell Biology*, Y.L. Wang and D.E. Discher, Editors. 2007.

259. Subbotin, A., et al., *Nonlinear rheology of confined polymer melts under oscillatory flow.* Macromolecules, 1996. **29**(4): p. 1296-1304.

260. Zhu, W., et al., *Viscoelastic shear properties of articular cartilage and the effects of glycosidase treatments.* Journal of Orthopaedic Research, 1993. **11**(6): p. 771-781.

261. Kusaka, K., et al., *Objective evaluation of liver consistency to estimate hepatic fibrosis and functional reserve for hepatectomy.* Journal of the American College of Surgeons, 2000. **191**(1): p. 47-53.

262. Butler, D.L., N. Juncosa, and M.R. Dressler, *Functional efficacy of tendon repair processes*, in *Annual Review of Biomedical Engineering*2004. p. 303-329.

263. Vincent, J.F.V., *Structural biomaterials.* Princeton: Princeton University Press, 1990.

264. Chen, C.H., et al., *Tendon Healing In Vivo: Gene Expression and Production of Multiple Growth Factors in Early Tendon Healing Period.* Journal of Hand Surgery, 2008. **33**(10): p. 1834-1842.

265. Gerber, C., et al., *Experimental rotator cuff repair. A preliminary study.* Journal of Bone and Joint Surgery - Series A, 1999. **81**(9): p. 1281-1290.

266. Gazielly, D.F., P. Gleyze, and C. Montagnon, *FUNCTIONAL AND ANATOMICAL RESULTS AFTER ROTATOR CUFF REPAIR.* Clinical Orthopaedics and Related Research, 1994(304): p. 43-53.

267. Cofield, R.H., et al., *Surgical repair of chronic rotator cuff tears: A prospective long-term study.* Journal of Bone and Joint Surgery - Series A, 2001. **83**(1): p. 71-77.

268. Fukuda, H., et al., *Pathology and pathogenesis of the intratendinous tearing of the rotator cuff viewed from en-bloc histologic sections.* Clinical Orthopaedics and Related Research, 1994(304): p. 60-67.

269. Reeves, B., *Experiments on the tensile strength of the anterior capsular structures of the shoulder in man.* Journal of Bone and Joint Surgery British Volume, 1968. **50-B**(4): p. 858-865.

270. Vincent, J., *Biomechanics Materials, A Practical Approach*. The Practical Approach Series, ed. H.B.D. Rickwood D.1992, New York: Oxford University Press. 242.

271. Lee, S.-B., et al., *The bursal and articular sides of the supraspinatus tendon have a different compressive stiffness.* Clinical Biomechanics, 2000. **15**(4): p. 241-247.

272. Cao, H. and S.Y. Xu, *Purification and characterization of type II collagen from chick sternal cartilage.* Food Chemistry, 2008. **108**(2): p. 439-445.

273. Potter, K., et al., *Imaging of collagen and proteoglycan in cartilage sections using Fourier transform infrared spectral imaging.* Arthritis and Rheumatism, 2001. **44**(4): p. 846-855.

274. Krafft, C., et al., *Differentiation of individual human mesenchymal stem cells probed by FTIR microscopic imaging.* Analyst, 2007. **132**(7): p. 647-653.

275. Tiong, W.H.C., et al., *Enhancing amine terminals in an amine-deprived collagen matrix.* Langmuir, 2008. **24**(20): p. 11752-11761.

276. Hashimoto, T., K. Nobuhara, and T. Hamada, *Pathologic Evidence of Degeneration as a Primary Cause of Rotator Cuff Tear.* Clinical Orthopaedics and Related Research, 2003(415): p. 111-120.

277. Sripriya, R., et al., *Influence of laboratory ware related changes in conformational and mechanical properties of collagen.* Journal of Applied Polymer Science, 2003. **87**(13): p. 2186-2192.

278. Wenger, M.P.E., et al., *Mechanical properties of collagen fibrils.* Biophysical Journal, 2007. **93**(4): p. 1255-1263.

279. Eppell, S.J., et al., *Nano measurements with micro-devices: Mechanical properties of hydrated collagen fibrils.* Journal of the Royal Society Interface, 2006. **3**(6): p. 117-121.

280. Porter, D. and F. Vollrath, *The role of kinetics of water and amide bonding in protein stability.* Soft Matter, 2008. **4**(2): p. 326.

281. Derfus, B., et al., *Human osteoarthritic cartilage matrix vesicles generate both calcium pyrophosphate dihydrate and apatite in vitro.* Calcified Tissue International, 1998. **63**(3): p. 258-262.

282. Jiang, E.Y. and J. Rieppo, *Enhancing FTIR imaging capabilities with two-dimensional correlation spectroscopy (2DCOS): A study of concentration gradients of collagen and proteoglycans in human patellar cartilage.* Journal of Molecular Structure, 2006. **799**(1-3): p. 196-203.

283. Sato, M., et al., *Hydroxyapatite maturity in the calcified cartilage and underlying subchondral bone of guinea pigs with spontaneous osteoarthritis: Analysis by Fourier transform infrared microspectroscopy.* Acta Histochemica Et Cytochemica, 2004. **37**(2): p. 101-107.

284. Camacho, N.P., et al., *FTIR microscopic imaging of collagen and proteoglycan in bovine cartilage.* Biopolymers, 2001. **62**(1): p. 1-8.

285. Schneeberger, A.G., R.W. Nyffeler, and C. Gerber, *Structural changes of the rotator cuff caused by experimental subacromial impingement in the rat.* Journal of Shoulder and Elbow Surgery, 1998. **7**(4): p. 375-380.

286. Maffulli, N., et al., *Movin and bonar scores assess the same characteristics of tendon histology.* Clinical Orthopaedics and Related Research, 2008. **466**(7): p. 1605-1611.

287. Hamilton, J.A., et al., *Human synovial fibroblast plasminogen activator. Modulation of enzyme activity by antiinflammatory steroids.* Arthritis and Rheumatism, 1981. **24**(10): p. 1296-1303.

288. Wong, M.W.N., et al., *Effect of dexamethasone on cultured human tenocytes and its reversibility by platelet-derived growth factor.* Journal of Bone and Joint Surgery-American Volume, 2003. **85A**(10): p. 1914-1920.

289. Kjaer, M., *Role of Extracellular Matrix in Adaptation of Tendon and Skeletal Muscle to Mechanical Loading.* Physiological Reviews, 2004. **84**(2): p. 649-698.

290. Wening, J.D., et al., *Quantitative morphology of full thickness rotator cuff tears.* Clinical Anatomy, 2002. **15**(1): p. 18-22.

291. Haut, R.C., R.L. Lancaster, and C.E. DeCamp, *Mechanical properties of the canine patellar tendon: Some correlations with age and the content of collagen.* Journal of Biomechanics, 1992. **25**(2).

292. Hamada, K., et al., *Localization of mRNA of procollagen ?1 type I in torn supraspinatus tendons: In situ hybridization using digoxigenin labeled oligonucleotide probe.* Clinical Orthopaedics and Related Research, 1994(304): p. 18-21.

293. Kumagai, J., et al., *Collagen type III in rotator cuff tears: An immunohistochemical study.* Journal of Shoulder and Elbow Surgery, 1992. **1**(4): p. 187-192.

294. Funakoshi, T., et al., *Application of tissue engineering techniques for rotator cuff regeneration using a chitosan-based hyaluronan hybrid fiber scaffold.* American Journal of Sports Medicine, 2005. **33**(8): p. 1193-1201.

295. Fan, L., et al., *Estimation of total collagen and types I and III collagen in canine rotator cuff tendons.* Calcified Tissue International, 1997. **61**(3): p. 223-229.

296. Frank, C., et al., *Optimisation of the biology of soft tissue repair.* Journal of Science and Medicine in Sport, 1999. **2**(3): p. 190-210.

297. Jozsa, L., et al., *Pathological alterations in human tendons.* Archives of Orthopaedic and Trauma Surgery, 1990. **110**(1): p. 15-21.

298. Miles, C.A., T.V. Burjanadze, and A.J. Bailey, *The kinetics of the thermal denaturation of collagen in unrestrained rat tail tendon determined by differential scanning calorimetry.* Journal of Molecular Biology, 1995. **245**(4): p. 437-446.

299. T√©treault, P., et al., *Glenoid version and rotator cuff tears.* Journal of Orthopaedic Research, 2004. **22**(1): p. 202-207.

300. Miles, C.A. and A.J. Bailey, *Thermal denaturation of collagen revisited.* Proceedings of the Indian Academy of Sciences-Chemical Sciences, 1999. **111**(1): p. 71-80.

301. Potau, J.M., X. Bardina, and N. Ciurana, *Subacromial space in African great apes and subacromial impingement syndrome in humans.* International Journal of Primatology, 2007. **28**(4): p. 865-880.

302. Bailey, A.J., et al., *Chemistry of collagen cross-links: Glucose-mediated covalent cross-linking of type-IV collagen in lens capsules.* Biochemical Journal, 1993. **296**(2): p. 489-496.

303. Willett, T.L., R.S. Labow, and J.M. Lee, *Mechanical overload decreases the thermal stability of collagen in an in vitro tensile overload tendon model.* Journal of Orthopaedic Research, 2008. **26**(12): p. 1605-1610.

304. Higgins, L.D., *Medicolegal aspects of the orthopaedic care for shoulder injuries.* Clinical Orthopaedics and Related Research, 2005(433): p. 58-64.

305. Willett, T.L., et al., *Increased proteolysis of collagen in an in vitro tensile overload tendon model.* Annals of Biomedical Engineering, 2007. **35**(11): p. 1961-1972.

306. Reilly, P., et al., *Dead men and radiologists don't lie: A review of cadaveric and radiological studies of rotator cuff tear prevalence.* Ann R Coll Surg Engl, 2006. **88**(2): p. 116-121.

307. Wiegand, N., et al., *Differential scanning calorimetric examination of the ruptured Achilles tendon in human.* Thermochimica Acta, 2010. **498**(1-2): p. 7-10.

308. Itoi, E., et al., *Isokinetic strength after tears of the supraspinatus tendon.* Journal of Bone and Joint Surgery - Series B, 1997. **79**(1): p. 77-82.

309. Szabo, I., et al., *Differential scanning calorimetric and histological examinations of the long head of the biceps in cadavers.* Journal of Thermal Analysis and Calorimetry, 2007. **88**(2): p. 343-349.

310. Toth, K., et al., *Further characterization of degenerated human cartilage with differential scanning calorimetry.* Thermochimica Acta, 2007. **464**: p. 75-77.

311. Doman, I., T. Illes, and D. Lorinczy, *Differential sacnning calorimetric examination of the human intervertebral disc: establishment of calorimetric standards of different stages of degeneration.* Thermochimica Acta, 2003. **405**(2): p. 293-299.

312. Miles, C.A., et al., *Differential scanning calorimetric studies of superficial digital flexor tendon degeneration in the horse.* Equine Veterinary Journal, 1994. **26**(4): p. 291-296.

313. Achet, D. and X.W. He, *Determination of the renaturation level in gelatin films.* Polymer, 1995. **36**(4): p. 787-791.

314. Gulotta, L.V., et al., *Application of bone marrow-derived mesenchymal stem cells in a Rotator cuff repair model.* American Journal of Sports Medicine, 2009. **37**(11): p. 2126-2133.

315. Thomopoulos, S., et al., *Variation of biomechanical, structural, and compositional properties along the tendon to bone insertion site.* Journal of Orthopaedic Research, 2003. **21**(3): p. 413-419.

316. Sweat, F., H. Puchtler, and P. Woo, *LIGHT-FAST MODIFICATION OF LILLIES ALLOCHROME STAIN.* Archives of Pathology, 1964. **78**(1): p. 73-&.

317. Cheng, V.W.T. and H.R.C. Screen, *The micro-structural strain response of tendon.* Journal of Materials Science, 2007. **42**(21): p. 8957-8965.

318. Miles, C.A., et al., *The increase in denaturation temperature following cross-linking of collagen is caused by dehydration of the fibres.* Journal of Molecular Biology, 2005. **346**(2): p. 551-556.

319. Hiemstra, L.A., P.B. MacDonald, and W. Froese, *Subacromial infection following corticosteroid injection.* Journal of Shoulder and Elbow Surgery, 2003. **12**(1): p. 91-93.

320. Willett, T.L., et al., *Changes in collagen with aging maintain molecular stability after overload: Evidence from an in vitro tendon model.* Journal of Biomechanical Engineering, 2010. **132**(3).

321. Slatter, D.A., C.A. Miles, and A.J. Bailey, *Asymmetry in the triple helix of collagen-like heterotrimers confirms that external bonds stabilize collagen structure.* Journal of Molecular Biology, 2003. **329**(1): p. 175-183.

322. Lapiere Ch, M., B. Nusgens, and G.E. Pierard, *Interaction between collagen type I and type III in conditioning bundles organization.* Connective Tissue Research, 1977. **5**(1): p. 21-29.

323. Schena, M., et al., *Quantitative monitoring of gene expression patterns with a complementary DNA microarray.* Science, 1995. **270**(5235): p. 467-70.

324. Wolf, B.R., W.R. Dunn, and R.W. Wright, *Indications for repair of full-thickness rotator cuff tears.* American Journal of Sports Medicine, 2007. **35**(6): p. 1007-1016.

325. Julien, R.E. and B.A. Williams, *Regional anesthesia procedures for outpatient shoulder surgery.* International Anesthesiology Clinics, 2005. **43**(3): p. 167-175.

326. Ireland, D., et al., *Multiple changes in gene expression in chronic human Achilles tendinopathy.* Matrix Biology, 2001. **20**(3): p. 159-169.

327. Reno, C., et al., *Temporal alterations in mRNA levels for proteinases and inhibitors and their potential regulators in the healing medial collateral ligament.* Biochemical and Biophysical Research Communications, 1998. **252**(3): p. 757-763.

328. Aigner, T., et al., *Anabolic and catabolic gene expression pattern analysis in normal versus osteoarthritic cartilage using complementary DNA-array technology.* Arthritis Rheum, 2001. **44**(12): p. 2777-89.

329. Schroeder, A., et al., *The RIN: an RNA integrity number for assigning integrity values to RNA measurements.* BMC Mol Biol, 2006. **7**: p. 3.

330. Jeong, J.A., et al., *Differential gene expression profiling of human umbilical cord blood-derived mesenchymal stem cells by DNA microarray.* Stem Cells, 2005. **23**(4): p. 584-593.

331. Butte, A., *The use and analysis of microarray data.* Nature Reviews Drug Discovery, 2002. **1**(12): p. 951-960.

332. Riley, G.P., *Gene expression and matrix turnover in overused and damaged tendons.* Scandinavian Journal of Medicine and Science in Sports, 2005. **15**(4): p. 241-251.

333. Bedi, A., et al., *The effect of matrix metalloproteinase inhibition on tendon-to-bone healing in a rotator cuff repair model,* in *J Shoulder Elbow Surg*2010. p. 384-91.

334. Tsuzaki, M., et al., *IL-1Œ≤ induces COX2, MMP-1, -3 and -13, ADAMTS-4, IL-1Œ≤ and IL-6 in human tendon cells.* Journal of Orthopaedic Research, 2003. **21**(2): p. 256-264.

335. Matthews, T.J., et al., *Pathology of the torn rotator cuff tendon. Reduction in potential for repair as tear size increases.* J Bone Joint Surg Br, 2006. **88**(4): p. 489-95.

336. Derwin, K.A., et al., *Commercial extracellular matrix scaffolds for rotator cuff tendon repair: Biomechanical, biochemical, and cellular properties.* Journal of Bone and Joint Surgery - Series A, 2006. **88**(12): p. 2665-2672.

337. Zheng, M.H., et al., *Porcine small intestine submucosa (SIS) is not an acellular collagenous matrix and contains porcine DNA: Possible implications in human*

implantation. Journal of Biomedical Materials Research - Part B Applied Biomaterials, 2005. **73**(1): p. 61-67.

338. Doro, L.C., et al., *Validation of an adapted MRI pulse sequence for quantification of fatty infiltration in muscle.* Magn Reson Imaging, 2009. **27**(6): p. 823-7.

339. Doro, L.C., et al., *Validation of an adapted MRI pulse sequence for quantification of fatty infiltration in muscle.* Magnetic Resonance Imaging, 2009. **27**(6): p. 823-827.

340. Walch, G., et al., *Musculotendinous infraspinatus ruptures: an overview.* Orthop Traumatol Surg Res, 2009. **95**(7): p. 463-70.

341. Altman, G.H., et al., *Silk-based biomaterials.* Biomaterials, 2003. **24**(3): p. 401-16.

342. Fan, H., et al., *In vivo study of anterior cruciate ligament regeneration using mesenchymal stem cells and silk scaffold.* Biomaterials, 2008. **29**(23): p. 3324-37.

343. Gokalp, G., et al., *Using chemical-shift MR imaging to quantify fatty degeneration within supraspinatus muscle due to supraspinatus tendon injuries.* Skeletal Radiology, 2010. **39**(12): p. 1211-1217.

344. Randelli, P.S., et al., *Autologous platelet rich plasma for arthroscopic rotator cuff repair. A pilot study.* Disability and Rehabilitation, 2008. **30**(20-22): p. 1584-1589.

345. Bond, J.L., et al., *Arthroscopic replacement of massive, irreparable rotator cuff tears using a GraftJacket allograft: Technique and preliminary results.* Arthroscopy-the Journal of Arthroscopic and Related Surgery, 2008. **24**(4): p. 403-409.

346. Barr, K.P., *Rotator cuff disease.* Physical Medicine and Rehabilitation Clinics of North America, 2004. **15**(2): p. 475-491.

347. Sclamberg, S.G., et al., *Six-month magnetic resonance imaging follow-up of large and massive rotator cuff repairs reinforced with porcine small intestinal submucosa.* Journal of Shoulder and Elbow Surgery, 2004. **13**(5): p. 538-541.

348. Iannotti, J.P., et al., *Porcine small intestine submucosa augmentation of surgical repair of chronic two-tendon rotator cuff tears: A randomized, controlled trial.* Journal of Bone and Joint Surgery - Series A, 2006. **88**(6): p. 1238-1244.

349. Metcalf, M.H., F.H. Savoie Iii, and B. Kellum, *Surgical technique for xenograft (SIS) augmentation of rotator-cuff repairs.* Operative Techniques in Orthopaedics, 2002. **12**(3): p. 204-208.

350. Walton, J.R., et al., *Restore orthobiologic implant: not recommended for augmentation of rotator cuff repairs.* The Journal of bone and joint surgery American volume, 2007. **89**(4): p. 786-91.

351. Badhe, S.P., et al., *An assessment of porcine dermal xenograft as an augmentation graft in the treatment of extensive rotator cuff tears.* Journal of shoulder and elbow surgery / American Shoulder and Elbow Surgeons [et al], 2008. **17**(1 Suppl): p. 35S-39S.

352. Soler, J.A., S. Gidwani, and M.J. Curtis, *Early complications from the use of porcine dermal collagen implants (Permacol) as bridging constructs in the repair of massive rotator cuff tears. A report of 4 cases.* Acta Orthop Belg, 2007. **73**(4): p. 432-6.

353. Encalada-Diaz, I., et al., *Rotator cuff repair augmentation using a novel polycarbonate polyurethane patch: Preliminary results at 12 months follow-up.* Journal of shoulder and elbow surgery 2010.

354. Halder, A., et al., *Mechanical properties of the posterior rotator cuff.* Clinical Biomechanics, 2000. **15**(6): p. 456-462.

355. Legerlotz, K., G.P. Riley, and H.R.C. Screen, *Specimen dimensions influence the measurement of material properties in tendon fascicles.* Journal of Biomechanics, 2010. **43**(12): p. 2274-2280.

356. Hashimoto, T., K. Nobuhara, and T. Hamada, *Pathologic evidence of degeneration as a primary cause of rotator cuff tear.* Clin Orthop Relat Res, 2003(415): p. 111-20.

357. Arner, O. and A. Lindholm, *Subcutaneous rupture of the Achilles tendon; a study of 92 cases.* Acta Chir Scand Suppl, 1959. **116**(Supp 239): p. 1-51.

358. Horan, R.L., et al., *In vitro degradation of silk fibroin.* Biomaterials, 2005. **26**(17): p. 3385-3393.

359. Lake, S.P., et al., *Tensile properties and fiber alignment of human supraspinatus tendon in the transverse direction demonstrate inhomogeneity, nonlinearity, and regional isotropy.* Journal of Biomechanics, 2010. **43**(4): p. 727-732.

360. Barber, F.A., M.A. Herbert, and D.A. Coons, *Tendon augmentation grafts: Biomechanical failure loads and failure patterns.* Arthroscopy-the Journal of Arthroscopic and Related Surgery, 2006. **22**(5): p. 534-538.

361. Chaudhury, S., et al., *Comparing normal and torn rotator cuff tendons using dynamic shear analysis.* Journal of Bone and Joint Surgery - Series B, 2011. **93 B**(7): p. 942-948.

362. Huang, T.F., S.M. Perry, and L.J. Soslowsky, *The effect of overuse activity on Achilles tendon in an animal model: A biomechanical study.* Annals of Biomedical Engineering, 2004. **32**(3): p. 336-341.

363. An, K.N., *In vivo force and strain of tendon, ligament, and capsule.* Functional Tissue Engineering, 2003: p. 96-105.

364. Gerber, C., B. Fuchs, and J. Hodler, *The results of repair of massive tears of the rotator cuff.* Journal of Bone and Joint Surgery - Series A, 2000. **82**(4): p. 505-515.

365. Iannotti, J.P., *Full-thickness rotator cuff tears: Factors affecting surgical outcome.* J Am Acad Orthop Surg, 1994. **2**: p. 87-95.

366. Bigliani, L.U., et al., *Operative repair of massive rotator cuff tears: Long-term results.* Journal of Shoulder and Elbow Surgery, 1992. **1**(3): p. 120-130.

367. Essman, J.A., R.H. Bell, and M. Askew, *FULL-THICKNESS ROTATOR-CUFF TEAR - AN ANALYSIS OF RESULTS.* Clinical Orthopaedics and Related Research, 1991(265): p. 170-177.

368. Arnoczky, S.P., et al., *Ex vivo static tensile loading inhibits MMP-1 expression in rat tail tendon cells through a cytoskeletally based mechanotransduction mechanism.* Journal of Orthopaedic Research, 2004. **22**(2): p. 328-333.

369. Gardner, K., S.P. Arnoczky, and M. Lavagnino, *Effect of In Vitro Stress-Deprivation and Cyclic Loading on the Length of Tendon Cell Cilia in Situ.* Journal of Orthopaedic Research, 2011. **29**(4): p. 582-587.

370. Screen, H.R.C., et al., *Cyclic tensile strain upregulates collagen synthesis in isolated tendon fascicles.* Biochemical and Biophysical Research Communications, 2005. **336**(2): p. 424-429.

371. Xu, Y. and G.A.C. Murrell, *The basic science of tendinopathy.* Clinical Orthopaedics and Related Research, 2008. **466**(7): p. 1528-1538.

372. Hettrich, C.M., et al., *The effect of muscle paralysis using Botox on the healing of tendon to bone in a rat model.* Journal of Shoulder and Elbow Surgery, 2011. **20**(5): p. 688-697.

373. Thomopoulos, S., G.R. Williams, and L.J. Soslowsky, *Tendon to bone healing: Differences in biomechanical, structural, and compositional properties due to a range of activity levels.* Journal of Biomechanical Engineering-Transactions of the Asme, 2003. **125**(1): p. 106-113.

374. Bosch, G., et al., *Effects of platelet-rich plasma on the quality of repair of mechanically induced core lesions in equine superficial digital flexor tendons: A placebo-controlled experimental study.* Journal of Orthopaedic Research, 2010. **28**(2): p. 211-217.

375. Gotoh, M., et al., *Interleukin-1-induced subacromial synovitis and shoulder pain in rotator cuff diseases.* Rheumatology (Oxford), 2001. **40**(9): p. 995-1001.

376. Potau, J.M., et al., *Quantitative study of the architecture of the human subacromial space and its relationship with rotator cuff tears.* European Journal of Anatomy, 2008. **12**(1): p. 39-45.

377. Mochizuki, T., et al., *Humeral insertion of the supraspinatus and infraspinatus.* Journal of Bone and Joint Surgery - Series A, 2008. **90**(5): p. 962-969.

378. Funakoshi, T., et al., *Application of tissue engineering techniques for rotator cuff regeneration using a chitosan-based hyaluronan hybrid fiber scaffold.* American Journal of Sports Medicine, 2005. **33**(8): p. 1193-1201.

379. Chen, J.M., et al., *Autologous tenocyte therapy using porcine-derived bioscaffolds for massive rotator cuff defect in rabbits.* Tissue Engineering, 2007. **13**(7): p. 1479-1491.

380. Oh, J.H., et al., *Prognostic Factors Affecting Anatomic Outcome of Rotator Cuff Repair and Correlation With Functional Outcome.* Arthroscopy - Journal of Arthroscopic and Related Surgery, 2009. **25**(1): p. 30-39.